Is it safe to go into the sea? Climate change and *Vibrio* spp. bacteria

A thesis submitted for the degree of Doctor of Philosophy to the School of Environmental Sciences, University of East Anglia.

Elizabeth Jasmine Archer

December 2023

Registration number: 100286473/1

Supervisory Team

Professor Iain Lake[1]

Dr Craig Baker-Austin[2]

Dr Felipe Colón González[3,4]

Professor Timothy Osborn[1]

1. School of Environmental Sciences,
   University of East Anglia,
   Norwich, UK

2. Centre for Environment, Fisheries and Aquaculture Science,
   Weymouth, UK

3. Data for Science and Health,
   Wellcome Trust,
   London, UK

4. Department of Infectious Disease Epidemiology,
   Centre for Mathematical Modelling of Infectious Diseases,
   London School of Hygiene & Tropical Medicine,
   London, UK.

Abstract

Bacteria of the *Vibrio* genus are natural inhabitants of low salinity coastal ecosystems yet pose an increasing risk to human health. Pathogenic *Vibrio* species are highly temperature-sensitive and can cause infection via the consumption of undercooked seafood or direct exposure of wounds to seawater. Emergence of *Vibrio* spp. wound infections in high-latitude regions has been linked to rising sea surface temperatures caused by human-driven climate change. Simultaneously, warming air temperatures may encourage coastal recreational behaviour, exposing a greater number of individuals to these bacteria.

In this thesis, the northwards expansion of *Vibrio vulnificus* wound infections along the US Gulf of Mexico and Atlantic coastlines over a three-decade period is demonstrated using epidemiological data from the US Centers for Disease Control and Prevention. Statistical modelling of the *V. vulnificus* infection distribution as a function of air temperature is used to predict the changing geographic spread of infections to the end of the 21st Century under different scenarios of climate change. At a finer temporal and spatial scale, environmental drivers of weekly *V. vulnificus* wound infections in Gulf Coast US states are explored with a multi-model inference framework. The thesis also includes an ecological sampling study of *Vibrio* spp. bacteria within an anonymised coastal lagoon in the United Kingdom (UK). *Vibrio* spp. bacterial abundance is quantified and examined for associations with temperature, salinity and pH over a 10-week summer period whilst individual bacterial isolates are identified with cutting-edge matrix-assisted laser desorption/ionisation time-of-flight (MALDI-TOF) mass spectrometry (MS), polymerase chain reaction (PCR) and 16S ribosomal RNA (rRNA) gene sequencing.

The thesis highlights the importance of temperature to the distribution of *V. vulnificus* wound infections and provides crucial long-term future risk projections for the US east coast. Further, the microbiological data presented contribute to initial information on potentially pathogenic *Vibrio* spp. bacteria in UK waters.

Contents

List of tables

List of figures

Dedicated to my mother, Rebecca Gooch, whose endless kindness and strength have supported me tirelessly, throughout this PhD journey and far beyond.

Acknowledgements

I would first like to thank my supervisory team: Professor Iain Lake, Dr Craig Baker-Austin, Dr Felipe Colón González and Professor Timothy Osborn for their expert knowledge, support, and guidance during my PhD. I am especially grateful to Iain for his time, the expertise he has shared with me, his commitment to providing detailed feedback on my work and for supporting the process of publishing my first paper. I would like to thank Craig for his specialist knowledge of *Vibrio* spp. bacteria and for enabling me to gain practical experience in microbiological techniques by hosting me for several months at Cefas in Weymouth. I am highly grateful to both Iain and Craig for their support in rescheduling and redirecting the course of my PhD when the original plans were disrupted by the COVID-19 pandemic. I am truly grateful to Felipe for his expertise in statistical modelling and technical assistance with R programming as well as for encouraging me to learn how to use Climate Data Operator software with his guidance. I would also like to thank Tim for providing his expertise in global climate model datasets and advice on statistical modelling which also informed the first two data chapters of this thesis.

I would also like to thank the following people from Cefas. For providing training in wet-lab microbiological techniques and for making fieldwork during one of the hottest UK summers so enjoyable, I wish to thank Alexandra Hughes. I am also extremely grateful to Andy Powell for his expertise in *Vibrio* spp. microbiology and for facilitating the use of matrix-assisted laser desorption/ionisation time-of-flight (MALDI-TOF) mass spectrometry (MS) on my samples. I would like to thank Megan Adaway for the huge amount of time she spent conducting MALDI-TOF MS on my bacterial isolates and for completing my remaining polymerase chain reactions (PCRs). I also wish to thank the staff involved with the sequencing of my samples.

I am indebted to all my friends and family for their patience, positivity and unwavering support. I especially wish to thank my mother, Rebecca, and grandmother, Hazel, for always believing in me and for being inspirational women to look up to. I am also grateful for the love and support from my father, Michael, and stepmother, Dannielle, across the pond. I am particularly grateful to my best friend, Alexandra, for always being there for me, cheering me on, and for the much-needed box of relaxation treats I received when writing-up. Thanks to fellow PhD students Emily, Jack and Huang for their friendship and all the laughter-filled games of badminton that have kept me sane over past months. Last, but by no means least, I am forever grateful to my fiancé, Cailean, for beaming sunshine into my life, supporting me through every up and down and for patiently answering my many questions on microbiology.

1 Introduction

1.1 Background overview

Vibrio is a genus of bacteria which can be found in a wide range of aquatic habitats (F. L. Thompson et al., 2004), from freshwater sources to the deep-sea (Urkawa and Rivera, 2006). There are over 100 *Vibrio* species, including 12 known to cause human disease (Baker-Austin et al., 2018). *Vibrio* spp. illnesses are grouped into cholera and non-cholera *Vibrio* spp. infections.

Cholera is caused by *V. cholerae* which have an O1 or O139 antigen within the bacterial cell membrane (Faruque and Mekalanos, 2012). This severe diarrheal disease is typically spread through contaminated drinking water as a result of poor sanitation and is estimated to cause 2.9 million illnesses, including around 95,000 fatalities, globally each year (WHO, 2023).

V. cholerae that do not possess the O1 or O139 antigen, non-O1/non-O139 *V. cholerae* (NOVC), do not cause cholera but can still cause human illness. NOVC are included in the 'big four' non-cholera *Vibrio* spp. pathogens alongside *V. vulnificus, V. parahaemolyticus* and *V. alginolyticus* (Baker-Austin et al., 2017). Although other non-cholera *Vibrio* spp. such as *V. mimicus, V. cincinnatiensis, V. metschnikovii, V. furnissii,* and *V. fluvialis* are also linked with human disease (Baker-Austin et al., 2018), this thesis will focus on the 'big four' due to their significance as environmental pathogens with increasing incidence of human infection (Baker-Austin et al., 2017, 2010). From here on, any reference to '*Vibrio* spp. bacteria' or 'vibrios' refers to non-cholera *Vibrio* species, unless stated otherwise. Equally, '*Vibrio* spp. infections' refers to non-cholera *Vibrio* spp. infections, unless else specified.

Vibrio spp. infections (also referred to as 'vibriosis') follow two main routes of transmission. The bacteria may enter and infect an open wound via seawater exposure or foodborne infection can be acquired through consumption of the bacteria in seafood (Almagro-Moreno et al., 2023). In contrast to cholera, vibriosis does not involve person-to-person transmission or transmission through the faecal-oral route (Almagro-Moreno et al., 2023). Unlike O1/O139 *V. cholerae,* which can be found in both fresh and marine

waters, other *Vibrio* spp. bacteria require salt for growth and are naturally present within warm, low salinity coastal waters and estuaries (Baker-Austin et al., 2018).

Vibriosis inflicts a global burden on human health; infections are reported across Asia (Kang et al., 2020; Li et al., 2020), Northern Europe (Amato et al., 2022), the Americas (Raszl et al., 2016; Sheahan et al., 2022) and Oceania (Harlock et al., 2022; Vasey et al., 2023). It is estimated that approximately 80,000 cases of vibriosis occur in the United States (US) annually, of which 45,000 cases are thought to be caused by *V. parahaemolyticus.* Around 52,000 of the total estimated *Vibrio* spp. infections in the US are attributed to the consumption of contaminated seafood (CDC, 2019). Infections vary in severity; symptoms are dependent on the *Vibrio* species and health of the individual, ranging from mild gastroenteritis to fatal septicaemia (Baker-Austin et al., 2018). Of particular concern is *V. vulnificus* which causes around 100-200 cases of vibriosis in the US each year (Sheahan et al., 2022). Despite the relatively low number of cases attributed to *V. vulnificus* (~11% of vibriosis reported in the US from 2007 to 2018; Sheahan et al., 2022), infections are especially severe and progress rapidly. *V. vulnificus* infections can prove fatal around just 48 hours after transmission (Baker-Austin and Oliver, 2016). Notably, foodborne *V. vulnificus* septicaemia possesses a case fatality rate of ~50%; the highest of all food-borne diseases (Rippey, 1994).

An increasing body of research links vibriosis disease dynamics to variability in climatic factors. Past studies have demonstrated *Vibrio* spp. bacteria's exceptional sensitivity to temperature in the laboratory and environment (Kelly, 1982; Pfeffer et al., 2003), and, more recently, multiple heatwave-associated outbreaks of human vibriosis have been documented in nonendemic regions (Baker-Austin et al., 2016, 2013; Brehm et al., 2021a). For instance, the emergence of vibriosis in Northern Europe has been attributed to anomalous sea surface temperatures (SSTs) in the Baltic Sea (Baker-Austin et al., 2013; Ebi et al., 2017). This temperature sensitivity led Baker-Austin et al. (2017) to designate *Vibrio* spp. pathogens "the microbial barometer of climate change". The increased risk of *Vibrio* spp. disease as a consequence of warming and extreme weather has also been recognised by the Inter-governmental Panel on Climate Change (IPCC) (Bindoff et al., 2019). The emergence of *Vibrio* spp. infections and their growing burden on human health stresses the need for investigations into their associated environmental factors.

1.2 Thesis structure

The main body of this thesis is comprised of an introductory literature review chapter and three data chapters. Each data chapter is presented in the format of a paper for potential submission to an academic journal.

Chapter 2

Chapter 2 provides an overview of the *Vibrio* spp. literature, covering the ecology of the bacteria within the marine environment to the epidemiology of vibriosis. North America and the Baltic Sea region of Northern Europe provide key case studies of locations experiencing increasing and emerging *Vibrio* spp. infections and so are the focal regions of this review. The impacts of climate change upon the bacterial dynamics of *Vibrio* spp. in the environment and human behaviour which drives exposure are explored. Socioeconomic impacts of *Vibrio* spp. infections are discussed as well as mitigation strategies to prevent future infections.

Chapter 3

Chapter 3 uses a 30-year epidemiological dataset of *V. vulnificus* wound infections from the US Centers for Disease Control and Prevention (CDC) to examine the northwards expansion of reported cases through time along the east coast of the US. As there is uncertainty surrounding the southern limit of cases due to the absence of a dedicated *Vibrio* spp. infection surveillance service in South America, this analysis aims to understand changes in *V. vulnificus* wound infections at the northern limit of cases reported only. An ecological niche modelling methodology is utilised to build a model which explains the current geographic extent of *V. vulnificus* cases based on environmental variables. The future northwards expansion of *V. vulnificus* wound infections is predicted across the 21st Century under multiple scenarios of climate change based on data from seven CMIP6 global climate models. In addition to mapping future geographic predictions, the population living within 200 km (1–2-hour journey) of the coastline at risk of reported infections is projected and used in combination with future age-structure data to estimate potential future annual case numbers.

This chapter was published in Nature Scientific Reports in March 2023 (see section 1.3) and has since been accessed over 20,000 times and cited 19 times in academic literature. It has also been cited in an official CDC health advisory issued in September 2023 (CDC, 2023) after several *V. vulnificus* infections were reported in the New York

and Connecticut area. The publication has received substantial media attention resulting in over 10 interviews with journalists from Forbes, TIME Magazine, NBC News, The New York Times, and WIRED Magazine resulting in written articles as well as TV broadcast and live radio. According to Altmetric, the publication has been mentioned by 328 news outlets including. Thesis author Elizabeth J. Archer (EJA), Dr Craig Baker-Austin (CBA) and Prof. Iain R. Lake (IRL) conceived the idea. All data analyses and figure creation were undertaken by EJA. The manuscript was written by EJA and IRL. Prof. Timothy J. Osborn (TJO) and CBA advised on data availability and Dr Felipe J. Colón González (FJCG) provided statistical expertise. All authors provided advice and interpretation of the analysis, edited multiple versions of the manuscript, and contributed to revisions.

Chapter 4

Chapter 4 builds on the analysis of chapter 3 by conducting a time-series analysis exploring the environmental drivers of *V. vulnificus* wound infection incidence for US states along the Gulf Coast. A multi-model inference approach was implemented to compare the relative importance of different environmental predictors including meteorological and oceanographic variables as well as hurricane landfalls and the El Niño and La Niña modes of the Southern Oscillation.

Chapter 5

Chapter 5 presents results from a 10-week ecological sampling study of *Vibrio* spp. in a UK coastal lagoon. The weekly abundance of *Vibrio* spp. bacteria during summer months was recorded using culture-dependent microbiological techniques and assessed for correlations with environmental parameters. In addition, 325 isolates were collected, purified and identified to species level using matrix-assisted laser desorption/ionisation-time-of-flight (MALDI-TOF) mass spectrometry (MS), polymerase chain reaction (PCR) and 16S ribosomal RNA (rRNA) gene sequencing. These isolates contribute to a preliminary database of *Vibrio* spp. strains retrieved from UK waters.

This work was conducted during EJA's CASE partner placement with the Centre for Environment, Fisheries and Aquaculture Science (Cefas). EJA and CBA planned the study. Water sampling was conducted by EJA and Exeter-Cefas PhD student Alexandra Hughes (AH). Training in microbiological techniques was provided within Cefas laboratories. EJA conducted all culture-dependent microbiological techniques including membrane filtration *Vibrio* spp. count plates and the isolation, purification and storage of individual isolates. MALDI-TOF MS was conducted by Andy Powell (AP, Cefas Staff) and Megan Adaway (MA, Cefas placement student). PCR was conducted by EJA and

MA. 16S rRNA gene sequencing was conducted by Cefas staff. All data analysis, figure creation and write-up of the work was conducted by EJA.

Chapter 6

Chapter 6 provides a breakdown of the key research outcomes produced from each data chapter of the thesis. Recurring themes present throughout the thesis are discussed and areas for future research are outlined before concluding with an overview of the contribution that this thesis makes to the literature.

1.3 Published work

Chapter 3 was published in Nature Scientific Reports, March 2023:

Archer, E.J., Baker-Austin, C., Osborn, T.J., Jones, N.R., Martínez-Urtaza, J., Trinanes, J., Oliver, J.D., Colón González, F.J., & Lake, I.R. Climate warming and increasing *Vibrio vulnificus* infections in North America. Sci Rep **13**, 3893 (2023). https://doi.org/10.1038/s41598-023-28247-2

2 Literature review

2.1 *Vibrio* spp. ecology and environmental drivers

Within the literature, sea surface temperature (SST) and salinity are frequently reported as the most significant factors determining the abundance of non-cholera *Vibrio* spp. bacteria (hereafter referred to as '*Vibrio* spp. bacteria'). However, many further variables such as abundance of plankton, turbidity, pH and nutrient concentrations have been recorded to significantly influence *Vibrio* spp. abundance and therefore, may be of importance when predicting future areas of increased disease risk. Table 2.1 highlights a number of papers which look at the environmental drivers of *Vibrio* spp. bacteria. Taking each environmental parameter in turn we now consider this literature.

2.1.1 Sea surface temperature

Temperature mediates both the survival and abundance of *Vibrio* spp. bacteria in the environment. In general, seawater temperatures above 18°C enable the bacteria to thrive and rapidly multiply to high densities (Baker-Austin et al., 2017; Ruppert et al., 2004). For instance, *V. parahaemolyticus* bacteria are able to replicate every 12-14 minutes in suitable conditions (Ulitzur, 1974). As a result of this responsiveness to temperature, patterns of *Vibrio* spp. abundance typically fluctuate in correspondence with SST and follow a seasonal pattern of abundance that peaks during summer months (Pfeffer et al., 2003). For this reason, temperature is described as one of the main drivers of the *Vibrio* spp. spatiotemporal distribution (Tantillo et al., 2004), particularly in temperate regions, e.g., Oberbeckmann et al. (2011) and Sterk et al. (2015).

Nevertheless, some studies do not find temperature to be a significant predictor of *Vibrio* spp. abundance. A systematic review by Sheikh et al. (2022a) into *Vibrio* spp. (including O1 *V. cholerae*) and temperature found that of 111 papers containing laboratory and ecological *Vibrio* spp. growth profiles, 10 (9%) did not find temperature to significantly influence *Vibrio* spp. growth. Fifty-two papers (47%) demonstrated a significant positive association between temperature and *Vibrio* spp. growth whilst 7 papers (6%) found significant negative associations between temperature and *Vibrio* spp. growth (Sheikh et al., 2022a). The remaining 42 papers (38%) suggested that

temperature's relationship with *Vibrio* spp. growth was not straightforward and could be non-linear or dependent on other environmental parameters (Sheikh et al., 2022a). Sampling over a period with a reduced range of temperatures, especially if conditions remain suitable for *Vibrio* spp. throughout the sampling period e.g., summer only, is one possible explanation for temperature's lack of significance. For example, Oberbeckmann et al. (2012) found that water temperature only had a significant positive relationship with *Vibrio* spp. abundance in spring, which recorded the greatest variability in temperature. Alternatively, species-specific temperature preferences amongst the vibrios (Sheikh et al., 2022a) may result in complex overall relationships between temperature and total *Vibrio* spp. growth.

Laboratory research suggests that optimal *V*. *vulnificus* growth typically lies between 37°C to 39°C (Kelly, 1982; Miles et al., 1997; Velez et al., 2023), but within the aquatic environment water temperatures above 30°C seem have an inhibitory effect on *V. vulnificus* (Oliver, 2015). This disparity in observations between a controlled environment and ecological sampling hints at the complexity of predicting *Vibrio* spp. abundance within natural systems where temperature fluctuations interact with many other important physico-chemical and biological parameters such as dissolved oxygen, pH and plankton abundance (Velez et al., 2023; Vezzulli et al., 2016) (see Table 2.1).

2.1.2 Salinity

Vibrio spp. bacteria require salt for growth (Urkawa and Rivera, 2006) and exhibit a general preference for salinities below 25 Practical Salinity Units (PSU) (Baker-Austin et al., 2013); the salinity of full strength seawater is considered 35 PSU. This biological importance of salt to the non-cholera vibrios suggests that, where temperature is not limiting, salinity typically determines the distribution of *Vibrio* spp. bacteria in the marine environment (Urkawa and Rivera, 2006). This was echoed in work by Froelich et al. (2013) where the importance of salinity and water temperature variables to *Vibrio* spp. abundance differed depending on whether the water was mixed or stratified with defined layers of salinity in the Neuse River Estuary, North Carolina. When mixed, water temperature and salinity together explained 55% of the variation in *Vibrio* spp. abundance with 99.6% of this attributed to water temperature. On the other hand, when the water was stratified, the two variables explained 49% of the variation in *Vibrio* spp. abundance of which salinity explained greater variability (70.6%) than water temperature (29.4%). Many ecological sampling studies find salinity to be a significant predictor of *Vibrio* spp. abundance, alongside temperature (see Table 2.1).

Although below 25 PSU is a general guide to *Vibrio* spp. suitability, optimal salinity range has been observed to differ between species by Esteves et al. (2015) who documented these interspecies differences within a coastal lagoon system. Peak bacterial concentrations were recorded between salinities of 5 and 12 PSU for non-O1/non-O139 *V. cholerae* (NOVC), 10 and 15 PSU for *V. vulnificus* and 10 and 20 PSU for *V. parahaemolyticus.* This may explain some conflicting results from environmental sampling studies as salinity has been recorded as having both positive and negative relationships with overall *Vibrio* spp. abundance (see Table 2.1).

2.1.3 Plankton

The environmental survival and persistence of *Vibrio* spp. is supported by an array of different organisms (see Figure 2.1). Associations with phytoplankton (Eiler et al., 2006; Frischkorn et al., 2013; Oberbeckmann et al., 2011) and zooplankton (Huq et al., 1983; Nalin et al., 1979) have been long been documented throughout members of the *Vibrio* genus (Huq et al., 1983).

Zooplankton

Vibrio spp. colonise the chitinous exoskeletons of zooplankton, especially copepods (Pruzzo et al., 2008). Living attached within a biofilm brings *Vibrio* spp. bacteria protection against changing physico-chemical conditions (Hall-Stoodley et al., 2004) and predation (Matz et al., 2005). In addition, *Vibrio* spp. are able to break down and use chitin as a source of energy (Aunkham et al., 2018; Hunt et al., 2008; Kaneko and Colwell, 1975; Svitil et al., 1997). It has been suggested that Asiatic strains of *V. parahaemolyticus* may have been transported to South America attached to the exoskeletons of zooplankton carried across the Pacific Ocean by El Niño currents (González-Escalona et al., 2015; Martinez-Urtaza et al., 2016). Overall, association with zooplankton sustains a dynamic microbial reservoir within the upper layer of the ocean, argued as crucial to *Vibrio* spp. persistence (Vezzulli et al., 2010).

Phytoplankton

Phytoplankton including dinoflagellates (Eiler et al., 2006), diatoms (Frischkorn et al., 2013) and cyanobacteria (Islam et al., 1999) have been associated with *Vibrio* spp. persistence. Direct attachment of *V. parahaemolyticus* to diatoms has been observed (Frischkorn et al., 2013) but phytoplankton blooms may also benefit *Vibrio* spp. survival through the release of dissolved organic matter (DOM). Within experimental Baltic Sea microcosms, addition of cyanobacterial DOM enhanced the abundance of total

Vibrio spp. by orders of magnitude, whilst temperature had no significant effect (Eiler et al., 2007). Interestingly, this response was species-specific as NOVC and *V. vulnificus* were the only *Vibrio* spp. to increase in abundance significantly (Eiler et al., 2007). The influence of phytoplankton on *Vibrio* spp. abundance has also been documented from environmental water samples. Chlorophyll-a, a proxy for phytoplankton density, has been recorded as a significant predictor of *Vibrio* spp. abundance in the Neuse River Estuary, North Carolina, US (Hsieh et al., 2008), the Arabian Sea off south-west India (Asplund et al., 2011) and the inland bays of Delaware, US (Main et al., 2015) (see Table 2.1). Within such environmental waters, chlorophyll-a concentration has been found to correlate with SST (Hsieh et al., 2008), suggesting the complexity of unpicking the importance of phytoplankton to *Vibrio* spp. abundance rather than their covariance with SST in environmental settings.

2.1.4 Nutrients

Vibrio spp. bacteria display a feast-or-famine lifestyle and are able to take advantage of increased availability of nutrients, dividing rapidly in their presence (Westrich et al., 2016). Determining which substances stimulate the growth of *Vibrio* spp. is vital for predicting their abundance and mitigating against surges in concentrations.

Counterintuitively, multiple ecology-based modelling studies have observed negative correlations between the concentration of some nutrients and *Vibrio* spp. abundance; ammonium nitrogen, nitrate and phosphate have all demonstrated this relationship (see Table 2.1). In fact, low levels of these substances are associated with high phytoplankton abundance (Oberbeckmann et al., 2011), creating conditions rich in DOM, suitable for *Vibrio* spp. growth, whilst supporting persistence through formation of an environmental reservoir (Asplund et al., 2011) (see section 2.1.3). This is a further example of the interactions between environmental variables and their effects on *Vibrio* spp. bacteria and why it is important to understand these interactions. As mentioned, chlorophyll-a, a proxy for phytoplankton density, has been identified as a significant predictor of *Vibrio* spp. abundance by multiple studies (Asplund et al., 2011; Hsieh et al., 2008; Julie et al., 2010; Main et al., 2015). This suggests that, rather than direct bacterial assimilation, the contribution of these nutrients to the development of phytoplankton blooms could be their dominant influence on *Vibrio* spp. abundance dynamics. The salinity and temperature of coastal systems is generally beyond our direct control, however, the input of bloom-stimulating nutrients should be mediated by terrestrial land

management to prevent proliferation of *Vibrio* spp. pathogens (Thickman and Gobler, 2017).

2.2 Environmental persistence of *Vibrio* spp.

Vibrio spp. bacteria are able to survive in the water column when conditions are suitable. When conditions are not suitable, the survival and persistence of *Vibrio* spp. populations relies upon bacteria living within environmental reservoirs that can seed the free-living water column population when conditions become favourable again. Many of these environmental reservoirs are documented in Figure 2.1. This section will discuss different environmental reservoirs of *Vibrio* spp. bacteria as well as the 'viable but nonculturable' (VBNC) survival mechanism.

2.2.1 Viable but nonculturable (VBNC) state

Lack of culturable *Vibrio* spp. cells each winter within aquatic systems was once wholly attributed to cell death in response to cold temperatures unsuitable for survival (Oliver, 2013). This changed when, in 1987, Roszak and Colwell, described the VBNC state in bacteria. Whilst transitioning to the VBNC state, bacteria undergo suspension of most metabolic activity (Nowakowska and Oliver, 2013), shrinking in size and shifting from rod to coccoid formation (Oliver et al., 1991). These VBNC cells do not divide, yet retain enough internal processing to still be classed as 'alive' (Roszak and Colwell, 1987).

Temperature conditions below ca. 10°C are believed to induce VBNC transition in *Vibrio* spp. bacteria (Vezzulli et al., 2013). Changes in salinity, oxygen concentration and reduced availability of nutrients may also prompt this survival strategy (Colwell, 2000; Oliver, 2005a). However, this is a complicated process with strain and growth phase recognised as additional influential factors (Wu et al., 2016). Many *Vibrio* species not limited to *V. vulnificus, V. parahaemolyticus, V. cholerae* and *V. alginolyticus* demonstrate this method of persistence (Albertini et al., 2006; Oliver, 2005b; Wagley et al., 2021) which delivers enhanced resilience to multiple other stressors including pH, antibiotics, ethanol and heavy metals, as demonstrated in VBNC *V. vulnificus* cells (Nowakowska and Oliver, 2013). Successful resuscitation and cell replication generally occurs upon the return of suitable levels of the inducing variable (Nowakowska and Oliver, 2013) and is essential for the VBNC response to be recognised as a survival mechanism (McDougald et al., 1998).

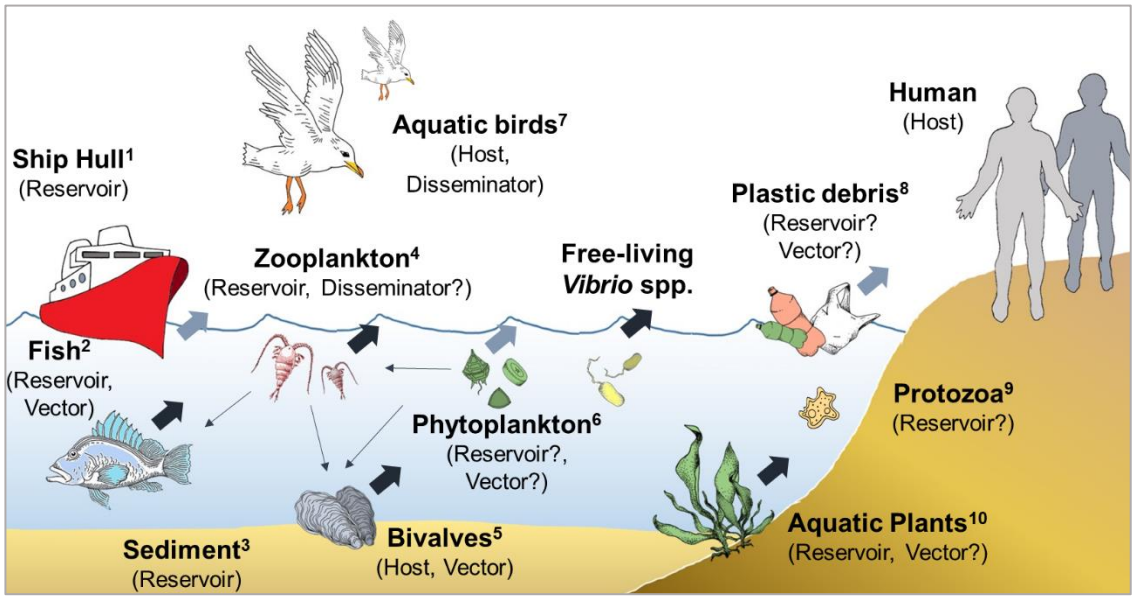

Figure 2.1 Environmental persistence and transmission amongst *Vibrio* spp. bacteria. Figure is based on Vezzulli et al. (2010) created from own illustrations and with additional components (plastic debris and ship hull). Question marks suggest potential interactions. Large arrows indicate transmission routes to humans (dark: evidenced in literature, light: potential route). Thin arrows represent ecological interactions between species. References: 1. (Shikuma and Hadfield, 2010); 2. (Halpern and Izhaki, 2017), 3. (Böer et al., 2013; Huehn et al., 2014) 4. (Colwell, 1996; Martinez-Urtaza et al., 2016; Vezzulli et al., 2013) 5. (Froelich and Noble, 2016) 6. (Frischkorn et al., 2013) 7. (Ayala and Ogbunugafor, 2023) 8. (Bowley et al., 2021; Zettler et al., 2013) 9. (Abd et al., 2005; Laskowski-Arce and Orth, 2008) 10. (Chase et al., 2015; Islam et al., 1994; Mahmud et al., 2007; Reilly et al., 2011).

2.2.2 Sediment

Vibrio spp. abundance is considerably higher within marine sediments (Blackwell and Oliver, 2008; Böer et al., 2013; Vezzulli et al., 2009). The benthic environment serves a protective role, providing bacteria with superior access to nutrients and more stable thermal conditions (Böer et al., 2013). *Vibrio* spp. bacteria over-wintering in sediments may recolonise the water column once favourable temperatures return (Kaneko and Colwell, 1973). Therefore, the function of sediment as a reservoir for pathogenic strains should not be overlooked.

2.2.3 Bivalves

Bivalves such as mussels, clams and oysters utilise a filtration method of feeding; a mechanism that draws in great densities of *Vibrio* spp. cells (Pruzzo et al., 2005). Uptake of these bacteria is aided by their association with particulates and planktonic organisms (Froelich and Noble, 2016). *Vibrio* spp. bacteria accumulate in bivalve tissues at significantly higher concentrations than within the surrounding water (DePaola et al., 2003; Wright et al., 1996), emphasising the elevated risk of infection from consumption of raw contaminated shellfish (Froelich and Noble, 2016). Moreover, bivalve larvae may supplement the planktonic *Vibrio* spp. population by returning cells to the water column, supporting the role of shellfish as a reservoir for these bacteria (Prado et al., 2014).

2.2.4 Abiotic biofilm associations

Amongst other man-made surfaces, e.g., ship hulls (Shikuma and Hadfield, 2010), oceanic plastic debris supplies a long-lasting, artificial, hydrophobic substrate, encouraging microbial biofilm formation (Zettler et al., 2013). *Vibrio* spp. have repeatedly been recorded to dominate microbial communities attached to plastic (the 'plastisphere'), representing as much as 33% of bacterial polypropylene colonisers in the North Atlantic open ocean (Amaral-Zettler et al., 2020; Zettler et al., 2013). Yet whether plastic debris functions as a microbial reservoir or potential vector of pathogenic *Vibrio* spp. is not known and warrants further scientific investigation (Amaral-Zettler et al., 2020; Bowley et al., 2022).

2.2.5 Other biotic associations

Further environmental reservoirs of *Vibrio* spp. have been included within Figure 2.1. Although some of these additional mechanisms of persistence have only been observed in select *Vibrio* species so far, including O1/O139 *V. cholerae*, they offer insight into the range of potential biological associations between *Vibrio* spp. and other marine organisms.

Protozoa may provide a form of environmental reservoir for *V. cholerae* as symbiosis with free-living amoebae such as *Acanthamoebea castellanii* has been demonstrated to support their survival (Abd et al., 2005). *A. castellanii* is also suggested to promote growth of *V. parahaemolyticus* through secretion of metabolic products, with no direct contact required (Laskowski-Arce and Orth, 2008).

Halpern and Izhaki, (2017) review the presence of O1/O139 *V. cholerae* and NOVC within the tissues of fish; most of these isolations being taken from healthy individuals. Fish, as hosts, may provide NOVC and other *Vibrio* spp. with protection from adverse conditions enabling their environmental dissemination and in return, may benefit from the bacteria's presence, for example, through improved digestion (Halpern and Izhaki, 2017).

A recent meta-analysis by Ayala and Ogbunugafor (2023) suggests that birds host many different pathogenic species of *Vibrio* including *V. cholerae, V. parahaemolyticus*, *V. vulnificus* and *V. alginolyticus* and are an understudied potential reservoir of *Vibrio* spp. bacteria. However, whether *Vibrio* spp. are opportunistic pathogens or active agents of avian disease and mortality is undecided (Ayala and Ogbunugafor, 2023).

Aquatic plants have been shown to support *Vibrio* spp. abundance (Chase et al., 2015; Gonzalez et al., 2014; Kalvaitienė et al., 2023; Mahmud et al., 2007). In Japan, seaweeds have been recognised as reservoirs for diverse populations of *V. parahaemolyticus* (Mahmud et al., 2007). Meanwhile, *V. parahaemolyticus* and a highly virulent genotype of *V. vulnificus* have been isolated from mats of the macroalga *Gracilaria vermiculophylla* on the US coast of Virginia (Gonzalez et al., 2014). In the first food safety assessment of macroalgae farmed for human consumption in the waters of the Northeast US, *V. parahaemolyticus* was detected from 78% of sugar kelp *Saccharina latissimi* samples, highlighting the importance of monitoring for bacterial pathogens in this industry (Barberi et al., 2020). Finally, a *V. alginolyticus* infection was reported as a result of direct contact of an open wound with gel extracted from *Fucus spiralis* (Reilly et al., 2011), suggesting contaminated macroalgae as a potential vector of extraintestinal *Vibrio* spp. disease. On the contrary, there is evidence to link the presence of seagrass with reduced *Vibrio* spp. load in the water column (Lamb et al., 2017; Reusch et al., 2021), yet the mechanism of this reduction remains unclear.

Table 2.1 Studies demonstrating significant (*p<0.05 minimum) interaction between microbial abundance of *Vibrio* spp. bacteria and environmental variables. Statistical methods used: [a]Regression-based modelling, [b]Independent correlation-based analyses. Unless presented in brackets, signifying a negative relationship, variables demonstrated positive relationships with *Vibrio* spp. abundance. **Positive below 15 PSU, negative above 15 PSU. SST (sea surface temperature), DOC (dissolved organic carbon), DON (dissolved organic nitrogen), DO (dissolved oxygen concentration), chl-a (chlorophyll-a), H' (Shannon-Weiner Index of diversity), POC (particulate organic carbon), TOC (total organic carbon), FPV (fine particulate volume).

Water Column			
Reference	**Location**	**Species**	**Significant* Variables**
Sea Surface Temperature (SST)			
Pfeffer et al., 2003[a]	Eastern North Carolina, USA	*Vibrio* spp.	SST, number of estuarine bacteria, phosphorous, (ammonia nitrogen), salinity, turbidity, (pH)
Vezzulli et al., 2009[a]	La Spezia Gulf, Italy	*Vibrio* spp.	SST, salinity, organic matter concentration
Froelich et al., 2015[b]	Eastern North Carolina, USA	*Vibrio* spp.	SST
Sterk et al., 2015[a]	The Netherlands, Europe	*Vibrio* spp.	SST, salinity, pH, enrichment method
Oberbeckmann et al., 2011[b]	Helgoland Roads, Germany, North Sea	*Vibrio* spp.	SST, SiO_2, (NO_2), (NO_3^-)
J. R. Thompson et al., 2004[b]	Barnegat Bay, New Jersey, USA	*Vibrio* spp.	SST
Neogi et al., 2011[b]	Eastern Atlantic Ocean (~50°N – ~24°S)	*Vibrio* spp.	SST, DOC, DON
Blackwell and Oliver, 2008[b]	Eastern North Carolina, USA	*Vibrio* spp.	SST, turbidity, total bacteria, total coliforms, *E. coli*, (DO), (ammonia nitrogen)

Table 2.1 continued…

Reference	Location	Species	Significant* Variables
Böer et al., 2013[a]	Germany, North Sea	*V. alginolyticus*	SST, rainfall
Blackwell and Oliver, 2008[b]	Eastern North Carolina, USA	*V. cholerae*	SST, (DO), (ammonia nitrogen)
Julie et al., 2010[a]	French Atlantic Coast	*V. parahaemolyticus*	SST, turbidity
Böer et al., 2013[a]	Germany, North Sea	*V. parahaemolyticus*	SST, (salinity)
Blackwell and Oliver, 2008[b]	Eastern North Carolina, USA	*V. parahaemolyticus*	SST, turbidity, (DO), (ammonia nitrogen)
Böer et al., 2013[a]	Germany, North Sea	*V. vulnificus*	SST, (wind- westerlies), (salinity)
Froelich et al., 2015[a]	Eastern North Carolina, USA	*V. vulnificus*	SST, salinity
Blackwell and Oliver, 2008[b]	Eastern North Carolina, USA	*V. vulnificus*	SST, turbidity, (DO), (ammonia nitrogen)
Salinity			
Hsieh et al., 2008[a]	Neuse River Estuary, North Carolina, USA	*Vibrio* spp.	salinity, SST, chl-a, DOC
Turner et al., 2009[a]	Georgia, USA	*Vibrio* spp.	salinity, SST
Hsieh et al., 2007[a]	Neuse River Estuary, North Carolina, USA	*Vibrio* spp.	salinity, POC
Froelich et al., 2013[a]	Neuse River Estuary, North Carolina, USA	*Vibrio* spp.	salinity, SST
Oberbeckmann et al., 2012[a]	Helgoland Roads, Germany, North Sea	*Vibrio* spp.	(salinity), SST, (PO_4^{3-}), (Secchi depth)
Wright et al., 1996[a]	Chesapeake Bay, USA	*V. vulnificus*	(salinity), depth of sample
Lipp et al., 2001[a]	Charlotte Harbor, Florida, USA	*V. vulnificus*	salinity**, SST

Table 2.1 continued…

Reference	Location	Species	Significant* Variables
Phytoplankton			
Asplund et al., 2011[a]	Arabian Sea, Mangalore, South-West India	*Vibrio* spp.	diatom biomass, (temperature), chl-a, total bacteria, phaeopigment absorbance, copepods, tides, *H'* phytoplankton, DOC, (salinity), (DO), DN, (SiO_2), pH, PO_4-P, heterotrophic flagellates, (ciliates), NO_3-N, (Secchi depth)
Within Sediment			
Sea Surface Temperature (SST)			
Vezzulli et al., 2009[a]	La Spezia Gulf, Italy	*Vibrio* spp.	SST
Böer et al., 2013[a]	Germany, North Sea	*V. alginolyticus*	SST, salinity, (wind - westerlies), TOC, rainfall
Blackwell and Oliver, 2008[b]	Eastern North Carolina, USA	*V. parahaemolyticus*	SST, turbidity
Böer et al., 2013[a]	Germany, North Sea	*V. parahaemolyticus*	SST, TOC, (wind – westerlies), rainfall (salinity)
Böer et al., 2013[a]	Germany, North Sea	*V. vulnificus*	SST, (wind - westerlies), (salinity)
pH			
Blackwell and Oliver, 2008[b]	Eastern North Carolina, USA	*V. vulnificus*	pH
Salinity			
Julie et al., 2010[a]	French Atlantic Coast	*V. parahaemolyticus*	salinity
Lipp et al., 2001[a]	Charlotte Harbor, Florida, USA	*V. vulnificus*	salinity, pH
Biofilm-Associated			
Particle-associated			
Hsieh et al., 2007[a]	Neuse River Estuary, North Carolina, USA	*Vibrio* spp.	FPV, (salinity)

Table 2.1 continued…

Reference	Location	Species	Significant* Variables
Main et al., 2015[b]	Delaware Inland Bays, USA	*Vibrio* spp.	raphidophyte abundance, diatom abundance, dinoflagellate abundance, chl-a, salinity
Plankton-associated (20-100µm)			
Oberbeckmann et al., 2011[b]	Helgoland Roads, Germany, North Sea	*Vibrio* spp.	SST, SiO2, (NO_2), (NO_3^-), (Secchi depth)
Plankton-associated (63-200µm)			
Turner et al., 2009[a]	Georgia, USA	*Vibrio* spp.	(copepod abundance), planktonic *Vibrio* conc., SST
Turner et al., 2009[a]	Georgia, USA	*Vibrio* spp.	(diatom abundance), planktonic *Vibrio* conc., SST, (DO)
Turner et al., 2009[a]	Georgia, USA	*Vibrio* spp.	(cyanobacteria abundance), (planktonic *Vibrio* conc.), SST, (salinity), (DO)
Plankton-associated (>100µm)			
Oberbeckmann et al., 2011[b]	Helgoland Roads, Germany, North Sea	*Vibrio* spp.	SST, SiO2, (NO_2), (NO_3^-), PO_4^{3-}
Plankton-associated (>200µm)			
Turner et al., 2009[a]	Georgia, USA	*Vibrio* spp.	copepod abundance, (planktonic *Vibrio* conc.), SST, (salinity)
Turner et al., 2009[a]	Georgia, USA	*Vibrio* spp.	(decapod abundance), (planktonic *Vibrio* conc.), SST
Shellfish-Associated			
Sea Surface Temperature (SST)			
Froelich et al., 2015[b]	Eastern North Carolina, USA	*Vibrio* spp.	SST
Oberbeckmann et al., 2011[b]	Helgoland Roads, Germany, North Sea	*Vibrio* spp.	SST, SiO2, (NO_2), (NO_3^-)
Cook et al., 2002[a]	Atlantic & Gulf Coast states, USA	*V. parahaemolyticus*	SST, salinity
Parveen et al., 2008[a]	Chesapeake Bay, Maryland, USA	*V. parahaemolyticus*	SST, turbidity, DO

Table 2.1 continued…

Reference	Location	Species	Significant* Variables
Froelich et al., 2015[a]	Eastern North Carolina, USA	*V. vulnificus*	SST, salinity
Chlorophyll-a			
Julie et al., 2010[a]	French Atlantic Coast	*V. parahaemolyticus*	chl-a

2.3 *Vibrio* spp. epidemiology

Vibrio spp. pathogens, including O1/O139 *V. cholerae*, are the dominant cause of human illness linked to bacteria from the marine environment (Almagro-Moreno et al., 2023; Baker-Austin et al., 2018). Ingestion of pathogenic *Vibrio* spp. in seawater or raw seafood can cause gastroenteritis which may lead to life-threatening primary septicaemia in immunocompromised individuals and those with predisposing chronic illnesses (Baker-Austin et al., 2018). Alternatively, cells may enter the body via an open cut exposed to contaminated seawater or seafood drippings (Daniels, 2011). Resultant wound infections vary in severity; most are resolved with antibiotic treatment but in some cases surgical debridement of tissue or limb amputation is necessary to prevent progression to secondary septicaemia which can be fatal (Leng et al., 2019). Such extreme cases are mainly associated with *V. vulnificus* infections in individuals with underlying health conditions (Leng et al., 2019).

Despite the overarching similarities in disease characteristics, interspecies differences in geographic spread, mortality rate and clinical manifestations will be explored in the following section.

2.3.1 *Vibrio vulnificus*

In contrast to *V. parahaemolyticus, V. alginolyticus* and *V. cholerae*, *V. vulnificus* is an opportunistic pathogen meaning it predominantly causes foodborne and wound infections in people with underlying health conditions (Baker-Austin and Oliver, 2018). Consequently, the number of infections caused by this pathogen is relatively low compared to other vibrios (Sheahan et al., 2022). Between 2007 and 2018, 1,573 cases of *V. vulnificus* were reported in the US Cholera and Other *Vibrio* Illness Surveillance

(COVIS) dataset, representing ~11% of *Vibrio* spp. infections and 53% of which were confirmed as non-foodborne manifestations (Sheahan et al., 2022).

High iron availability enables rapid proliferation and progression of *V. vulnificus* host infection (Baker-Austin et al., 2018; Wright et al., 1981), resulting in rapid symptom onset, e.g., within 26 hours after oyster consumption (Oliver, 2013). Consequently, illnesses that result in excess iron levels in the blood, including liver cirrhosis, cancer, and hereditary hemochromatosis, generate a greater risk of fatality from *V. vulnificus* infections (Khan et al., 2007; Oliver, 2005c; Payne et al., 2016).

The rapidity of *V. vulnificus* disease progression stresses the importance of responsive intervention with appropriate antibiotics, as likelihood of survival diminishes with delay in treatment (Klontz, 1988; Oliver, 2005c). Correct diagnosis within a short window of symptom onset is vital for maximising chance of survival, therefore highlighting the need for widespread awareness and education of disease risks amongst both medical practitioners and the general public. This is especially important when considering non-endemic regions such as the Baltic Sea region of Northern Europe and Atlantic Coast of the United States, where *Vibrio* spp. cases are emerging (Baker-Austin et al., 2013; King et al., 2019).

Interestingly, a large proportion of cases affect persons aged between 45-60 years (Baker-Austin et al., 2018), with greatest prevalence repeatedly observed in men (Hlady and Klontz, 1996; Jones and Oliver, 2009). These biases may be linked to trends in liver cirrhosis diagnoses, as middle-aged males are more frequently affected by this condition (Sajja et al., 2014; Scaglione et al., 2015). However, the protective role of the female hormone, oestrogen, against *Vibrio* spp. Endotoxic shock may also influence this disparity (Merkel et al., 2001).

V. vulnificus foodborne infections

The case fatality rate (CFR) of *V. vulnificus* primary septicaemia infections (~50%) is greater than that of any other foodborne disease (Baker-Austin et al., 2018; Rippey, 1994). Between 1992 and 2007, 51.6% of patients (459 cases), died in the US according to Food and Drug Administration (FDA) records (Jones and Oliver, 2009). FDA data available for 180 primary septicaemia cases reported between 2002 and 2007, revealed 95.3% of individuals had at least one underlying condition and the ingestion of raw oysters preceded 92.8% of infections (Jones and Oliver, 2009). Consumption of raw bivalves, mainly oysters, is a common factor amongst primary septicaemia cases (Baker-

Austin and Oliver, 2018), highlighting the risk of consuming this seafood product for those with high risk predispositions.

***V. vulnificus* wound Infections**

Whilst *V. vulnificus* wound infections have a lower mortality rate (~18%) (Ralston et al., 2011), they are more frequently reported than foodborne *V. vulnificus* infections (Sheahan et al., 2022). Seawater exposure to this marine pathogen arguably still presents a substantial risk for those with the risk factors mentioned above. Prompt surgical removal of infected tissue (Chao et al., 2013) and amputation can be necessary to prevent the rapid onset of systemic infection resulting in secondary septicaemia and death; survival is significantly enhanced in those patients subjected to this treatment within 24 h of infection (Kuo et al., 2007). The rapidity of *V. vulnificus* infections is exemplified in a case report of a 59-year-old male who exposed an insect bite to seawater whilst fishing in the Gulf of Mexico (Baker-Austin and Oliver, 2016). The fast progression of the illness resulted in the death of this individual around 48 hours after exposure (Baker-Austin and Oliver, 2016).

2.3.2 *Vibrio parahaemolyticus*

V. parahaemolyticus is a common cause of seafood-related illnesses that are typically self-limiting (Almagro-Moreno et al., 2023) and seawater exposure infections that resolve after antibiotic treatment (Baker-Austin et al., 2017). This said, individuals with health conditions can still develop more severe forms of *V. parahaemolyticus* infection such as primary septicaemia (Zhang and Orth, 2013).

Perhaps due to the high number of *V. parahaemolyticus* infections relative to other *Vibrio* spp. pathogens (e.g., in the US, *V. parahaemolyticus* caused ~40% of vibriosis cases between 2007 and 2018; Sheahan et al., 2022), there are more data available on the history and global dispersal of this pathogen compared to other *Vibrio* species. The first recorded outbreak of *V. parahaemolyticus* occurred in Japan during the 1950s (Shinoda, 2011) and by 1969, *V. parahaemolyticus* was isolated from sporadic vibriosis cases across the United States (Baker-Austin et al., 2018). Since then, a unique serotype (strains grouped by possession of the same surface antigens within the cell membrane) of *V. parahaemolyticus*, serotype O3:K6, emerged from Asia in 1996 and has spread globally, resulting in the first *V. parahaemolyticus* pandemic (Velazquez-Roman et al., 2014).

V. parahaemolyticus foodborne infections

V. parahaemolyticus is responsible for the greatest prevalence of seafood-related food-poisoning in the US (Newton et al., 2012) and about 20-30% of all food-poisoning incidences in Japan (Alam et al., 2002). In the US, between 2007 and 2018, 4,530 foodborne cases of *V. parahaemolyticus* were reported to COVIS (Sheahan et al., 2022).

Whilst most cases of gastroenteritis are self-limiting (Baker-Austin et al., 2017), the risk of developing a severe primary septicaemia infection following ingestion of raw oysters is high for persons with an underlying chronic illness (Su and Liu, 2007). Outbreaks within the US are now regularly linked to consumption of oysters harvested from coastlines off the Gulf of Mexico, Atlantic and Pacific (Altekruse et al., 2000; Centers for Disease Control and Prevention, 1999, 1998).

V. parahaemolyticus wound infections

V. parahaemolyticus wound infections are mainly recorded during summer months (Hlady and Klontz, 1996) and regularly require antibiotic treatment (Baker-Austin et al., 2017). This clinical manifestation of *V. parahaemolyticus* is much less common than foodborne *V. parahaemolyticus* illnesses. Only 14% (n = 755) of *V. parahaemolyticus* cases reported to COVIS between 2007 and 2018 were confirmed as non-foodborne infections compared to 80% which were confirmed as foodborne (Sheahan et al., 2022). The reason for lower prevalence of wound infections compared to foodborne infections is unclear.

2.3.3 Non-O1/non-O139 *Vibrio cholerae* (NOVC)

NOVC cause wound infections, ear infections and gastroenteritis (Deshayes et al., 2015). During the progression of an infection, NOVC can enter the bloodstream, described as ‘bacteraemia’ (Deshayes et al., 2015). Bacteraemia is infrequently diagnosed, yet poses a high risk for those individuals with underlying illnesses (Ou et al., 2003). As with *V. vulnificus*, liver-related disorders are repeatedly identified as the greatest predisposing factor for bacteraemia development (Deshayes et al., 2015). Other significant risk factors include malignancies and steroid use (Ou et al., 2003). Based on an extensive literature review of 350 cases by Deshayes et al. (2015), NOVC bacteraemia presents a CFR of ~33%. Most of the bacteraemia patients were male (77%), middle-aged individuals (median age 56 years) and nearly all (96%) were known to have a predisposing condition, e.g., liver cirrhosis (55%) (Deshayes et al., 2015).

NOVC foodborne infections

Gastroenteritis is a frequent form of NOVC infection (Chen et al., 2015; Vezzulli et al., 2020) and can range from mild to severe, similar to *V. parahaemolyticus* (Anderson et al., 2004). Progression to NOVC bacteraemia has predominantly been linked to seafood consumption (54%), of which oysters, fish and shrimps constitute the greatest risk (associated with 41%, 23% and 18% of cases, respectively) (Deshayes et al., 2015).

NOVC wound infections

NOVC can also cause extraintestinal infections such as wound and ear infections associated with seawater exposure (Baker-Austin et al., 2018). The 2014 heatwave experienced across Northern Europe, saw a sudden associated surge in reported *Vibrio* spp. infections within Sweden and Finland; NOVC was responsible for 77% of these cases, most of which were wound infections (Baker-Austin et al., 2016). NOVC wound infections also increased in Europe during the following heatwave year of 2018, with 100 cases reported across Sweden, Finland, Norway, Denmark, Estonia and Poland (Amato et al., 2022). This information suggests NOVC infections are a developing human health hazard and therefore should be monitored closely.

2.3.4 *Vibrio alginolyticus*

V. alginolyticus predominantly causes wound and ear infections which can usually be treated with antibiotics (Jacobs Slifka et al., 2017; Pezzlo et al., 1979); progression of these cases to bacteraemia or necrotising fasciitis is rare, but may occur in immunocompromised individuals (Reilly et al., 2011). Foodborne *V. alginolyticus* infections are not considered a common form of illness caused by this pathogen, although cases of seafood-associated gastroenteritis are present within the literature (Baker-Austin et al., 2018; Uh et al., 2001), therefore here we focus on extraintestinal *V. alginolyticus* wound infections only.

Within Europe, *V. alginolyticus* infections have been reported sporadically (Baker-Austin et al., 2016, 2013; Hartley et al., 1991; Reilly et al., 2011). In the US, reported cases of *V. alginolyticus* increased 12-fold between 1988 and 2012 with 1331 total reported infections, 86% of which were related to water-based activities (Jacobs Slifka et al., 2017). This bacterium was responsible for 131 (15.7%) of 834 *Vibrio* spp. infections reported in Florida between 1998 and 2007 (Weis et al., 2011). Cases were sporadic and non-fatal (Weis et al., 2011). This mirrors the percentage of vibriosis cases caused by *V. alginolyticus* nationally in the US between 2007 and 2018 (15.8%) (Sheahan et al.,

2022). Whilst in 2007 *V. alginolyticus* caused around 100 cases per year, recent data suggests there are now nearly 300 per year (Sheahan et al., 2022). This highlights the growth of *V. alginolyticus* in significance as a human pathogen with warming sea surface temperatures (Amato et al., 2022; Sheahan et al., 2022).

2.4 Understanding reporting: burden of illness pyramid

The 'burden of illness' pyramid is a concept used by FoodNet (CDC, 2015) (see Figure 2.2) to understand the stages leading up to a case of foodborne illness being reported to a surveillance body. Each stage, represented by a level of the pyramid, contains fewer individuals than the level beneath. This concept is particularly relevant for *Vibrio* spp. pathogens such as NOVC and *V. parahaemolyticus* which can cause self-limiting gastroenteritis (Baker-Austin et al., 2018). For example, a large number of the population may be exposed to these pathogens through eating seafood but only some individuals will become ill. Only a small proportion of those persons will seek medical attention and fewer still will have a sample taken and tested. A confident species-level identification is obtained for some of the tests. Not all confirmed test results will get reported to the centralised surveillance body therefore, as a result, many cases of vibriosis are not reported. Unlike in the US, where vibriosis is legally notifiable (CDC, 2019), vibriosis is not a notifiable disease in Europe which further decreases the likelihood of reporting. There may also be differences in the extent of underreporting between different *Vibrio* spp. pathogens. For instance, *V. vulnificus* symptoms are typically severe and foodborne infection can rapidly develop to primary septicaemia (Warnock and MacMath, 1993), which unquestionably requires medical intervention. In comparison, the generally self-limiting nature of gastrointestinal symptoms caused by *V. parahaemolyticus* (Baker-Austin et al., 2018) suggest a lower frequency of infected individuals reporting their illness to a doctor. Therefore, it could be proposed that proportionally, there is greater underreporting of *V. parahaemolyticus* than *V. vulnificus*, with consequences for understanding the true extent of the health burden these bacteria pose.

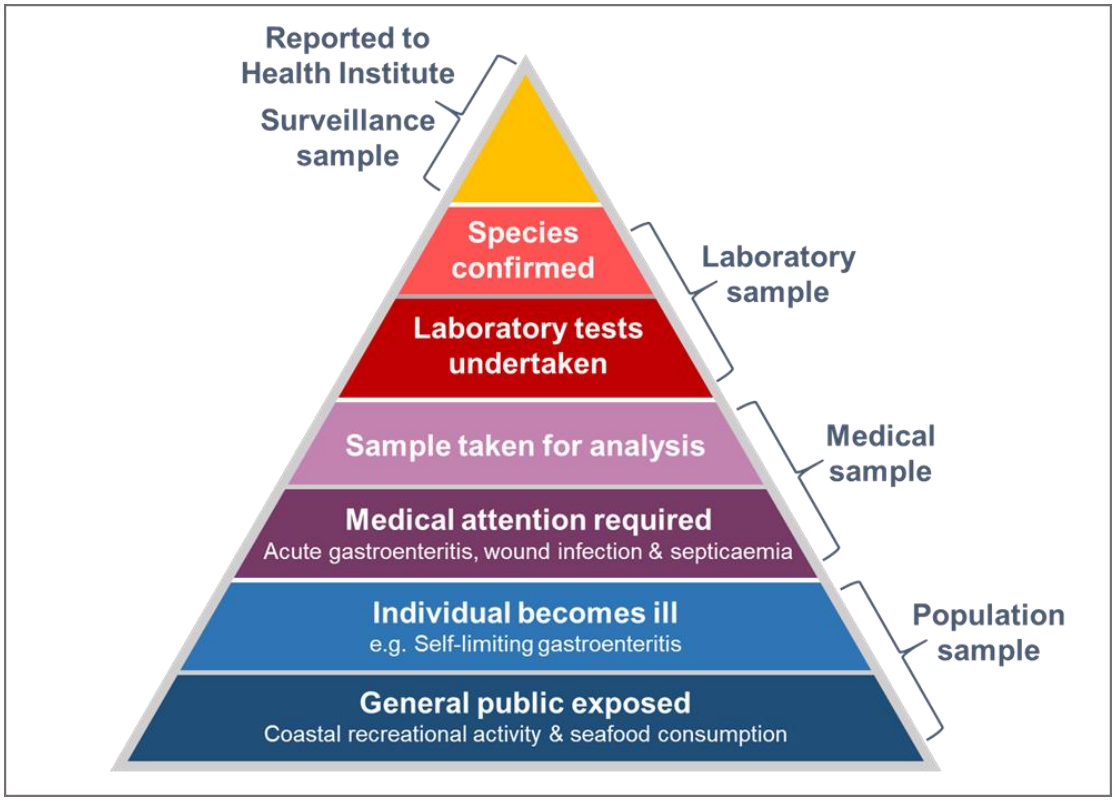

Figure 2.2 *Vibrio* spp. burden of illness pyramid. Adapted from FoodNet Surveillance example (CDC, 2015).

2.5 Threat of antimicrobial resistance (AMR)

The genome of *Vibrio* spp. bacteria is distributed across two chromosomes; a trait present across the *Vibrionaceae* family (Okada et al., 2005). *Vibrio* spp. bacteria are highly receptive to free genetic material; species constantly evolve through the mechanism of horizontal gene transfer (HGT) (Le Roux et al., 2015), threatening potential recombination of antimicrobial resistance (AMR) genes. In fact, attachment to chitin (a key component of marine invertebrate exoskeletons; see section 2.1.3 for *Vibrio* spp. attachment to plankton) induces natural competence in *Vibrio* spp., i.e., enables the uptake of free DNA which could harbour virulence or AMR genes (Blokesch, 2014).

Regular, excessive use of antibiotics to suppress disease within aquaculture environments, as well as increasing use for treatment of human infection, has created a selection pressure within natural aquatic habitats for AMR bacteria (Allen et al., 2010). Such environments are considered reservoirs of AMR bacteria (Marti et al., 2014) which enter via wastewater from homes and hospitals, as well as run-off from agricultural

sources (Reverter et al., 2020). These factors are thought to have led to the occurrence of multi-drug resistant (MDR) *Vibrio* spp. strains (Letchumanan et al., 2015). MDR *Vibrio* spp. isolates have been found in seafood products (Letchumanan et al., 2015), coastal water and sediment samples (Baker-Austin et al., 2008), and clinical isolates from human infections (Baker-Austin et al., 2009).

Shaw et al. (2014) tested 120 *V. vulnificus* and 77 *V. parahaemolyticus* environmental strains isolated from the Chesapeake Bay and Maryland Coastal Bays for their susceptibility to 26 different antibiotics. *V. vulnificus* isolates were resistant to 12 of 26 antibiotics whilst *V. parahaemolyticus* isolates demonstrated resistance to 15 of 26 antibiotics (Shaw et al., 2014). Importantly, the majority of isolates were susceptible to those antibiotics recommended for treating *Vibrio* spp. infections (Shaw et al., 2014).

AMR strains pose a significant risk to human health as the outcome of life-threatening *Vibrio* spp. infections is shown to depend on the timing of effective antibiotic treatment (Klontz, 1988). Increasing incidence of infections (Baker-Austin et al., 2010) stress the need for alternative therapies and effective methods of mitigation to reduce the likelihood of further resistant strains developing (Heng et al., 2017).

2.6 Climate change impacts on *Vibrio* spp. transmission and disease

Greenhouse gas emissions from human activity have unequivocally increased global temperatures (IPCC, 2021) with widespread negative consequences for people and nature (IPCC, 2022). As the average global temperature rises, impacts continue to manifest in long term, incremental changes whilst also enhancing disruptive, extreme events (Bindoff et al., 2019; Collins et al., 2019).

The IPCC Special Report on the Ocean and Cryosphere in a Changing Climate states that there is ‘very high confidence’ in the link between warming, extreme weather events and increased *Vibrio* spp. disease risk (Bindoff et al., 2019). An overview of how climate change may influence *Vibrio* spp. disease risk is presented in Figure 2.3 resulting from a synthesis of the literature presented. Prediction of this risk involves multiplying the level of hazard by the level of exposure in the population; climate change affects both of these components. This diagram identifies how climate change may influence SST, through warming trends, and salinity, via changing precipitation and glacier melt (IPCC, 2014). Both may have direct microbial effects which could modify the abundance and

distribution of *Vibrio* species as well as indirect effects through changes to plankton populations (see section 2.1.3). Climate change could also affect human behaviour. Changing air temperature and precipitation are likely to impact the frequency and locations of recreational activities such as fishing, coastal bathing and seafood consumption which enhance the risk of coming into contact with *Vibrio* spp. Furthermore, a feedback mechanism may occur whereby awareness of rising *Vibrio* spp. disease risk results in a small proportion of individuals limiting their exposure. Together, the hazard and exposure combine to influence the spatiotemporal distribution of *Vibrio* spp. disease.

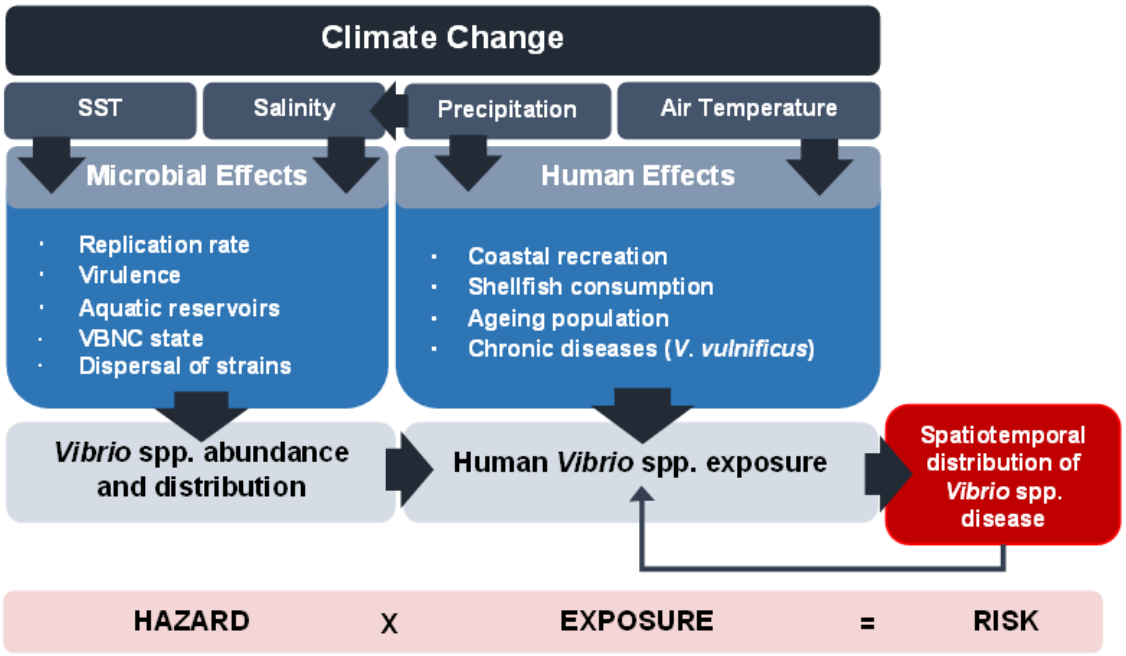

Figure 2.3 Potential influences of climate change on the spatiotemporal distribution of *Vibrio* spp. disease. Impacts of climate change include changing SST, precipitation and air temperature (IPCC, 2014), with proposed influences on microbial communities and human behaviour. The resultant effects on *Vibrio* spp. abundance (hazard) and human *Vibrio* spp. exposure (exposure) can be multiplied together to determine the spatiotemporal distribution of *Vibrio* spp. disease risk.

2.6.1 *Vibrio* spp. spatiotemporal abundance and distribution (hazard)

In terms of the hazard, climate change may influence the spatiotemporal abundance of *Vibrio* spp., changing opportunities for human exposure, and thus infection. There are several environmental factors that promote *Vibrio* spp. survival in the aquatic environment, and these may influence both the geographic range of *Vibrio* spp. as well

as the seasonal patterns of its abundance. The possible influences of climate change on each of these environmental factors with potential consequences for *Vibrio* spp. spatiotemporal abundance and distribution will be considered in turn.

Geographic range

Temperature and salinity directly influence *Vibrio* spp. bacteria's replication rate and survival (see section 2.1, '*Vibrio* spp. ecology and environmental drivers'). Changes in these environmental parameters therefore majorly determine the capacity for growth and persistence in the marine environment of *Vibrio* spp. (Vezzulli et al., 2013).

The ocean has absorbed greater than 90% of the excess heat generated from anthropogenically driven warming (Zanna et al., 2019) and many impacts of climate change affecting the ocean are accelerating (Bindoff et al., 2019). Average global sea temperature continues to rise at an increasing rate, disproportionately affecting the upper ocean and causing widespread stratification of the surface layer (Bindoff et al., 2019). At the time of writing (August 2023), average daily global SST for 2023 has consistently reached well beyond 2 standard deviations from the 1981-2011 mean (Climate Reanalyzer, Climate Change Institute, University of Maine, 2023; Huang et al., 2021) (see Figure 2.4). With time, stratification is likely to be strengthened by the freshening of marine ecosystems in high latitude regions in response to future patterns of heavy precipitation (Bindoff et al., 2019). As these changes occur, warm, low salinity conditions suitable for *Vibrio* spp. growth may expand poleward, extending the spatial area within which vibrios can persist (Baker-Austin et al., 2013; Vezzulli et al., 2013). One analysis predicts that the length of global coastlines suitable for *Vibrio* spp. growth could expand by up to 38,000km by the end of the 21st Century (Trinanes and Martinez-Urtaza, 2021). Multi-decadal evidence presented by (Vezzulli et al., 2016) suggests that rising SSTs, correlated with warming trends of the Northern Hemisphere Temperature (NHT) and Atlantic Multidecadal Oscillation (AMO) climatic indices, have driven an increase in the relative abundance of *Vibrio* spp. amongst plankton-associated bacteria sampled within the temperate North Atlantic and North Sea regions. However, long term changes in climatic variables also affects the dynamics of *Vibrio* spp. indirectly, by altering the populations of organisms that encourage *Vibrio* spp. survival, particularly plankton communities (Hays et al., 2005) (see section 2.1.3).

There is high confidence that the poleward movement of marine organisms has in-part been enabled by increasing ocean temperatures (Bindoff et al., 2019). As warm water species shift in range, the structure of plankton communities in high latitude regions

changes, with potential consequences for *Vibrio* spp. persistence (Vezzulli et al., 2015). In the North Atlantic and North Sea regions, a multi-decadal increase in phytoplankton abundance with SST and a more recent shift in phytoplankton community structure were observed (Vezzulli et al., 2016). Differential competitive ability of phytoplankton species under changing ocean conditions is thought to have resulted in a reduction in dinoflagellates, whilst diatoms have increased in abundance in this region (Hinder et al., 2012; Vezzulli et al., 2016). These community composition alterations have occurred in tandem with a sharp increase in *Vibrio* spp. abundance relative to other members of the bacterioplankton since the year 2000 (Vezzulli et al., 2016). It is difficult to ascertain whether *Vibrio* spp. have benefitted directly from these changes in the phytoplankton community or whether phytoplankton dynamics mirror that of *Vibrio* spp. due to the relationship of these organisms with temperature. However, (Main et al., 2015) found a greater positive relationship between *Vibrio* spp. and diatoms than with dinoflagellates, supporting the consideration of changing phytoplankton community structures as a potential factor in the prediction of future *Vibrio* spp. abundance.

Climate change may also influence the survival of *Vibrio* spp. bacteria transported to new, suitable regions via natural or artificial (e.g., ship ballast tanks) means (Colwell, 1996; Martinez-Urtaza et al., 2016; Shikuma and Hadfield, 2010). The likelihood of the establishment of *Vibrio* spp. populations in non-endemic locations will arguably increase with the effects of climate change as these locations become more favourable for growth (Vezzulli et al., 2013). The climate phenomenon ‘El Niño’ results in extensive warming of surface waters along the west coast of South America with irregular frequency every two to seven years (Martinez-Urtaza et al., 2016). These events are contended to provide a “long-distance biological corridor”, connecting the waters from South America to those of East Asia through an intercontinental body of warm water (Martinez-Urtaza et al., 2016). Analysis of oceanographic variables has linked the 1997 emergence of *V. parahaemolyticus* serotype O3:K6 along the coast of South America to the movement of El Niño waters from Southeast Asia (Martinez-Urtaza et al., 2008). *Vibrio* spp. may be transported across this distance in biofilm association with the exterior surfaces of zooplankton, enabling them to reach new habitats for colonisation whilst protected from starvation and physiological changes (Martinez-Urtaza et al., 2016). Extreme El Niño events are predicted to double in frequency throughout the 21st century (Collins et al., 2019), potentially creating more frequent opportunities for the geographic transmission of pathogenic *Vibrio* spp.

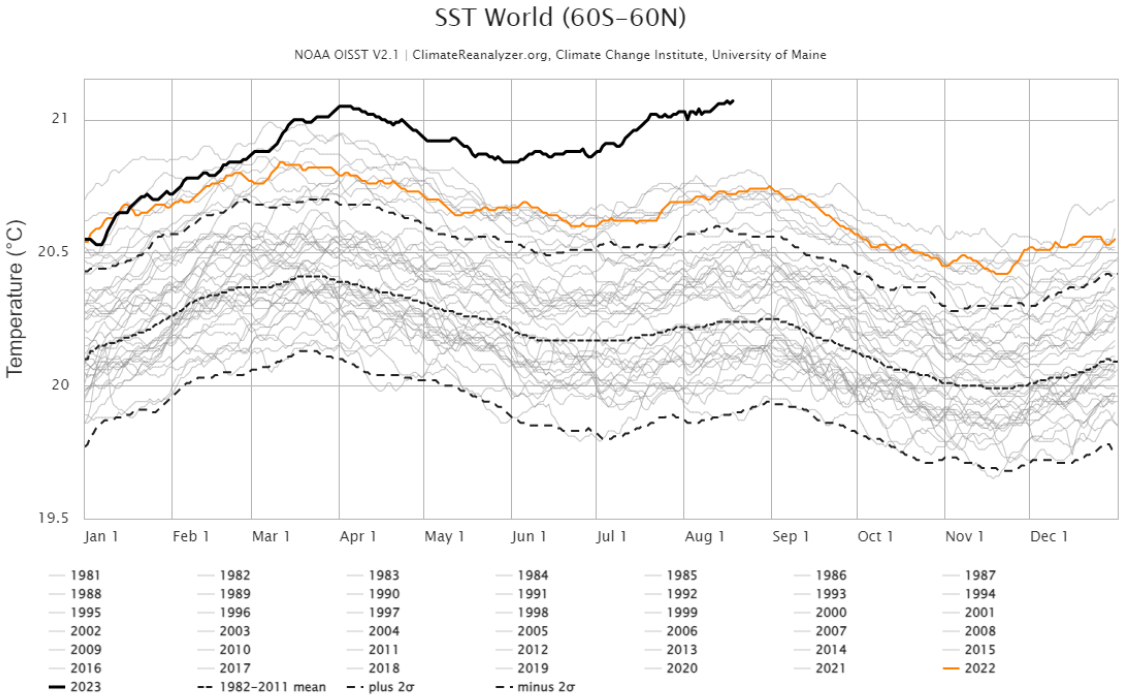

Figure 2.4 Daily global average sea surface temperatures from the NOAA Optimum Interpolation SST (OISST) version 2.1 dataset (1981-2023) (Huang et al., 2021). Light grey lines represent each year from 1981 to 2021. The orange and bold black lines show data from 2022 and 2023, respectively. The small dashed line represents the 1982-2011 mean with larger dashed lines for 2 standard deviations above and below that mean. Image courtesy of Climate Reanalyzer, Climate Change Institute, University of Maine, (2023) under a Creative Commons Attribution 4.0 International License.

Temporal abundance

One impact of ocean warming is the extended duration of summer SSTs (Baker-Austin et al., 2013), likely leading to longer growing seasons for temperature-mediated organisms. Rapid replication is common amongst the *Vibrio* genus; some species double in under 10 minutes (Aiyar et al., 2002), therefore, prolonged periods of optimal SST for *Vibrio* spp. proliferation can lead to the accumulation of high cell densities within near-shore waters (Ruppert et al., 2004). *Vibrio* spp. concentrations may be further supplemented by the regrowth of VBNC cells (see section 2.2.1), which can be initiated by temperature upshifts (Coutard et al., 2007). However, it is worth noting that some locations could become less suitable for *Vibrio* spp. bacteria if salinity is sufficiently increased because of strong evaporation during periods of high temperature. This is more likely in coastal waters that are semi-enclosed or have less tidal exchange such as coastal lagoons.

Vibrio spp. abundance could be enhanced by other environmental factors, including changes to precipitation. It is predicted that greater average annual rainfall at higher latitudes will cause increased volumes of freshwater run-off (IPCC, 2014). As well as reduced salinity, this may lead to subsequent nutrient loading of coastal areas, potentially fuelling phytoplankton and zooplankton blooms, ultimately boosting *Vibrio* spp. survival (Andersson et al., 2015; Heisler et al., 2008) (see sections 2.1.3 and 2.1.4). Furthermore, seasonality of peak *Vibrio* spp. abundance may be influenced by changes to the timing of phytoplankton spring blooms which are observed to occur earlier in response to climate change impacts on physiology, water column stratification and changing light and nutrient availability (Winder and Sommer, 2012). Furthermore, the species composition of zooplankton communities is also an important factor in the seasonal timing of *Vibrio* spp. abundance (Constantin de Magny et al., 2014; Turner et al., 2009).

In addition to long term seasonal changes, increasing frequency of extreme weather events is associated with climate change (IPCC, 2014). There is high confidence that anthropogenic global warming was responsible for 84-90% of Marine heatwave (MHW) events recorded between 2006 and 2015 (Collins et al., 2019). MHWs have doubled in frequency since 1982, whilst also increasing in severity, geographic extent and duration; trends predicted to continue into the 21st Century (Collins et al., 2019). Anomalously high SSTs associated with heatwave events stimulate *Vibrio* spp. abundance (Ruppert et al., 2004), therefore MHWs represent an increasingly frequent source of elevated hazard.

Short periods of high volume rainfall can cause coastal flooding, creating the brackish, low salinity conditions within which *Vibrio* spp. bacteria flourish (Baker-Austin et al., 2018). Hurricanes are associated with an elevated risk of *Vibrio* spp. infections as extensive brackish coastal floodwaters resulting from hurricane storm surges can expose large numbers of people to the bacteria leading to a spike in wound-associated vibriosis (Rhoads, 2006; Sodders et al., 2023). For example, a total of 38 vibriosis cases were reported in Florida, US after exposure to Hurricane Ian's floodwaters in 2022 (Sodders et al., 2023). This included 11 fatalities, 9 of which were caused by *V. vulnificus* (Sodders et al., 2023). Climate change is predicted to increase the intensity of hurricanes (Collins et al., 2019) which may influence the vibriosis risk associated with these events. More generally, heavy precipitation events are becoming more frequent with climate change (IPCC, 2014). Rising sea levels due to glacial melt and thermal expansion, in response to ocean warming (IPCC, 2014), may exacerbate the severity and extent of coastal flooding during extreme events, suggesting greater exposure of human populations to *Vibrio* spp. bacteria in future.

2.6.2 Human factors (exposure)

Coastal recreation

Environmental variables also affect human behaviour; for example the duration of coastal recreational activity increases with air temperature (Elliott et al., 2019), exhibiting a visible surge in popularity during summer periods. Nevertheless, literature addressing how weather affects specific human behaviours involved in *Vibrio* spp. disease transmission such as seafood consumption, bathing and fishing is not extensive.

Future patterns of recreational activity have the potential to alter the extent to which human populations are exposed to *Vibrio* spp. pathogens. Climate predictions of increased air temperature and more frequent heatwave events (IPCC, 2014) could be accompanied by concomitant patterns of recreational behaviour, potentially resulting in higher incidence of infections. However, the influence of environmental factors upon human behaviour may not be linear; for example, anomalously high temperatures experienced during some heatwaves may reduce recreation and thus exposure (Coombes et al., 2008).

Demographic changes influencing exposure

Demographic factors also influence the burden of *Vibrio* spp. infections. Concomitant with global trends of coastal migration (Hugo, 2011), between 2000 and 2016, the population of coastal counties along the Gulf of Mexico grew by >3 million (24.5%) in comparison to an overall 14.8% growth in population of the US within this time (Cohen, 2018). These factors are important as more people are potentially exposed to *Vibrio* spp. bacteria and some chronic underlying conditions that predispose individuals to greater risk of developing a severe manifestations of *Vibrio* spp. infection, for example liver cirrhosis, are associated with older individuals (Scaglione et al., 2015). Ageing populations are highly likely to mean predisposing conditions rise in frequency amongst the general population with higher proportion of individuals susceptible to suffer from life-threatening forms of vibriosis. Meanwhile, population growth in many parts of the world (UN DESA, 2019) may lead to more individuals interacting with coastal resources which would likely result in a general increase in infections.

Temporal patterns in consumption of seafood imply a further source of altering levels of exposure. As well as short term seasonality, long term trends suggest a general increase in seafood consumption in some regions (Gudmundsson et al., 2006).

2.7 Changing *Vibrio* spp. disease risk

The true burden of *Vibrio* spp. disease risk is unknown (see section 2.4). Despite this, data indicate a global rise in reported *Vibrio* spp. illnesses (Vezzulli et al., 2013). Reported *Vibrio* spp. infections are increasing both over time and in geographic extent (Baker-Austin et al., 2013). For example, the annual incidence of vibriosis per 100,000 individuals in the US more than doubled in less than a last decade from 0.42 in 2010 to 0.90 in 2019 (Newton et al., 2012; Tack et al., 2020). The geographic expansion of vibriosis cases is noted in their emergence at high latitudes in northern Europe (Baker-Austin et al., 2013) and Alaska (McLaughlin et al., 2005) as well as temperate regions of Israel (Paz et al., 2007), Northwest Spain (Baker-Austin et al., 2010), Chile (González-Escalona et al., 2005) and Peru (Martinez-Urtaza et al., 2008); representing a developing human health hazard in these locations. However, in many of these locations no systematic collection and investigation of epidemiological *Vibrio* spp. data takes place, therefore, emergence is based upon case reports which may give a poor estimate of incidence.

In the following sections the changing risk of *Vibrio* spp. disease in North America and Northern Europe will be considered in turn. Whilst vibriosis does also occur in other locations around the world, many academic papers focus on these two regions thus providing substantial data to discuss.

2.7.1 North America

Vibrio spp. bacteria have been a known cause of illness in the US for decades. The earliest reports of *V. parahaemolyticus* and *V. alginolyticus* infections occurred in the late 1960s (Twedt et al., 1969) followed by the first *V. vulnificus* infections which were described in 1976 (Hollis et al., 1976; Kang et al., 2020). *Vibrio* spp. account for a large number of mild and therefore unreported cases. The US CDC estimate that around 80,000 vibriosis infections occur each year in the US, of which 65% are believed to be caused by *V. parahaemolyticus,* (CDC, 2019).

The Pacific Northwest region, which includes the US states of Washington, Oregon and Alaska as well as the Canadian province of British Columbia, and the US Gulf of Mexico coastline are hotspots for *Vibrio* spp. disease (Sheahan et al., 2022). The Pacific Northwest has harvested shellfish for over 150 years and brings $270 million to the local economy annually (NOAA, 2022). However, the consumption of shellfish from this region

has been associated with vibriosis, including several *V. parahaemolyticus* outbreaks occurring in 1997 (CDC, 1998), 2004 (McLaughlin et al., 2005) and 2021 (Washington State Department of Health, 2021). Meanwhile, in the Gulf of Mexico region, reports of vibriosis prompted the first US coordinated surveillance of *Vibrio* spp. infections in 1989, resulting in the establishment of the Cholera and Other *Vibrio* Illness Surveillance (COVIS) system by the CDC, FDA and states of Texas, Alabama, Louisiana, and Florida (CDC, 2022; Levine and Griffin, 1993). Additional states voluntarily joined the COVIS reporting scheme as they experienced infections and vibriosis was made nationally notifiable in the US in 2007 (CDC, 2019).

Numbers of all vibriosis cases declared to COVIS have grown since mandatory reporting began in 2007 according to data presented by Sheahan et al. (2022). Between 2007 and 2018, 14,017 cases were reported (Sheahan et al., 2022). Around 70% of cases occurred in the latter half of this 12-year dataset with ca. 3,000 cases in 2018 alone, representing about 20% of all cases (Sheahan et al., 2022). Using these data Sheahan et al. (2022) were able to build models of monthly vibriosis occurrence for individual *Vibrio* spp. pathogens using SST, supporting the influence of warming temperatures on the increasing number of vibriosis cases reported in the US. This is also evidenced in case reports of vibriosis at new, higher latitudes along the East Coast of the US (e.g., Delaware Bay; King et al., 2019).

V. parahaemolyticus was the dominant species reported to COVIS between 2007 and 2018, causing around 40% of all infections (Sheahan et al., 2022). Around 900 cases of *V. parahaemolyticus* were reported in 2018, demonstrating a ~50% increase compared to the previous year and approximately quadruple the number reported in 2007 (Sheahan et al., 2022). Cases of *V. vulnificus* and *V. alginolyticus* also increased over time from fewer than 100 cases before 2009 to around 200 and 300 cases per year attributed to these species by 2018, respectively (Sheahan et al., 2022). Interestingly, 2017 and 2018 also saw substantial increases in the number of infections caused by *Vibrio* species other than *V. parahaemolyticus, V. vulnificus,* and *V. alginolyticus* (Sheahan et al., 2022). The number of infections caused by these 'other' *Vibrio* species, including NOVC, increased from around 300 cases in 2016 to 1,600 cases in 2018 (Sheahan et al., 2022). The inclusion of cases confirmed with culture-independent diagnostic tests (CIDTs) from 2017 onwards is believed to have contributed to this significant rise in reporting through improvements in the accuracy of diagnoses (Sheahan et al., 2022). This may also be linked to the recent increases in *V. parahaemolyticus* infections.

2.7.2 Northern Europe

The emergence of *Vibrio* spp. infections in northern Europe has corresponded with spatial and temporal changes in SST (Baker-Austin et al., 2013). In conjunction with other high latitude regions, northern Europe is warming at a rate disproportionate to the global average (Belkin, 2009). Sudden increases in domestically contracted *Vibrio* spp. illnesses have accompanied multiple heatwave events (1994, 1997, 2003, 2006, 2010, 2014, 2018) experienced in this geographic area (Amato et al., 2022; Baker-Austin et al., 2016).

For example, Sweden and Finland reported a total of 89 *Vibrio* spp. infections in association with the summer heatwave of 2014 (Baker-Austin et al., 2016). NOVC caused the majority (77%) of cases with 10 of these infections reported at latitudes greater than 63°N, including 6 documented at ~65°N (Baker-Austin et al., 2016). At the time of reporting, the *Vibrio* spp. cases observed represented the largest yearly totals recorded for Sweden and Finland, as well as documenting the most northerly cases of vibriosis ever recorded (Baker-Austin et al., 2016). Generalised linear modelling determined maximum annual SST as the key predictor of cases in these countries (Baker-Austin et al., 2016), similar to previous results (Baker-Austin et al., 2013). Analysis of all cases reported within the Baltic Sea area between 1985 and 2010 revealed that alongside maximum annual SST, time explained significant amounts of variability in the number of cases reported (Baker-Austin et al., 2013). Trends that may have led to time being a significant variable include: changes in reporting such as greater medical awareness leading to higher rates of diagnosis, shifting population demography and increased exposure (Baker-Austin et al., 2013).

Analysis of Hadley SST data sets revealed the Baltic Sea, considered the world's most rapidly warming marine ecosystem (Belkin, 2009), has been warming by more than 1°C per decade since 1987; seven times faster than the global average (Baker-Austin et al., 2013; Belkin, 2009). Baker-Austin et al. (2013) predict the future extension of summer SSTs, with average SST set to exceed 18°C for the majority of the summer season under the highest levels of warming. Temperatures above 18°C are preferential for *Vibrio* spp. growth (Vezzulli et al., 2013), highlighting the increased risk of *Vibrio* spp. disease under a changing future climate. Furthermore, the spatial extent of Baltic Sea waters favourable for *Vibrio* spp. growth is predicted to double from 140,000 km^2 in July 2015 to 309,966 km^2 in July 2050 under the RCP 4.5 climate change scenario; or to 317,793 km^2 in July 2050 under RCP 8.5 (Semenza et al., 2017).

Notably, since 2014, Sweden has reported a new record number of annual *Vibrio* spp. infections with 135 cases reported in 2018 (see Figure 2.5); a year of extreme heat for Europe, especially Scandinavia (Herring et al., 2020). Across Norway, Sweden, Finland, Denmark, Poland and Estonia, 445 vibriosis cases were reported in 2018, surpassing the previous record of 272 total cases reported in 2014 (Amato et al., 2022). Recent work demonstrates a strong significant correlation (r = 0.95) of average annual seawater temperature and annual total *Vibrio* spp. cases reported in Denmark (Gildas Hounmanou et al., 2023).

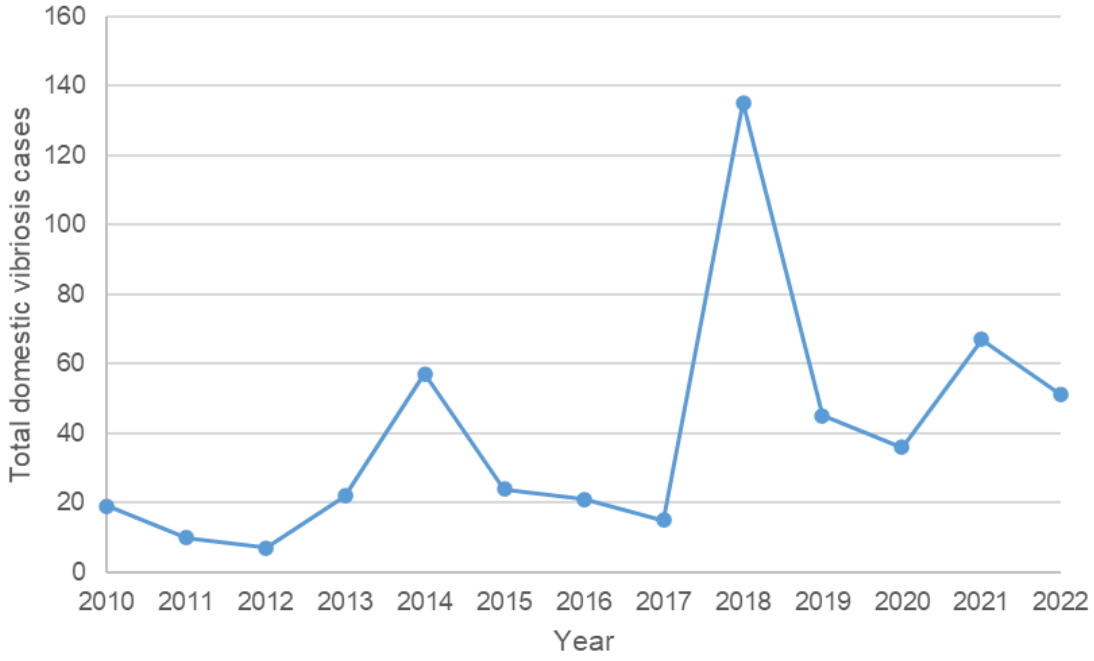

Figure 2.5 Annual totals of domestically acquired vibriosis cases in Sweden during years 2010-2022. Created with data from the Public Health Agency of Sweden (Public Health Agency of Sweden, 2023, 2019)**.**

2.8 Socioeconomic impacts of changing *Vibrio* spp. disease

2.8.1 Economic impacts on tourism

Tourism often provides coastal communities with a substantial proportion of their economic gain (Ghosh, 2012). A study by (Czajkowski et al., 2015), estimates the economic benefits from recreational activity within Baltic Sea region at 15 billion euros per year. This same study identifies that degradation of the Baltic's marine environment may lead to annual losses of 1-2 billion euros due to a reduction in citizens' perceived value of this region, and thus reduced likelihood of recreational use. Therefore, potential negative associations of a geographic area with *Vibrio* spp. may dramatically reduce tourism and result in harmful economic impacts to the detriment of coastal towns and cities around the world affected by these pathogens. This could be particularly relevant for associations with *V. vulnificus* infections, as this pathogen is colloquially referred to as "flesh-eating" in the media (e.g., Hassan, 2022).

Increased public awareness of rising *Vibrio* spp. incidence rates and shellfish harvesting closures could also have negative implications for local seafood industries (Anderson and Plummer, 2017; Luk et al., 2019). The comparatively low carbon footprint of shellfish to other protein sources (Nijdam et al., 2012) indicates their value as an important sustainable resource. However, failure to cook thoroughly, or raw ingestion, increases risk of *Vibrio* spp. infection. Association of illness with local fisheries may damage their reputation and consequent in economic loss which could also negatively impact the mental health of these communities (Sheahan et al., 2022). This could be especially detrimental due to the coincidence of the summer tourism season and peak conditions for *Vibrio* spp. growth and abundance.

2.8.2 Healthcare costs

Health-related costs resulting from *Vibrio* spp. infection include those directly incurred from doctor appointments, antibiotic treatments and hospitalisation, whilst indirect costs are also associated with inability to work during illness. Given the rising rates of *Vibrio* spp. infections (Baker-Austin et al., 2010; Newton et al., 2012), increases in the economic burden of this disease are expected. It is especially important to consider the burden of increasing cases of *V. vulnificus*; the severity of these infections makes them

particularly costly due to high rates of hospitalisation, often involving high-cost intensive care units (Seidel et al., 2006), and death. An analysis by Sheahan et al. (2022) estimates that in 2018 vibriosis cost the US $2.2 billion when accounting for medical care, productivity losses due to time off work and premature death. By 2090, these infections could cost the US between $5.2 billion - $7.3 billion each year, depending on global greenhouse gas emissions (Sheahan et al., 2022). Higher emissions are expected to have a stronger positive influence on SSTs which would likely lead to greater numbers of cases and therefore higher cost (Sheahan et al., 2022).

The economic impacts mentioned may be concentrated spatially and temporally, because of the seasonality of infections (Baker-Austin et al., 2013) and localised suitability of conditions for *Vibrio* spp. growth. Rising cases of infection will likely intensify pressure on public health services – some of which may already be stressed by the impacts of escalating ageing populations (United Nations, Department of Economic and Social Affairs, 2015) and increasingly frequent heatwave periods (Hoegh-Guldberg et al., 2018).

2.9 Mitigation of *Vibrio* spp. infections

The sensitivity of *Vibrio* spp. abundance to temperature indicates these marine bacteria represent a rapidly changing hazard (Baker-Austin et al., 2017). Infections can be fatal, especially amongst the most vulnerable (Oliver, 2005c), therefore, it is important that steps are taken to minimise *Vibrio* spp. disease risk.

One key element in mitigation is ascertaining when *Vibrio* spp. concentrations are at their highest. This can be conducted either through direct water sampling for bacterial enumeration (Gyraite et al., 2020) or growth risk models based on climatic data. One example is the European Centre for Disease Control and Prevention (ECDC) *Vibrio* Map Viewer, which enables real-time monitoring of *Vibrio* spp. growth risk as well as generation of a 5-day risk forecast based on SST and salinity in the Baltic Sea (ECDC, 2016). This forecast is examined weekly by the ECDC who publish their observations within Communicable Disease Threat Reports (CDTR); such information can be evaluated by public health authorities, who then decide whether further action is required (Semenza et al., 2017). Communication of increased *Vibrio* spp. risk may take the form of public alerts, educating immunocompromised persons of elevated exposure risk, warning signs or beach closures (Semenza et al., 2017). By further developing predictive models of *Vibrio* spp. disease, risks to human health can be more reliably evaluated,

allowing clear guidance to be relayed to the public which can limit exposure, thus potentially reducing the burden of *Vibrio* spp. disease on human health.

However, monitoring *Vibrio* spp. case data for recent reports and issuing alerts in response is another strategy. In September 2023 the US CDC issued a Health Alert Network (HAN) advisory to increase awareness of recent serious and fatal *V. vulnificus* infections that had been reported on the Atlantic coast (CDC, 2023). The HAN advisory encouraged healthcare workers to consider *V. vulnificus* as a potential cause of wound infections where exposure to seawater has occurred, as well as urging them to share guidance and news of the recent reports across departments and laboratories (CDC, 2023). Specifically, due to the rapidity of disease progression, clinicians are advised not to wait for laboratory confirmation of a suspected *V. vulnificus* infection before starting a patient's treatment including antibiotic therapy and surgical tissue removal. Guidance from the CDC to the public includes to not enter seawater or brackish water with an open cut and to wash any cuts that have been exposed to seawater, brackish water or raw seafood with soap and water immediately (CDC, 2023).

In addition to measures which limit exposure through water-related activities, it is important to consider methods which reduce *Vibrio* spp. risk from seafood consumption. The CDC recommend that raw oysters and other shellfish should be cooked thoroughly before eating (CDC, 2023). The closure of waters to shellfish harvesting has proved an effective tactic to control the progression of foodborne *Vibrio* spp. outbreaks, for example, the 1997 outbreak of *V. parahaemolyticus* within the US Pacific Northwest (CDC, 1998). However, frequent repetition of this approach may result in significant negative economic impacts for shellfishery owners and their workers. In light of this, research efforts are now focused on establishing post-harvest purification treatments which can reduce *Vibrio* spp. densities with minimal impact on the quality of the seafood product. Processes being tested for use on oysters include: UV-sterilized seawater depuration (Phuvasate et al., 2012), irradiation (Andrews et al., 2003), low temperature pasteurization (Andrews et al., 2000), high hydrostatic pressure (Kural and Chen, 2008), flash freezing with frozen storage (Liu et al., 2009), chlorine dioxide treatment (Wang et al., 2010) and bacteriophage application (Rong et al., 2014; Zhang et al., 2018).

Knowledge gained from the management of similar hazards, such as harmful algal blooms (HABs) could be utilised to inform the development of mitigation strategies regarding *Vibrio* spp. risk. Berdalet et al. (2015) describe the importance of clear scientific communication of human health risks regarding HABs in the context of coastal tourism and the fishing industry. Lack of uniform understanding of HAB risk amongst

affected communities can lead to the ‘halo effect’ whereby human activities within that location, unrelated to HAB risk, are reduced or halted (Berdalet et al., 2015). For example, consumption of all forms of seafood is reduced, despite bivalves presenting particularly high risk by concentrating HAB biotoxins (Berdalet et al., 2015).

3 Climate warming and increasing *Vibrio vulnificus* infections in North America

3.1 Abstract

Vibrio vulnificus is an opportunistic bacterial pathogen, occurring in warm low-salinity waters. *V. vulnificus* wound infections due to seawater exposure are infrequent but mortality rates are high (~18%). Seawater bacterial concentrations are increasing but changing disease pattern assessments or climate change projections are rare. Here, using a 30-year database of *V. vulnificus* cases for the Eastern USA, changing disease distribution was assessed. An ecological niche model was developed, trained and validated to identify links to oceanographic and climate data. This model was used to predict future disease distribution using data simulated by seven Global Climate Models (GCMs) which belong to the newest Coupled Model Intercomparison Project (CMIP6). Risk was estimated by calculating the total population within 200km of the disease distribution. Predictions were generated for different "pathways" of global socioeconomic development which incorporate projections of greenhouse gas emissions and demographic change. In Eastern USA between 1988 and 2018, *V. vulnificus* wound infections increased 8-fold (10-80 cases p.a.) and the northern case limit shifted northwards 48km p.a. By 2041-2060, *V. vulnificus* infections may expand their current range to encompass major population centres around New York (40.7^{o}N). Combined with a growing and increasingly elderly population, annual case numbers may double. By 2081-2100 *V. vulnificus* infections may be present in every Eastern USA State under medium-to-high future emissions and warming. The projected expansion of *V. vulnificus* wound infections stresses the need for increased individual and public health awareness in these areas.

3.2 Introduction

Greenhouse gas emissions from human activity are changing our climate (IPCC, 2021). The global mean temperature has risen 1.2°C since the pre-industrial period (World Meteorological Organisation, 2021). Despite the aim of the Paris Climate Agreement to limit this increase in global average temperature to "well below two degrees" (United Nations, 2016), 1.5°C of warming may occur by the early 2030s (IPCC, 2021).

Impacts may be especially acute on the world's coastlines which provide a major interface between natural ecosystems and human populations and are a particular source of human disease. Vibrios are naturally occurring and commonly found Gram-negative bacteria in marine waters, which thrive in warm, brackish water and are highly sensitive to temperature (Vezzulli et al., 2013). These associations with climate have led to *Vibrio* species being collectively recognised as a "microbial barometer of climate change" (Baker-Austin et al., 2017). Despite being endemic to subtropical regions (e.g. south-eastern USA (King et al., 2019)), *Vibrio* spp. infections have recently emerged at higher latitudes such as Delaware Bay, USA (King et al., 2019) and the Baltic Sea (Baker-Austin et al., 2013). The latter geographical shift has been formally attributed to climate change (Ebi et al., 2017). Recent modelling studies indicate that climate change will increase the suitability and distribution of pathogenic *Vibrio* species, particularly at high latitudes (Trinanes and Martinez-Urtaza, 2021).

Of particular concern is *V. vulnificus* infection which can occur from exposure to seawater through small skin lesions (Baker-Austin and Oliver, 2016) and can quickly turn necrotic, requiring urgent surgical tissue removal or limb amputation in around 10% of cases (Dechet et al., 2008). *V. vulnificus* is the most pathogenic of the *Vibrio* genus: wound infection mortality rates are as high as 18% (Ralston et al., 2011) and fatalities have occurred as soon as 48 hours following exposure (Baker-Austin and Oliver, 2016). Alongside causing around 100 cases annually in the USA (Brumfield et al., 2021), the economic burden of *V. vulnificus* wound infections is estimated at over US$ 28 million/year (Ralston et al., 2011). When also considering the economic burden of foodborne cases (USDA, 2020), overall annual costs associated with this pathogen are estimated at over US$ 360 million, making it the most expensive marine pathogen in the USA to treat.

Despite a changing *V. vulnificus* infection distribution, there are few attempts to quantify this change, or to map the likely climate change effects. This is due to the lack of high-

quality epidemiological data. Some studies have made future *Vibrio* spp. risk predictions based on the projected distribution of ideal environmental conditions (e.g., Trinanes and Martinez-Urtaza, (2021)) but these predictions indicate the probable presence of *Vibrio* spp. bacteria rather than disease risk (Brumfield et al., 2021).

Here, we produce a systematic assessment of the changing distribution of *V. vulnificus* infections along the east USA coast using a unique 30-year *V. vulnificus* infection database. The study area includes the USA Gulf Coast, a global hotspot for *V. vulnificus* infection (Huang et al., 2016), and the Atlantic coastline where reported *V. vulnificus* infections are increasingly common (King et al., 2019). We then explore the influence of climate change upon the spatial distribution of *V. vulnificus* wound infections using an Ecological Niche Model (ENM), a common tool for predicting species distribution based upon biogeographic variables and increasingly used for modelling disease transmission (Johnson et al., 2019).

Future changes to the *V. vulnificus* wound infection distribution were predicted using the ENM and future data simulated by seven Global Climate Models (GCMs) which belong to the newest Coupled Model Intercomparison Project (CMIP6) (Eyring et al., 2016). These GCM projections were available for different Shared Socioeconomic Pathways (SSPs) which enabled the influence of climate change in the *V. vulnificus* distribution to be assessed. SSPs offer an update to the previous Representative Concentration Pathways as they combine different socioeconomic "narratives", which shape trends including economic growth, population change and urbanisation with corresponding levels of greenhouse gas emissions by the end of the 21st century (O'Neill et al., 2014; "The CMIP6 landscape," 2019). We focus on scenarios SSP1-2.6 which is set against the SSP1 narrative of "sustainability" and is a low emissions scenario, and SSP3-7.0, which is set against the SSP3 socioeconomic backdrop of "regional rivalry" (Riahi et al., 2017) where resurgent nationalism and regional conflicts shift focus away from climate mitigation leading to medium-to-high emissions. These are referred to hereafter as SSP126 and SSP370. Analysis was based upon climate data (temperature and precipitation) obtained from seven GCMs and oceanographic data (sea surface temperature and salinity) for one GCM (see Methods and Table S1 for GCM references).

3.3 Methods

3.3.1 *Vibrio vulnificus* data

Since 1988 the CDC has maintained the Cholera and Other *Vibrio* Illness Surveillance database (COVIS) for the reporting of human cases of vibriosis and cholera. Laboratory-confirmed cases of *V. vulnificus*, where the transmission route was confirmed as non-foodborne, foreign travel was not reported, and the patient did not live in the Pacific Region of the US (or travel outside this Region) were extracted (1375 cases) for the years 1988-2018. For a few cases (69) a symptom date was not present, but in all but 3 cases one was generated by applying the modal lag between cases where a symptom date and specimen date were present.

An accurate location of exposure is important, and for most cases this was based on the city/county where the individual lived or travelled to in the days preceding symptoms. Cases were excluded (128) where the home/travel location was coarser than city/county. A further 75 cases were excluded as the home/travel location was further than 200km from the coast (>2-hour drive), introducing uncertainty into location of exposure which is predominantly coastal. The analysis proceeded with 1169 cases (85% of total) which were matched to their nearest coastline. Equivalent *V. vulnificus* data from Canada were unavailable, and an absence of case reports in the literature strongly suggests negligeable incidence.

3.3.2 Baseline oceanographic, climate and climate change projection data

V. vulnificus is known to be affected by both sea surface temperature (SST) and seawater salinity. Gridded historical and future data sets of SST (°C) and salinity (PSU) were downloaded for the Alfred Wegener Institute Climate Model (AWI-CM-1-1-MR) at a spatial resolution of 25km (Semmler et al., 2018). Historical data were downloaded between 2007 and 2014 (data were not available beyond 2014). Future data were downloaded for the years 2018 – 2100 under SSP126, SSP245, SSP370 and SSP585. For baseline and all future time periods (2021-2040, 2041-2060, 2061-2080 and 2081-2100) the mean monthly temperature for each month during the period of interest was calculated. The mean and maximum salinity and mean and maximum SST were then calculated from these 12 values.

Meteorological conditions such as air temperature and precipitation not only influence SST and salinity (SST and air temperature are highly correlated (Feng et al., 2018; Galbraith et al., 2012)) but can also affect human behaviour and hence exposure to *V. vulnificus*. They are also known to influence coastal recreational behaviour (Elliott et al., 2019). Crucially they are available at finer grid resolutions. For baseline conditions, gridded historical monthly maximum air temperature (°C) and monthly total precipitation (mm) were obtained from the WorldClim database (https://www.worldclim.org/) for the years 2007 to 2018. The air temperature data (Harris et al., 2014) which has been bias corrected using WorldClim 2.1 (Fick and Hijmans, 2017) to a spatial resolution of 2.5 arcminutes (~4.6km), represents monthly means of the daily maximum air temperatures. Future maximum air temperature (°C) and total precipitation (mm) were obtained from the WorldClim 'Future Climate' dataset which had been downscaled and bias-corrected with the same WorldClim 2.1 baseline. These data were available for four future 20-year time periods under four SSPs as gridded monthly averages across each 20-year period for January to December, respectively. Individual data were obtained for seven GCMs (BCC-CSM2-MR, CNRM-CM6-1, CNRM-ESM2-1, CanESM5, IPSL-CM6A-LR, MIROC-ES2L, MIROC6) downscaled at a spatial resolution of 2.5 arcminutes (~4.6km) (see Table S1 for GCM references).

To ensure the compatibility of historical and future temperature data, monthly averages of maximum air temperature were calculated for each calendar month across the 11-year historical period of 2007 to 2018. Therefore, each grid cell contained 12 values (one average value per calendar month) for the historical period and 12 for a given future time period.

From the air temperature data tmean was calculated as the average of 12 monthly values for each time period. The maximum of these values was also calculated (tmax). Using the monthly total precipitation, mean precipitation, and maximum precipitation variables were also calculated in the same way.

3.3.3 Historic and future population scenario data

Baseline population at risk and age distribution was calculated using 2010 subsets of Gridded Population of the World, Version 4: Population Count and Gridded Population of the World, Version 4: Basic Demographic Characteristics, respectively (Center for International Earth Science Information Network - CIESIN - Columbia University, 2018a, 2018b), at a resolution of 2.5 arcminutes (~4.6km). These data were subdivided into 20-year age categories (0-19, 20-39, 40-59, 60 and older).

SSP-specific future population data were obtained at the same spatial resolution as annual projections (Jones and O'Neill, 2016). These data were subdivided into age categories using SSP-specific future U.S. County-Level Population Projections (Hauer and Center for International Earth Science Information Network - CIESIN - Columbia University, 2021).

3.3.4 Changing distribution

To assess whether the geographical distribution of cases has shifted over time, the mean latitude, 5th percentile (southern extent) and 95th percentile of latitude (northern extent) was calculated for the dataset in annual time steps. These data were plotted and trends assessed.

3.3.5 Model specification and creation

The current spatial distribution of *V. vulnificus* cases (presence:absence) was calculated using cases from 2007 onwards (n=709) to ensure a contemporary distribution and because *V. vulnificus* became notifiable in 2007 (therefore there was potential for earlier cases to be unreported). The northern extent of the distribution was set as the 95th percentile latitude of cases (39.93°N adjacent to Philadelphia). The distribution was assumed to extend southwards along the US coastline to the Mexican border (25.95ºN; cases were reported along the entire coastline to this border; Figure 3.1), as results indicated no change in the southern extent and *V. vulnificus* has been isolated in shellfish throughout the Gulf of Mexico. The coastline absent of *V. vulnificus* infections was defined as northwards from 39.93°N to the northernmost point of Newfoundland and Labrador located (60.35°N). Grid cells directly intersecting the coastline were used to define presence:absence locations (oceanographic data, SST and salinity, 318 presence cells, 596 absence cells; climate data, air temperature and precipitation, 2990 presence cells, 5252 absence cells).

The creation of each model was based upon cells along the coast that were labelled as present/absent for *V. vulnificus*. The oceanographic (SST and salinity) and climate (air temperature and precipitation) data were assigned to each cell. Models were generated using oceanographic and climate data. For each model, the proportion of presence:absence points was kept constant and 10% of the data were set aside for model validation whilst the remaining 90% were carried forward for model creation and testing. From this remaining 90% of the data, 100 random samples were obtained which contained all the presence points and an identical number of randomly selected absence

points to ensure that the models were not biased towards predicting either presence or absence. Each of the 100 random samples of data were split 70:30 into training and testing subsets whilst maintaining a 50:50 ratio of presence:absence points in both training and testing subsets. Binomial logistic regression models of *V. vulnificus* presence-absence were fitted using 10-fold cross validation on each of the 100 training subsets using a Generalised Linear Model (GLM) method within the package 'caret' (Kuhn, 2021) in R version 4.0.2 (R Core Team, 2021). Model predictive power was measured using the mean AUC calculated for each of the 100 model replicates on the corresponding testing subsets using R package 'pROC' (Robin et al., 2011). Multiple variations of oceanographic and climate variables were fitted as univariate models, and each was tested to check that the assumption of linearity between the predictor variable and logit of the outcome had been met. All coefficients and metrics of model performance were averaged over the 100 replicates. Each model produced this way (i.e., as an average of the 100 replicates) was used to predict on the corresponding 10% validation dataset which had been held out of the model creation process for each variable tested. A further AUC was generated to check the ability of the model to predict on unseen data, this is referred to as the 'Validation AUC'.

3.3.6 Distribution maps

After the final models were selected, predictors from the historical data set and from every future SSP / time period combination were passed through the model to produce estimates of current and future *V. vulnificus* distribution. For the future time period the output from all 7 GCMs were averaged to generate a multi-model mean prediction of the future distribution. The model outputs were the probability of *V. vulnificus* wound infection presence and these probabilities were converted into a binary map using the 'PresenceAbsence' package (Moisen and Freeman, 2008) in R version 4.0.2 (R Core Team, 2021). This package translates probability of occurrence into a binary (presence:absence) parameter based on a given 'Required Sensitivity'. A required sensitivity of 0.85 (ReqSens85) was chosen to ensure that that no more than 15% of risk locations were missed whilst maintaining the highest degree of specificity possible. The ReqSens85 threshold meant that probabilities greater than or equal to 0.999 were classified as presence and probabilities below 0.999 as absences. A lower Required Sensitivity threshold was not applied as *V. vulnificus* is a rare infection and it is important not to misidentify true locations as absences (Freeman and Moisen, 2008). Modifying this parameter made negligeable difference to the distribution due to the strong predictive power of the chosen models (tmean AUC 0.999, tmax AUC 0.998).

3.3.7 Coastlines, population at risk and projected cases

The sum of the coastline length within climate cells where presence was calculated for each SSP scenario and future time period. The population at risk of *V. vulnificus* infection was determined as the sum of the population that reside within a 200km buffer surrounding these coastal cells and clipped to the maximum latitude of predicted risk (to be consistent with the method used to assign cases to coastal locations). To estimate likely cases, the current case rates by 20-year age bands (0-19, 20-39, 40-59, 60 and older) were calculated using age data within COVIS. These rates were multiplied by the age profile in the risk zone (200km buffer surrounding coastline where *V. vulnificus* infections are present) to estimate likely baseline and future cases.

3.4 Results

3.4.1 Changing incidence and distribution of *V. vulnificus* infections

The historical distribution of *V. vulnificus* infections between 2007-2018 is presented in Figure 3.1. This presents all cases where either the home or travel location was reported within 200 km of the eastern USA coastline. Cases were reported from the Mexican border along the entire coast of the USA to Maine. The total reported *V. vulnificus* cases has increased, from around 10 p.a. in 1988 to around 80 p.a. by 2018. Figure 3.2 presents the latitudinal distribution of *V. vulnificus* cases by year and shows that the 5th percentile of latitude (henceforth southern extent) of cases has remained constant at the Mexican border and not shifted northwards (linear trend $p=0.237$), whereas the mean case latitude has moved northward at 0.13^{o} (~15 km) p.a. (linear trend $p<0.001$). The 95th latitude percentile (henceforth northern extent) of *V. vulnificus* cases has extended northwards at 0.43^{o} (~48 km) p.a. (linear trend $p<0.001$). On Figure 3.2 the non-linear progression of the northern extent is likely a consequence of cases of this low probability disease only occurring when reaching high population density areas (e.g., Virginia, Maryland see Figure 3.1).

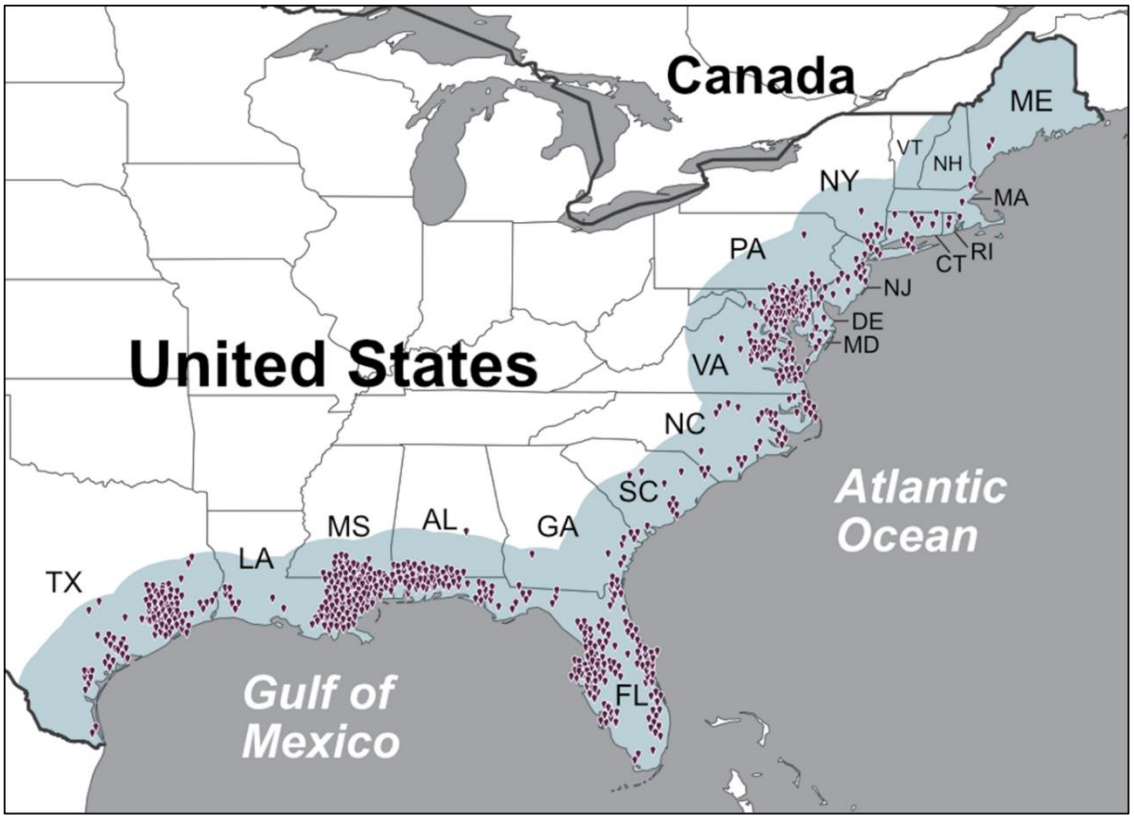

Figure 3.1 Original locations of the 709 confirmed non-foodborne *V. vulnificus* infections reported to the Cholera and Other *Vibrio* Illness Surveillance (COVIS) database between 2007 and 2018 within 200 km of the east USA coastline (blue shading).

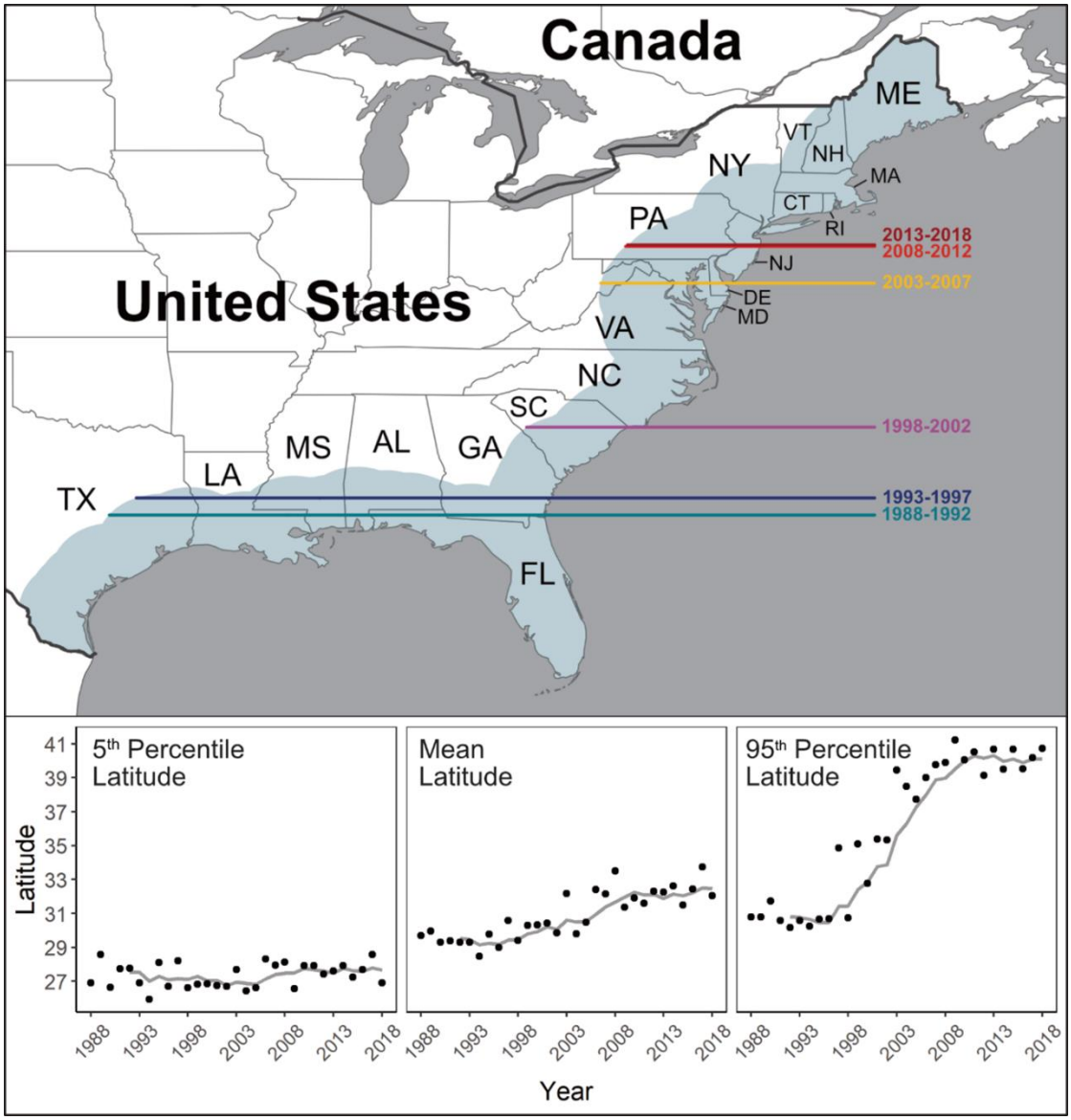

Figure 3.2 Latitudinal shifts by year of confirmed non-foodborne *V. vulnificus* infections in the USA reported to the Cholera and Other *Vibrio* Illness Surveillance (COVIS) between 1988 – 2018. The 95th latitude percentile in 5-year bands is presented in the upper panel. The lower panel presents the 5th percentile, mean and 95th latitude percentile for individual years alongside 5-year rolling means.

Binary logistic regression models of the *V. vulnificus* infection distribution (presence-absence between the Mexican border and northern extent) were fitted using 10-fold cross validation on 100 data subsets using generalised linear models (see Methods). Both mean air temperature (tmean) and maximum air temperature (tmax) were individually statistically significant ($p<0.001$) with a high area under the receiver operator characteristic curve (AUC; 0.999 and 0.998, respectively) and high validation AUCs (0.999 and 0.997, respectively) indicating good predictive accuracy for *V. vulnificus* infection presence. Mean precipitation and maximum precipitation were also significant ($p<0.001$) but each had a lower AUC (0.833 and 0.687). Sea surface temperature and salinity were considered but the coarse dataset resolution (25 by 25km vs 5 by 5km for air temperature and precipitation) meant that they were unable to capture conditions close to the coast (where there can be sharp gradients particularly in salinity near to estuaries) especially as the effective resolution (i.e., including density of the underlying salinity observations) may be coarser. For example for every coastal grid cell (25 x 25km) in the study area for every month, salinity values were never in the suitable range for *V. vulnificus* (2-25 practical salinity units (PSU) (Baker-Austin et al., 2018)) (see Figure S1), yet *V. vulnificus* infections are present in all these states (Figure 3.1). This indicates that the true salinity of these near-shore waters is within the ideal range for *V. vulnificus*, but we are unable to observe the true salinity values due the coarse resolution of these data. This resulted in poor statistical relationships with *V. vulnificus*. Model fit was not improved by multivariable models hence the two models with the highest AUC were selected (i.e., tmean and tmax), to represent different temperature variations. These models were used to predict the *V. vulnificus* infection distribution into the future, using air temperature projections from seven GCMs.

3.4.2 Future Distribution and Incidence of *V. vulnificus* Infections

Projections are presented as maps of infection distribution, length of coastline within this distribution, population at risk within 200km of the distribution and estimated annual case numbers. Results were produced for multiple time periods (2021-2040, 2041-2060, 2061-2080, 2081-2100) and SSPs (SSP126, SSP245, SSP370, SSP585). We focus on SSP126 and SSP370 to represent a range of likely socioeconomic trends and greenhouse gas emissions (Hausfather and Peters, 2020). We focus on 2041-2060 and 2081-2100 to make our projection periods comparable with other impact modelling groups (e.g., The Inter-Sectoral Impact Model Intercomparison Project [ISIMIP]

(Warszawski et al., 2014)). Results for other SSPs and time periods are found in Supplementary Information (Table S2-S3 and Figures S2-S9).

Tmean and tmax were the strongest predictors of infection distribution, and projections of future distribution from both are compared in Figure 3.3 and Figure 3.4. Projections were produced for both tmean and tmax to evaluate how sensitive the projections are to predictor choice. Baseline predictions are almost identical to the current distribution (Figure 3.2), with the upper limit around Philadelphia (40.0°N). Under both SSP126 and SSP370, the tmean model (Figure 3.3) predicts a northward expansion of *V. vulnificus* infection distribution to New Jersey (40.0ºN) and southern New York state (40.9ºN) by 2041-2060. Under SSP126, the projected distribution changes little from 2041-2060 to 2081-2100. Under SSP370 the distribution extends northwards to include the Connecticut (41.3ºN), New Hampshire (43.0ºN) and southern Maine (43.3ºN) coastlines.

Under the tmax model (Figure 3.4) by 2041-2060 SSP126 and SSP370 the *V. vulnificus* infection distribution extends further northward into Connecticut (41.3ºN) and as far north as Boston, Massachusetts (42.4°N). By 2081-2100, there is a notable between-scenario difference with little further change in the distribution under SSP126 but an expansion towards the southern Maine coastline (43.3°N) under SSP370. Under SSP370, the distribution of *V. vulnificus* infections encompasses every Eastern USA coastal state by 2081-2100. Figure 3.5 presents the length of coastline within the infection distribution and population at risk for every SSP and time period. SSPs incorporate changes in climate and changes in population. Table 3.1 focusses on SSP126 and SSP370 for 2041-2060, and 2081-2100 and indicates that *V. vulnificus* infections are currently present along ~10,000km of the eastern USA coastline. Tmax produced a lower baseline of infection distribution estimate than tmean (9,000 vs 10,000km). In the near future (i.e., 2021 – 2040), the length of the coastline where infections are present increases to between 10,800km and 10,900km under all scenarios. After this increase, the coastline lengths where infections are present diverges depending upon SSP. By 2041-2060, *V. vulnificus* infections may be present along ~11,100km (SSP126) to ~11,500km (SSP585) of USA coastline. However, far future predictions indicate a ~2,100km difference in coastline where infections are present between SSP126 and SSP585. Under SSP585, the tmax model (2081-2100) indicates 14,400km of coastline where infections are present and stretches as far North as the St Lawrence River. However, this is an unlikely worst-case scenario that is at odds with increasing clean energy use (Hausfather and Peters, 2020).

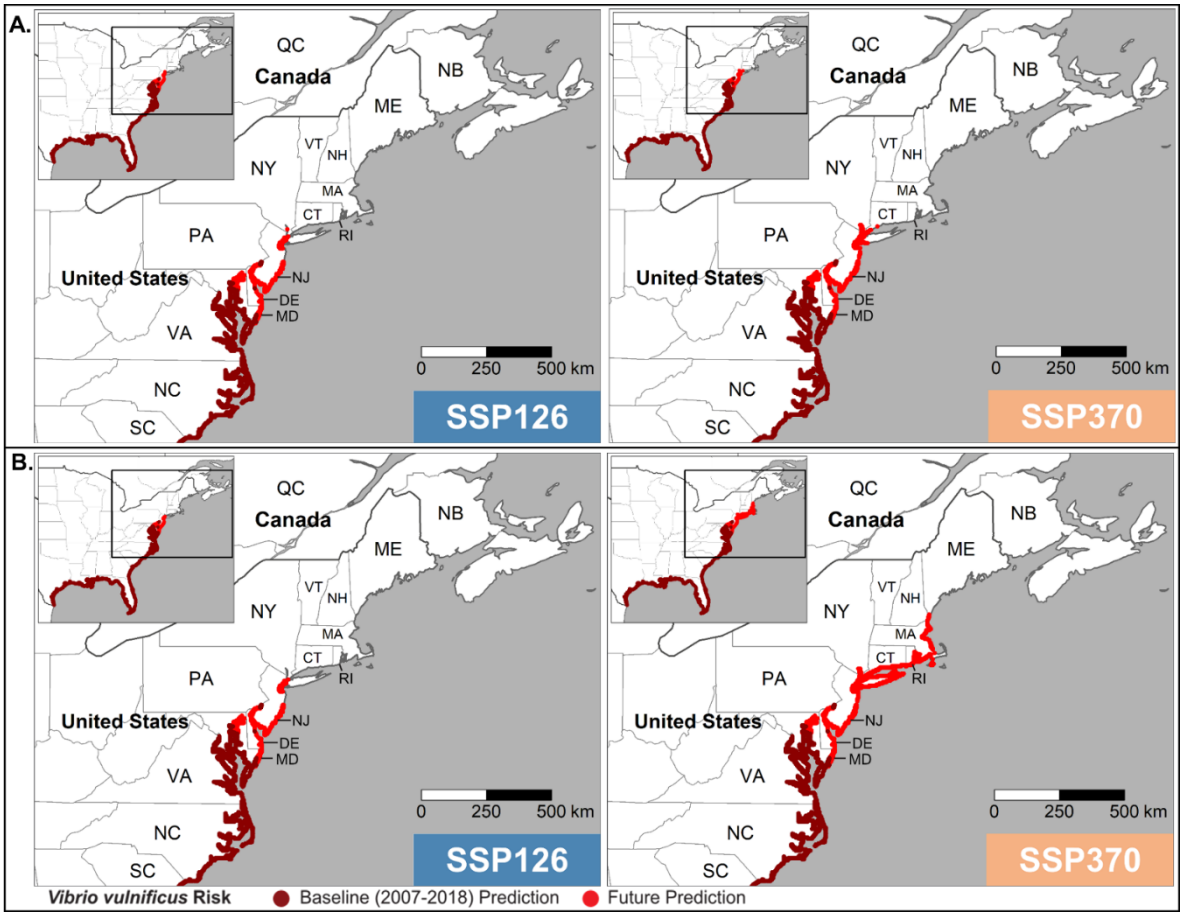

Figure 3.3 Baseline and projected *V. vulnificus* infection distribution (presence) predicted using tmean and then averaged across seven CMIP6 global climate models for A. 2041 – 2060 and B. 2081 – 2100 under CMIP6 SSP126 and SSP370.

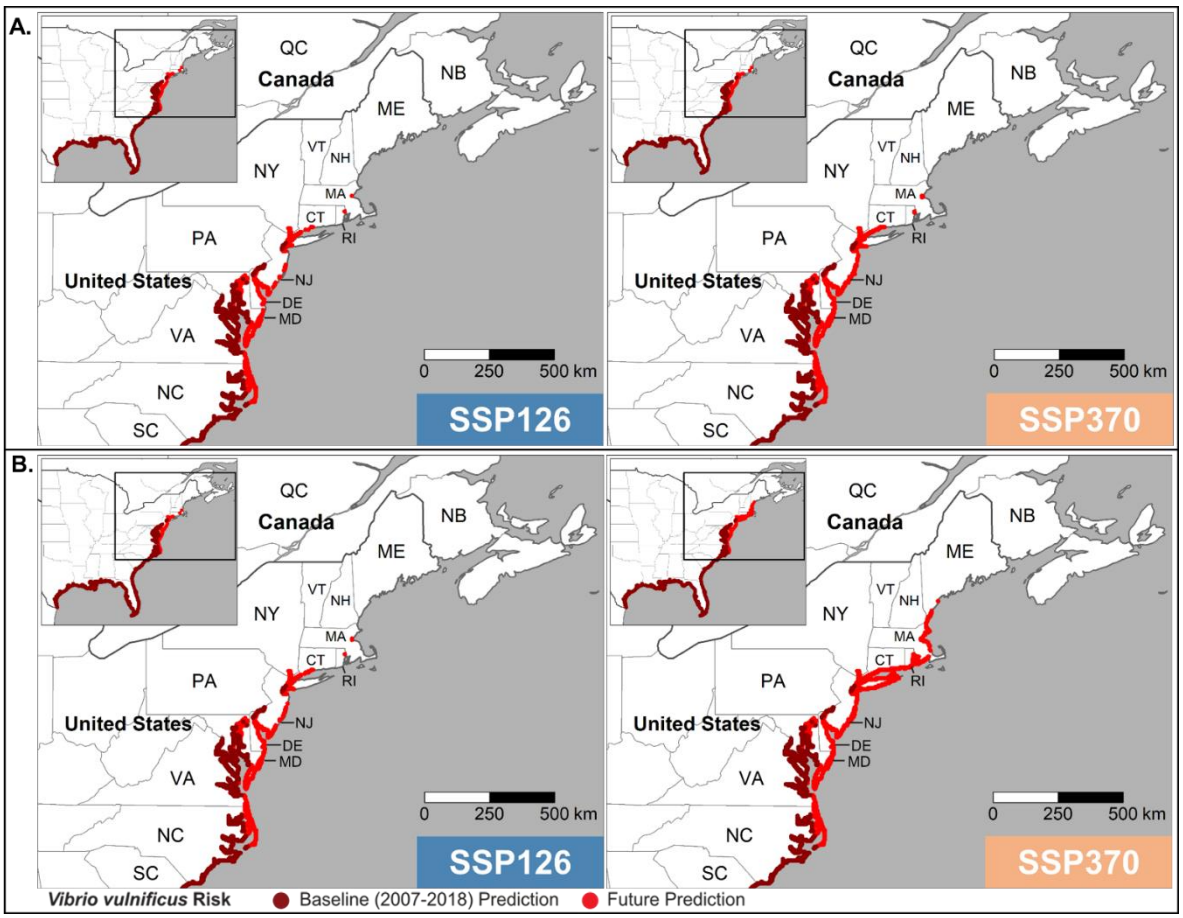

Figure 3.4 As Figure 3.3 but predicted using tmax.

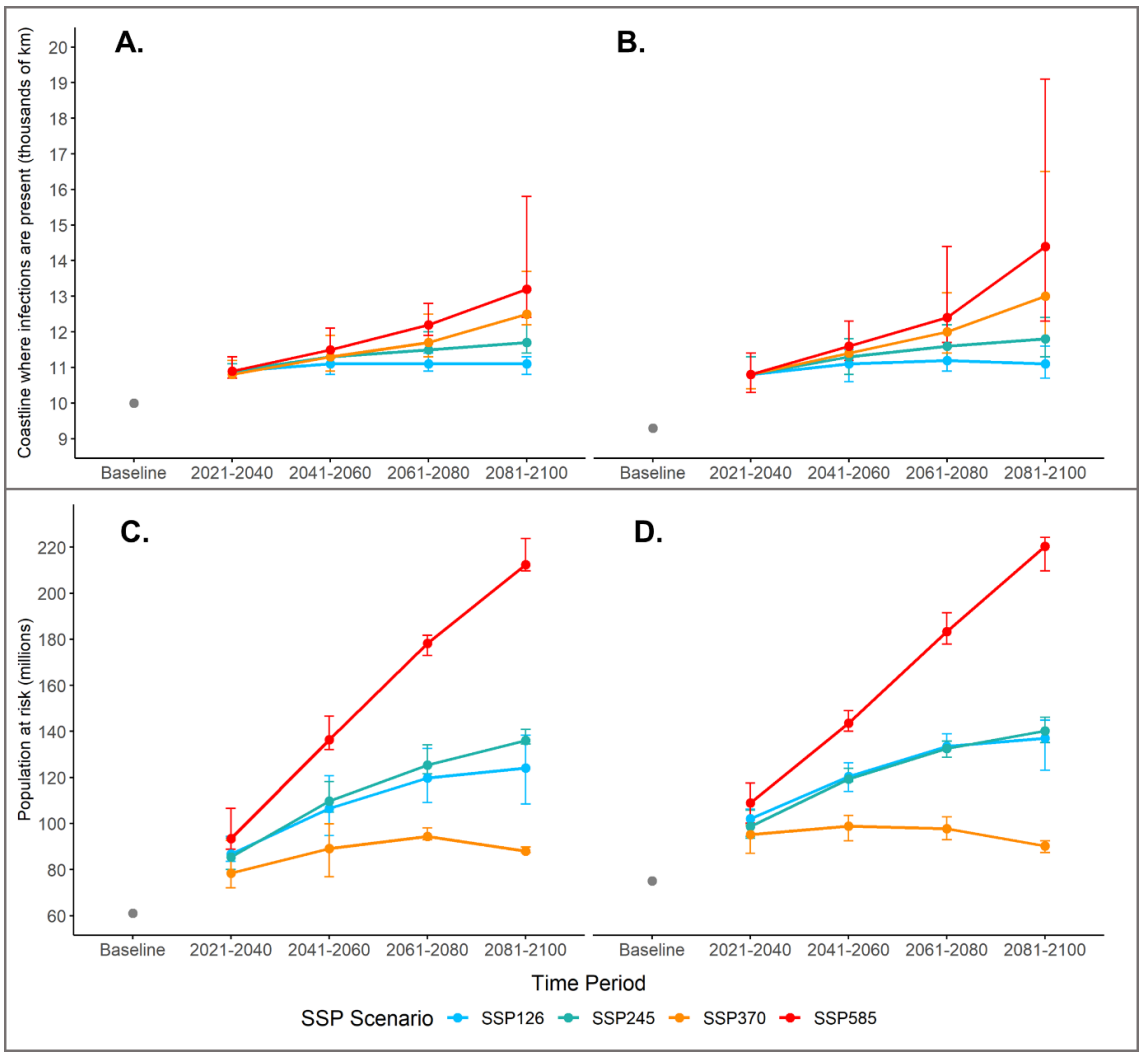

Figure 3.5 Length of the coastline where *V. vulnificus* infections are present (thousands of km) for the tmean (A) and tmax model (B). Total population at risk (millions) for the tmean (C) and tmax model (D). Future values represent an average across seven CMIP6 global climate models (GCMs). Error bars represent the highest and lowest estimate from individual GCM predictions.

Table 3.1 Length of coastline where *V. vulnificus* infections are present (thousand km) population at risk (millions), percentage of population aged ≥ 60 and estimated annual number of *V. vulnificus* cases under CMIP6 Shared Socioeconomic Pathways SSP126 and SSP370. Values are the ensemble mean from seven global climate models and the minimum and maximum estimates are given in square brackets.

Scenario	Time Period	Coastline where infections are present (thousands of km)	Total projected population at risk (millions)	Percentage of projected population at risk aged ≥60 years (%)	Estimated annual total number of cases
tmean model					
Baseline	**2007 – 2018**	10.0	61.0	16.9	61
SSP126	**2041-2060**	11.1 [10.8-11.3]	106.6 [94.8-120.7]	32.5 [32.7-32.4]	145 [130-164]
	2081-2100	11.1 [10.8-11.3]	124.1 [108.4-138.3]	43.1 [43.3-42.9]	204 [178-228]
SSP370	**2041-2060**	11.3 [10.9-11.9]	89.1 [76.9–99.9]	31.4 [31.5-31.3]	120 [104-135]
	2081-2100	12.5 [12.2-13.7]	88.0 [87.4-89.7]	41.1 [41.1-40.8]	141 [141-143]
tmax model					
Baseline	**2007 – 2018**	9.3	75.1	16.9	76
SSP126	**2041-2060**	11.1 [10.6-11.5]	120.5 [113.9-126.3]	32.4 [32.5-32.4]	164 [156-172]
	2081-2100	11.1 [10.7-11.6]	137.0 [123.2-144.8]	42.9 [43.1-42.9]	224 [202-237]
SSP370	**2041-2060**	11.4 [11.1-12.3]	98.9 [92.5-103.5]	31.3 [31.4-31.3]	133 [125-140]
	2081-2100	13.0 [11.8-16.5]	90.2 [87.4-92.5]	40.4 [41.1-39.6]	142 [141-144]

When the coastline where infections are present is combined with the SSP-specific population, the impacts diverge further between SSPs. These impacts combine climate change and population change. Under all SSPs there is a large increase in population at risk between the baseline and 2021-2040 as New York and nearby states become incorporated. By 2081-2100 the population at risk varies between ~90 million (SSP370) and ~210 million (SSP585). The tailing off of population at risk for many SSPs between 2041-2060 and 2081-2100 is notable. This is due to reductions in population associated with these SSPs (Jones and O'Neill, 2016) and for SSP370, this represents a reduction in the population at risk in spite of a larger coastline where *V. vulnificus* infections are present, due to a lower future population under SSP3, particularly in NE USA (Jiang et al., 2020).

Aged populations are more susceptible to *V. vulnificus* infections and when the projected population aged over 60 is calculated large increases in this age group are observed across all models from 17% at the baseline to 31% by 2041-2060, and over 40% by 2081-2100. When the estimated number of cases is calculated based upon current age specific case rates (20-year age bands) the results indicate a case doubling by 2041-2060 under most SSPs and models. By 2081-2100 cases increase again to more than 3 times baseline under SSP126. Under SSP370 by 2081-2100 there is a smaller increase over 2041-2060 numbers due to the smaller future population under this SSP. Currently the case fatality rate for *V. vulnificus* wound infections is around 18% (Ralston et al., 2011). The projections combine climate change and population change and in Table S4 these are replicated focussing on population change only (i.e., *V. vulnificus* distribution is held constant). For SSP126 around half the change in case numbers is associated with climate change and the other half population change. For SSP370 between 67% and 75% of the change is climate related.

3.5 Discussion

Our projections of *V. vulnificus* infection distribution and population at risk have multiple strengths. They are based upon one of the most detailed databases of *V. vulnificus* cases to date (Cholera and Other *Vibrio* Illness Surveillance [COVIS]; Newton et al. (2012)), which covers the Gulf and Atlantic USA coasts spanning 30 years (1988-2018). COVIS data trained and validated the models which were generated using 100 different samples of historical data and had strong predictive power. Each GCM produced similar *V.*

vulnificus infection distributions and uncertainty is presented as the range between different GCMs.

V. vulnificus is an increasingly recognized human pathogen with a low incidence but a high wound infection fatality rate of ~18% (Ralston et al., 2011). Here we show that in Eastern USA the total reported *V. vulnificus* cases have increased 8-fold between 1988 and 2018, accompanied by a profound geographical expansion. In the late 1980's infections were rare above Georgia (32^{o}N) but by 2018 were regularly reported as far north as Philadelphia (40^{o}N). On average the *V. vulnificus* infection distribution has been shifting northwards at ~48km p.a. Our analyses confirm studies which have documented *Vibrio* spp. infection emergence in new US locations (King et al., 2019). Between 1988 and 2016 there have been over 1100 wound infections reported in the USA with 159 associated fatalities, highlighting the significant yet underappreciated impact of this pathogen.

Our projections indicate that climate change will have a major effect on *V. vulnificus* infection distribution and number in Eastern USA, likely due to warming coastal waters favouring presence of bacteria and elevated temperatures leading to more coastal recreation. By 2041-2060 the coastline where *V. vulnificus* infections are present increases by over 1000km under both SSP126 and SSP370 and both tmean and tmax models. This shift increases the population at risk into the densely populated coastal regions of New Jersey and New York. Alongside population growth and an increasingly elderly population, this translates into a doubling of cases by 2041-2060.

By 2081-2100 the patterns increasingly diverge between SSPs. Under SSP126 the coastline where *V. vulnificus* infections are present remains relatively static but increases in the elderly population under this 'sustainability' scenario led to further increases in the projected population at risk and cases. Conversely, under SSP370, the coastline where *V. vulnificus* infections are present increases by another 1000km into southern Maine, to encompass every state along the Eastern USA coastline. However, this shift occurs into less densely populated areas, and within SSP370 there are population reductions under this 'regional rivalry' scenario. For context, the population within the current *V. vulnificus* disease distribution (see Figure 3.2), is projected to decrease by 9.3 million over the 21st Century under the SSP3 pathways (Table S4). The overall impacts under SSP370 are a small increase in the projected number of cases in comparison to 2041-2060. Under all SSPs and time periods, tmax gave a marginally greater increase in coastline where *V. vulnificus* infections are predicted compared to tmean.

The 4º shift in the northern coastline extent where *V. vulnificus* infections are present under SSP370 projected by 2080 (~0.06º p.a.) is slower than the rate observed between 1988-2018 (0.43º p.a.). Potential reasons include steeper latitude-temperature gradients at higher latitudes or few reported cases early in the observational period (1988-2018) in mid-latitudes. This is plausible due to the rare nature of a *V. vulnificus* illness intersecting an area of lower population (i.e., North and South Carolina, Figure 3.1).

Our work uses an ENM to evaluate *V. vulnificus* infection spread. The best model is based upon air temperature, a surrogate for both sea surface temperature (the two are strongly correlated (Feng et al., 2018; Galbraith et al., 2012)) and coastal recreation (Elliott et al., 2019). This approach contrasts to previous studies (Trinanes and Martinez-Urtaza, 2021) which focus on the ecological suitability for the *V. vulnificus* bacteria, which even if present, may not lead to human disease (van Zyl, 2022). Therefore, within our current and future *V. vulnificus* disease distribution there will be coastal areas where conditions are unsuitable for *V. vulnificus* bacteria. However, it is worth noting that despite this limitation, *V. vulnificus* infections currently occur along the USA coastline from Southern Texas to New Jersey (Figure 3.1). The current and future oceanographic data resolution (25 x 25km) is a particular challenge for coastal studies as the underlying observations are often poorly representative of near coastal conditions where *V. vulnificus* thrive and ultimately come into contact with the human population.

This work has uncertainties. Exposure case location was assumed as the nearest coastline to an individual's home/travel county, but case location was only used to define the current *V. vulnificus* distribution. Population at risk was based upon residents within 200km of the coast (~2-hour travel time), but different distance buffers could have been used. Projected cases were based upon current age-specific incidence rates, but these may change. The analysis used future downscaled climate data, bias corrected with current observational data, but future weather patterns may be different. We were unable to model changes to the *V. vulnificus* southern extent, but this bacterium has been isolated from oysters as far south as Tabasco (18.5°N) (Fernández-Rendón et al., 2019).

The northward *V. vulnificus* infection expansion stresses the need for increased individual and public health *V. vulnificus* awareness in these areas. This is crucial as prompt action when symptoms occur is necessary to prevent major health outcomes (Coerdt and Khachemoune, 2021). Individuals and health authorities could be warned in real time about particularly risky environmental conditions through marine (Frölicher and Laufkötter, 2018) or *Vibrio*-specific early warning systems (Semenza et al., 2017). Active control measures could include greater awareness programmes for at risk groups (e.g.,

the elderly, individuals with underlying conditions), and coastal signage during high-risk periods.

4 Environmental predictors of *Vibrio vulnificus* infections reported on the United States' Gulf Coast

4.1 Abstract

Vibrio vulnificus is a climate-sensitive marine pathogen which causes severe wound infections via exposure to seawater. The Gulf of Mexico and Atlantic coasts of the United States (US) are a global hotspot for these infections and recent work predicts that the number and distribution of *V. vulnificus* infections is likely to increase with climate warming in this region. In this study we use a multi-model inference approach to systematically assess potential environmental drivers of *V. vulnificus* infection variability at a weekly timescale across five US states along the Gulf of Mexico coastline. Air temperature and sea surface temperature were independently the most important environmental drivers of *V. vulnificus* infection variability. A baseline model without the addition of environmental variables containing parameters of year, month, occurrence of a holiday and random effect of US state demonstrated similarly good predictive power (baseline AUC: 0.816 vs air temperature AUC: 0.817 and SST AUC: 0.818). This observation suggests that a model accounting for seasonal trends alone may provide reasonable predictive skill for *V. vulnificus* infection occurrence in this region. This work reinforces the association of *V. vulnificus* infection with environmental temperatures and thus highlights *V. vulnificus* disease as a continued and growing human health risk in a warming world. This research presents a critical call to action to policymakers, emphasizing the urgency of climate adaptation strategies, public health interventions, and surveillance measures to mitigate the growing threat of *V. vulnificus* infections in vulnerable coastal regions. It underscores the need for proactive policies and resources dedicated to safeguarding public health in the face of climate-induced health risks, particularly those linked to marine pathogens.

4.2 Introduction

With the recent finding that 58% of human pathogenic diseases are exacerbated by climate change (Mora et al., 2022), the interconnectedness of human health and the health of the environment has never been more apparent. Intensifying climatic hazards such as heatwaves, extreme rainfall events, hurricanes and sea-level rise can influence pathogens, host and vector populations, as well as human behaviour resulting in changes to disease transmission in space and time (Epstein, 2001; IPCC, 2022). Waterborne disease caused by marine *Vibrio* spp. bacteria, which infect open wounds exposed to seawater, is a key example of how changing environmental conditions can influence the spread of disease due to the sensitivity of these pathogens to environmental temperatures (Baker-Austin et al., 2017). *Vibrio* spp. infections have emerged in the Baltic Sea region of Northern Europe in accordance with anomalous sea surface temperatures (SSTs) associated with climate change (Baker-Austin et al., 2013; Ebi et al., 2017) and at new, higher latitude locations along the east coast of the United States (US) (Archer et al., 2023; King et al., 2019). Continued warming is estimated to provide up to 38,000 km of additional coastline suitable for *Vibrio* spp. growth worldwide by 2100, depending on greenhouse gas emissions (Trinanes and Martinez-Urtaza, 2021), highlighting the potential growth of *Vibrio* spp. disease as a human health issue throughout the 21st Century.

Of the *Vibrio* spp. pathogens, *V. vulnificus* presents a major threat to human health (Almagro-Moreno et al., 2023; Amaro and Carmona-Salido, 2023), especially along the coastlines of subtropical eastern Asia, the Gulf of Mexico and Atlantic coasts of North America and countries bordering the Baltic Sea in Northern Europe, where these infections are mainly reported (Archer et al., 2023; Gildas Hounmanou et al., 2023; Huang et al., 2016). *V. vulnificus* is opportunistic, therefore most infections occur in individuals who are immunocompromised or have a chronic health condition (Baker-Austin and Oliver, 2018). As a consequence, the numbers of infections reported are low (e.g., ~80 *V. vulnificus* wound infections are reported along the US Gulf of Mexico and Atlantic coasts combined each year (Archer et al., 2023)). Despite this, *V. vulnificus* infections are high impact due to the severity of the disease and consequences for patient health. *V. vulnificus* wound infections can quickly become systemic so rapid diagnosis and treatment with antibiotics is essential (Baker-Austin and Oliver, 2016). Survival of this illness can also depend on life-changing surgery such as amputation (Dechet et al., 2008) and the mortality rate for *V. vulnificus* wound infection is estimated

at ~18% (Ralston et al., 2011). Individuals with chronic conditions associated with elevated blood iron levels, e.g., liver cirrhosis and haemochromatosis, are especially susceptible to severe *V. vulnificus* infections as the bacterium can replicate rapidly under increased iron availability (Baker-Austin et al., 2018; Wright et al., 1981). Current demographic trends indicate that many populations are ageing (United Nations Department of Economic and Social Affairs, 2023): a characteristic associated with increased prevalence of chronic conditions (Boutayeb and Boutayeb, 2005). For context, by 2050, the world population aged 65 and above is expected to rise to 1.6 billion (1 in 6) which is more than double the 761 million (1 in 10) people within this age group in 2021 (United Nations Department of Economic and Social Affairs, 2023). This suggests that globally, future populations are likely to contain a greater proportion of individuals with risk factors that make them susceptible to *V. vulnificus* infections.

A key epidemiological feature of *V. vulnificus* infections is that they are highly seasonal (Hlady and Klontz, 1996; Newton et al., 2012). Warm summer months coincide with the majority of waterborne *V. vulnificus* infections which mainly occur between May to October (Baker-Austin et al., 2016; Baker-Austin and Oliver, 2018; Brehm et al., 2021a). This trend is also present in the annual cycle of *V. vulnificus* bacterial abundance which demonstrates a seasonal peak in summer months in accordance with changes in water temperature (Jacobs et al., 2014; Pfeffer et al., 2003). *V. vulnificus* bacteria prefer warm (~20°C), low salinity (10-25 Practical Salinity Units, PSU) conditions (Noorian et al., 2023) and sea surface temperature (SST) is frequently identified as the primary driver of *V. vulnificus* bacteria in the environment, often explaining >50% of the variability in its abundance, whilst salinity demonstrates less explanatory power (Blackwell and Oliver, 2008; Motes et al., 1998; Nigro et al., 2011; Randa et al., 2004). Other environmental factors associated with *V. vulnificus* abundance include chlorophyll-a concentration (a proxy for phytoplankton biomass), and zooplankton. Phytoplankton blooms, which increase nutrient availability for bacterial growth, have been linked to increased *V. vulnificus* abundance (Eiler et al., 2007; Greenfield et al., 2017). Meanwhile, *V. vulnificus* attach directly to zooplankton (Gugliandolo et al., 2008; Toubiana et al., 2019); here, the bacteria are sheltered from harsh changes in physical conditions whilst provided with a source of nutrients and protection from predators (Hall-Stoodley et al., 2004; Matz et al., 2005; Vezzulli et al., 2016). *V. vulnificus* has been positively associated with zooplankton, notably copepods (Diner et al., 2021), which are highlighted as one of the most important environmental reservoirs for *Vibrio* spp. bacteria (Vezzulli et al., 2010). Although presence of *V. vulnificus* bacteria alone does not result in human infection due to the many other elements involved in disease transmission (i.e., number of bacteria,

virulence of strains, human exposure, host susceptibility), environmental variables associated with *V. vulnificus* growth are arguably important precursors to human disease and should be explored when constructing models to explain *V. vulnificus* infection variability.

Further variables potentially important to *V. vulnificus* infection variability include precipitation, air temperature, hurricane landfall, and El Niño, and La Niña Southern Oscillation (ENSO) and these are detailed below. Heavy precipitation increases freshwater runoff from the land which can dilute coastal salinities to brackish conditions preferred by *V. vulnificus,* influencing the abundance of this bacterium (Bullington et al., 2022). Alternatively, in terms of human behaviour, precipitation may decrease coastal recreation (Morgan and Ozanne-Smith, 2013) and thus human exposure to *V. vulnificus* but extreme rainfall may increase exposure through coastal flooding. Air temperature positively influences coastal recreation (Elliott et al., 2019), including the number of bathers immersed in coastal waters (Morgan and Ozanne-Smith, 2013). Consequently, summer months are considered the peak of coastal recreational activity and thus a period of elevated human exposure to *Vibrio* spp. bacteria. However, air temperature strongly correlates with sea surface temperature (Ayala et al., 2023; Sheahan et al., 2022) so possible influences on human behaviour are challenging to isolate from temperature effects on *V. vulnificus* bacteria in the water.

Hurricane landfalls and ENSO events may represent longer-term, upstream changes in conditions that are not visible within weekly air temperature and rainfall variables but have relevance to *V. vulnificus* infections. In 2005, exposure to the brackish flood waters of Hurricane Katrina was associated with 14 cases of *V. vulnificus* infection, including 3 fatalities (CDC, 2005) (see Figure S10). In 2022, Hurricane Ian was linked to 29 *V. vulnificus* cases in Florida, including nine deaths (Sodders et al., 2023). Finally, changes in environmental conditions induced by the ENSO climate phenomenon have been linked to increased risk of vibriosis in the US nationally (Logar-Henderson et al., 2019). The two opposing modes of ENSO: La Niña and El Niño, are associated with increased and suppressed hurricane activity in the Atlantic basin, respectively (Bell and Chelliah, 2006), thus upstream effects of the ENSO modes may influence coastal conditions and human exposure of *V. vulnificus* along the Gulf Coast of the US, the focal location of this study.

Presently, few studies seek to explain the variability in *V. vulnificus* human infections. In the US, SST has been used to model monthly likelihood of *V. vulnificus* infection by Sheahan et al. (2022). However, other factors known to influence *Vibrio* spp. bacteria in

the environment are not explored as the aim of Sheahan et al. was to provide future projections of *Vibrio* spp. incidence, so models were limited by future data availability. Other recent work by Ayala et al. (2023) examines air temperature, water temperature, windspeed and air pressure recorded by NOAA buoys for associations with monthly *V. vulnificus* infections reported in Florida. Both air and water temperatures were found to be significantly higher in months when *V. vulnificus* cases occurred whilst negative associations were found for wind speed and air pressure variables. A logistic regression model including these four environmental variables plus dummy month variables to account for seasonal trends was determined to be the best explanatory model of monthly *V. vulnificus* infection occurrence, but strong correlation between air temperature and water temperature variables may have reduced the precision of the model estimates due to multicollinearity. To the best of our knowledge, no study has yet examined the environmental drivers of weekly variability in *V. vulnificus* infections nor included attempts to validate the strength of models on withheld data.

In Chapter 3 the sustained northwards expansion in the distribution of *V. vulnificus* infections along the eastern coastline of the United States was documented and predictions for further extension to the geographic range of *V. vulnificus* infections with climate warming were produced (Archer et al., 2023). In contrast, this chapter seeks to explore a wide range of environmental predictors of *V. vulnificus* infections on a weekly, short-term basis after accounting for seasonal and long-term trends. Despite studies into the geographic spread of *Vibrio* spp. infections, there is a lack of research investigating the environmental drivers of variability in *Vibrio* spp. infections through time, particularly at short intervals. This omission is important as *Vibrio* spp. bacteria respond to environmental changes rapidly and thus represent a dynamic risk to human health. Unravelling which factors are important in driving weekly variability in *V. vulnificus* infections is therefore a key knowledge gap yet to be addressed in a systematic way.

In this study we use a multi-model inference (MMI) approach (Burnham and Anderson, 2002) to rank and compare the relative importance of a number of different environmental variables by their ability to explain the variability in reported *V. vulnificus* infections at weekly intervals. The MMI approach offers an alternative to null hypothesis testing which often seeks to provide one final model without considering model uncertainty (Whittingham et al., 2006). In contrast, within the MMI framework, models containing different combinations of the predictor variables are fitted and compared simultaneously using metrics that assess how likely each model represents the best approximating model for the data (Symonds and Moussalli, 2011). Therefore, this

approach represents a robust methodology for considering multiple possible predictor variables.

The MMI framework has been widely applied in ecology and examples of its use include to understand features of hedgerow habitat associated with bat activity (Boughey et al., 2011) and to explore factors associated with household infestation by *Triatoma infestans* in rural Argentina (Gurevitz et al., 2011). We focus this *V. vulnificus* wound infection modelling exercise on five US states bordering the Gulf of Mexico (Texas, Mississippi, Louisiana, Alabama and Florida). This coastline is a key hotspot for *V. vulnificus* infection (Huang et al., 2016; Miles et al., 2023) with at least one case reported in each of the five states to the US Centres for Disease Control and Prevention (CDC) Cholera and Other Vibrio Illness Surveillance (COVIS) monitoring programme every year between 2009 and 2018 (n = 391 cases).

4.3 Methods

4.3.1 *Vibrio vulnificus* health data

A dataset of confirmed non-foodborne *V. vulnificus* infections reported at county-level between 1988 and 2018 was obtained from the US Cholera and Other Vibrio Illness Surveillance (COVIS) service (CDC, 2022) and coastal cases were determined (see Chapter 3 for details). A subset of *V. vulnificus* data for 1993 to 2018 were used to match the availability of environmental data (see section 4.3.2).

Only infections reported along the Gulf of Mexico coastline of the United States (Texas, Mississippi, Louisiana, Alabama and Florida; n = 711) were included in this analysis (see Figure 4.1). The Gulf of Mexico has been a hotspot for *V. vulnificus* infections continuously over the temporal range of the *V. vulnificus* dataset and therefore provides more data points for model creation than other east coast states which have more recently started reporting *V. vulnificus* infections (e.g., the first *V. vulnificus* wound infection in Maryland, where *V. vulnificus* cases are often associated with Chesapeake Bay, was reported to COVIS in 2003).

To ensure only Gulf of Mexico cases of *V. vulnificus* were included, the coastline of Florida was divided into Gulf Coast and Atlantic Coast with north and west of Highway 1 determined as the Gulf Coast of Florida. South and east of Highway 1 was determined to be the Atlantic Coast of Florida and was excluded from the analysis. Highway 1 runs south-west from approximately 25.173°N, -80.374°E to 24.556°N, -81.780°E (see Figure

4.1). The majority (72%; 255/354) of Florida's *V. vulnificus* infections between 1993 and 2018 were associated with the Gulf of Mexico coastline.

V. vulnificus infection occurrence within each ISO week (January to December) between 1993 to 2018 was determined for each Gulf Coast state (Texas, Louisiana, Mississippi, Alabama, and Florida [Gulf Coast only]). Wound infection reports were aggregated to state-level due to uncertainty regarding the location of exposure and to reduce zero-inflation from the high number of weeks across counties when no *V. vulnificus* cases were reported. Although within 200 km of the coast, many cases were reported in counties not directly on the coastline resulting in uncertainty in the location of exposure on the coastline. For ~30% of cases (196/711), the exact 'location of exposure' description, which provides location detail beyond the county-level of reporting, was missing whilst this information was ambiguous for many additional cases.

Whilst the incubation period for *V. vulnificus* wound infections is short, usually within 24 hours of exposure (Baker-Austin and Oliver, 2016; Sakihara et al., 2023), a weekly time interval was chosen to account for uncertainty in the time between exposure and reporting and provides the average coastal conditions associated with presence of an infection in each US state. This was included in the models as a Boolean variable whereby '1' indicates the occurrence of at least one case reported within the state in a given week and '0' indicates that no cases were reported. A Boolean variable of infection occurrence was used due to the low variability in total weekly cases as in (Sheahan et al., 2022). When aggregated to state-level the maximum weekly total *V. vulnificus* infections was 9 cases in Louisiana on the week beginning 29th August 2005 and there was a high frequency of weeks where no infections were reported because of the relative rarity of *V. vulnificus* infections. For example, cases were reported on the Gulf Coast of Florida during 15% (207/1357) of weeks between 1993 to 2018 and just 3% of weeks (49/1357) in Alabama.

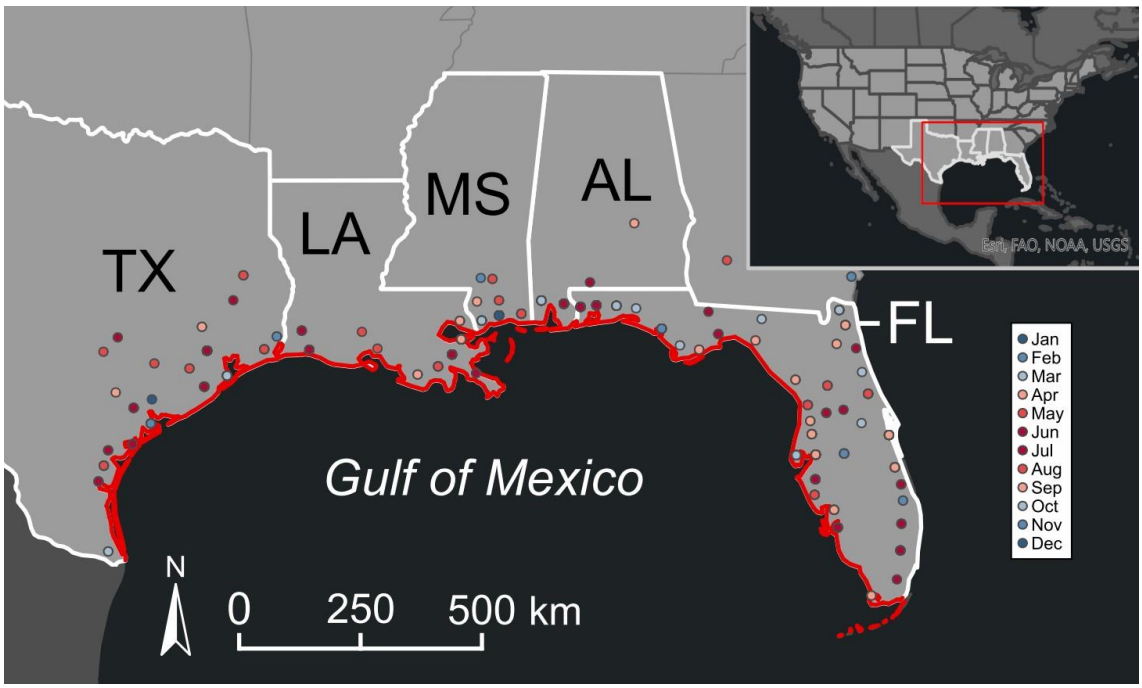

Figure 4.1 United States Gulf of Mexico coastline included in the study (red). Location of Gulf Coast-associated *Vibrio vulnificus* wound infections during study period (1993-2018) shown by points coloured by month of infection onset. Inset map of United States, North America to contextualise the study region.

4.3.2 Environmental data

Oceanographic and weather data

Daily SST and salinity data from the Global Ocean Physics Reanalysis dataset for 1993 to 2018 (Copernicus Marine Service, 2022a) and daily zooplankton biomass (expressed as carbon in seawater, C g m^{-2}) data from the Global Ocean Low and Mid Trophic Levels Biomass Content Hindcast product for 1998 to 2018 (Conchon, 2016; Copernicus Marine Service, 2022b; Lehodey et al., 2015, 2010) were downloaded at 0.083º (~9 km) resolution from the Copernicus Marine Service. Satellite-derived chlorophyll-a concentration (mg m^{-3}) data was downloaded from the Ocean Colour Daily dataset (version 5.0.1) at 0.042º (~5 km) resolution for 1998 to 2018 from the Copernicus Climate Data Store (Copernicus Climate Data Store, 2019).

Hourly 2m air temperature (°C) and total precipitation (m) reanalysis data of the ERA5-Land dataset were obtained from the Copernicus Climate Data Store at 0.1º (~11 km) resolution (Muñoz Sabater, 2019). Total precipitation was converted into mm as this was a more appropriate unit for comparison with the remaining environmental variables using the same y-axis (see Figure 4.2) and later standardisation of the variables would mean

no impacts on this variable within model creation. These weather data were downloaded for the 1993-2018 time-period and were processed into daily means to match the available temporal range and frequency of the oceanographic data using Climate Data Operator (version 1.9.8) (Schulzweida, 2019) on the High Performance Computing Cluster supported by the Research and Specialist Computing Support service at the University of East Anglia.

Weather and oceanographic data, except for chlorophyll-a, were extracted at the Gulf of Mexico coastline where the data grid cells touch the coastline. As most chlorophyll-a data grid cells did not intersect the US coastline, and to account for patchiness in data availability due to clouds, values for this variable were extracted within a 30 km buffer of the coastline as most coastal human activity occurs within this distance from the coast (Trinanes and Martinez-Urtaza, 2021).

Using ISO weeks, the weekly minimum (weekmin), weekly mean (weekmean) and weekly maximum (weekmax) value of each cell within the weather and oceanographic datasets was calculated from the daily data using the Climate Data Operator software (version 1.9.8) (Schulzweida, 2019).

All further data analysis was conducted in R version 4.2.1 (R Core Team, 2022). For every ISO week within the 1993 to 2018 time-period the weekmin, weekmean and weekmax values of each weather and oceanographic variable (with the exception of chlorophyll-a and zooplankton, which were available from 1998 to 2018) were averaged spatially across the coastline of each Gulf Coast state. These averages were weighted by the human population count within 200 km of each cell on the coastline to reflect the environmental conditions of locations with increased human presence and therefore potentially greater coastal recreational activity. Data were missing for 19/1036 (1.8%) of weeks for the chlorophyll-a and zooplankton variables combined.

Population count data were obtained at 0.042º (~5km) resolution at 5-year intervals from version 3 (years 1990 – 1995) and version 4 (years 2000 – 2015) of the Gridded Population of the World dataset (CIESIN - Columbia University, 2018; CIESIN - Columbia University et al., 2005). Due to the availability of the population data, environmental data for 1993-1994 were weighted by 1990 population data, 1995-1999 weighted by 1995 data and so on.

Hurricane landfall data

Hurricane landfall data was obtained from NOAA's 'Continental United States Hurricane Impacts/Landfalls 1851-2022' dataset which lists the states affected by hurricanes each

month (https://www.aoml.noaa.gov/hrd/hurdat/All_U.S._Hurricanes.html). Presence of a hurricane landfall impact of any hurricane category was included in relevant models as a binary variable.

El Niño Southern Oscillation (ENSO)

Oceanic Niño Index (ONI) data which quantify SSTs anomalies in Pacific equatorial waters using the Niño 3.4 region [5°N-5°S, 120°-170°W], were obtained from NOAA's 'Cold and Warm Episodes by Season' dataset (https://origin.cpc.ncep.noaa.gov/products/analysis_monitoring/ensostuff/ONI v5.php). Five consecutive 3-month running means with an ONI of at least +0.5°C, or -0.5°C within the Niño 3.4 region are considered an El Niño or La Niña period, respectively (Norel et al., 2021). The occurrence of El Niño and La Niña conditions were each included as binary variables.

State and Federal holidays

In the absence of a freely available US holiday API, the dates of non-working Federal and State holidays in Gulf Coast US states were obtained from the timeanddate.com web page and included as a single Boolean variable to indicate a holiday occurred within a particular week of the dataset.

4.3.3 Statistical analysis

An MMI approach using mixed effects logistic regression models was taken to explore and compare the ability of different factors to explain the weekly variability in *V. vulnificus* wound infections within Gulf Coast states of the US. Modelling was conducted in three main stages: initial models to determine the best versions of weather and oceanographic variables, model comparison using these 'best' variables and assessment of the impact of additional hurricane landfall, ENSO and plankton variables on model fit and predictive power.

All models contained a random effect for US state to account for potential increased similarity in observations reported in the same state. The performance of environmental models is compared to both 'null' and 'baseline' models which lack environmental parameters throughout. The 'null' model of weekly *V. vulnificus* infection occurrence contains an intercept and a random effect of US state only. The 'baseline' model builds on the null model to account for seasonal and long-term trends by also including a polynomial term of year (due to sigmoid relationship between year and the logit of the model from preliminary analyses), dummy categorical variables for each month to control

for monthly variation, and a Boolean variable to indicate the presence or absence of a non-working holiday within each week to control for potentially greater exposure during public holidays when more people have the opportunity for coastal recreation. Dummy variables for each week of the year were also explored as an alternative to monthly dummy variables but resultant predictive power was lower for all models so monthly dummy variables were used. All environmental models contain parameters present in the baseline model in addition to weather and/or oceanographic variables.

'Best' versions of weather and oceanographic variables

The weekmin, weekmean and weekmax of the SST, salinity, air temperature, and total precipitation variables were assessed to determine the 'best' version of each variable, i.e., the version with greatest relative importance to weekly *V. vulnificus* infections, to carry forward into the final model set (see 'Modelling approach' below for relative importance calculation). As demonstrated in Chapter 3, different versions of variables (minimum, mean, maximum) can have different strength as predictors, so this step was included to ensure the strongest version of each variable was used for final multi-model comparisons.

Variables were first tested for covariance using Spearman's Rho Rank Correlation and all possible pairs of variables that did not correlate ≥0.7 were generated. SST and air temperature variables correlated strongly ($\rho(6783) = 0.96$, $p<0.001$) therefore two sets of candidate models, one including SST variables and one including air temperature variables were assessed separately. Only one version of each environmental variable was included in each model so that they could be compared but also due to correlation across variable versions (e.g., weekmean air temperature correlates with weekmin and weekmax air temperature), and to ensure each predictor variable occurs within the model set the same number of times for balanced calculation of relative importance.

Each environmental model contained all variables present in the baseline model plus a unique combination of environmental predictors (n = 63), resulting in 65 models per initial candidate set (see Table S5). The relative importance of each version (weekmin, weekmean and weekmax) of the predictors was determined (see 'Modelling approach' below) with only the version with the greatest average relative importance carried forward to the final model comparisons. The two model sets were reduced to the combinations of the best versions of the environmental variables only (n = 7) alongside the null and baseline models and model metrics were recalculated based on the reduced model set.

Modelling approach

For each set of models analysed, the following method was applied:

As in Chapter 3, an initial 90:10 split of the dataset was used to set aside 10% of the data for later validation whilst 90% of the data was for training and testing models. The 90% subset was randomly sampled to generate 100 subsets of data, each containing a balanced proportion of weeks where *V. vulnificus* infections were present versus absent (50:50). Each subset was split 70:30 with 70% of the data for model training and 30% of the data for model testing (i.e., generation of an area under the receiver operator characteristic curve [AUC] value, a measure of predictive power). Therefore, each random subset of the data (n = 100) provided a replicate for all models within the set.

Model results including coefficients and metrics were averaged over 100 replicates to reflect a more robust choice of 'best' model (see below). Median values as an alternative to taking the mean were explored as the median is less sensitive to outliers, however, resultant values were highly similar and made negligeable difference to the conclusion of results.

The lme4 package (Bates et al., 2015) in R (version 4.2.1) (R Core Team, 2022) was used to generate all generalised linear mixed models. For each model, the corrected Akaike Information Criterion (AIC_c) to account for a large number of predictors (k) relative to sample size (n), i.e., n/k < 40, was generated as described by Symonds and Moussalli, 2011:

$$AIC_c = AIC + \frac{2k(k+1)}{n-k-1}$$

For each data subset, the fitted models were ordered by ascending AIC_c and the 'best' model was that with the lowest AIC_c. The difference between the AIC_c of each model and the best model was generated (Δ_i). To quantify the probability that each model is the best model given the data subset, the Akaike Weight (w_i) of each model was calculated as described by (Burnham and Anderson, 2004):

$$w_i = \frac{\exp\left(-\frac{1}{2}\Delta_i\right)}{\sum_{r=1}^{R}\exp\left(-\frac{1}{2}\Delta_r\right)}$$

The mean AIC_c was calculated for each model from the 100 subsets of data to generate averaged model results. This enabled the overall 'best' model with the greatest average model Akaike Weight to be determined.

The relative importance of each individual environmental predictor included in the models was calculated by adding together the model Akaike Weight of every model in the set where that predictor was present. Relative importance values for each predictor were also averaged across the 100 subsets of data.

The mean AUC was generated for each model from across the 100 test data subsets that were held out from model training. A validation AUC was generated from the raw unbalanced 10% validation subset that was held out from model training and testing.

Models with a mean difference in AIC_c from the best model (Δ_i) of less than 2, indicating that they are amongst the best competing models (Symonds and Moussalli, 2011), were selected for averaging. Model averaging was conducted with R package MuMIn (Bartoń, 2023).

Impact of additional variables

To assess whether the addition of further potentially relevant variables improved model fit, final models were rerun with the addition of terms for El Niño, La Niña, hurricane landfall, chlorophyll-a concentration and zooplankton biomass. Final models were rerun with data from 1998-2018 due to the restricted availability of chlorophyll-a and zooplankton data. The decision to include plankton variables at a later stage in the modelling was taken so that oceanographic and weather variables could be assessed first with the greatest time-range of data available. ENSO and hurricane landfall variables were included at a later stage as they potentially have 'upstream' effects on *V. vulnificus* disease, and we first wanted to explore environmental variables with more direct associations to *V. vulnificus* described the literature.

The difference in average AIC_c and AUC values between the original model and the model with the addition of each variable in turn was reviewed. Differences in AIC_c greater than two suggest that the new model is substantially different from the original model (Burnham and Anderson, 2004).

All possible model combinations of the final weather and oceanographic variables and the above-mentioned additional variables were generated and fitted to 100 subsets of the 1998-2018 dataset alongside null and baseline models (n = 257). Covariance between all variables was tested beforehand and ensured that none of the additional variables were correlated ≥0.7 with the final model variables. Average standardised coefficients, 95% confidence intervals of coefficient estimates, and the relative importance of all variables was generated for comparison.

4.4 Results

4.4.1 Environmental conditions in US Gulf Coast states

The mean environmental conditions between 1993 and 2018 for individual Gulf Coast states for each month of the year are presented in Figure 4.2 with mean monthly *V. vulnificus* wound infections displayed using a secondary y-axis. Air temperature and SST variables both display a seasonal trend, highlighting the strong correlation between these temperature predictors. For all Gulf Coast states, temperature peaks around mid-July and the seasonal trend of *V. vulnificus* infections shows strong similarity to that of temperature.

There are distinct differences in the patterns of salinity exhibited between states. According to these data, little variation in salinity is present along the Gulf Coast of Florida throughout the year as conditions remain typical of seawater at around 35 PSU. Louisiana, Mississippi, and Alabama display a decrease in mean salinity to their lowest values at around April to May. Of these three states, Mississippi observed the lowest minimum salinity values of around 10 PSU, reflecting brackish conditions. A sharp spike in maximum precipitation is noticeable around the time of the reduction in salinity in Mississippi and Louisiana. Conversely, Texas demonstrates a temporary increase in salinity around mid-late summer.

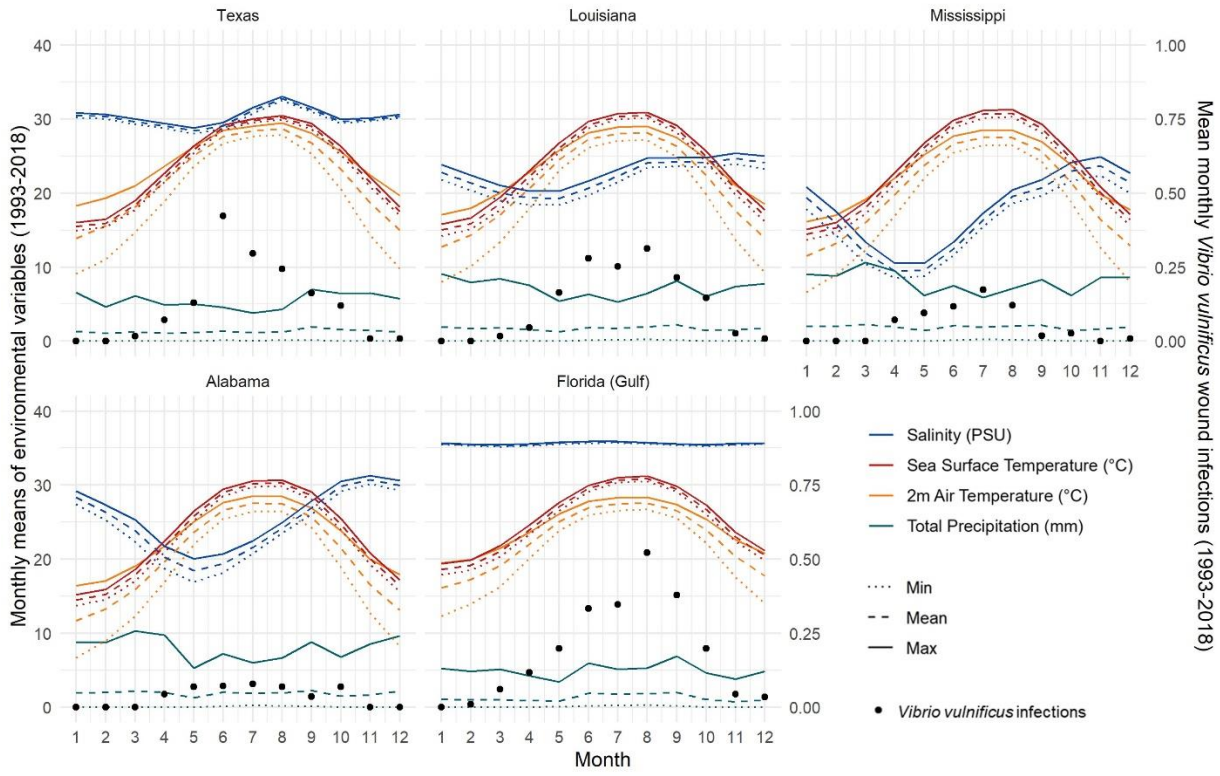

Figure 4.2 Monthly environmental conditions and number of *V. vulnificus* wound infections for US Gulf Coast states averaged over 1993-2018 time-period. Environmental means are weighted by population count within 200 km of the coast.

Table 4.1 Models of weekly *V. vulnificus* infection occurrence ranked by highest Akaike weight (w_i). Results shown for a sea surface temperature and air temperature model sets, which each contain 7 possible combinations of environmental variables. Model sets include a 'null' model (intercept and random effect of US state only) and 'baseline' model which contains variables present in all environmental models. K indicates the number of model parameters. Model results were generated for and averaged over 100 random subsets of the dataset: bias corrected AIC (AIC_c), difference in AIC_c from the best model (Δ_i), area under the ROC curve (AUC), validation (V.) AUC and Akaike weight (w_i). Top models ($\Delta_i < 2$) indicated above line.

Rank (n = 9)	Model[a, b]	K	Mean (n = 100)				
			AIC_c	Δ_i	AUC	V. AUC	w_i
Sea surface temperature model set							
1	sst weekmean	18	765.696	0.378	0.818	0.823	0.378
2	sst weekmean + totprec weekmean	19	766.436	1.118	0.818	0.819	0.267
3	sal weekmax + sst weekmean	19	767.133	1.815	0.817	0.823	0.189
4	sal weekmax + sst weekmean + totprec weekmean	20	767.866	2.548	0.817	0.819	0.132
5	baseline model	17	778.148	12.831	0.816	0.817	0.011
6	totprec weekmean	18	778.204	12.886	0.817	0.812	0.009
7	sal weekmax	18	778.815	13.498	0.817	0.821	0.008
8	sal weekmax + totprec weekmean	19	778.823	13.505	0.817	0.817	0.007
9	null model	2	988.338	223.020	0.646	0.612	0.000
Air temperature model set							
1	temp weekmean	18	765.875	0.322	0.817	0.822	0.407
2	temp weekmean + totprec weekmin	19	767.066	1.513	0.816	0.822	0.228
3	sal weekmax + temp weekmean	19	767.147	1.594	0.817	0.823	0.219
4	sal weekmax + temp weekmean + totprec weekmin	20	768.380	2.828	0.816	0.823	0.119
5	baseline model	17	778.148	12.596	0.816	0.817	0.010
6	sal weekmax	18	778.815	13.263	0.817	0.821	0.008
7	totprec weekmin	18	779.487	13.935	0.815	0.816	0.005
8	sal weekmax + totprec weekmin	19	780.151	14.598	0.816	0.820	0.004
9	null model	2	988.338	222.785	0.646	0.612	0.000

[a]All environmental models and the baseline model contain a random effect for US state, 3rd order polynomial terms of year, dummy month variables and binary term for whether it is a public holiday (state or federal) or not. [b]Predictor labels: weekmin = weekly minimum, weekmean = weekly mean, weekmax = weekly maximum, sst = sea surface temperature (°C), temp = air temperature (°C), sal = salinity (PSU), totprec = total precipitation (mm).

Table 4.2 Standardised coefficient estimates (β), standard errors, and 95% confidence intervals of coefficients. Each value is averaged over the top models ($\Delta_i < 2$, see Table 4.1) and 100 random subsets of the dataset. Relative predictor importance (Σw_i) calculated from 9 model subset (Table 4.1). Confidence intervals that do not overlap 0 are highlighted in bold.

	Predictor	β	SE	Lower CI	Upper CI	Σw_i
Sea surface temperature model set	sst weekmean	1.926	0.526	**0.896**	**2.957**	0.966
	totprec weekmean	-0.061	0.109	-0.274	0.152	0.414
	sal weekmax	-0.019	0.110	-0.234	0.196	0.335
	poly(year, 3)1	14.766	3.319	**8.260**	**21.272**	
	poly(year, 3)2	-1.259	2.852	-6.850	4.331	
	poly(year, 3)3	0.304	3.221	-6.009	6.617	
	holiday	-0.357	0.483	-1.304	0.591	
	Jan	-15.630	1117.162	-2205.267	2174.008	
	Feb	-15.885	1256.215	-2478.067	2446.296	
	Mar	-0.831	0.660	-2.125	0.462	
	May	-0.965	0.514	-1.972	0.043	
	Jun	-0.848	0.862	-2.537	0.842	
	Jul	-1.177	0.829	-2.802	0.448	
	Aug	-1.516	0.889	-3.257	0.226	
	Sep	-1.792	0.726	**-3.214**	**-0.369**	
	Oct	-1.117	0.641	-2.373	0.139	
	Nov	-1.222	0.643	-2.482	0.039	
	Dec	-1.459	6.198	-13.608	10.689	
Air temperature model set	temp weekmean	1.278	0.340	**0.611**	**1.945**	0.973
	totprec weekmin	-0.065	0.098	-0.257	0.127	0.356
	sal weekmax	0.021	0.111	-0.196	0.238	0.350
	poly(year, 3)1	17.429	2.966	**11.616**	**23.242**	
	poly(year, 3)2	-0.143	2.762	-5.557	5.270	
	poly(year, 3)3	-2.025	2.878	-7.665	3.615	
	holiday	0.306	0.320	-0.322	0.934	
	Jan	-16.963	1080.210	-2134.174	2100.248	
	Feb	-16.876	1015.379	-2007.019	1973.266	
	Mar	-0.767	0.633	-2.008	0.473	
	May	-0.720	0.475	-1.650	0.210	
	Jun	0.325	0.579	-0.810	1.459	
	Jul	-0.135	0.599	-1.309	1.040	
	Aug	-0.296	0.614	-1.500	0.908	
	Sep	-0.119	0.444	-0.988	0.750	
	Oct	-0.901	0.536	-1.952	0.149	
	Nov	-0.548	0.623	-1.770	0.673	
	Dec	-2.084	6.008	-13.860	9.691	

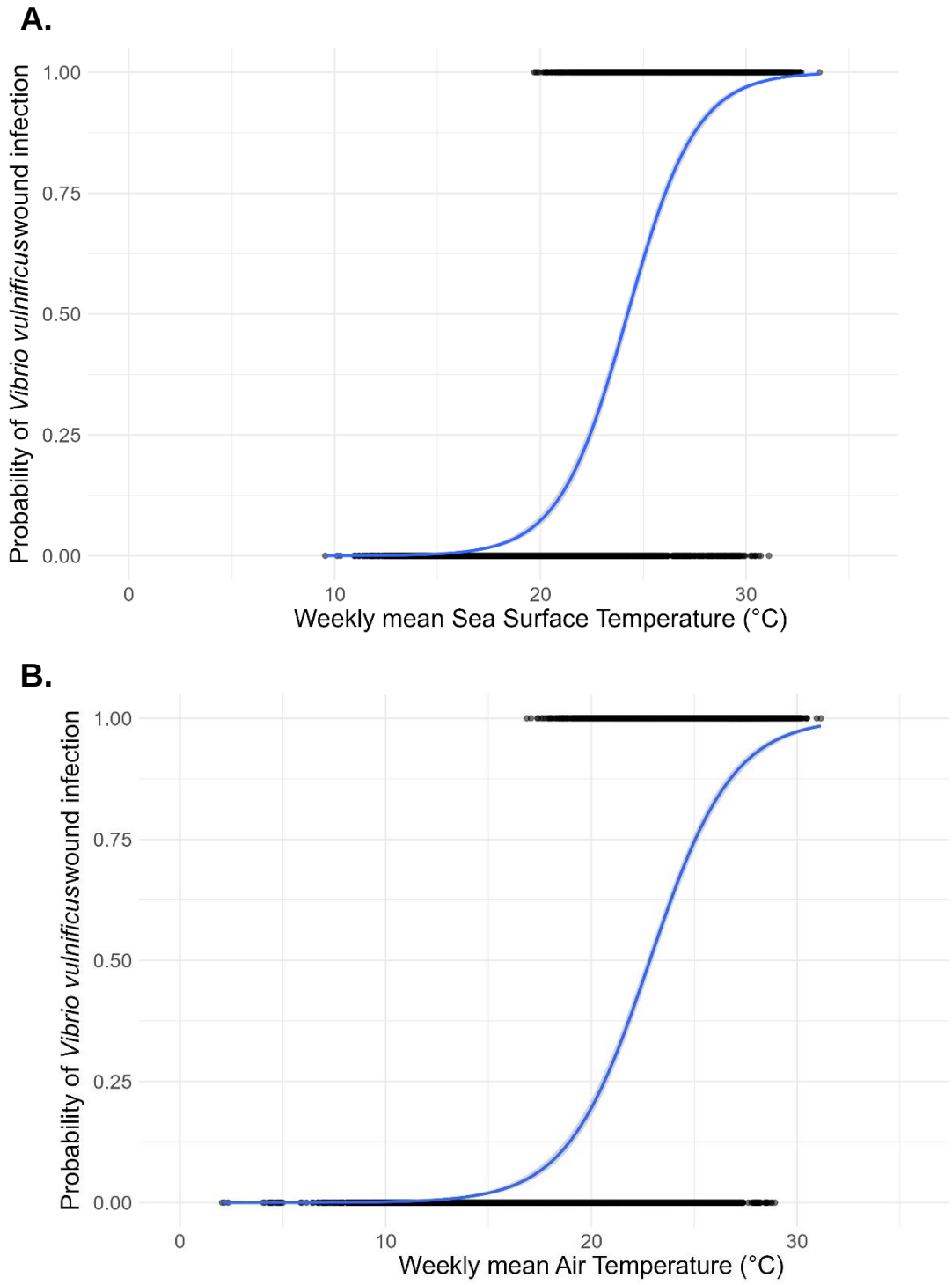

Figure 4.3 Logistic regression equation of model averaged parameters A. Weekly mean sea surface temperature (°C) and B. Weekly mean air temperature (°C). Grey shading indicated Standard Error. Models with a mean difference in AIC_c from the best model (Δ_i) < 2 (see Table 4.1) included in averaging.

4.4.2 Model results

An initial modelling step was conducted to assess the 'best' version (i.e., weekmin, weekmean, or weekmax) of each weather and oceanographic variable to investigate, based on their initial 'relative importance' score. Due to strong correlation between air temperature and SST variables, two respective initial model sets (n = 65 models each) were generated. In the SST initial model set, 'SST weekmean', 'total precipitation weekmean' and 'salinity weekmax' were the best performing versions of the variables. In the air temperature initial model set, 'air temp weekmean', 'total precipitation weekmin' and 'salinity weekmax' performed best (see Table S5 and Table S6 for initial model results).

Models containing these best performing versions of variables were retained in the two final model sets (n = 9 models each) and Akaike model weights were recalculated based on the smaller model sets. Results of the final model sets are shown in Table 4.1. All model sets include a 'null' model which contains only the intercept and random effect of US state, a 'baseline' model which builds on the null model with a third order polynomial of year, dummy variable for month and a Boolean holiday variable and the environmental models which contain all variables of the baseline model in addition to the environmental variables.

For both final model sets, the null model was ranked lowest in terms of Akaike Weight and had an AUC of 0.646 indicating poor predictive power (an AUC >0.8 indicates good predictive power; Hosmer et al., 2013). The addition of year, month and holiday terms to the null model increased the average AUC from 0.646 to 0.816, indicating good predictive power of the resulting baseline model. Despite large differences in the average Akaike Weight across models, predictive power (AUC) did not vary substantially across the remaining models. Models including temperature had a greatly reduced AIC_c compared to the baseline model, yet negligible increases in their predictive power are recorded as AUC improves by 0.002 at most. More specifically, once baseline terms that account for a long-term positive trend, monthly variation and holidays are included, the addition of temperature may increase model fit, but makes little improvement to the model's predictive power. The validation dataset which represents 10% of the raw dataset held out from core model training and testing confirmed these results with similar model AUC scores produced (SST model and air temperature model improve baseline AUC by 0.006 and 0.005 using validation dataset).

Within both final model sets, including a single environmental variable of temperature alongside baseline variables has the greatest average Akaike Weight and lowest average AIC_c. Within the SST model set, on average, an SST weekmean model of *V. vulnificus* infection variability had a 37.8% chance of being the best model given the data available compared to 1.1% for the baseline model which lacks any environmental parameters. The baseline model had an average Δ_i of 12.831, indicating a substantial difference in AIC_c from the best model over the 100 replicate data subsets compared to a Δ_i of 0.378 for the SST weekmean model. As the latter is not 0, this highlights that although best performing on average, the SST weekmean model was not the best model in all 100 data subsets.

The average Δ_i of models 'SST weekmean + total precipitation weekmean' and 'SST weekmean + salinity weekmax' is less than 2 (1.118 and 1.815, respectively), suggesting that on average, they do not differ substantially from the best model. Nonetheless, precipitation and salinity models without a temperature variable performed less well than the baseline model, each with negligible Akaike Weights which imply a <1% chance of being the best model, emphasising that SST is still an important factor in weekly *V. vulnificus* infection variability. Model results within the air temperature set displayed strong similarity to those of the SST set due to the strong correlation between these temperature variables. Air temperature weekmean was on average 40.7% likely to be the best model for the data.

The relative importance of each environmental predictor is displayed in Table 4.2 alongside averaged standardised coefficients and 95% confidence intervals of the coefficients. SST and air temperature were the most important predictors with strong average relative importance of 0.966 and 0.973, respectively. The 95% confidence intervals for both temperature predictors did not overlap zero, indicating a strong positive influence of temperature on weekly *V. vulnificus* infection variability in Gulf Coast states. The positive impact of SST (average standardised beta coefficient = 1.926) was stronger than that of air temperature (average standardised beta coefficient = 1.278). The relationship of these variables with the probability of a *V. vulnificus* wound infection being reported in a Gulf Coast state is visualised in Figure 4.3.

Precipitation and salinity both displayed a negative association with weekly *V. vulnificus* infection occurrence, yet high standard errors and zero-overlapping confidence intervals indicate a lack of statistical importance.

Interestingly, the holiday variable, included to control the potential impact of state and federal holidays on weekly *V. vulnificus* infections, was not statistically important and had

a small standardised coefficient of 0.049 and 0.051 in the SST and air temperature model sets, respectively.

4.4.3 ENSO, hurricane landfall, and plankton variables

Additional variables of potential importance to weekly *V. vulnificus* infection occurrence based on existing literature including El Niño and, La Niña events, hurricane landfall, chlorophyll-a, and zooplankton (see Introduction), were investigated. Each variable was added individually to the final environmental models to determine differences in AIC_c (ΔAIC_c) and AUC (Δ AUC) metrics of the final environmental models with the addition of each variable (see Table S7 and Table S8). Table 4.3 presents the averaged standardised coefficients and relative importance of the additional variables when compared to all other environmental variables in the final model sets.

The addition of La Niña and hurricane landfall terms individually resulted in a marginal reduction in AIC_c for all models (ΔAIC_c range for La Niña: -0.288 to -1.758, hurricane landfall: -0.414 to -0.971) indicating slight improvements to model fit but no substantial difference to the original models ($\Delta AIC_c < 2$; Burnham and Anderson, 2004). La Niña somewhat improved predictive power for 9/14 models by a positive Δ AUC of 0.001 whilst the addition of the hurricane landfall variable resulted in no change in AUC for all but one model, where AUC decreased by 0.001.

The impact of El Niño on AIC_c was inconsistent; AIC_c was slightly reduced for models which included SST (ΔAIC_c range: -0.018 to -0.080) and AUC improved by 0.001 at most. Table 4.3 shows that the direction of association with weekly *V. vulnificus* infections for La Niña was negative whilst this was positive for El Niño and hurricane landfall variables. This suggests that *V. vulnificus* wound infections could be more likely to be reported during El Niño events and hurricane landfall impacts and less likely during La Niña events. However, these coefficients possessed large standard errors and all respective confidence intervals overlapped zero so no statistically significant conclusions can be drawn.

Chlorophyll-a and zooplankton variables unanimously increased AIC_c across models, indicating a small reduction in model fit with the inclusion of these variables (ΔAIC_c range for chlorophyll-a: 1.261 to 1.530, zooplankton: 0.298 to 1.442). Neither variable improved predictive power; chlorophyll-a reduced the AUC of 13/14 models by a maximum of 0.002 and zooplankton reduced the AUC of 9/14 models by 0.001. Small negative and positive coefficients were generated for chlorophyll-a and zooplankton variables respectively.

Nonetheless, zero-overlapping confidence interval estimates imply a lack of statistical importance to weekly *V. vulnificus* infection variability.

Results in Table 4.3 show that the temperature variables maintain the highest relative importance when additional variables are included in the modelling set (relative importance: SST weekmean = 0.965, air temperature weekmean = 0.940). La Niña scores second highest with a relative importance of 0.649 in the SST model set and 0.633 within the air temperature model set.

Overall, none of the additional predictors were found to be statistically important to weekly *V. vulnificus* infection occurrence.

Table 4.3 Standardised coefficient estimates (β), standard errors, relative predictor importance (Σw_i) and 95% confidence intervals of coefficients. Each value is averaged over all models (n = 257) and 100 random subsets of the dataset. Confidence intervals that do not overlap 0 are highlighted in bold. Ordered by relative importance.

Predictor[a]	β	SE	Σw_i	95% CIs	
				Lower	Upper
Sea surface temperature set					
sst weekmean	1.448	0.429	0.965	**0.608**	**2.289**
La Niña	-0.415	0.245	0.649	-0.895	0.065
zooplankton	0.072	0.211	0.449	-0.342	0.486
El Niño	0.273	0.267	0.412	-0.251	0.797
totprec weekmean	-0.094	0.101	0.398	-0.292	0.105
hurricane landfall	0.369	0.489	0.381	-0.589	1.326
sal weekmax	-0.071	0.255	0.366	-0.571	0.428
chlorophyll-a	-0.020	0.154	0.342	-0.322	0.282
Air temperature set					
temp weekmean	1.083	0.355	0.940	**0.388**	**1.778**
La Niña	-0.405	0.244	0.633	-0.884	0.074
El Niño	0.262	0.267	0.401	-0.262	0.786
hurricane landfall	0.343	0.488	0.368	-0.614	1.301
sal weekmax	-0.112	0.259	0.368	-0.619	0.395
totprec weekmean	-0.079	0.102	0.357	-0.278	0.12
zooplankton	0.008	0.208	0.351	-0.399	0.416
chlorophyll-a	-0.007	0.154	0.334	-0.309	0.294

[a]Predictor labels: weekmin = weekly minimum, weekmean = weekly mean, weekmax = weekly maximum, sst = sea surface temperature (°C), temp = air temperature (°C), sal = salinity (PSU), totprec = total precipitation (mm).

4.5 Discussion

This study uses a structured MMI approach to explore and rank different environmental predictors identified in the literature as potentially important to weekly *V. vulnificus* wound infection variability in the Gulf Coast region of the United States. Our results suggest that both air temperature and SST are key environmental drivers of weekly variability in *V. vulnificus* wound infections in this region, however, seasonal factors alone appear good predictors of *V. vulnificus* disease.

Both sea surface temperature and air temperature variables had statistically significant coefficient estimates and demonstrated the greatest relative importance of all environmental predictors. Models with a single temperature parameter in addition to baseline variables generated the lowest average AIC_c scores and therefore explained the greatest amount of variation in weekly *V. vulnificus* infections. These models support studies that note a greater number of *V. vulnificus* cases in warm summer periods (Baker-Austin and Oliver, 2018). Significance of both temperature variables at the weekly time scale suggests the importance of weekly temperature for *V. vulnificus* wound infections beyond monthly variability, which was accounted for in the models. However, as air temperature and SST are highly correlated, it is not possible to unpick the mechanism of temperature's impact on *V. vulnificus* infections.

Possible pathways that increase the likelihood of infection include an increased density of *V. vulnificus* bacterial cells in response to higher water temperature. The short generation times of *Vibrio* spp. bacteria (Eagon, 1962; Ulitzur, 1974) coupled with temperature upshifts can lead to rapid accumulation of bacterial cells in coastal bathing waters, increasing risk to bathers (Ruppert et al., 2004). As well as increased abundance, it is suggested that temperature affects the infectious capability of *V. vulnificus* (Hernández-Cabanyero et al., 2020). From a human behaviour perspective, warm air temperatures have been associated with increased coastal recreation (Elliott et al., 2019; Morgan and Ozanne-Smith, 2013) including increased coastal bathing (Morgan and Ozanne-Smith, 2013) thus weeks with higher-than-average air temperature could be associated with higher levels of human exposure. However, we are unable to untie the importance of different temperature-related mechanisms for *V. vulnificus* infections at the weekly scale with the current data.

Despite the strong relative importance of temperature variables, a baseline model incorporating month, year and holiday variables exhibited good predictive power with an

AUC of 0.816, just 0.002 less than that of the SST model and 0.001 less than the AUC of the air temperature model. This implies that the seasonal pattern of *V. vulnificus* infections is captured by dummy month variables within the model, enabling good predictive power without the requirement of environmental variables. A model built with these baseline variables may be useful for generating predictions of *V. vulnificus* infection risk in similar locations where environmental data are difficult to obtain. Nevertheless, it is important to note that outside of the Gulf of Mexico US coastline, other states may observe different results using the same modelling analysis.

A model based on seasonal factors alone may not be as helpful in regions that experience greater interannual variability in temperature and other environmental conditions that may differ from the seasonal pattern in *V. vulnificus* wound infections experienced by Gulf of Mexico states. In fact, linear models reveal that along the Gulf of Mexico coastline used in this study, monthly dummy variables explained 82% of the variability in the mean weekly air temperature variable (temp weekmean) whilst along the Atlantic Coast of the US, only 68% of air temperature variation is explained by month (see Table S9 and Table S10). This also indicates the challenge of isolating the effect of temperature from its seasonal pattern present in monthly dummy variables, especially in this coastal region.

V. vulnificus bacteria prefer low salinity (<25 PSU) environments such as brackish estuarine waters (Noorian et al., 2023); however, salinity was not found to be a statistically important parameter in weekly *V. vulnificus* infection variability. This lack of statistical importance may be partly explained by the low levels of variability in weekly salinity observed in our dataset (see Figure S12). This was especially noted for the Gulf Coast of Florida, where ~50% of infections (354/711) were reported over the study's time range (1993-2018). The oceanographic data used are 0.083º (~9 km) resolution gridded reanalysis data whereby observational data are incorporated into computer models. The gridded nature of these data means that small-scale spatial changes in salinity that can occur across the coastal zone (e.g., within inlets, bays, and estuaries) are aggregated into the coarser resolution grid cells, meaning some loss of granularity in the values. Data were also averaged spatially across the coastline of each state weighted by population count to account for uncertainty in exposure location. As a result, weekly salinity values reflect broad trends along the most populated areas of the coastline of each state and may not pick up variation at the smaller geographic scale.

We hypothesised that precipitation may reduce coastal salinities which could encourage *V. vulnificus* growth and increase the likelihood of infection or, alternatively, reduce

coastal bathing (as found by Morgan and Ozanne-Smith (2013) in an Australian coastal setting) and therefore exposure which could have a decreasing impact on infections. However, precipitation was not found to significantly influence *V. vulnificus* wound infection variability. The precipitation data reveal high week-to-week variability and no clear seasonal trends, emphasising the stochasticity of this environmental factor (see Figure 4.2).

This analysis did not find hurricane landfalls to have a significant contribution to the variability in weekly *V. vulnificus* infections above the effects of the weather and oceanographic factors explored. This was surprising given the cases of *V. vulnificus* associated with hurricanes Katrina (CDC, 2005) and Ian (Sodders et al., 2023). However, *V. vulnificus* infection risk may depend on the specific characteristics of the hurricane landfall event e.g., demographic characteristics of the impacted population, healthcare access in the aftermath, extent of coastal flooding. For instance, although Hurricane Katrina made landfall as a category 3 hurricane, storm surges >25 ft in height combined with failure of the levee system in New Orleans resulted in 80% of the city flooding (Knabb et al., 2023; Sodders et al., 2023). Such widespread coastal flooding in combination with an elevated risk of cuts and grazes from debris would have resulted in especially high levels of human exposure to *V. vulnificus* bacteria present.

Extremely high storm surges reaching 12-18 ft were also documented during Hurricane Ian, which made landfall as a category 4 hurricane and was associated with 29 *V. vulnificus* cases (Sodders et al., 2023). In contrast, just 6 vibriosis cases were associated with Hurricane Irma which also made landfall in Florida as a category 4 hurricane, but resulted in lower storm surge heights of 5-6 ft (Sodders et al., 2023). This information alludes to the complexity of factors that may influence the *V. vulnificus* health burden of hurricanes events which are likely not captured by the binary hurricane landfall impact variable included in our modelling analysis.

Additionally, the Atlantic hurricane season runs from 1st June to 30th November (NOAA, 2023a), overlapping with summer months during which most *V. vulnificus* infections occur (May to October;), therefore, the upstream environmental impacts of hurricanes are likely incorporated into the seasonal and environmental components of the model. Despite absence of a statistically significant association with hurricane landfall in our analysis, coastal flooding following a hurricane remains a *V. vulnificus* safety concern for residents as brackish floodwaters can provide ideal growth conditions for this pathogen (Rhoads, 2006).

Variables representing the two different modes of the ENSO climate phenomenon were included in the modelling analysis: El Niño and La Niña. During El Niño, winter conditions in the Gulf Coast states are cooler and wetter due to changes to the jet stream (Lindsey, 2017). Despite more severe weather and increased rainfall leading to a greater risk of flooding in south-eastern coastal states, Atlantic hurricane activity is reduced during El Niño (Bell and Chelliah, 2006). Conversely, La Niña is conducive to greater Atlantic hurricane activity but also warmer, drier winter weather overall (Bell and Chelliah, 2006; Lindsey, 2017).

Neither ENSO mode had a significant impact on weekly *V. vulnificus* infection variability overall. This result agrees with previous work by Logar-Henderson et al. (2019) who demonstrate increased risk of vibriosis in association with a yearly average of NOAA's multivariate ENSO Index (MEI) both across the US nationally and along the Pacific Coast but find no significant association with vibriosis reported along the Gulf and Atlantic Coasts. Alternatively, changes in weather conditions related to ENSO may have been accounted for by the seasonal and temperature variables present. The strength of the ENSO mode, as indicated by the numerical ONI value or alternative ENSO indices, could be explored in future work in addition to different lag periods between ENSO events and *V. vulnificus* infections.

Further variables explored also include chlorophyll-a (a proxy for phytoplankton density) and zooplankton biomass. Inclusion of these variables in the analysis was based on ecological associations of phytoplankton and zooplankton with greater *V. vulnificus* bacterial abundance (Brumfield et al., 2023a; Eiler et al., 2007; Greenfield et al., 2017; Turner et al., 2014) which may precede human infections. However, neither variable was found to significantly explain weekly variability in *V. vulnificus* infections. Several studies indicate that relationships between *Vibrio* spp. bacteria and plankton are complex and species-specific (Diner et al., 2021; Turner et al., 2014, 2009). Unfortunately, species-specific relationships are not captured by the upper taxonomic level data available in a spatially and temporally continuous gridded format, so a lack of significance may be related to this issue.

Data availability was a key challenge to this analysis. The rarity of *V. vulnificus* wound infections and limited temporal range of high-resolution environmental data restricted the amount of data available for constructing models. The choice of a logistic regression model was based on the small variability in number of weekly cases per state in the dataset and the high number of weeks with zero cases which may have led to overdispersion in a count-based model. To improve the reliability of results despite the

reduced sample size as a result of the rarity of *V. vulnificus* infections, 100 subsets of the data were randomly drawn. Model sets were run on each data subset and metrics averaged to ensure that models were ranked based on their performance on all 100 subsets. The reduced amount of *V. vulnificus* data available was an unavoidable limitation of the analysis due to the opportunistic nature of this pathogen but steps were taken to increase the robustness of model results.

Another limitation of this study was the use of state-wide spatial averages of environmental conditions due to uncertainty in the location of human exposure resulting in disease transmission. The counties of all reported infections were within 200 km of the coastline but the exact point of exposure on the coastline was unclear in many cases. Using large spatial averages will have somewhat reduced the variability in the environmental data used for modelling. Consequently, some variables that may have effects at the county-level may not have been picked up as important within the state-wide analysis. Environmental state-wide averages were weighted by population count to reflect values along the coastline with potentially greater human exposure, but alternative human activity data (e.g., smartphone-GPS data such as in Filazzola et al., 2022) could have been used here if freely and easily accessible.

Overall, this study offers the first attempt to explore a range of potential environmental drivers of weekly *V. vulnificus* infection variability using a MMI approach. Although temperature is frequently associated with *Vibrio* spp. bacteria and infections, we use a structured, quantitative approach that ranks the relative importance of temperature variables alongside other tentatively important environmental parameters. Our finding that a model containing seasonal parameters alone has good predictive power suggests that predictive models of weekly *V. vulnificus* infection risk could be straightforward to implement for Gulf Coast US states. Future research may include repeating this analysis on Atlantic Coast states where different environmental conditions and patterns of variability may yield different results. The inclusion of lag periods for some variables, especially those hypothesised to have an indirect impact on the variability of *V. vulnificus* wound infections i.e., El Niño, La Niña, chlorophyll-a and zooplankton biomass could also be explored in future work.

5 An environmental investigation of *Vibrio* spp. abundance and isolation of potentially pathogenic *Vibrio* spp. in a UK coastal hotspot during summer months

5.1 Abstract

Non-cholera *Vibrio* spp. infections are an emerging threat to human health in Northern Europe. High numbers of infections have been reported in countries bordering the Baltic Sea during recent heatwave years due to the sensitivity of these pathogens to temperature but, at present, *Vibrio* spp. infections are believed to be extremely rare in the UK. This study records the abundance of *Vibrio* spp. bacteria within a UK coastal lagoon over a 10-week period in the summer of 2022 and investigates potential associations with environmental parameters including water temperature, salinity, and pH. High *Vibrio* spp. abundance of up to 1.03 x10^5 CFU/100ml was recorded but no significant correlations with environmental parameters were found. A collection of 325 isolates from water samples were identified using matrix-assisted laser desorption/ionisation time-of-flight (MALDI-TOF) mass spectrometry (MS), polymerase chain reaction (PCR) and 16S ribosomal RNA (rRNA) gene sequencing. The presence of potentially pathogenic *Vibrio* species was confirmed; strains belonging to three of the four key human pathogenic species: *V. alginolyticus*, *V. parahaemolyticus* and *V. cholerae* were recovered and represented 142 of 325 isolates (44%). Continued sea surface temperature warming with climate change could increase the suitability for *Vibrio* spp. pathogens in UK waters therefore more research is needed to determine the key environmental influences on *Vibrio* spp. abundance and assess the risk to human health in this region.

5.2 Introduction

Non-cholera *Vibrio* spp. (henceforth '*Vibrio* spp.') pathogens are climate-sensitive marine bacteria that represent an emerging risk to human health in Northern Europe (Baker-Austin et al., 2017, 2013) (see section 1.1 for overview). There are two key routes of disease transmission; foodborne infections are acquired through the consumption of contaminated undercooked seafood whilst wound infections develop from bacterial colonisation of a cut or wound when exposed to the pathogen in seawater (Baker-Austin et al., 2018). Due to pathogenic *Vibrio* species' affinity for warm (>18 °C), low salinity (<25 PSU) waters (Vezzulli et al., 2015), *Vibrio* spp. infections have historically been associated with subtropical locations such as the Gulf of Mexico (Newton et al., 2012; Strom and Paranjpye, 2000; Weis et al., 2011). Yet, recent decades have witnessed increasing reports of *Vibrio* spp. infections at higher latitudes in temperate regions, including Northern Europe (Baker-Austin et al., 2016, 2013), Alaska (McLaughlin et al., 2005), Chile (González-Escalona et al., 2005) and the Northeast United States (Archer et al., 2023; King et al., 2019).

To date, *Vibrio* spp. infections reported in Europe have predominantly resulted from exposure to the low salinity waters of the Baltic Sea (Baker-Austin et al., 2016; Brehm et al., 2021a; Gildas Hounmanou et al., 2023). Here, rapidly rising sea surface temperatures in response to climate change are considered key to the emergence and unprecedented numbers of wound infections reported in countries bordering the Baltic Sea, particularly Sweden, Finland, Denmark and Germany (Baker-Austin et al., 2016; Brehm et al., 2021a; Ebi et al., 2017; Gildas Hounmanou et al., 2023). Between 2010 and 2018, 638 *Vibrio* spp. infections were reported in Denmark (Gildas Hounmanou et al., 2023). Notably, around a quarter of these cases were reported in 2018 alone; a heatwave year which saw increased *Vibrio* spp. incidence in many Baltic Sea countries totalling 445 cases across Norway, Denmark, Sweden, Finland, Poland and Estonia which surpassed the record 272 total reported *Vibrio* spp. cases set across these countries during the previous 2014 heatwave (Amato et al., 2022). Although less frequent, *Vibrio* spp. wound infections have also been reported on the North Sea coastlines of Denmark, Germany and The Netherlands (Brehm et al., 2021b; Gildas Hounmanou et al., 2023; Schets et al., 2011, 2006), highlighting that *Vibrio* spp. risk in Europe is not limited to the Baltic Sea. Despite the higher salinity of the North Sea compared to the brackish Baltic Sea (Lehmann et al., 2022), low salinities suitable for

pathogenic *Vibrio* spp. growth still exist in near-shore estuarine environments along North Sea coastlines (Fleischmann et al., 2022; Huehn et al., 2014).

At present, few domestically acquired *Vibrio* spp. infections have been reported in the United Kingdom (UK) (Hartley et al., 1991; Hooper et al., 1974; Reilly et al., 2011); most UK *Vibrio* spp. cases are associated with travel outside of the country (Baker-Austin et al., 2020). However, the current and future risk of infections is highlighted by several recent studies that confirm the presence of potentially pathogenic *Vibrio* species in UK waters (Ford et al., 2020; Harrison et al., 2022), including a pandemic strain of *V. parahaemolyticus* (Powell et al., 2013). However, it is important to note that the presence of these bacteria alone does not necessarily result in local human infections. For example, potentially pathogenic *Vibrio* species have been isolated from waters off the east coast of Canada (Badley et al., 1990), yet, to the best of our knowledge, there are currently no reports of seawater-associated *Vibrio* spp. wound infections in this region present in the available literature. Nevertheless, *V. vulnificus* wound infections have been reported further northwards over time along the east coast of North America and further expansion of the infection distribution into non-endemic locations within the Northeast United States is predicted with climate warming (Archer et al., 2023). This highlights the need to monitor *Vibrio* spp. risk to human health in locations where potentially pathogenic *Vibrio* species are present. Worryingly, UK sea surface temperatures have warmed significantly by around 0.3°C per decade over the last 40 years, with strongest surface warming trends in the southern North Sea (Cornes et al., 2023). This spatially overlaps with where Harrison et al., (2022) found water temperatures exceeding 18°C, and therefore suitable for *Vibrio* spp. growth, to occur for up to 70 days per year on average between 2015-2017. Presence of potentially pathogenic *Vibrio* spp. combined with continued warming of UK sea surface temperatures expected with climate change (Cornes et al., 2023) stresses the need to examine *Vibrio* spp. risk in the UK.

In locations where *Vibrio* spp. are endemic, strategies to reduce *Vibrio* spp. concentrations in seafood (e.g., UV-sterilised water depuration (Phuvasate *et al*., 2012) and bacteriophage application (Zhang et al., 2018)) are being developed. Nevertheless, *Vibrio* spp. bacteria cannot be removed from the coastal waters in which they naturally occur. Instead, management of *Vibrio* spp. wound infection risk must centre around enhanced monitoring and forecasting of *Vibrio* spp. in coastal waters, as well as epidemiological surveillance and increased awareness within risk groups. The UK is able to investigate the potential risk of *Vibrio* spp. infections and plan appropriate mitigation

actions prior to *Vibrio* spp. potentially emerging as a notable health risk as seen within the Baltic Sea region of Northern Europe. In line with this, Ford et al., (2020) conducted the first ecological and genomic study of *Vibrio* spp. in the UK over the summers of 2018 and 2019. A coastal lagoon in the Southwest UK was chosen for its warm, shallow brackish waters to provide insight into *Vibrio* spp. populations in the UK where conditions are suitable for their growth. Ford et al., (2020) recorded a peak water temperature of 32.1°C and levels of *Vibrio* spp. abundance up to 10^5 colony forming units (CFU) per 100ml. Concerningly, this maximum level of *Vibrio* spp. abundance is comparable to that found in some North Sea coastal areas of The Netherlands where *Vibrio* spp. infections have been reported in previous years (Schets et al., 2011, 2006; Sterk et al., 2015). However, this magnitude of *Vibrio* spp. abundance was only present in one week during the summers of 2018 and 2019 at the study location, which is considered a hotspot for *Vibrio* spp. bacteria (Ford et al., 2020). The rarity of pathogenic *Vibrio* species at high abundances in both space and time which also coincide with human exposure may be one reason why *Vibrio* spp. infections remain highly uncommon in the UK, but further studies of *Vibrio* spp. abundance and virulence in more UK coastal environments are needed. Yet, even with additional environmental sampling data, the actual number of *Vibrio* spp. illnesses is not known. Individuals with mild, self-limiting infections are not likely to seek medical attention but, even if medical testing and treatment is required, *Vibrio* spp. disease is currently not notifiable to the UK Health Security Agency. All these factors imply that infections are underreported.

Understanding which environmental factors influence *Vibrio* spp. abundance in the UK is a first step towards identifying other 'hotspot' locations with elevated *Vibrio* spp. risk. Temperature and salinity are regularly identified as important drivers of *Vibrio* spp. bacterial abundance in ecological sampling studies (Froelich et al., 2013; Takemura et al., 2014; Turner et al., 2009; Vezzulli et al., 2009; Wetz et al., 2014) and therefore have been used to produce *Vibrio* spp. risk map tools in multiple locations. In the United States, the ecology of *Vibrio* spp. bacteria has been explored in locations such as the Chesapeake Bay in Maryland and the Neuse River Estuary in North Carolina, to develop predictive models of *Vibrio* spp. abundance to inform monitoring efforts and anticipate increased *Vibrio* spp. risk (Froelich et al., 2013; Jacobs et al., 2010). Meanwhile, in Northern Europe, an existing tool for *Vibrio* spp. risk prediction is the ECDC *Vibrio* Map Viewer (ECDC, 2016) which is an excellent resource for predicting suitable water temperature and salinities for *Vibrio* spp. growth in the Baltic Sea (Semenza et al., 2017). Although the ECDC *Vibrio* Map Viewer risk output can be seen for UK waters, development of a UK-specific model would offer more reliable predictions across UK

coastlines. Both near-term and far-term predictions could be generated to allow the identification of coastal hotspots predicted to exhibit high levels of future *Vibrio* spp. abundance and therefore where efforts to increase awareness of *Vibrio* spp. disease could be targeted. The identification of high *Vibrio* spp. risk locations could also inform where to conduct enhanced shellfish testing as high *Vibrio* spp. abundance in bivalves, such as oysters, may pose a challenge to the shellfish industry through the risk of foodborne illnesses. Yet so far there has been little attempt to investigate the environmental drivers of *Vibrio* spp. abundance in UK waters.

In this study, we investigate *Vibrio* spp. abundance and its potential associations with environmental parameters within the same coastal lagoon hotspot in the Southwest UK as used by Ford et al. (2020). The identity of the coastal lagoon is kept anonymous in agreement with the sampling permit and is henceforth referred to as 'Lagoon X'. A large collection of isolates are identified with molecular methods, including MALDI-TOF MS, PCR and 16S rRNA gene sequencing which confirm the presence of potentially pathogenic *Vibrio* species in this UK coastal hotspot. Given the further warming of UK waters (Cornes et al., 2023) and increased frequency of UK heatwave events expected with climate change (Christidis *et al*., 2020), more research into *Vibrio* spp. as a potential future human health risk in the UK is needed.

5.3 Methods

5.3.1 Sampling sites

Three sampling locations were used along the length of 'Lagoon X', a shallow coastal lagoon located in Southwest England (see Figure 5.1). There is limited freshwater input at one end of the Lagoon via several freshwater streams and seawater intrusion at the other where the Lagoon meets full strength seawater (see Figure 5.2). This results in varying salinity across the sites. Site A is located near the freshwater input which dilutes the water to brackish conditions. Site B is shallow in depth and therefore exhibits strong salinities during times of increased evaporation. Site C is closest to seawater influx. These sites are the same as described in Ford et al. (2020) which enables comparison to previous years' results.

Water samples of 1 litre volume were collected in duplicate at low tide at each sampling site along Lagoon X once a week on the same day (where possible) between 14th July 2022 and 13th September 2022. Given that *Vibrio* spp. bacteria prefer warm water

temperatures, this summer period was chosen with the aim of recording peak *Vibrio* spp. abundance. The samples were obtained using 1 litre plastic bottles fixed to a 3-metre-long collection pole. Each bottle was rinsed three times in the Lagoon water to the side of the collection spot to avoid disturbing the sediment near where the water sample was to be collected. Water samples were taken just below the surface of the water.

In situ water temperature and salinity was recorded at time of sampling using a conductivity, temperature, and depth (CTD) instrument which was attached to the end of the sampling pole. Measurements of pH were taken using a hand-held pH-meter within the sample bottle immediately after water sample collection. All environmental measurements were repeated three times to account for measurement uncertainty. Samples were transported on ice back to the laboratory within 3 hours and microbial analyses took place within 24 hours.

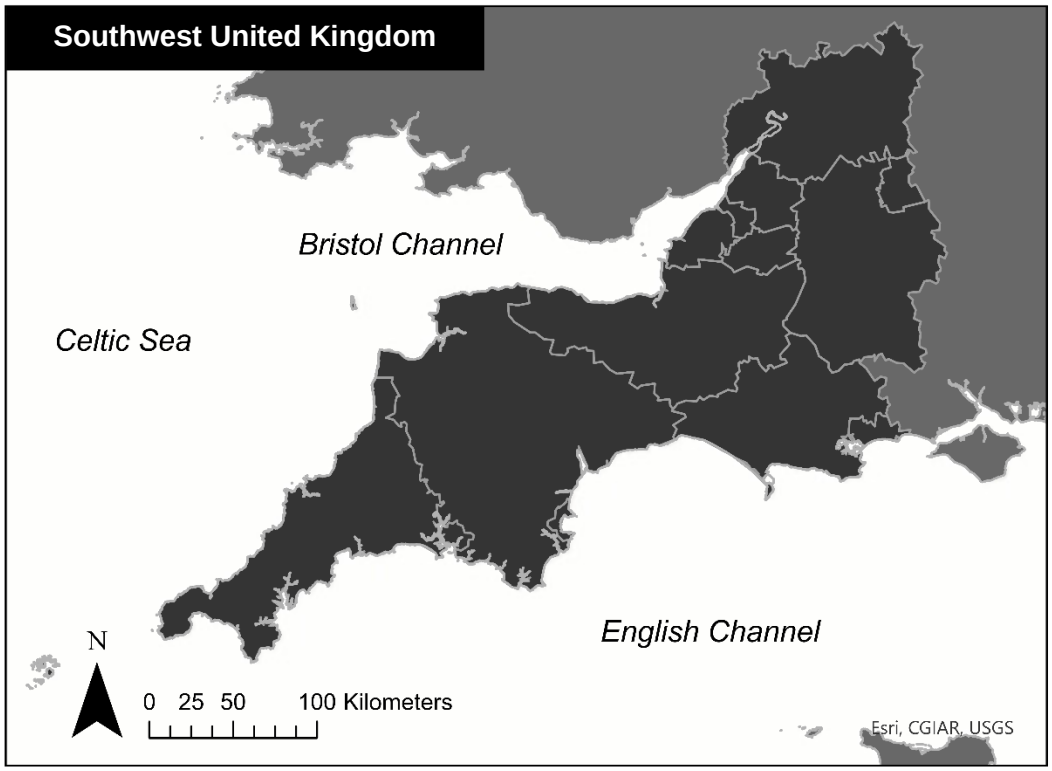

Figure 5.1 Generalised location of anonymous coastal lagoon study site in the Southwest United Kingdom.

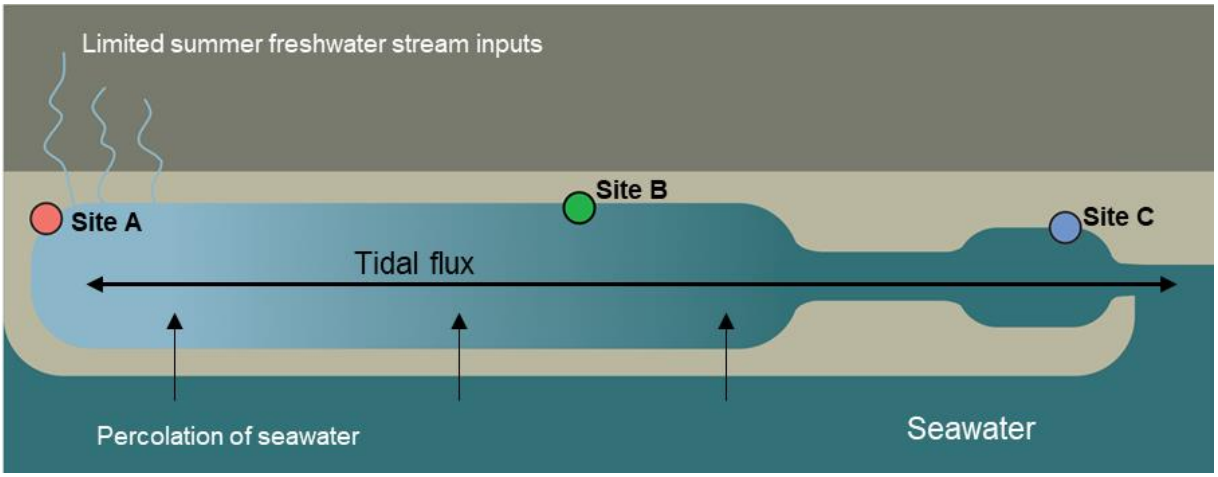

Figure 5.2 Schematic of coastal lagoon study site in Southwest United Kingdom.

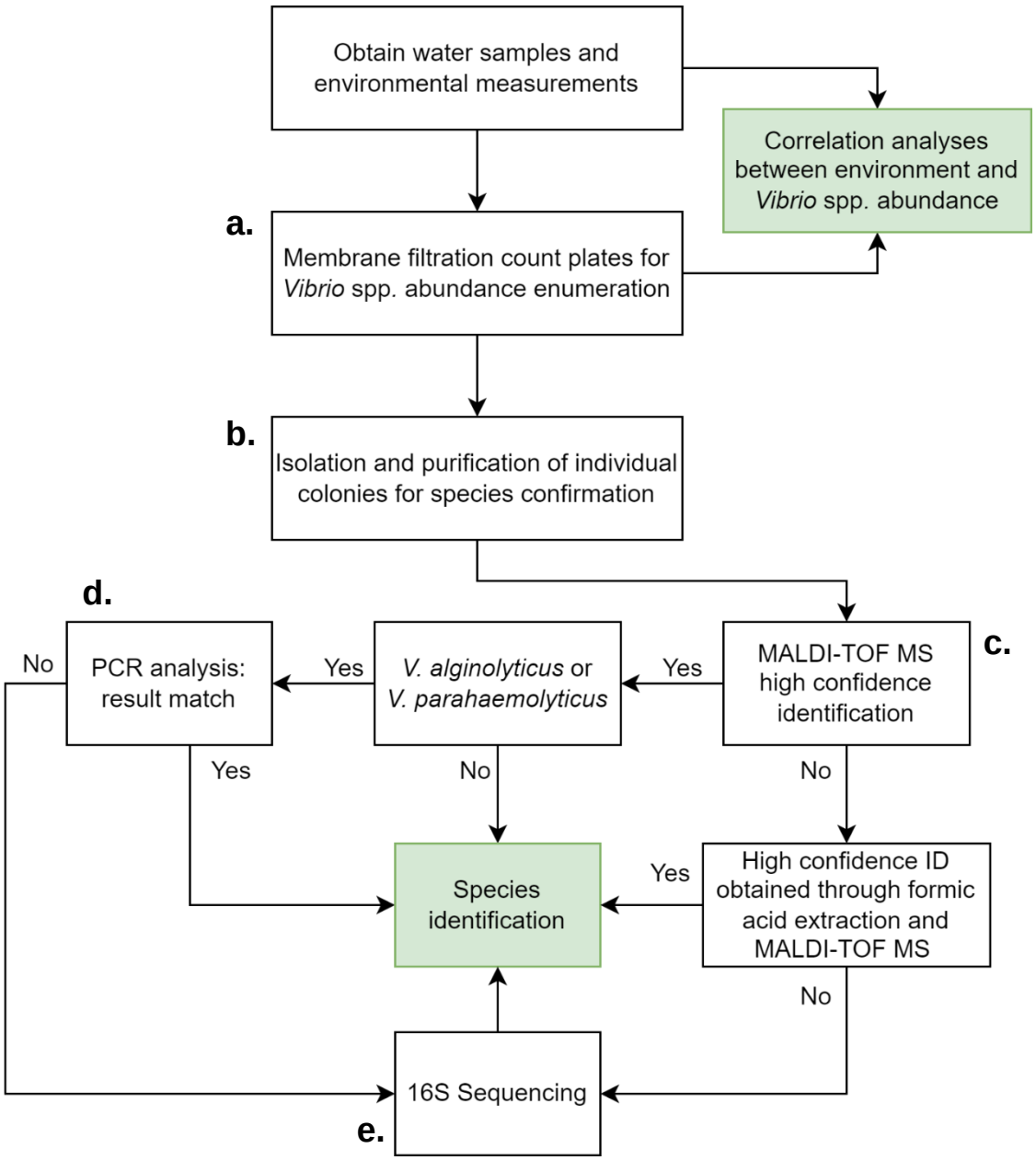

Figure 5.3 Method workflow from collection of water samples to end points (highlighted in green): correlation analyses between environmental parameters and *Vibrio* spp. abundance; identification of bacterial species present. Steps labelled a-e are referred to within the text.

5.3.2 Culture-dependent microbial analysis

Culture-dependent microbiological techniques were used to estimate *Vibrio* spp. abundance in the collected water samples for correlational analyses with environmental parameters. Individual colonies from count plates matching the morphology of potentially pathogenic *Vibrio* species (*V. parahaemolyticus*, *V. vulnificus, V. cholerae*, *V. alginolyticus*) were isolated and grown in pure culture for species identification with molecular techniques (see section 5.3.3). A flowchart documenting the stages of analysis is presented in Figure 5.3 for clarity.

a. Membrane filtration plate counts for Vibrio spp. enumeration

Enumeration of *Vibrio* species present in the water samples used procedures set out in the BSI Standard publication and Ford et al. (2020). For each replicate water sample, subsamples of different volumes (1, 10 and 100 ml) were filtered through a 0.45 µm pore membrane, using a vacuum pump, which was then placed onto ChromID *Vibrio* (VID) agar (Biomériux, Marcy l'Etoile, France) using sterile forceps. This process was repeated for Thiosulfate Citrate Bile Sucrose (TBCS) agar (Oxoid, UK). Both sets of plates were incubated at 37°C for 18 hours.

After incubation, the number of presumptive *Vibrio* spp. colony forming units (CFU) on each plate within the readable range (30-300 colonies) was counted using colony morphology and colour for identification of *Vibrio* species. The CFU per 100 ml water (CFU/100ml) was subsequently calculated.

b. Isolation and purification of isolates

For weeks 1 to 9 (sampling dates: 14/07/2022 to 06/09/2022), individual selected colonies were isolated and grown in pure culture for later species confirmation using molecular methods (see section 5.3.3). Where available, a minimum of two colonies from each morphology (TCBS: small-green, large-green, small-yellow, large-yellow and VID: blue-purple, blue with halo, creamy, pink-orange) from each site were sub-cultured for purity by streak-plating onto their respective agar type. Purification plates were incubated for 18 hours at 30°C. After incubation, a 10µL loop of pure culture was inoculated onto protect beads (Technical Service Consultants Ltd, UK) which were stored at -80°C for later species confirmation with molecular methods (see section 5.3.3).

5.3.3 Molecular methods for species confirmation

Molecular methods were used to confirm the species identification of the isolates collected. Matrix assisted laser desorption/ionization time-of-flight (MALDI-TOF) mass spectrometry (MS) is a relatively new method for identifying *Vibrio* spp. that gives a level of confidence with each result (see below section for details). PCR, a long-established technique used to confirm the presence of a species-specific gene, was conducted on isolates identified as *V. parahaemolyticus* and *V. alginolyticus* by MALDI-TOF MS to check the validity of these 'high confidence' results. PCR was also used to check for the presence of virulence-associated genes *tdh* and *trh* which encode production of virulence factors thermostable direct hemolysin (TDH) and TDH-related hemolysin (TRH) in *V. parahaemolyticus* (Ceccarelli et al., 2013). For those MALDI-TOF MS results that were low confidence, the isolate was sent for 16S rRNA sequencing to confirm species identification.

c. MALDI-TOF MS

MALDI-TOF MS was used to confirm the bacterial species identification. In preparation for MALDI-TOF MS analysis, isolates were grown from inoculation of a single protect bead onto saltwater agar (SWA) and incubated overnight at 30°C.

Using a sterilised toothpick, a sample of a single colony from each plate was directly transferred to the target well of a 96-well target plate. After the initial spot, a second spot was applied immediately after, without further sample being collected. This double-spot method was used to reduce the amount of sample in the target well with the aim to increase accuracy; MALDI-TOF MS requires an especially small amount of sample. This process was performed in duplicate for each isolate. A 1 µL volume of HCCA matrix solution was applied to each spotted sample on the target plate and dried at room temperature before MALDI-TOF MS analysis on the Bruker MALDI Biotyper (www.bruker.com). Each resultant species identification was accompanied by a level of confidence (log score) between 0.0 and 3.0 generated by MBT Compass HT software (www.bruker.com). A log score of ≥2.0 indicates an identification to species-level (also described in Mougin et al. (2020) and Moussa et al. (2021)). Isolates with a best match species identification log score of <2.0 (indicating low confidence identification) were reanalysed using the extended direct transfer method, as per the manufacturer's instructions.

For the extended direct transfer method, the sample double-spot procedure was repeated as detailed above followed by a formic acid extraction. A 1 µL volume of 70%

formic acid was applied to the sample in each target well and allowed to dry at room temperature before application of the HCCA matrix. If a high confidence species identification could not be obtained after the extended direct transfer method was applied, the isolate was sent for 16S rRNA gene sequencing.

d. Conventional PCR for species confirmation

All isolates confidently identified as *V. alginolyticus* or *V. parahaemolyticus* using MALDI-TOF MS were also tested using conventional polymerase chain reaction (PCR).

Isolates were grown on marine agar. A single colony was inoculated into 500 µL of molecular grade water in a 1.5ml tube and boiled at 95°C for 5 minutes. This step was repeated for positive control samples (*V. parahaemolyticus* reference strain NCTC 10885; *V. alginolyticus* reference strain NCTC 12160) and the negative control (molecular grade water). Species-specific primers were used to confirm the species identification via PCR (see Table 5.1).

Mastermix was prepared containing per reaction: 10 µl Green GoTaq flexi reaction buffer (Promega), 5 µl MgCl2, 0.625 µl dNTPs, 0.5 µl forward primer, 0.5 µl reverse primer, 30.625 µl molecular grade water, 0.25 µl GoTaq G2 flexi DNA polymerase (Promega). PCR reactions were conducted in a 500 µl tube containing 5 µl of bacterial suspension and 45 µl of mastermix. Thermocycler programmes for *toxR* and *alg* can be found in Table 5.2 and Table 5.3, respectively.

PCR products were run on a 2 % agarose gel containing 1.0 µg/ml ethidium bromide, at 120 V for 30 minutes to visualise the PCR results.

Table 5.1 Primer sequences used for *V. parahaemolyticus* (toxR) (Kim et al., 1999) and *V. alginolyticus* (Alg) (Luo and Hu, 2008) PCR assays.

Primer	Sequence
toxR (forward)	5`- GTCTTCTGACGCAATCGTTG -3`
toxR (reverse)	5`- ATACGAGTGGTTGCTGTCATG -3`
Alg (forward)	5`- TCAGAGAAAGTTGAGCTAACGATT -3`
Alg (reverse)	5`- CATCGTCGCCTGAAGTCGCTGT -3`

Table 5.2 Thermocycler programme for toxR *V. parahaemolyticus* PCR assay.

N Cycles	Temperature (°C)	Time (min)
1	94	3
30	94	1
	58	1
	72	1
1	72	5

Table 5.3 Thermocycler programme for Alg *V. alginolyticus* PCR assay.

N Cycles	Temperature (°C)	Time (min)
1	94	4
31	94	0.5
	64	0.5
	72	1
1	72	8

Conventional PCR for presence of the tdh and trh gene in V. parahaemolyticus

Conventional PCR for haemolysin genes *tdh and trh* were carried out on all confirmed *V. parahaemolyticus* strains essentially as previously described (Bej et al., 1999) and briefly comprised of 30.62µL nuclease-free water, 0.72µL dNTPs, 10µL GoTaq Flexi Buffer, 5µL $MgCL_2$, 0.58µl *tlh* forward and reverse primers (µM) 0.25µl GoTaq Flexi G2 DNA Polymerase. The thermal cycle protocol for both *tdh* and *trh* assays can be found in Table 5.5. Samples were separated on 2% agarose gels and subjected to a 120V, 400mA electrophoresis run for 25-35 minutes.

Table 5.4 Primer sequences for *tdh* (Nishibuchi M and Kaper J B, 1985) and *trh* (Honda et al., 1991) PCR assays.

Primer	Sequence
tdh (forward)	5`- GTAAAGGTCTCTGACTTTTGGAC -3`
tdh (reverse)	5`- TGGAATAGAACCTTCATCTTCACC -3`
trh (forward)	5`- TTGGCTTCGATATTTTCAGTATCT -3`
trh (reverse)	5`- CATAACAAACATATGCCCATTTCCG -3`

Table 5.5 Thermocycler programme for *tdh* and *trh* PCR assays.

N Cycles	Temperature (°C)	Time (min)
1	94	3
30	94	1
	58	1
	72	1
1	72	5

e. 16S rRNA Gene Sequencing

The PCR reactions were performed in a 50 µl volume containing 2.5 µl cDNA samples in reaction volumes of; 0.5 µl of 25 mM dNTPs, 10 µl 5x green GoTaq flexi buffer, 5 µl of 25 mM MgCl2, 0.25 µl GoTaq G2 Flexi DNA Polymerase (Promega), 0.5 µl of forward and reverse primer at 10 pmol, and 30.75 µl of molecular grade water. The thermocycler programme can be found in Table 5.7.

PCR products were resolved on a 2 % agarose gel containing 1.0 µg/ml ethidium bromide, at 120 V for 30 minutes, products of the expected size were excised, and the DNA purified using the freeze and squeeze method using spin modules (MP biomedicals). Both strands of the DNA were sequenced by Sanger sequencing using big dye terminator 3.1 methodology (Life technologies) using the manufacturer's recommended protocol and the sequences were analysed on a 3500xl genetic analyser

(Applied Biosystems). Consensus sequences were generated using CLC workbench 7 software.

Where different forward and reverse matches were identified, the match with the greatest similarity was used as the identification for that isolate.

Table 5.6 Primer sequences for 16S rDNA amplification (Weisburg et al., 1991).

Primer	Sequence
fD1 (forward)	5`- AGAGTTTGATCCTGGCTCAG -3`
rP2 (reverse)	5`- ACGGCTACCTTGTTACGACTT -3`

Table 5.7 Thermocycler programme for 16S rDNA amplification.

N Cycles	Temperature (°C)	Time (min)
1	94	5
30	94	1
	55	1
	72	1
1	72	10

5.3.4 Statistical analysis

Spearman's Rho Rank Correlation was used to check for correlation between each environmental parameter and *Vibrio* spp. abundance at each site independently. The Spearman's Rho Rank Correlation was used due to a small number of data points for each test (n = 10; one pair of datapoints per week per site). Each value of water temperature, salinity and pH is a mean of three repeat measurements taken at the time of sampling. Each *Vibrio* spp. abundance value is a mean of two replicate plate counts.

5.3.5 Weather conditions at sampling sites

Weather conditions at the sites between 01/07/2022 and 30/09/2022 were obtained from Visual Crossing (www.visualcrossing.com). This platform uses the integrated surface database (ISD) from NOAA and observations from local weather stations to provide daily data for a range of parameters. Daily data for the following parameters were obtained: air temperature (°C), maximum air temperature (°C), precipitation (mm), wind speed (kph), solar radiation (W/m^2) and cloud cover (%). Results for weather conditions are included in the Supplementary Material.

5.4 Results

5.4.1 Environmental conditions in Lagoon X

Week-by-week variation in mean environmental conditions across the sampling period (14/07/2022 – 13/09/2022) is presented in Figure 5.4A. All three sites had an overall mean water temperature above 20°C. Site B had the highest mean water temperature (22.67 ± 5.58°C [± 2 SD]) and recorded the maximum weekly temperature during week 2 (19/07/2022) of 26.42°C when sites A and C measured 22.50°C and 21.98°C, respectively. Water temperature at site B was also the most variable with the greatest standard deviation. Site A had an overall mean water temperature of 20.15 ± 4.28°C whilst site C measured 20.83 ± 2.68°C. Over the 10-week sampling period, the three sites displayed a similar pattern in water temperature (see Figure 5.4A). After an initial increase in week 2 (19/07/2022) and sharp decline to below 20°C in week 3 (26/07/2022), water temperatures increased again in week 4 (02/08/2022) at the beginning of August followed by a fluctuating decrease in temperature over the remaining weeks of the study. During this time, mean water temperature remained above 20°C for five consecutive weeks between 02/08/2022 and 30/08/2022 at sites B and C.

Strong differences in mean salinity were observed between sampling sites. The highest overall mean salinity of 39.12 ± 5.28 PSU was recorded at site B followed by site C with 35.68 ± 1.08 PSU, which is located where Lagoon X meets seawater (typically 35 PSU). The lowest salinities were consistently recorded at site A (mean: 28.93 ± 5.80 PSU), which is nearest to freshwater input. Throughout the sampling period, mean weekly salinity was distinct for each site. Salinity at site C showed little variation over time whilst noticeable drops in salinity were recorded at sites A (week 5; 09/08/2022) and B (week 4; 02/08/2022).

The overall mean pH measurements of all sites reflected alkaline (pH >7) conditions. Site B had the greatest mean pH of 9.24 ± 0.46 and measured consistently higher in pH than the remaining two sites over the whole study period. Sites A and C showed a similar trend in pH through time and had an overall mean pH of 8.42 ± 0.52 and 8.45 ± 0.34, respectively.

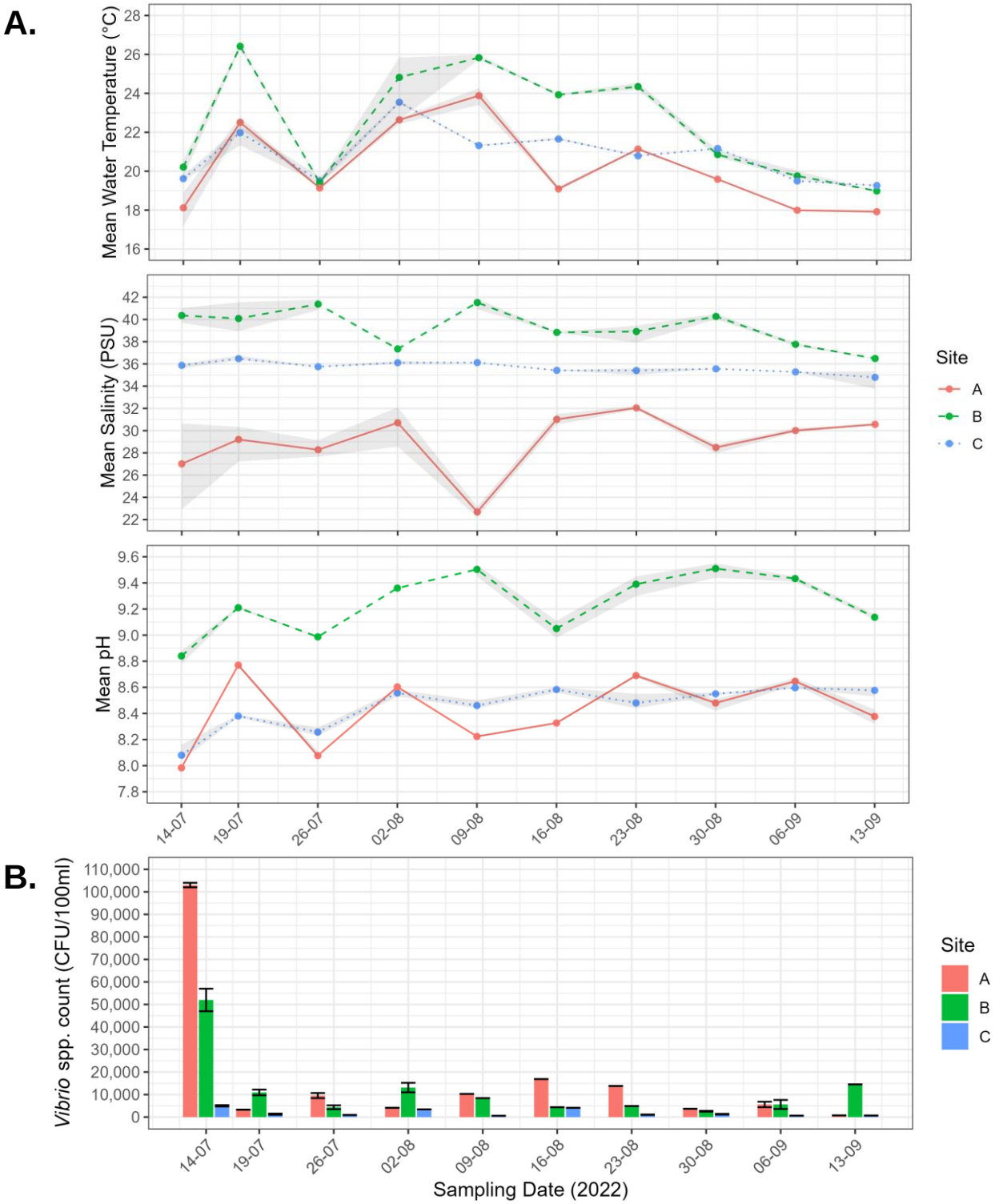

Figure 5.4 Weekly **A.** environmental conditions (mean with shaded area between minimum and maximum values to show measurement uncertainty) **B.** *Vibrio* spp. abundance (CFU/100ml) across the three Lagoon X sampling sites during 10-week sampling period (14/07/2022 – 13/09/2022). Mean with error bars to show minimum and maximum *Vibrio* spp. count.

5.4.2 Culture-dependent *Vibrio* spp. abundance

Vibrio spp. bacteria were detected using culture-dependent methods every week across the sampling period (see Figure 5.4B). Site A had the highest overall mean *Vibrio* spp. count of 2.22 $x10^4$ CFU/100ml water followed by site B at 1.30 $x10^4$ CFU/100ml. The overall mean *Vibrio* spp. abundance of site C was an order of magnitude lower than sites A and B at 1.75 $x10^3$ CFU/100ml. The maximum weekly *Vibrio* spp. abundance recorded was 1.03 $x10^5$ CFU/100ml recorded during week one (14/07/2022) at site A. All sites experienced their maximum *Vibrio* spp. count during this same week: 5.20 $x10^4$ CFU/100ml at site B and 5.00 $x10^3$ CFU/100ml at site C. Over the remaining weeks, trends in *Vibrio* spp. concentrations appear to vary independently across sites, however, sites A and B recorded consistently greater numbers of *Vibrio* spp. colonies than site C. After the initial high *Vibrio* spp. numbers recorded during week one, the number of colony forming units sharply reduced and remained below 2.00 $x10^4$ CFU/100ml, with most observations below 1.00 $x10^4$ CFU/100ml.

5.4.3 Influence of environmental parameters on *Vibrio* spp. abundance

Mean weekly *Vibrio* spp. abundance was plotted against mean environmental measurements for each sampling site and associations were assessed using Spearman's Rho Rank correlations which are presented in Figure 5.5.

Visually, the scatter plots do not appear to show any clear patterns of association between *Vibrio* spp. counts and environmental parameters which is confirmed by all non-significant Spearman's rank tests. The overall highest recorded *Vibrio* spp. count of 1.03 $x10^5$ CFU/100ml at site A during week one occurred when salinity measured 27.0 PSU and water temperature was 18.1°C; warmer water temperatures were recorded across 7 out of 9 other weeks in the sampling period and reached up to 23.9°C at this site. Site B recorded its highest *Vibrio* spp. abundance of 5.20 $x10^4$ CFU/100ml at 20.2°C and 40.4 PSU.

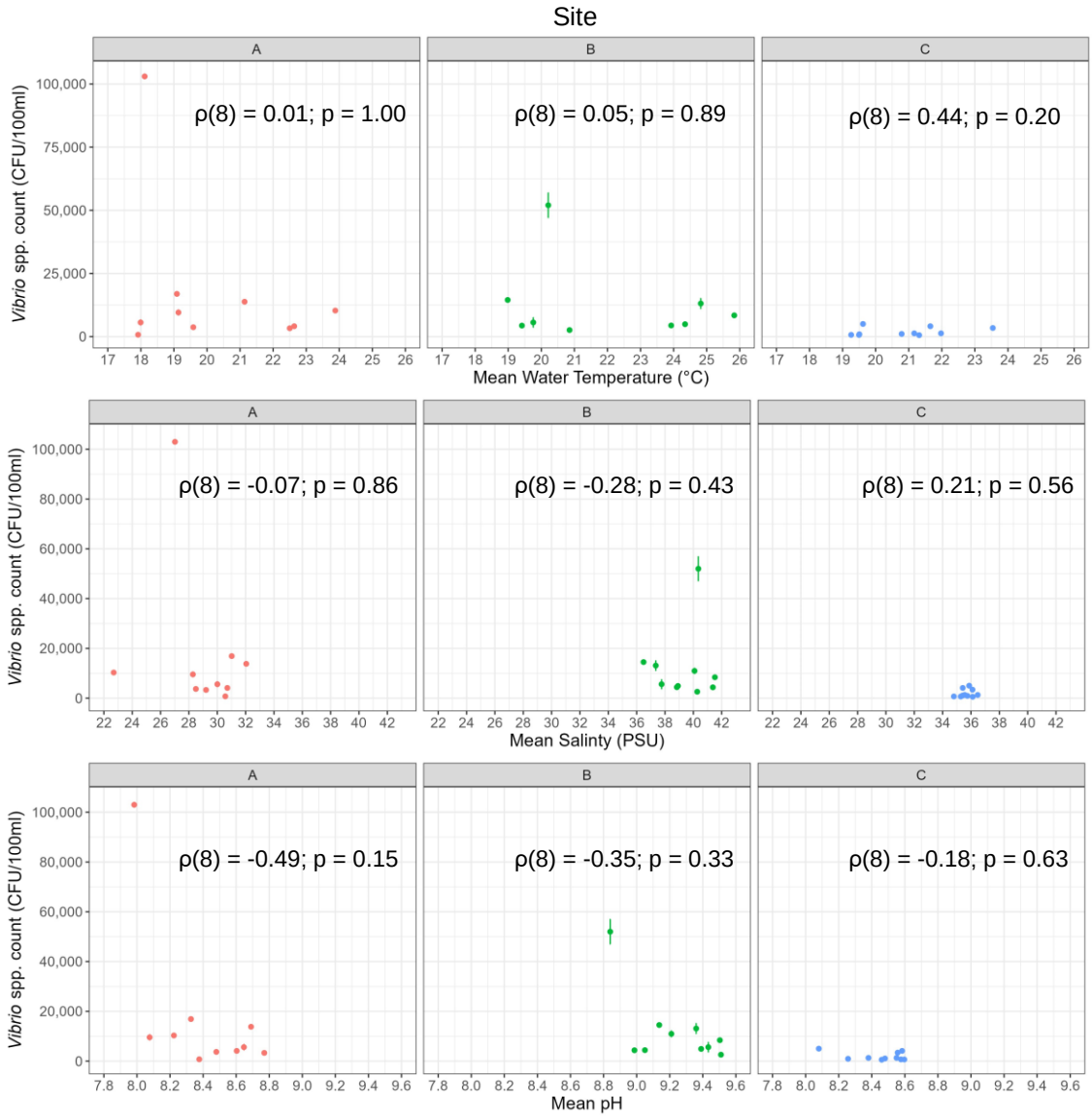

Figure 5.5 Presumptive *Vibrio* spp. counts (mean with minimum and maximum range) plotted against environmental conditions across sites A-C in Lagoon X. Results of Spearman's rank correlation displayed.

5.4.4 Isolate species identification

Performance of identification methods

Table 5.8 details the methods used to identify strains isolated from Lagoon X. A total of 335 isolates were analysed for species identification using MALDI-TOF MS. Of these, 216 isolates (65%) had a high confidence (log score ≥2.0) species identification that matched both replicates tested. One high confidence species result was obtained for 53 isolates (16%). Sixty isolates (18%) had low-confidence MALDI-TOF MS scores.

16S rRNA gene sequencing was carried out for 65 isolates (60 low confidence MALDI-TOF MS and 5 strains which returned different high confidence species identifications for the same isolate. Twenty-five (38%) were subsequently identified to species-level whilst 23 (35%) were identified as *Vibrio* spp. at genus-level (including the 5 isolates that obtained multiple high confidence scores for different species using MALDI-TOF MS).

All isolates confidently identified as *V. parahaemolyticus* and *V. alginolyticus* using MALDI-TOF MS (n = 129) were tested again with PCR which yielded 96% agreement (5 conflicting identifications). Five isolates identified as *V. alginolyticus* via MALDI-TOF MS were PCR negative for *V. alginolyticus*. Fourteen isolates with low confidence MALDI-TOF MS identifications suspected of being *V. alginolyticus* from close match results were also tested with PCR and all obtained positive results. However, upon sequencing, 1 of the 14 isolates was differentially identified as *Grimontia hollisae*. Therefore, conflicting species identifications exist for 6 out of 335 isolates (1.8%). No identification was possible for 4 of 335 isolates (1.2%). Overall, 325 isolates obtained a species identification.

Table 5.8 Breakdown of methods used to confirm identity of isolates collected.

	Identification method	N (%)
1	MALDI-TOF MS: two high confidence ID replicates in agreement	213 (63.6)
2	MALDI-TOF MS: at least one high confidence ID	51 (15.2)
3	Low confidence MALDI-TOF MS ID: identified using PCR*	13 (3.8)
4	Low confidence MALDI-TOF MS ID: identified using 16S rRNA gene sequencing	25 (7.5)
5	Low confidence MALDI-TOF MS ID: identified to genus level using 16S rRNA gene sequencing	23 (6.9)
6	Conflicting results between methods	6 (1.8)
7	No identification possible	4 (1.2)
	Total	**335**

**V. alginolyticus* and *V. parahaemolyticus* isolates only

Species Identified

Between 14/07/2022 and 06/09/2022, 20 bacterial species from 6 genera were represented across 325 isolates from Lagoon X (see Figure 5.6 and Table 5.9). *Vibrio* species made up 79% of strains identified (258/325). Twelve different *Vibrio* species were isolated including three of four key human *Vibrio* spp. pathogens: *V. cholerae* (4/325)*, V. parahaemolyticus* (21/325) and *V. alginolyticus* (117/325) which together represented 55% of *Vibrio* spp. isolates (142/258) and 44% of all isolates (142/325). *V. alginolyticus* was the most numerous bacterial species overall, making up 36% of the total isolates (117/325) and close to half of *Vibrio* spp. isolates alone (117/258; 45%). Twenty-one isolates were identified as *V. parahaemolyticus* (8% of *Vibrio* spp.; 6% overall), and 4 as *V. cholerae* (2% of *Vibrio* spp.; 1% overall). Three of the *V. parahaemolyticus* strains were PCR-positive for the *trh* gene which is associated with virulence in *V. parahaemolyticus* (Ceccarelli et al., 2013). The second most numerous species identified was *V. harveyi* with 54 isolated strains (21% of *Vibrio* spp.; 17% overall). Twenty-three isolates (9% of *Vibrio* spp.; 7% overall) were classified as *Vibrio* species, however, could not be identified to species-level.

In addition to *Vibrio,* species from the *Photobacterium, Shewanella, Exiguobacterium, Stenotrophomonas,* and *Grimontia* genera were also isolated as *Vibrio* spp. false-positives due to similar colony appearance to the target *Vibrio* species. Although using growth media selective for *Vibrio* species (TCBS and VID), some non-*Vibrio* species can still grow on selective media (Nigro and Steward, 2015). The genus *Photobacterium* consisted of 43 isolates of *P. damselae* (previously *V. damsela*)*,* a potential human and aquatic animal pathogen, and was the next most common genus represented amongst the isolates (43/325; 13%) after *Vibrio*. Three species of *Shewanella* were isolated (10/325; 3%), including 7 isolates of *S. algae*, an emerging human pathogen (Srinivas et al., 2015).

Overall, 252 of the 302 isolates identified to species level (83%) were species with the potential to cause infections in humans and 264/302 (87%) were species potentially pathogenic to aquatic animals (278/302; 92% potentially pathogenic isolates in total).

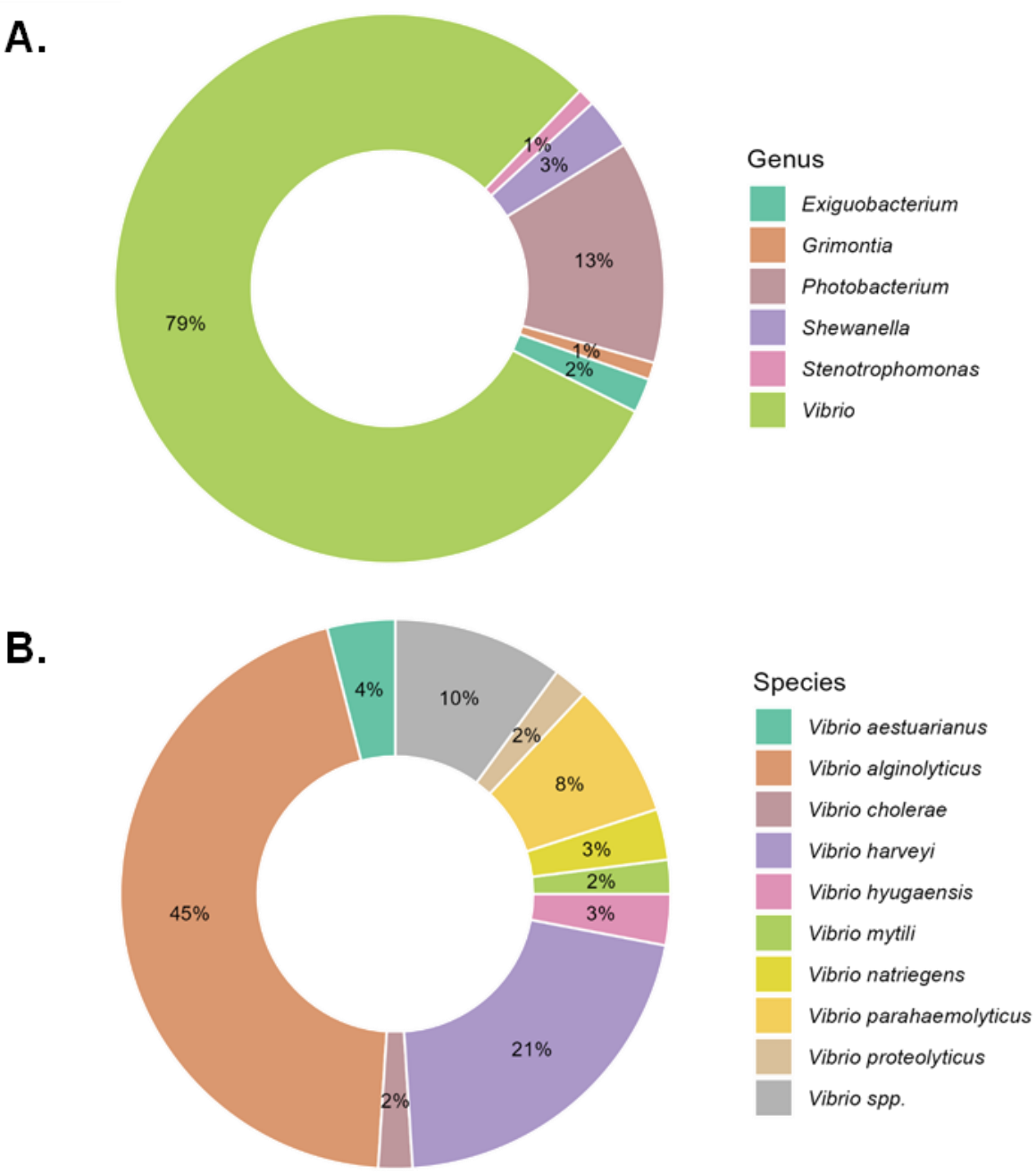

Figure 5.6 **A.** Percentage breakdown of the genera isolated from Lagoon X (n = 325). **B.** Percentage breakdown of *Vibrio* species isolated (n = 258). *Vibrio* species for which only one isolate was obtained (n = 3) were merged with *Vibrio* spp.

Table 5.9 Species identification of isolates obtained across Lagoon X sampling sites A-C during 9 weeks of the sampling period (14/07/2022 – 06/09/2022).

	Species[a]	Site			Total	Reference(s)
		A	B	C		
	Exiguobacterium artemiae	1	0	0	**1**	López-Cortés et al., 2006
	Exiguobacterium marinum	4	2	1	**7**	Kim et al., 2005
●	*Grimontia hollisae*	0	0	2	**2**	Edouard et al., 2009; Hinestrosa et al., 2007
●○	*Photobacterium damselae*	13	3	27	**43**	Osorio et al., 2018; Rivas et al., 2013
●	*Shewanella algae*	4	3	0	**7**	Hong et al., 2020; Srinivas et al., 2015; Tseng et al., 2018
	Shewanella insulae	1	0	1	**2**	Park et al., 2020
○	*Shewanella marisflavi*	1	0	0	**1**	Li et al., 2010
●	*Stenotrophomonas maltophilia*	0	0	4	**4**	Brooke, 2012
○	*Vibrio aestuarianus*	1	0	10	**11**	Garnier et al., 2007; Labreuche et al., 2006; Zhang et al., 2011
●○	***Vibrio alginolyticus***	33	48	36	**117**	Cai et al., 2006; Chen et al., 2000; Reilly et al., 2011
●○	***Vibrio cholerae***	1	1	2	**4**	Chen et al., 2022; Engel et al., 2016; Vezzulli et al., 2020
○	*Vibrio europaeus*	1	0	0	**1**	Dubert et al., 2016; Rojas et al., 2021
●○	*Vibrio harveyi*	11	32	11	**54**	Brehm et al., 2020; Zhang et al., 2020
	Vibrio hepatarius	1	0	0	**1**	Ramirez et al., 2022; Thompson et al., 2003
	Vibrio hyugaensis	0	2	5	**7**	Urbanczyk et al., 2015
	Vibrio mytili	2	4	0	**6**	Pujalte et al., 1993
○	*Vibrio natriegens*	5	0	3	**8**	Zhang et al., 2023
○	*Vibrio neptunius*	1	0	0	**1**	Galvis et al., 2020
●○	***Vibrio parahaemolyticus***	15	0	6	**21**	Gildas Hounmanou et al., 2023; Yang et al., 2022
○	*Vibrio proteolyticus*	0	4	0	**4**	Cervino et al., 2008; Verschuere et al., 2000
-	*Vibrio spp.*	11	5	7	**23**	**-**
	Total	**106**	**104**	**115**	**325**	

[a]Species is noted as a potential pathogen of humans (●) or aquatic animals (○). Species included in the 'big four' *Vibrio* human pathogens (Baker-Austin et al., 2017b) highlighted in bold.

5.4.5 Distribution of species across sites and weeks

Distribution across sites

V. alginolyticus was isolated from all three sampling sites with 48 of 117 isolates (41%) obtained at site B (hypersaline) whilst isolated from sites A (33/117; 28%) and C (36/117; 31%) a similar number of times. *V. parahaemolyticus* was only isolated from sites A (brackish salinity) and C (salinity of seawater), with most isolates (15/21; 71%) from site A and remaining 6/21 (29%) from site C. Four isolates of *V. cholerae* were recovered including 2 at site C and 1 each at sites A and B. The distribution of *V. harveyi* isolates across sites was similar to that of *V. alginolyticus. V. harveyi* was predominantly isolated from site B (32/54; 59%) followed by an equal number of 11 isolates at both sites A and C. Ten of 11 *V. aestuarianus* isolates were obtained from site C and 1 at site A.

The majority of *P. damselae* isolates originated from site C (27/43; 63%) with 13/43 (30%) from site A and 3/43 (7%) from site B. *S. algae* was recovered from sites A (4/7) and B (2/7) only.

Distribution across sampling weeks

Figure 5.7 displays the number and distribution of *V. alginolyticus, V. parahaemolyticus* and *V. cholerae* isolates recovered from the three sites across the sampling period.

V. alginolyticus was isolated across all sites and weeks except week 9 (06/09/2022) at site C. The highest number of *V. alginolyticus* isolates (10) was recovered on week 1 (14/07/2022) at site B and week 4 (02/08/2022) at site C. With the exception of these weeks, the number of *V. alginolyticus* isolates at sites B and C gradually declined over the 9-week period. A weekly maximum of 5 *V. alginolyticus* isolates was identified for several weeks across the latter half of the study period at Site A.

V. parahaemolyticus was isolated in 6 of 9 sampling weeks at site A, where a weekly maximum of 6 isolates was recovered on week 4 (02/08/2022). *V. parahaemolyticus* was isolated during the last 3 weeks (23/08/2022 to 06/09/2022) at site C and no isolates for this species were recovered from site B.

V. cholerae was recovered sporadically across the study period. A single isolate of this species was identified at sites A and B during weeks 3 (26/07/2022) and 5 (09/08/2022), respectively. Two isolates of *V. cholerae* were isolated at site C: 1 in week 5 (09/08/2022) and 1 in week 6 (16/08/2022).

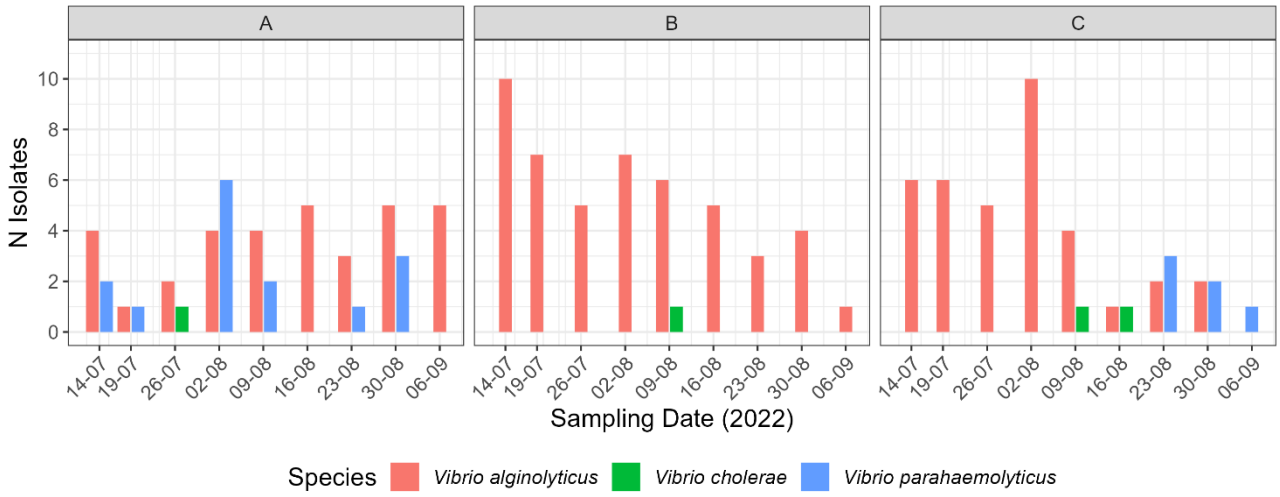

Figure 5.7 Number of potentially pathogenic *V. alginolyticus, V. cholerae, V. parahaemolyticus* isolates obtained across 9 weeks of the sampling period (14/07/2022 – 06/09/2022) for sites A-C.

5.5 Discussion

The emergence and increasing reports of *Vibrio* spp. infections in Northern Europe associated with warming sea surface temperatures (Baker-Austin et al., 2013; Ebi et al., 2017) demonstrates the interdependence of the environment and human health, especially within the context of climate change. Whilst *Vibrio* spp. infections are not an endemic health issue in the UK, the ongoing warming of coastal waters (Cornes et al., 2023) stresses the importance of investigating environmental *Vibrio* spp. bacteria in this region to better understand the risk to human health. This study is one of the first to collect and examine *Vibrio* spp. bacterial abundance for associations with environmental conditions in the UK and also involved the collection and identification of a large number of *Vibrio* spp. isolates. Our analysis did not find significant associations between those environmental parameters tested (water temperature, salinity, and pH) and *Vibrio* spp. abundance. However, *Vibrio* species known to cause illness in humans, including three of the 'big four' *Vibrio* spp. pathogens affecting human health (*V. parahaemolyticus, V. cholerae* and *V. alginolyticus*) (Baker-Austin et al., 2017) were isolated, supporting existing evidence of their presence in UK waters during summer months (Ford et al., 2020; Harrison et al., 2022). This is concerning as the sampling site, Lagoon X, is used for recreational water sports and swimming in several locations along its length and has

a shellfish harvesting area. This work highlights the need for ongoing research into *Vibrio* spp. human health risk in the UK.

Vibrio spp. abundance and environmental conditions in Lagoon X

Using the culture-dependent membrane filtration method, *Vibrio* spp. bacteria were recovered in all 10 weeks of the summer 2022 study period (14/07/2022 – 13/09/2022) across the three sites sampled in Lagoon X. The shallow bathymetry of Lagoon X in combination with heatwave conditions present in the UK during summer 2022 (Kendon, 2022) led to water temperatures of around 18°C or above recorded at all sites throughout the study, thus within an ideal range for *Vibrio* spp. bacterial growth (Vezzulli et al., 2015). Meanwhile, the varying salinity across Lagoon X sites demonstrates the ability of members of the *Vibrio* genus to inhabit a range of salinities from brackish (site A; 28.93 ± 5.80 PSU [mean ± 2 SD]) to that of seawater (site C; 35.68 ± 1.08 PSU) to hypersaline (site B; 39.12 ± 5.28 PSU). Lagoon X has minimal freshwater input (nearest to site A) and shallow bathymetry; therefore, evaporation is likely a key source of this variability in salinity, mediated by both the depth of the waters and amount of tidal seawater influx at each site. The average pH levels of sites A and C were similar (8.42 ± 0.52 and 8.45 ± 0.34, respectively), reflecting values typical of seawater (~8; Marion et al., 2011) whilst average pH measured 9.24 ± 0.46 at site B. A potential reason for this strong alkalinity at site B is the presence of photosynthesising seagrass flats which remove dissolved carbon dioxide from the water, thus reducing acidity and increasing pH (Frankignoulle and Distèche, 1984).

For all sites, peak *Vibrio* spp. abundance occurred during week one of the study (14/07/2022). A maximum *Vibrio* spp. abundance of 1.03 $x10^5$ CFU/100ml was recorded at site A, similar to that found by Ford et al. (2020) (1.26 $x10^5$ CFU/100ml) at the same site along Lagoon X on 10/07/2018. This suggests that *Vibrio* spp. abundance at such order of magnitude is not a one-off occurrence in this location. Interestingly, this maximum *Vibrio* spp. abundance in 2022 was recorded at 18.1°C which was the third lowest water temperature measured at site A. Site A also had the highest average *Vibrio* spp. abundance across the 10-week sampling period (2.22 $x10^4$ CFU/100ml), despite observing the lowest average water temperature of the three sites over the study period. The brackish salinity of site A may have increased the suitability for *Vibrio* spp. bacteria. However, no significant correlations were found between *Vibrio* spp. abundance and water temperature, salinity or pH at the three sites. Similar average levels of total *Vibrio* spp. abundance have been recorded in the Delaware and Chesapeake Bays (7.9 $x10^4$ and 5.1 $x10^3$ CFU/100ml, respectively; Parveen et al.,

2020), where *Vibrio* spp. infections have recently emerged (King et al., 2019). Nevertheless, it is not possible to reliably compare the risk of human infections between locations based on *Vibrio* spp. numbers alone, especially as different methods of enumeration are used and average values are often calculated across different time ranges (i.e., May through October in Parveen et al. (2020) versus July to September in this study).

The maximum water temperature recorded at Lagoon X was 26.42°C at site B on 19/07/2022, 6°C lower than the overall maximum of 32.1°C recorded at site A during the 2018 heatwave by Ford et al. (2020). Investigation of the weather conditions during the study reveals strong correlations between local daily air temperature and in situ water temperatures at the sites (site A: $\rho(8) = 0.82$, $p < 0.01$; site B: $\rho(8) = 0.94$; $p < 0.001$; site C: $\rho(8) = 0.70$; $p < 0.05$) (see Figure S13). According to these weather data, maximum daily air temperature between July and September (31.0°C) occurred on 10/08/2022 across all three sites, one day after sampling on 09/08/2022 (week 5) (see Figure S14). This suggests that peak water temperature may have occurred on a non-sampling day. Regardless, in both the present study and Ford et al. (2020), the maximum water temperature and highest *Vibrio* spp. abundance did not occur in the same week, indicating the influence of a factor other than temperature on *Vibrio* spp. abundance. These results contrast with many ecological studies which frequently find temperature and salinity to be the two most important environmental influences on *Vibrio* spp. abundance, (Froelich et al., 2013; Takemura et al., 2014; Turner et al., 2009; Vezzulli et al., 2009; Wetz et al., 2014). Yet the significance of these variables is not unanimous. Salinity and temperature have been found to vary in their importance as predictors of total *Vibrio* spp. abundance with season (Froelich et al., 2013; Oberbeckmann et al., 2012). For example, Oberbeckmann et al. (2012) found temperature and chlorophyll-a to be significant predictors of *Vibrio* spp. abundance in German North Sea waters in spring whereas salinity, Secchi depth (turbidity) and chlorophyll-a were significant predictors during the summer. The authors suggest that this could indicate the existence of a water temperature threshold that allows increasing *Vibrio* spp. growth to occur. In our study, temperature remained near or above 18°C at all sites for the duration of the sampling period but there was no evidence of increasing *Vibrio* spp. growth with increases in water temperature. This suggests that temperature was not the factor limiting *Vibrio* spp. growth during the time range of the study. Additional complexities include the interaction of temperature and salinity on *Vibrio* spp. abundance (e.g., as seen for *V. vulnificus*: Randa et al., 2004) as well as the species-specific relationships with these variables (Esteves et al., 2015).

Our results show that, for all sites, the weeks with greatest *Vibrio* spp. abundance occurred at their lowest pH values (pH 8.0 - 8.8), but no overall correlation with this variable was found. Although there has been less focus on the effect of pH on *Vibrio* spp. abundance, the importance of this parameter to *Vibrio* spp. growth has recently been discussed and investigated by Velez *et al.*, (2023). *Vibrio* spp. can survive across pH 5 to 10 by induction of the viable but nonculturable (VBNC) state of bacterial dormancy at the extremes of acidity and alkalinity (Nowakowska and Oliver, 2013; Wong and Wang, 2004). Under controlled conditions, Velez *et al.*, (2023) found the highest growth rates of environmental *V. parahaemolyticus* and *V. vulnificus* strains occurred within neutral to acidic pH levels. Meanwhile, water sampling of the Chesapeake Bay recorded the highest abundances of *V. parahaemolyticus* and *V. vulnificus* at around pH 8 (Brumfield et al., 2023a).

Isolation of potentially pathogenic Vibrio spp. strains

A selection of suspected *V. parahaemolyticus, V. vulnificus, V. cholerae* and *V. alginolyticus* colonies were isolated from the membrane filtration count plates and sub-cultured each week so that the presumed *Vibrio* species' identifications could be confirmed by molecular methods. The presence of *V. parahaemolyticus, V. cholerae* and *V. alginolyticus*, three of the 'big four' *Vibrio* species known for their burden on human health (Baker-Austin et al., 2017), was confirmed by a combination of MALDI-TOF MS, PCR and 16S rRNA sequencing. These three species constituted 55% of the 258 *Vibrio* spp. strains identified. *V. alginolyticus* was the most numerous overall with 117 isolates recovered across the sites including a high proportion (48/117; 41%) from hypersaline site B (39.12 ± 5.28 PSU). Pathogenic *V. alginolyticus* strains cause typically mild ear and wound infections that are treatable with antibiotics; only a small number of cases develop into septicaemia or necrotising fasciitis, usually in immunocompromised individuals (Baker-Austin et al., 2018). This pathogen caused over half (52.2%) of all *Vibrio* spp. infections reported in Denmark between 2010 and 2018 (n = 638), where vibriosis is an emerging health issue (Gildas Hounmanou et al., 2023). The majority (74.5%) of these *V. alginolyticus* cases were ear infections. In the UK, reports of *V. alginolyticus* infections are rare and sporadic with only a handful of cases present in the available literature (Hartley et al., 1991; Reilly et al., 2011). The most recent case report was published in 2011 after a woman in her 70s wrapped an existing cut with a homemade dressing containing the seaweed *Fucus spiralis* collected from the shoreline which became infected (Reilly et al., 2011). As vibriosis is not a notifiable illness in the UK, the true number of *V. alginolyticus* cases is not known.

V. parahaemolyticus was predominantly isolated from site A (15/21; 71%), the site with lowest average salinity (28.93 ± 5.80 PSU), whilst absent from hypersaline site B (39.12 ± 5.28 PSU). These differences may reflect broader salinity tolerance by *V. alginolyticus* compared to *V. parahaemolyticus.* A meta-analysis of ecological studies by Takemura et al. (2014) suggests that *V. parahaemolyticus* may inhabit salinity ranges between around 5 to 33 PSU which matches the absence of this species at the hypersaline site B and reduced recovery from site C where salinity was around 35 PSU. Where *Vibrio* spp. infections are endemic, *V. parahaemolyticus* can be a common cause of mild seafood- and seawater exposure-related infections, e.g., in the United States it is estimated to cause around 45,000 infections each year (Centers for Disease Control and Prevention, 2019). In Denmark between 2010 and 2018, *V. parahaemolyticus* caused 45.9% of reported *Vibrio* spp. wound and deep tissue infections (Gildas Hounmanou et al., 2023). Most *V. parahaemolyticus* infections are self-limiting or resolve following antibiotic treatment but can be life-threatening in some cases, especially for individuals with underlying health conditions (e.g., Guillod et al., 2019). Concerningly, three *V. parahaemolyticus* strains isolated from Lagoon X tested positive for the *trh* gene which encodes TRH, a major *V. parahaemolyticus* virulence factor associated with disease (Ceccarelli et al., 2013). Unfortunately, the PCR assay for detection of the thermostable direct hemolysin (TDH) gene, *tdh*, did not work and therefore will be the focus of future work.

Four isolates of *V. cholerae* were recovered from across the sites. Similar to *V. parahaemolyticus*, non-O1/non-O139 *V. cholerae* generally cause self-limiting gastroenteritis as well as wound and ear infections (Deshayes et al., 2015). A large proportion (77%) of *Vibrio* spp. infections reported in Sweden and Finland after a 2014 heatwave event in Northern Europe were attributed to non-O1/non-O139 *V. cholerae,* including several infections reported less than 100 miles from the Arctic Circle (Baker-Austin et al., 2016).

Interestingly, *V. vulnificus* was not isolated throughout the sampling period despite being recovered from all three sites at Lagoon X in both 2018 and 2019 (Ford et al., 2020). This could have been in response to lower average salinities recorded in 2018 (17.0 - 37.9 PSU) and 2019 (21.0 - 35.0 PSU) which may have been more favourable for *V. vulnificus* (Ford et al., 2020). The optimal salinity range for *V. vulnificus* growth is around 10 to 25 PSU (Esteves et al., 2015; Noorian et al., 2023) but has been observed to expand to between 5 and 30 PSU at higher water temperatures (>22°C) (Randa et al., 2004). Yet, this is just one possible explanation and other environmental factors may

have been involved. *V. vulnificus* is a serious opportunistic human pathogen that can cause deadly necrotising wound and seafood-related infections, mainly in susceptible individuals with chronic underlying health conditions (Baker-Austin and Oliver, 2018). Despite the rarity of *V. vulnificus* disease, the high fatality rates associated with wound (~18%; Ralston et al., 2011) and foodborne (~50%; Jones and Oliver, 2009) infections emphasise the severity of this pathogen. Therefore, the presence of *V. vulnificus* isolates possessing multiple virulence genes in UK waters is concerning (Ford et al., 2020). Heavy summer rainfall events may increase the suitability of coastal waters for *V. vulnificus* bacteria in the UK by reducing salinities during peak seasonal water temperature. Heavy rainfall did not occur during the sampling period conducted in this study, which may partially explain the absence of *V*. *vulnificus* bacteria.

Molecular methods

MALDI-TOF MS was used for rapid species identification of isolates recovered from the waters of Lagoon X. Of the 335 isolates, 261 (78%) returned a high confidence species identification via MALDI-TOF MS. PCR of isolates identified as *V. alginolyticus* or *V. parahaemolyticus* by MALDI-TOF MS (n = 129) returned 96% identification agreement between the two methods. These findings support the use of MALDI-TOF MS for *Vibrio* species identification within the context of monitoring *Vibrio* spp. risk by providing rapid, cost-effective results (Dieckmann et al., 2010; Erler et al., 2015; Mougin et al., 2020). The sensitivity and rapid proliferation of *Vibrio* spp. means that high abundances of these bacteria can accumulate quickly in coastal waters with favourable conditions. Being able to routinely identify the presence of *Vibrio* spp. pathogens in coastal waters shortly after a sample is taken would enable the timely use of warning signs or public text alerts if necessary.

The use of culture-independent methods for the quantification of *Vibrio* spp. abundance would benefit this analysis. Quantitative real-time PCR (qPCR) uses species-specific primers to enumerate target *Vibrio* species and therefore would enable species-specific relationships with environmental variables to be assessed (Randa et al., 2004; Wetz et al., 2014). The *Vibrio* spp. abundance presented in this study includes some non-*Vibrio* species, as 21% of isolated strains did not belong to the *Vibrio* genus; qPCR would enable the enumeration of chosen target *Vibrio* species only and therefore reduce false-positive counts. Furthermore, although the chromogenic media used for culture-dependent counts should allow for species-specific enumeration based on morphology, later testing with MALDI-TOF MS revealed inconsistent colony appearance within species. In particular, *V. alginolyticus* colonies exhibited a wide range of colours on VID

media. This species grew as pink, blue and purple colonies which more closely match the description of *V. parahaemolyticus, V. vulnificus* and *V. cholerae* on this media (see Table S11). The intense selection pressure experienced by environmental *Vibrio* spp. strains results in natural variation that can be observed in the variable morphologies of isolates (personal communication with A. Powell, Cefas), further strengthening the need for species-specific enumeration using qPCR.

Isolates that obtained a low confidence MALDI-TOF MS identification or multiple contrasting high confidence MALDI-TOF MS identifications were sent for 16S rRNA gene sequencing. From 16S rRNA gene sequencing, species-level results were obtained for just 31/65 (48%) of isolates whilst 29/65 (45%) were identified to genus level and 5/65 (8%) could not be identified. High genetic similarity amongst *Vibrio* species (especially within the *V. harveyi* clade (Lin et al., 2010)) can make it challenging to decipher between species with this method (Mougin et al., 2020). Future work could include whole genome sequencing (WGS) of isolates recovered to aid identification to species level where this has not been possible or where conflicting identifications have been obtained across methods. WGS would provide higher resolution genetic data to enable comparisons of closely related species to build a phylogenetic tree of *Vibrio* spp. strains and could be used to assess whether similar strains reappear in the same location each year. WGS data would also reveal whether the strains possess genes associated with virulence or antibiotic resistance (Janecko et al., 2021). Concerningly, the presence of genes associated with virulence amongst *V. parahaemolyticus, V. vulnificus* and *V. cholerae* isolates from Lagoon X was noted by Ford *et al*. (2020) and within three *V. parahaemolyticus* isolates in in our study. Gathering knowledge of the virulence genes present in environmental *Vibrio* spp. strains and assessing the relative virulence of different strains (e.g., via the *Galleria mellonella* infection model for *V. parahaemolyticus*; Wagley et al., (2018)) would help to assess the human health risk of *Vibrio* spp. found in UK waters.

Limitations and future work

This snapshot ecological study adds to a preliminary dataset of *Vibrio* spp. abundance in the UK and the large number of *Vibrio* spp. isolates collected (n = 258) contribute to an increased understanding of the *Vibrio* species present. Unfortunately, the short timeframe of the study and necessary independent treatment of the sampling sites meant only ten pairs of datapoints were available to test for each correlation between *Vibrio* spp. abundance and environmental factors, reducing the reliability of the statistical results. Therefore, future work could include more extensive sampling across seasons,

starting earlier in the year, and samples could also be collected at more frequent intervals (e.g., twice a week).

In this study three environmental factors were measured. However, the ecological complexity of coastal environments increases the number of factors that likely influence *Vibrio* spp. populations. For example algal blooms can provide a source of nutrients to *Vibrio* spp. (Hsieh et al., 2007) and storms can disturb the sediment, releasing more *Vibrio* spp. cells into the water column (Wetz et al., 2008). Therefore, the measurement of additional potentially important environmental factors that have also been identified as important to *Vibrio* spp. abundance in some locations, i.e., nutrient levels, chlorophyll-a concentration, dissolved oxygen and turbidity (Blackwell and Oliver, 2008; Hsieh et al., 2008; Oberbeckmann et al., 2011; Pfeffer et al., 2003; Vezzulli et al., 2009), should also be explored alongside water temperature, salinity and pH in future work. Further complexity is introduced by the rare physical characteristics of Lagoon X which influence the movement and mixing of water and its biological inhabitants. Different coastal environments in the UK such as estuaries and bays have different physical characteristics which means that our observations cannot be generalised to all other coastal environments in the UK. Sampling a range of coastal environments in different locations along the UK coastline would provide greater insight into *Vibrio* spp. abundance and risk.

Conclusion

Overall, this study confirms that a high abundance of *Vibrio* spp. bacteria can be found within a UK coastal environment in summer months, but no correlation of *Vibrio* spp. abundance with water temperature, salinity or pH was found. However, given that our results provide evidence of potentially pathogenic *Vibrio* species in UK coastal waters, further scientific investigation of the *Vibrio* spp. community and monitoring is warranted to provide a continued assessment of the risk to human health.

6 Outlook & discussion

Here, the key research outcomes of the thesis are summarised for each data chapter followed by a discussion of the key reoccurring themes throughout the thesis and priorities for future research. The chapter concludes by stating the contributions of this thesis to the field.

6.1 Key research outcomes

The work conducted in Chapter 3 represents one of the first studies to systematically assess the historical changes in the geographic distribution of *V. vulnificus* wound infections in the eastern United States (US). Previously, the northwards shift of *V. vulnificus* infections was inferred with sporadic case reports of infections in non-endemic locations (e.g., King et al., 2019) yet here, Chapter 3 visualises 30 years of data from the Cholera and Other *Vibrio* Illness Surveillance (COVIS) database to map the northwards shift in distribution over this period. Results indicate that the upper limit of the infection distribution has been moving northwards at ~48 km per year on average. Cases that were once restricted to the southern US along the Gulf of Mexico coastline in the 1980s are now reported in the Chesapeake and Delaware Bays and waters off the coast of New Jersey. Also in Chapter 3, an ecological niche modelling methodology was used to build models of *V. vulnificus* wound infection risk based on average air temperature conditions where *V. vulnificus* infections are mainly reported. These models were then used to predict future expansion of the areas conducive to *V. vulnificus* infections under different scenarios of climate change. This work highlights future at-risk regions on the Northeast US Atlantic coast that may benefit from increased awareness of *V. vulnificus* infections. It also indicates the long-term benefit of limiting greenhouse gas emissions; the predicted geographic expansion of the *V. vulnificus* infection distribution by the end of the 21st Century was limited under SSP126, a low emissions scenario, to around Connecticut compared to medium-to-high scenario, SSP370, whereby the risk distribution reached Maine. However, estimations of the population living within 200 km of the coastline at risk of *V. vulnificus* infections reveal that more individuals within a high-risk age group (60 and older) are expected to live within this risk region in the future under SSP126 than SSP370 and this was reflected in the higher number of cases expected per year. This is a key finding that emphasises the need to

explore demographic change as well as environmental change when examining *V. vulnificus* risk.

Whilst the work of Chapter 3 focused on long-term, large-scale changes in historical and future *V. vulnificus* infection risk, the role of Chapter 4 was to examine *V. vulnificus* infections at a finer temporal resolution. Environmental factors were assessed for their influence on the variability of weekly *V. vulnificus* infections. The work focused on the Gulf of Mexico coastline, where *V. vulnificus* infections have historically been reported, and employed a robust multi-model inference (MMI) approach for comparison of the relative importance of a range of environmental factors to weekly infection variability. Overall, air temperature and sea surface temperature (SST) variables had the greatest relative importance and were the only significant environmental parameters. However, the baseline model which included a random effect of US state, as well as accounting for seasonality (month), year and national or state US holiday, had a similarly good predictive power compared to the best models which included air temperature or SST alongside these baseline variables. This suggests that a model where seasonal changes in temperature are accounted for within the 'month' variable may provide good predictions of whether a *V. vulnificus* infection may be reported in a given week along the Gulf of Mexico coastline. Assessments of the different variables influencing *V. vulnificus* infection variability as opposed to variability in *V. vulnificus* bacterial abundance are limited and, to the best of our knowledge, only one such study has been published in the United States, which was conducted with data for Florida only at a monthly temporal resolution (Ayala et al., 2023).

The work of Chapter 3 and Chapter 4 indicates the importance of temperature to the occurrence of waterborne *V. vulnificus* disease in the US. The constructed models encapsulate the processes that lead to disease including *V. vulnificus* bacterial presence and abundance in the environment, human behaviour leading to exposure and host susceptibility in a "black box" approach. This approach means we are unable to unpick the influence of temperature on *V. vulnificus* bacteria versus human-related factors, such as behaviour. Therefore, the aim of Chapter 5 was to focus on the microbiology and investigate the environmental factors driving *Vibrio* spp. bacterial abundance by conducting an ecological study within a *Vibrio* spp. hotspot located in Southwest England. To date, no *V. vulnificus* infections have been reported in the UK and domestic infections caused by other *Vibrio* spp. are believed to be extremely low in number. Yet it has been suggested that warming waters along the UK coastline may encourage pathogenic *Vibrio* spp. growth and therefore the risk to human health should be

investigated (Ford et al., 2020). Due to the microbiological techniques used, a much wider range of *Vibrio* species could be considered in Chapter 5, rather than solely investigating *V. vulnificus*. By understanding the environmental factors influencing *Vibrio* spp. abundance, other "hotspot" locations with similar conditions could potentially be identified and targeted for future monitoring of pathogenic *Vibrio* spp. Over a 10-week period, water samples were obtained, and environmental parameters were measured in situ. Associations between environmental parameters (i.e., water temperature, salinity and pH) and culture-dependent *Vibrio* spp. bacterial abundance were tested but no significant correlations were identified. This alludes to the complexity of capturing patterns in the abundance of one bacterial genus within a dynamic coastal environment at weekly intervals over a short time period. Yet, the study did reveal high levels of *Vibrio* spp. abundance which peaked at 10^5 colony forming units (CFU) per 100ml of water, confirming that such magnitude of *Vibrio* spp. abundance, as recovered in Ford et al. (2020), is not a unique event in the study location. A further key finding from this work was the confirmation of potentially pathogenic *Vibrio* species within the 325 isolates identified, including *V. alginolyticus*, *V. cholerae* and *V. parahaemolyticus* using molecular methods, including matrix-assisted laser desorption/ionisation time-of-flight (MALDI-TOF) mass spectrometry (MS). Additional testing revealed that three isolates of *V. parahaemolyticus* possessed the *trh* gene, associated with virulence (Ceccarelli et al., 2013). The presence of potentially pathogenic *Vibrio* species within a UK coastal site used for recreation and shellfish harvesting is concerning and strengthens the need to conduct additional research on *Vibrio* spp. bacteria in the UK to identify and understand *Vibrio* spp. risk in more locations.

6.2 Reoccurring themes

6.2.1 Data availability

Health data

For building models of *Vibrio* spp. risk based on human infections, good quality epidemiological data is key. Chapters 3 and 4 use *V. vulnificus* wound infection data from the Centers for Disease Control and Prevention (CDC) COVIS database: the most comprehensive *Vibrio* spp. infection database in the US. The COVIS system collates reports of *Vibrio* spp. infections from across all states, meaning that only one data request is needed. As a result, it is much easier to obtain *Vibrio* spp. infection data for the US as opposed to, for example, the Baltic Sea region of Northern Europe which

requires data requests to be sent individually to the health institutes of different countries; a centralised *Vibrio* spp. surveillance system for all of Europe is yet to be established. *Vibrio* spp. infections were made legally notifiable in the US in 2007, however, the severity of *V. vulnificus* infections made their occurrence medically noteworthy, even before this date. As a result, there is reasonable confidence that the *V. vulnificus* infections reported to the CDC represent close to the true number of infections. The *V. vulnificus* pathogen is opportunistic and therefore infections are rare (around 80 wound infection cases are reported per year on the east coast of the US (Archer et al., 2023)).

Vibrio spp. infections caused by other species such as *V. parahaemolyticus* and *V. alginolyticus* are greater in prevalence (Sheahan et al., 2022), but symptoms are typically not as severe as *V. vulnificus* infections leading to many unreported self-limiting infections. This uncertainty in the true number of cases is relevant for Chapter 5 located in the UK, where *Vibrio* spp. infections are thought to be rarely domestically acquired. There is currently no legal requirement for cases to be reported to the UK Health Security Agency (UKHSA) so, even if mild ear or wound *Vibrio* spp. infections were being contracted from exposure to UK waters, this information may not be reported. Underreporting of *Vibrio* spp. infections in non-endemic locations may mean that mitigation efforts such as enhanced shellfish testing and bathing water monitoring are not considered until serious, potentially life-threatening, systemic infections, typically caused by *V. vulnificus* and non-O1/O139 *V. cholerae,* are reported. *Vibrio* spp. infections are a classic example of the 'Burden of Illness' pyramid (see section 2.4 in Chapter 2) for which there are many unreported mild infections in the community with fewer, more severe cases reported to health authorities, especially when reporting is not mandatory.

Within Chapters 3 and 4, a common theme was that the low number of cases restricted the statistical analyses that could be performed. For instance, binomial logistic regression models which aggregated the infection distribution into presence or absence along the coastline in Chapters 3 and at the weekly state-level in Chapter 4 were used rather than count-based models as the low number of cases would have meant limited variability present in the dependent variable. The low number of cases was also considered in Chapter 3's visualisation of the changing distribution of *V. vulnificus* infections. A low number of cases can result in large jumps northwards in the northern limit of *V. vulnificus* infections, therefore, the 95th percentile latitude of cases was

averaged over 5-year periods to represent the expanding upper limit of the infection distribution.

Despite confidence in the number of *V. vulnificus* infections reported to COVIS, the exact location of exposure, beyond county-level, of the cases is a source of uncertainty. Although the CDC COVIS reporting form asks for the specific water body the patient has been exposed to in the last 7 days before infection began (https://www.cdc.gov/nationalsurveillance/pdfs/cdc5279-covis-vibriosis-508c.pdf), the exact location is often unclear or missing in the retrieved case database entries for *V. vulnificus* wound infections. Chapter 3 considers cases 'coastal' if the US county where the infection was reported (or travel county within US, if stated), are within 200 km of the US coastline. The same method was applied in Chapter 4, but the locations of cases were then aggregated to state-level for the modelling analysis. Currently, location of exposure is recorded on the COVIS reporting form but relies on the patient's ability to accurately and reliably recall where and when they interacted with coastal waters. This information recall may be affected by the time taken to record the information or if the patient is recovering from a severe infection. However, the timescale is likely reduced for *V. vulnificus* infections as symptoms require urgent medical attention usually within hours of exposure (Baker-Austin and Oliver, 2016). Additionally, how specifically the question of exposure location was asked may affect the information provided. Many exposure locations were vague and stated "ocean" or large geographic areas such as "Gulf of Mexico" or "Atlantic Ocean". Having a more specific location of exposure for each case in the COVIS dataset would enable more focussed analyses into the environmental conditions associated with cases of waterborne *V. vulnificus* infection.

An alternative method of determining the exact locations that a patient has been exposed to brackish waters would be to use the GPS location data from a device such as their mobile phone. This method has many ethical considerations relating to the privacy of individuals which were raised recently with the use of mobile GPS data for contact-tracing during the COVID-19 pandemic (Grantz et al., 2020). However, the responsible and effective use of such data could bring positive benefits to public health. For instance, this information may help to identify hotspot *Vibrio* spp. risk areas that could be studied or monitored more closely. At a broader population scale, anonymised mobile phone GPS data could reveal trends in human activity at the coast that could be examined alongside trends in reported *Vibrio* spp. infections. Anonymised mobile phone GPS data has recently been used to explore and quantify human activity within green space, including the amount of time spent within different land cover types (Filazzola et al.,

2022). Similarly, data on human activity at the coast could be used to weight coastal environmental data used in *Vibrio* spp. infection modelling, similar to Chapter 4 whereby population count data was used as a proxy for human activity and therefore exposure. A better understanding of where and how people spend time at the coast could also potentially inform *Vibrio* spp. risk mitigation efforts by focussing resources (e.g., monitoring *V. vulnificus* bacterial load, signage, regional risk modelling) on popular bathing locations.

Collating *Vibrio* spp. health data into a global *Vibrio* spp. surveillance system would enable more efficient and greater collaboration between healthcare professionals, researchers, and decision makers to allow for more responsive and informed mitigation actions. Such a system could introduce standardised reporting across multiple countries which may currently have different reporting forms and therefore different metadata collected. Standardised reporting would be useful for tracking trends in incidence across broader geographical regions, improving the availability of epidemiological data for research and for identifying the emergence of *Vibrio* spp. infections in new locations. However, there are huge challenges to standardising reporting of disease cases across multiple states or countries, including how you define a case of a particular disease. The European Surveillance System (TESSy) collects case data for infectious diseases reported across the European Union and European Economic Area but discrepancies in the data reported still exist between countries. For example, there is no standardised reporting date for campylobacteriosis cases submitted to TESSy so whether the date of onset, date of diagnosis or date of notification is used depends on the country submitting the data (Lake et al., 2019).

Increased availability of *Vibrio* spp. health data could enable regular development and optimisation of existing *Vibrio* spp. risk models which help to protect public health (discussed in section 6.3.1). Nonetheless, any expansion in epidemiological surveillance of *Vibrio* spp. disease would be costly, requiring continuous funding and many resources that need to be considered against the benefits of such a system.

Environmental data

One of the first challenges to constructing a statistical model is obtaining high quality data; models are only as good as the information they are trained with. Within Chapter 3, the challenge of obtaining suitable data for constructing an ecological niche model of *V. vulnificus* infections on the east coast of the US is discussed. A core aim of this analysis was to construct a model to predict potential changes in the geographic disease

distribution into the future, therefore, future environmental data obtained had to be downscaled and bias-corrected with the same baseline dataset as used for the historical data. Such data was available from WorldClim (https://www.worldclim.org) for meteorological variables at a fine resolution of 2.5 arcminutes (~4.6 km) and for seven different Coupled Model Intercomparison Project phase 6 (CMIP6) global climate models (GCMs) for the chosen Shared Socioeconomic Pathways (SSPs) at the time of download. However, similarly paired historical and future oceanographic data could not be found at the same high spatial resolution nor for the same number of CMIP6 models and SSPs. Having more than one GCM enables predictions to be made from an ensemble of models that account for a range of possible futures, as in (Colón-González et al., 2018).

Oceanographic variables such as SST and salinity were obtained at a resolution of 25 km from the Alfred Wegener Institute Climate Model (AWI-CM-1-1-MR), the highest resolution available for future oceanographic data from CMIP6 GCMs. Given the size of these data grid cells, large offshore areas were incorporated into the value of each cell, rather than reflecting the conditions nearshore and within the intertidal zone, at the interface between land and sea where most recreational exposure is likely to take place. When extracting these 25 km resolution data at the coastline, it became apparent that the historical values obtained were not within the tolerance of *V. vulnificus* bacteria which are mainly found in conditions below 25 practical salinity units (PSU) (Randa et al., 2004). All salinity values were above 25 PSU, even within states where *V. vulnificus* wound infections are endemic. As a consequence, oceanographic variables could not be reliably used to generate a model of *V. vulnificus* infections in Chapter 3. The intertidal zone is noted as having a particularly high number of microclimates which stresses the need for appropriately fine-scale environmental data when constructing models of a species' niche or distribution (Robinson et al., 2011). This heterogeneity of the coastal environment was highlighted in Chapter 5 which, for example, documented large differences in salinity between sampling sites located ~7 km apart (Site A: 28.93 ± 5.80 PSU, Site B: 39.12 ± 5.28 PSU [mean ± 2 SD]). Moreover, the resolution of data used to construct species distribution models has been found to influence the relative importance of variables and the extent of suitable habitat predicted (Basher et al., 2014). Fortunately, the lack of available high-resolution future SST data was overcome by using finer coastal air temperature instead. A strong correlation between air temperature and SST had been suggested in the literature (Feng et al., 2018; Galbraith et al., 2012) and was later also observed along the Gulf of Mexico coastline during the analyses for Chapter 4 ($\rho(6783) = 0.96$, $p<0.001$). Unfortunately, no proxy was available for other

oceanographic variables of interest such as salinity. Yet even these air temperature data of comparatively fine resolution are only able to predict broad areas of risk at ~4.6 km resolution. *V. vulnificus* risk is likely to vary spatially within these broad areas as the suitability of conditions for the bacteria fluctuate.

Lack of high-resolution future oceanographic data is especially an issue for marine species distribution modelling and ecological niche modelling studies aiming to assess climate change impacts. For example, von Hammerstein et al. (2022) sought to assess the impact of climate change on SSTs within humpback whale breeding grounds. The authors state that the 25 km resolution of CMIP6 data was not suitable for their analysis as the whale's breeding grounds would be represented by just a few grid cells. As an alternative solution, they conducted statistical downscaling using the *delta* method (Ramírez Villegas and Jarvis, 2010) to provide access to high resolution (~5 km) SST data for future time periods. However, this downscaling method assumes that changes in future climate are constant over large areas that match the resolution of the GCM data used (i.e., 25 km; cell area 625 km^2) and that the relationships between variables in the baseline period remain the same over time (Ramírez Villegas and Jarvis, 2010). Therefore, despite daily SST data of ~1 km resolution being available from the Group for High-Resolution Sea Surface Temperature (GHRSST) for 2002 onwards (Chin et al., 2017), downscaling these data is still limited by the coarse resolution of future CMIP6 SST projections which do not overlap sufficiently with the coastline.

Even with future data available, predictions of *Vibrio* spp. risk could potentially be limited by the GCMs' ability to account for extreme events as upshifts in case numbers are associated with heatwave events (Baker-Austin et al., 2016; Brehm et al., 2021a). Indeed, predictions of future *V. vulnificus* infection risk in Chapter 3 were generated from models based on maximum air temperature data. However, recent studies that have explored the ability of CMIP6 models to predict climate extremes retrospectively find that the models have been able to capture observed historical extreme temperatures well (Engdaw et al., 2023; Kim et al., 2020; Wu et al., 2021). Yet, climatic tipping points, defined as a "level of change in system properties beyond which a system reorganizes" (IPCC, 2022) are a source of uncertainty. This is owing to the challenge of estimating when they are predicted to bring about abrupt and often irreversible change. One such tipping point is the collapse of the Atlantic Meridional Overturning Circulation (AMOC) which is predicted to cool the Northern Hemisphere as ocean circulation slows (Vellinga and Wood, 2002). Rapid cooling of North Atlantic sea surface temperatures in response to the AMOC shutting down (Orihuela-Pinto et al., 2022) would likely influence the burden

of *Vibrio* spp. illnesses along the coasts of North America and Europe due to the climate sensitivity of *Vibrio* spp. disease. A recent study predicts that the AMOC may collapse as soon as the middle of the 21st Century (Ditlevsen and Ditlevsen, 2023). However, the timing of this tipping point being reached is hotly debated. Although the IPCC have high confidence that the AMOC is “very likely” to weaken this century, they state with medium confidence that the full collapse of the AMOC by 2100 is “very unlikely” (Collins et al., 2019). Across the CMIP6 GCMs, including those used to generate future predictions of *V. vulnificus* infection burden in Chapter 3, there are large differences in predicted declines in AMOC strength but most models do not predict an abrupt shutdown (Bellomo et al., 2021). Nevertheless, GCMs may be subject to model-biases that underestimate the likelihood of AMOC collapse (Liu et al., 2017). Therefore, the highly improbable but still physically possible collapse of the AMOC this century (Collins et al., 2019) is not represented within Chapter 3 predictions.

By only exploring variables for their ability to explain the variability in past *V. vulnificus* infections, rather than attempt future predictions, the environmental data available for Chapter 4’s analysis was expanded. Higher resolution historical data could be obtained for multiple oceanographic variables from the Copernicus Marine Service at 0.083º (~9 km) resolution from the Global Ocean Physics Reanalysis dataset for 1993 onwards. These data are outputs from computer models which are used to interpolate the values between observational datapoints. Model output data are highly valuable as they can provide access to a range of variables over continuous space and time and are often freely available. A study by Becker et al. (2016) compared models of cetacean density constructed with oceanographic variables from model output data versus in situ measurement data and found that both models had highly similar, good predictive capabilities, supporting the use of model output data for species distribution and ecological niche modelling studies. However, ~9 km is still highly coarse and may homogenise small-scale changes in environmental conditions that could influence bacterial abundance of *Vibrio* spp., especially within the intertidal zone. The use of these data represents a trade-off between the spatial resolution and the temporal range of data available. With a low frequency of *V. vulnificus* cases, having a longer temporal range of the Global Ocean Physics Reanalysis dataset available i.e., 1993 onwards, kept a greater number of weeks when *V. vulnificus* infections occurred within the model training dataset compared to ~1 km resolution GHRSST data which were available from 2002 onwards (Chin et al., 2017). A comparison of models built with these two different datasets is beyond the scope of this thesis but may offer insight into whether to prioritise

spatial resolution or temporal range when selecting gridded environmental datasets for similar analyses with a low number of observations.

In contrast, Chapter 5 used in situ measurements of environmental conditions at the time of sampling for *Vibrio* spp. abundance, rather than existing gridded datasets. Whilst a model of *Vibrio* spp. abundance could potentially have been created with the measured variables (sea surface temperature, salinity and pH) if they demonstrated significant relationships, the ability to predict *Vibrio* spp. abundance in the UK would require the availability of gridded oceanographic data with good resolution at the coast. High resolution (~1.5 km by ~3 km) reanalysis data with 7-day forecast are available for the UK from the Copernicus Marine Service for SST and salinity variables (CMS, 2023a). However, this resolution would cover the three sampling sites in Chapter 5 within a few grid cells and so may not provide enough datapoints for calibrating a model of *Vibrio* spp. bacterial abundance to the gridded data. SST data finer than ~1 km resolution such as 300m (at daily temporal resolution) and 100m (at 16-day temporal resolution) can be obtained through CoastObs (www.coastobs.eu) but are not open access. For additional potentially relevant variables such as dissolved oxygen, turbidity and chlorophyll-a concentration, the Sentinel-2 satellite has recently enabled the availability of 100m resolution data spatially ranging from Europe's coastlines to 20 km offshore which can be obtained for 2020 onwards (e.g., CMS, 2023b). Yet pH remains difficult to obtain at a similarly high spatial resolution.

6.2.2 Understanding the influence of climate change on pathways of *Vibrio vulnificus* disease transmission

Understanding the pathways through which climate change may influence waterborne *V. vulnificus* infections via environmental impacts on human behaviour and the suitability of the coastal environment for *V. vulnificus* bacteria is complex. Additionally, as *V. vulnificus* infections are mainly acquired by older individuals, often with health conditions (Baker-Austin and Oliver, 2018), demographic change in coastal populations (and those visiting the coast) may also influence the future health burden of this disease. This complexity has been summarised in Figure 6.1 which is a directed acyclic graph of the many different pathways that climate change and demographic change may influence waterborne *V. vulnificus* infections, based off reading conducted for this thesis.

Pathogenic *Vibrio* spp. bacteria are known for their sensitivity to temperature (Baker-Austin et al., 2017) but human behaviour and therefore exposure to seawater potentially containing *Vibrio* spp. pathogens can also be influenced by temperature (Elliott et al.,

2019; Morgan and Ozanne-Smith, 2013). Although temperature variables were found to be statistically important in both Chapter 3 and Chapter 4, it is not possible to infer the underlying mechanism of temperature within the disease transmission pathway for these analyses due to collinearity between air temperature and SST. Air temperature may influence human recreational behaviour and therefore exposure to the bacteria in the environment, whilst SST could affect the abundance of *V. vulnificus* bacteria, both directly and indirectly e.g., by mediating plankton blooms (see Figure 6.1).

For example, in Northern Europe, the emergence of *Vibrio* spp. infections occurred in accordance with anomalous SSTs, closely mirroring the spatial and temporal patterns (Baker-Austin et al., 2013). In addition to an increase in suitability for *Vibrio* spp. pathogens, human recreational behaviour in the waters of the Baltic Sea may have also increased due to heatwave conditions but, without reliable human activity data and concurrent microbiological sampling in areas where infections are reported, it is not possible to unpick how much each response to temperature may have contributed to the increased number of infections. Here, more research into how people interact with the coast under different weather conditions e.g., fishing, bathing or beach use only would be useful. Combined with *Vibrio* spp. surveillance data, this information could be used to identify especially 'risky' activities during periods of increased suitability for *Vibrio* spp. infections.

Within the environment, many different factors are found to significantly impact *Vibrio* spp. bacterial abundance (see Table 2.1 in Chapter 2). Yet, of a range of variables considered, air temperature and SST were the only environmental terms found to be statistically relevant at the human *V. vulnificus* infection level along the US Gulf Coast in Chapter 4. Here, the 'hurricane landfall impact' variable is discussed as an example. Hurricane landfall impact was not a significant predictor of weekly *V. vulnificus* infection variability despite 14 reports of infection associated with Hurricane Katrina (CDC, 2005). As discussed in Chapter 4, it is likely that the specific characteristics of individual hurricane landfall events are more important to the *V. vulnificus* health burden than the occurrence of a hurricane landfall itself. For instance, Hurricane Katrina caused an especially high storm surge which coupled with the failure of protective levees, resulted in widespread flooding and exposure (Knabb et al., 2023). Hurricane Ian was also associated with increased reports of *V. vulnificus* infections (Sodders et al., 2023). A recently published study by Brumfield et al. (2023) observed increases in SST before and immediately following Hurricane Ian that were above the 10-year average. Chlorophyll-a concentrations were greater than five times the 10-year standard deviation

during and after Hurricane Ian, suggesting an increased suitability of conditions for growth of *Vibrio* spp. bacteria (Brumfield et al., 2023b). However, as this event occurred in 2022 it was beyond the temporal range of the COVIS data used in this thesis (1988 – 2018). Therefore, the rarity of a hurricane landfall impact resulting in cases of *V. vulnificus* (a relatively rare form of infection) may mean that no statistically significant effect is detectable when analysing many years of data.

This relates to ideas discussed by Levin (1992), whereby "different processes are likely to be important on different scales". For example, although Chapter 4 did not find salinity to be important for weekly *V. vulnificus* infection variability at the state-level, salinity might still be important to the variability of infections if studied at a local level. Different bathing areas within a county may vary in salinity due to their specific physical characteristics (such as proximity to freshwater inputs) which mediates the suitability for *V. vulnificus* growth. However, when aggregated to weekly values at the state-level, spatial and temporal variation in salinity is reduced (although some states demonstrated greater variability in weekly salinity than others; see Figure S12) (see section 6.2.1, 'Data availability' for discussion on spatial resolution). Nevertheless, when conducting an ecological study of *Vibrio* spp. bacteria in the UK (Chapter 5), no significant environmental drivers of *Vibrio* spp. abundance (including water temperature and salinity) were found. This highlights the challenge of understanding the key environmental drivers of *Vibrio* spp. bacteria as geographic location, season, and

taxonomic resolution (i.e., investigating the abundance of all *Vibrio* spp. rather than specific species) can influence findings.

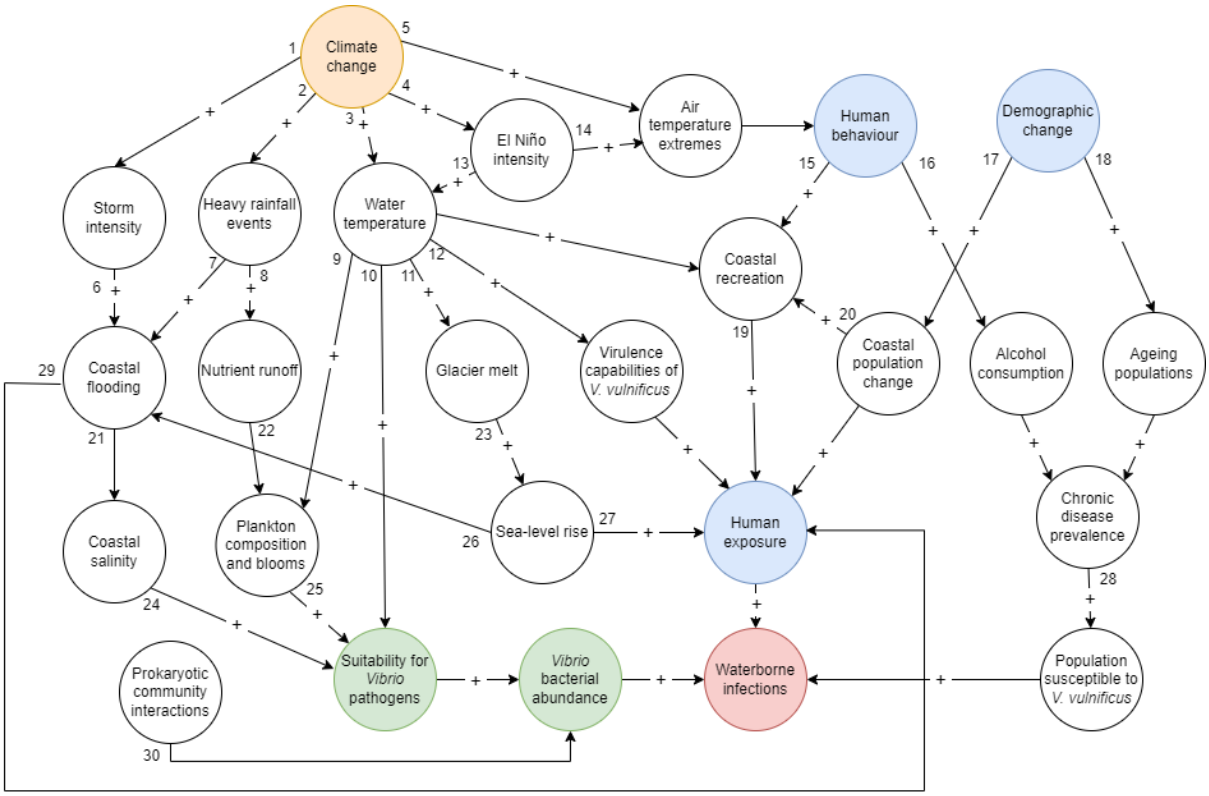

Figure 6.1 Directed acyclic graph of the pathways through which climate change and demographic change may influence waterborne *Vibrio vulnificus* infections generated from reading conducted during the creation of this thesis. Each edge (arrow) may contain a '+' to identify an increasing effect on the connecting node. Orange highlights the climate change node, blue represents key human-related nodes, green highlights *Vibrio* spp. bacteria within the environment and red signifies the waterborne infection node. References: 1. Kang and Elsner (2015), 2-3. IPCC (2021), 4. Wang et al. (2019), 5. IPCC (2021), 6-7. Collins et al. (2019b), 8. Fong et al. (2020), 9. (Henson et al., 2021; United States Environmental Protection Agency, 2013; Yamaguchi et al., 2022), 10. Sheikh et al. (2022b), 11. IPCC (2021) 12. Hernández-Cabanyero et al. (2020), 13. Wang et al. (2019), 14. IPCC (2021), 15. Elliott et al. (2019); Morgan and Ozanne-Smith (2013), 16. Julien et al. (2020), 17. Neumann et al. (2015), 18. United Nations Department of Economic and Social Affairs (2023), 19. Baker-Austin et al. (2016), 20. Neumann et al. (2015), 21. United States Environmental Protection Agency (2013), 22. IPCC (2021), 23. Rhoads (2006), 24. Eiler et al. (2007); Greenfield et al. (2017) , 25. IPCC (2021), 26. Deeb et al. (2018), 27-28. Baker-Austin and Oliver (2018), 29. Rhoads (2006).

6.2.3 Improving the robustness of results

A reoccurring theme throughout the thesis is the importance of ensuring the robustness of analysis results in response to the low frequency of *V. vulnificus* infections, and potential uncertainties and errors in the data. In both Chapter 3 and Chapter 4 the data for modelling were split 90:10 so that 90% of the data could be used for model training and testing (split 70:30) and the remaining 10% would be held out for model validation as an unseen set of data applied at the end of the modelling process. Calculating model metrics such as the area under the receiver operating characteristic curve (AUC; a measure of predictive power) with the validation set is important to assess whether the model performs as well on completely unseen raw data (Chicco, 2017; Quinn et al., 2021).

Chapter 3 model parameter estimates were averaged across 100 replicate models which were constructed with 100 random subsets of the data. Averaging over multiple models generally reduces prediction error compared to the use of just one model, as supported by an assessment of 180 studies by Dormann et al. (2018). Predictions of future risk were also averaged across results from 7 CMIP6 GCMs to account for differences in their simulations of future climate. Generating model predictions from an ensemble of GCMs is a useful method to account for differences in their simulations of future climate and enables the range of predicted values across GCMs to be assessed alongside the mean, as seen for predictions of dengue fever cases in Colón-González et al. (2018). Model averaging was also used in Chapter 4. Here, an MMI approach was used to obtain average parameter estimates across a set of models containing different combinations of environmental variables. Using MMI enables models to be ranked by their fit to the data and means that variables of interest can be explored for their relative importance to the dependent variable in a systematic way (Symonds and Moussalli, 2011). This process was repeated across 100 random subsets of data and results were averaged.

Although vastly contrasting to Chapter 3 and Chapter 4 in methodology, Chapter 5 also included efforts to improve the robustness of results. Multiple methods were used to confirm *Vibrio* species identification of the bacterial isolates obtained from a coastal lagoon. For example, those isolates identified as *V. alginolyticus* and *V. parahaemolyticus* by MALDI-TOF MS were also tested with conventional PCR to confirm these results. MALDI-TOF MS is a relatively new method for identifying *Vibrio* spp. (Dieckmann et al., 2010) therefore confirmation via a secondary, more established method was important to understand the accuracy of MALDI-TOF MS for *Vibrio* spp. identification. This said, the gold standard for microbial species identification

is currently whole genome sequencing (WGS) (UKHSA, 2018). Future work could include comparison of results generated with MALDI-TOF MS and WGS.

6.3 Future research

6.3.1 Future *Vibrio* spp. risk

Early warning systems

Moving forward, a key area of research is the further development of predictive risk models for *V. vulnificus* and other *Vibrio* spp. pathogens. Both long-term predictions (e.g., spanning decades into the future) and short-term early warning systems (e.g., a 5-day forecast) are needed to inform effective mitigation strategies which can help to prevent *Vibrio* spp. infections. Chapter 3 provides an example of long-term prediction of *V. vulnificus* infection risk for the east coast of the US. Whereas early warning systems like the ECDC *Vibrio* Map Viewer (Semenza et al., 2017) provide a resource for forecasting *Vibrio* spp. risk over the next five days based off SST and salinity data which can be used for decision making by local government as well as the general public. Similar near-term risk models may be useful for predicting *Vibrio* spp. risk in other locations where infections are emerging e.g., east coast of the United States (Archer et al., 2023), Australia (Harlock et al., 2022) and New Zealand (Vasey et al., 2023). On the other hand, Schütt et al. (2023) argue that the ECDC *Vibrio* Map Viewer is less helpful for estimating *Vibrio* spp. infection risk as the model does not account for species-specific preferences of temperature and salinity and that models focused on a particular *Vibrio* species, would be more valuable and robust. Even so, regardless of whether they visualise predicted *V. vulnificus* risk only or general *Vibrio* spp. risk, mapped forecasts of *Vibrio* spp. risk using gridded environmental data are useful for estimating risk over large areas which would be impractical and highly costly to sample directly. Monitoring *Vibrio* spp. bacteria with laboratory techniques, which can take several hours, would also delay the dissemination of warning messages to the public. Nevertheless, it is still important that model results are validated with microbiological analysis of water samples (Mälzer et al., 2016).

A key aim of Chapter 5 was to assess the relationship of environmental variables with *Vibrio* spp. abundance in a UK coastal lagoon. The resultant environmental conditions suitable for high *Vibrio* spp. abundance could then potentially be mapped to identify other coastal *Vibrio* spp. hotspots for further microbiological investigation (nonetheless,

extrapolation of relationships between *Vibrio* spp. abundance and environmental parameters to wider geographic locations would need to be validated by in situ microbiological testing). Unfortunately, this was not possible as no significant relationships between water temperature, salinity or pH and Vibrio spp. abundance were found over the 10-week study, emphasising the complex ecology of this environment. However, given the high *Vibrio* spp. abundance (10^5 CFU/100ml) recorded in some water samples from UK 'Lagoon X' in Chapter 5 and the number of potentially pathogenic isolates recovered, future work should continue to investigate *Vibrio* spp. risk to bathers in the UK.

Figure 6.2 is an interactive *Vibrio* spp. risk map created by mapping thresholds of SST (>18°C) and salinity (<25 PSU) recognised as preferred for *Vibrio* spp. growth (Vezzulli et al., 2013) (similar to the ECDC *Vibrio* Map Viewer; Semenza et al. (2017)) with high resolution (~1.5km by ~3km) oceanographic data. As seen in Figure 6.2, several alternative locations are identified as potential UK *Vibrio* spp. risk hotspots during the 2022 heatwave (Kendon et al., 2023). Nevertheless, the elevated risk identified in this mapping exercise should be taken as a starting point for future microbiological investigation and validation which is needed before such risk map application can be considered useful.

Future advancements in satellite sensors, oceanographic sensors and computer models used to interpolate data between observations, may provide opportunities to include further relevant variables in addition to SST and salinity in near-real-time *Vibrio* spp. risk models to improve predictions. This may be especially useful for developing more complex models in smaller, high *Vibrio* spp. risk locations that have specific hydrological dynamics. For instance, Bullington et al. (2022) generated hourly real-time predictions of *V. vulnificus* concentrations in the Ala Wai Canal of Honolulu, Hawai'i using 40m resolution SST and salinity forecast data from the Regional Ocean Modeling System for the Waikīkī area (Waikīkī ROMS), five-day average rainfall, daily maximum air temperature and, using a moored fluorometer sensor, dissolved organic matter (DOM). The inclusion of DOM increased the risk model's ability to explain the variability in *V. vulnificus* concentration by 17%, highlighting the importance of this parameter at the study location (Bullington et al., 2022). Work to predict DOM in estuaries has been conducted (Bowers and Brett, 2008; Wang et al., 2021). Future availability of DOM forecasts alongside other open-source data products would enable this parameter to be included in near-term forecasts of *V. vulnificus* concentration.

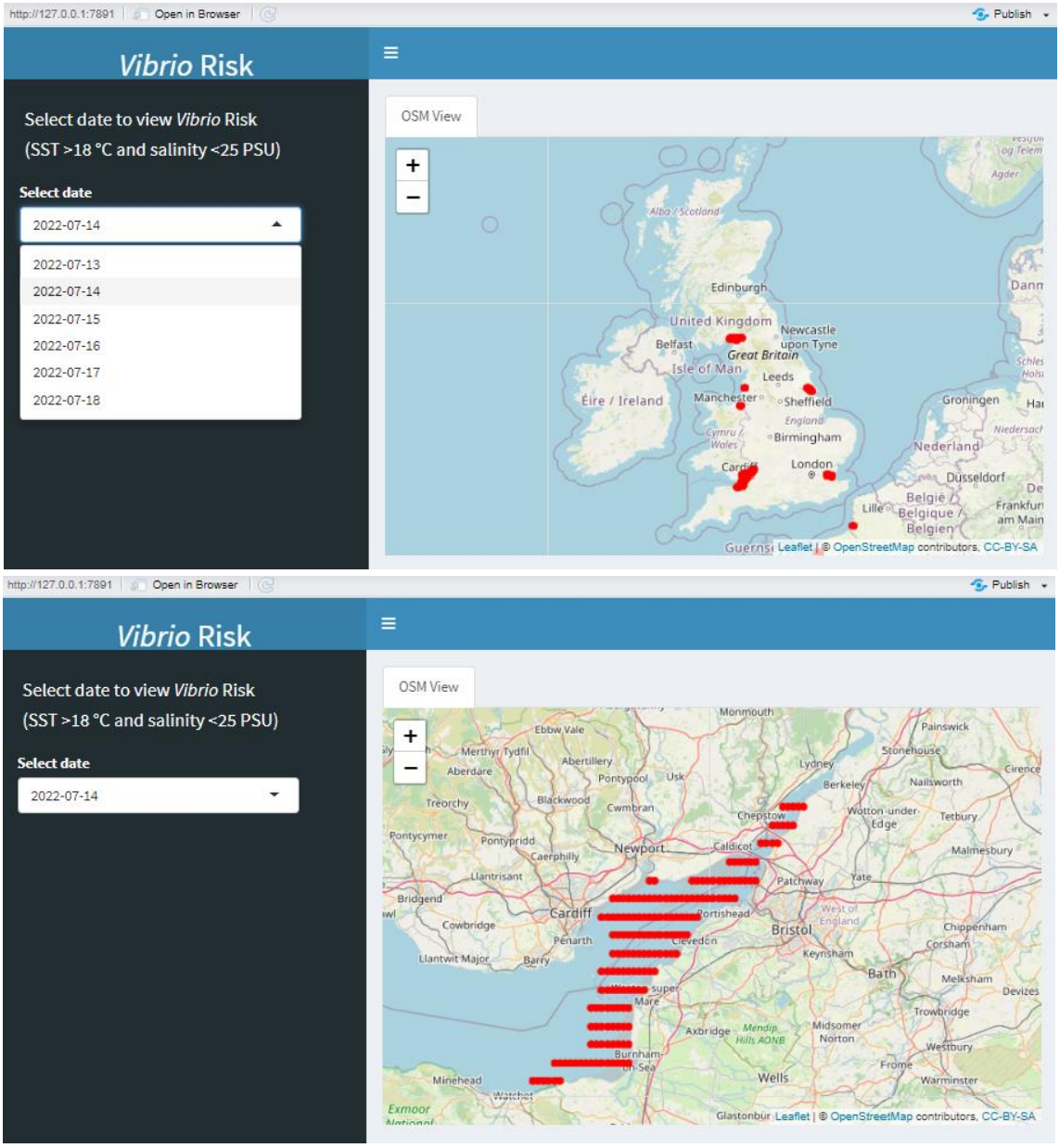

Figure 6.2 *Vibrio* spp. risk in the UK on 14/07/2022 during the July 2022 heatwave (Kendon et al., 2023) based on suggested suitable sea surface temperature (>18°C) and salinity (<25 PSU) for *Vibrio* spp. growth (Vezzulli et al., 2013). Daily risk plus 5-day forecast using data from the Atlantic – European North West Shelf – Ocean Physics Analysis and Forecast dataset available from the Copernicus Marine Service (Copernicus Marine Service, 2023a). Application made by author using RShiny (Chang et al., 2022). Top: UK view. Bottom: zoom-in of waters suitable for *Vibrio* spp. growth in the Severn Estuary leading into the Bristol Channel.

Current bathing water quality classifications in Europe and the US are determined by counting the number of viable faecal indicator bacteria (FIB) in water samples obtained

and tested during the bathing season (typically May to September) (Tiwari et al., 2021). The quantification of waterborne pathogens is not included in these assessments as FIB are considered more easily isolated from the environment and an indication of faecal pollution and its associated pathogens (US Environmental Protection Agency, 2001). Alternatively, Gyraite et al. (2020) propose an integrated bathing water quality assessment that also takes into consideration specific *Vibrio* spp. indicators: less than 19 *V. vulnificus* infections per 1000 bathers and a *V. cholerae* count of less than 10^6 cells/100ml are required to stay below the high-risk level. Although promising in concept, the proposed risk level considered acceptable for *V. vulnificus* should be examined to ensure that the rate of infections is appropriate for the geographic area and time period (19 cases represents roughly a quarter of annual *V. vulnificus* cases on the east coast of the US (Archer et al., 2023)). Support for the inclusion of additional bathing water quality parameters alongside FIB comes from Farrell et al. (2021) who conducted a review of waterborne organisms of public health concern isolated within designated bathing waters of Europe across multiple studies (Farrell et al., 2021). The authors found that *Vibrio* spp. were the most frequently detected bacterial organisms and were found in 84.1% of samples tested (392/466) (Farrell et al., 2021).

Another limitation of existing bathing water quality monitoring is the infrequency of sample collection. Even if *Vibrio* spp. counts were to be measured alongside FIB, the sensitivity of *Vibrio* spp. to changing environmental conditions means that four samples per season (the minimum required under the EU Bathing Water Directive; E. U. Directive (2006)) would not be adequate to provide a reliable estimation of risk to bathers. This is evident through results of *Vibrio* spp. bacterial counts in Chapter 5 which demonstrate strong weekly variability in abundance. For other rapidly changing environmental hazards such as harmful algal blooms (HABs), wider monitoring efforts are enabled using citizen science initiatives such as the US Phytoplankton Monitoring Network which has existed for over 20 years (NCCOS, 2021). This strategy proves effective for HABs as they are often highly visible and citizen scientists can be trained to obtain water samples and identify different phytoplankton species with optical microscopy. Unfortunately, the same methods cannot be used to identify *Vibrio* spp. bacteria which are typically identified with techniques requiring use of specialist laboratory equipment and methods. However, there is ongoing development of lateral flow assays as a low-cost, portable test to detect *Vibrio* spp. pathogens in seafood samples (Sohrabi et al., 2022; Yang et al., 2021; Ying et al., 2021) and drinking water in rural regions (Mayry et al., 2022). Such tests are rapid, taking just over one hour to complete without the need for laboratory thermocycler instruments (Ying et al., 2021) or expensive reagents (Mayry et al., 2022)

and so may provide a promising tool for citizen science monitoring of *Vibrio* spp. in local waters in the future.

6.3.2 *Vibrio* spp. ecology and disease

Paired environmental and epidemiological data

In addition to environmental data, genetic information obtained from sequencing the causal *Vibrio* spp. pathogen could also be incorporated into the same dataset. Applications like NextStrain (https://nextstrain.org/) and Microreact (https://microreact.org/) currently enable the genetic information of pathogens such as the DENV1 dengue virus and *Mycobacterium tuberculosis*, the causal agent of tuberculosis, to be shared and evolving strains to be tracked globally. By mapping the geographic locations of clinical *Vibrio* spp. strains in space and time, the evolution and movement of *Vibrio* spp. pathogens could be visualised and considered in conjunction with *Vibrio* spp. early warning systems for the benefit of public health preparedness (Baker-Austin et al., 2020).

Building on the above mapping of *Vibrio* spp. genetic information, future epidemiological *Vibrio* spp. surveillance should aim to incorporate environmental and demographic attributes into records of infections. In the context of the COVID-19 pandemic, the integration of data from multiple sources including meteorological data, policy data and air quality data alongside epidemiological data has been valuable for elucidating COVID-19 risk factors (Badr et al., 2023). For *Vibrio* spp. researchers, the availability of this information at local, regional, and global scales would prove invaluable for investigating the geographic expansion of *Vibrio* spp. pathogens with climate change and the environmental conditions conducive to infections. It could also highlight human populations with demographic characteristics that make them particularly vulnerable to *Vibrio* spp. infections, particularly those caused by *V. vulnificus*. An example of a similar framework is the Medical & Environmental Data Mash-up Infrastructure (MEDMI) project which was active between 2013-2016 and is now accessible through the UKHSA Environmental Public Health Surveillance System (EPHSS) (https://www.ecehh.org/research/medmi/). MEDMI provided a platform for researchers to extract and combine epidemiological, environmental, and demographic data (described by MEDMI as “data linkage”) for a variety of human health projects e.g., examining the seasonality of pathogens in connection with weather (Cherrie et al., 2018) and night-time temperature and mortality risk (Murage et al., 2017). A key challenge highlighted by researchers working with the MEDMI platform was the difficulty in matching data from different sources at different temporal and spatial resolutions, available at different temporal

ranges and frequencies (Leonelli and Tempini, 2021) (similar to points discussed in section 6.2.1 'Data availability'). However, it is argued that with careful, purposeful choice of datasets and acknowledgement of their limitations, analyses that make use of "data linkages" can still provide important findings (Leonelli and Tempini, 2021).

Human interaction with the environment leading to disease

Detailed information on what activities individuals were engaged with whilst exposed to *Vibrio* spp. pathogens resulting in disease should be collated to help better understand if particular behaviours are associated with elevated risk of infection or the most severe health outcomes such as sepsis or death. For example, it might be helpful to understand to what extent fishing activity versus swimming increases a person's risk of aquiring a *V. vulnificus* infection but obtaining these data is a challenge. Within the confirmed waterborne *V. vulnificus* COVIS data subset used in this thesis, about 20% of entries include a specific statement on the presumed route of transmission such as "scraped arm on crab trap" or "cut by catfish spine". Yet even of these cases, many statements are vague or incomplete, e.g., "lives next to sea" and "slipped". Having access to this information would be valuable for identifying groups of people to target for *V. vulnificus* interventions.

6.3.3 Climate change attribution of *Vibrio vulnificus* infection emergence along Northeast United States coastline

The emergence of *Vibrio* spp. infections in Northern Europe was attributed to anomalous sea surface temperatures that arose as a consequence of climate change due to the strong similarity in the spatial and temporal patterns of temperatures and disease emergence (Baker-Austin et al., 2013; Ebi et al., 2017). Future work could include an attribution study to determine the role of climate change in the emergence of *V. vulnificus* wound infections along the northeast coastline of the US. Detection and attribution studies for health-related outcomes such as *Vibrio* spp. disease are highly important for many reasons. From a financial perspective, demonstrating the link between climate change and particular poor health outcomes can aid in loss and damage calculations as well as open up sources of funding reserved for climate change related issues (Ebi et al., 2020). The further benefit of attributing health impacts to climate change includes an increase in the general public's understanding that climate change is affecting health now and it is not just a problem for tomorrow, boosting the significance of climate action (Ebi et al., 2020).

6.4 Contribution of the thesis to the field

This thesis includes one of the first studies to explore the changing spatial distribution of *V. vulnificus* wound infections on the east coast of the US over a three-decade historical period. Temperature-sensitive *V. vulnificus,* is considered a 'microbial barometer of climate change' (Baker-Austin et al., 2017); research into changes in the spatial distribution of such pathogens is crucial for further understanding the impacts of climate change on the marine microbial community and human health. By mapping the historical changes in *V. vulnificus* risk, we have demonstrated the northwards expansion of *V. vulnificus* wound infections through time, bringing together 30 years of data and, more generally, highlighting the increasing burden of climate-sensitive diseases in a warming world. Meanwhile, the predictions of future *V. vulnificus* risk along the Northeast coast of the US provide incentive for greater awareness of *V. vulnificus* infections and their risk factors amongst residents, visitors, and healthcare professionals. With these predictions we also demonstrate the need for a reduction in greenhouse gas (GHG) emissions to limit the burden of *V. vulnificus* infections on human health in the long term, as predictions of risk diverged with climate change scenarios mostly in the far-future time period (2081-2100). This is because even if GHG emissions were reduced now, stabilisation of global temperature may still not occur for 20-30 years (IPCC, 2021), i.e., we have already 'locked in' a certain amount of warming. However, as the number of predicted infections was also heavily influenced by the age structure and count of the population, this work stresses the need for research to consider the intersection of demographic change and *V. vulnificus* risk.

In 2023, higher than average SSTs have been recorded globally, including along US coastlines (NOAA, 2023b). Fatalities from *V. vulnificus* infections have been reported in Connecticut (CT DPH, 2023), New York (Governor Kathy Hochul, 2023) and North Carolina (NCDHHS, 2023). This has prompted the US CDC to issue an official health advisory to warn citizens of the risk of *V. vulnificus* infections associated with warm coastal waters (CDC, 2023). Chapter 3 (Archer et al., 2023) has been cited in this official advisory, therefore part of the thesis has already supported public health awareness efforts in the US. Further, press attention surrounding the study has potentially increased awareness of *V. vulnificus* more generally in the US and Canada, as well as an awareness of climate change's impact on the marine environment and human health.

Using the same CDC dataset, the second modelling study presented in this thesis (Chapter 4) explores the drivers of *V. vulnificus* wound infection occurrence at a weekly

timescale for Gulf of Mexico states. This analysis demonstrated the strength in the seasonality of *V. vulnificus* infections within this region. The importance of temperature as an environmental driver of weekly infections compared to other environmental factors was supported but weekly temperature was not essential to the generation of a good predictive model which already contained a seasonal component (i.e., month). This not only demonstrates how predictable the occurrence of *V. vulnificus* wound infections is in the Gulf of Mexico region, but it also highlights the potential accuracy of an early warning system using a model only containing seasonal components in this location.

Challenges resulting from studying a low probability, high impact form of infection have been confronted and discussed throughout this thesis. Both Chapter 3 and Chapter 4 tailored the modelling methodologies used to *V. vulnificus* wound infections. The methods detailed in these chapters may be of use to researchers wishing to study other diseases with similar characteristics. Further to the methodologies, the importance of using high quality environmental and epidemiological datasets, especially when the frequency of infection cases is low, is highlighted by this work.

To improve the understanding of *Vibrio* spp. abundance and its environmental drivers in the UK, an ecological sampling study (Chapter 5) was conducted. Analysis of *Vibrio* spp. abundance in UK waters is rare so this work has helped to develop current knowledge of *Vibrio* spp. in a hotspot location. MALDI-TOF MS was used to aid rapid identification of a large collection of isolates recovered, supporting its potential future use in *Vibrio* spp. monitoring efforts. Multiple potentially pathogenic *Vibrio* species were isolated. These findings suggest the need for further investigation of *Vibrio* spp. in UK waters.

The impacts of climate change on microorganisms are not well documented nor widely discussed (Cavicchioli et al., 2019). Yet, human infections caused by *Vibrio* spp. pathogens offer a tangible indicator of marine microbial communities facing environmental change (Baker-Austin et al., 2017) and therefore could be considered a vehicle for increased understanding of the link between environment and health.

Appendix:

Supplementary material

Table S1 Global Climate Models (GCMs) used in this study.

Model Name	Institution(s)	Main Reference(s)
AWI-CM-1-1-MR	Alfred Wegener Institute	(Semmler et al., 2020)
BCC-CSM2-MR	Beijing Climate Center	(Xin et al., 2018)
CNRM-CM6-1	Centre National de Recherches Meteorologiques and Centre Europeen de Recherche et Formation Avancees en Calcul Scientifique	(Voldoire, 2018; Voldoire et al., 2019)
CNRM-ESM2-1	Centre National de Recherches Meteorologiques and Centre Europeen de Recherche et Formation Avancees en Calcul Scientifique	(Séférian et al., 2019)
CanESM5	Canadian Center for Climate Modelling and Analysis	(Swart et al., 2019)
IPSL-CM6A-LR	Institut Pierre-Simon Laplace Climate Modelling Centre	(Boucher et al., 2020)
MIROC-ES2L	Japan Agency for Marine-Earth Science and Technology; Atmosphere and Ocean Research Institute, The University of Tokyo; National Institute for Environmental Studies; RIKEN Center for Computational Science	(Hajima et al., 2020)
MIROC6	Japan Agency for Marine-Earth Science and Technology; Atmosphere and Ocean Research Institute, The University of Tokyo; National Institute for Environmental Studies; RIKEN Center for Computational Science	(Tatebe et al., 2019)

Table S2 Length of coastline where *V. vulnificus* infections are present (thousand km) population at risk (millions), percentage of population aged ≥ 60 and estimated annual number of *V. vulnificus* cases under CMIP6 Shared Socioeconomic Pathways SSP126, SSP245, SSP370 and SSP585. Values are for the tmean model and are the ensemble mean from seven global climate models and the minimum and maximum estimates are given in square brackets.

Scenario	Time Period	Coastline where infections are present (thousands of km)	Total projected population at risk (millions)	Percentage of projected population at risk aged ≥60 years (%)	Estimated annual total number of cases
Baseline	**2007 - 2018**	10.0	61.0	16.9	61
SSP126	**2021 - 2040**	10.9 [10.7 - 11.1]	86.7 [83.6 - 94.4]	27.2 [27.2-27.2]	106 [102-115]
	2041 - 2060	11.1 [10.8-11.3]	106.6 [94.8-120.7]	32.5 [32.7-32.4]	145 [130-164]
	2061 - 2080	11.1 [10.9 - 11.4]	119.8 [109.1 - 132.6]	43.0 [43.2-42.9]	196 [179-216]
	2081 - 2100	11.1 [10.8-11.3]	124.1 [108.4-138.3]	43.1 [43.3-42.9]	204 [178-228]
SSP245	**2021 - 2040**	10.9 [10.7 - 11.1]	85.4 [80.1 - 93.6]	26.3 [26.3-26.2]	102 [95-112]
	2041 - 2060	11.3 [11.1 - 11.5]	109.7 [105.0 - 118.2]	30.1 [30.1-30.0]	142 [136-153]
	2061 - 2080	11.5 [11.3 - 12.0]	125.4 [121.5 - 134.1]	38.8 [38.8-38.7]	192 [186-204]
	2081 - 2100	11.7 [11.4 - 12.2]	136.0 [134.5 - 140.9]	38.7 [38.8-38.7]	208 [205-215]
SSP370	**2021 - 2040**	10.8 [10.7 - 11.2]	78.4 [72.0 - 92.6]	27.0 [27.0-27.0]	95 [88-113]
	2041 - 2060	11.3 [10.9-11.9]	89.1 [76.9–99.9]	31.4 [31.5-31.3]	120 [104-135]
	2061 - 2080	11.7 [11.3 - 12.5]	94.4 [92.9 - 98.0]	41.2 [41.2-41.1]	152 [149-158]
	2081 - 2100	12.5 [12.2-13.7]	88.0 [87.4-89.7]	41.1 [41.1-40.8]	141 [141-143]
SSP585	**2021 - 2040**	10.9 [10.7- 11.3]	93.5 [88.8 - 106.5]	25.7 [25.7-25.8]	110 [103-124]
	2041 - 2060	11.5 [11.3 - 12.1]	136.4 [132.1 - 146.6]	28.9 [28.9-28.8]	170 [165-182]
	2061 - 2080	12.2 [11.9 - 12.8]	178.2 [172.9 - 181.7 [2]]	35.2 [35.2-35.2]	251 [244-257]
	2081 - 2100	13.2 [12.4 - 15.8]	212.4 [209.6 - 223.7]	34.9 [35.2-33.4]	298 [296-300]

Table S3 As Table S2 but for the tmax model.

Scenario	Time Period	coastline infections are present (thousands of km)	Total projected population at risk (millions)	Percentage of projected population at risk aged ≥60 years (%)	Estimated annual total number of cases
Baseline	**2007 - 2018**	9.3	75.1	16.9	76
SSP126	**2021 - 2040**	10.8 [10.4 - 11.3]	102.0 [94.4 - 106.3]	27.3 [27.2-27.4]	124 [115-131]
	2041 - 2060	11.1 [10.6-11.5]	120.5 [113.9-126.3]	32.4 [32.5-32.4]	164 [156-172]
	2061 - 2080	11.2 [10.9 - 11.6]	133.5 [132.6 - 138.9]	42.9 [42.9-42.9]	218 [216-228]
	2081 - 2100	11.1 [10.7-11.6]	137.0 [123.2-144.8]	42.9 [43.1-42.9]	224 [202-237]
SSP245	**2021 - 2040**	10.8 [10.4 - 11.3]	98.7 [93.6 - 105.8]	26.3 [26.2-26.4]	117 [112-126]
	2041 - 2060	11.3 [10.8 - 11.8]	119.3 [118.2 - 123.9]	30.0 [30.0-30.0]	154 [153-159]
	2061 - 2080	11.6 [11.2 - 12.2]	132.5 [128.7 - 135.8]	38.7 [38.8-38.7]	203 [197-208]
	2081 - 2100	11.8 [11.3 - 12.4]	140.3 [135.1 - 146.1]	38.6 [38.7-38.0]	213 [207-218]
SSP370	**2021 - 2040**	10.8 [10.4 - 11.4]	95.2 [87.1 - 99.4]	27.0 [26.9-27.0]	116 [105-121]
	2041 - 2060	11.4 [11.1-12.3]	98.9 [92.5-103.5]	31.3 [31.4-31.3]	133 [125-140]
	2061 - 2080	12.0 [11.4 - 13.1]	97.7 [93.0 - 103.4]	40.9 [41.2-39.6]	156 [149-160]
	2081 - 2100	13.0 [11.8-16.5]	90.2 [87.4-92.5]	40.4 [41.1-39.6]	142 [141-144]
SSP585	**2021 - 2040**	10.8 [10.3 - 11.4]	108.9 [100.2 - 117.5]	25.8 [25.7-25.9]	128 [116-138]
	2041 - 2060	11.6 [11.2 - 12.3]	143.5 [140.0 - 149.0]	28.8 [28.8-28.9]	180 [174-187]
	2061 - 2080	12.4 [11.7 - 14.4	183.4 [177.9 - 191.5]	34.7 [35.2-33.5]	256 [251-258]
	2081 - 2100	14.4 [12.3 - 19.1]	220.4 [209.6 - 224.2]	33.8 [35.2-33.3]	299 [296-300]

Table S4 Length of coastline at risk (thousands km) population (millions) within 200 km of predicted *V. vulnificus* risk, percentage of population aged ≥ 60 and estimated annual number of *V. vulnificus* cases under CMIP6 Shared Socioeconomic Pathways SSP126 and SSP370 assuming no shift in the distribution of *V. vulnificus* (95th percentile latitude of cases: ~40^{o}N).

Model	Scenario	Time Period	Length of coastline at risk (in thousands of km)	Total projected population at risk (in millions)	Percentage of projected population at risk aged ≥60 years (%)	Estimated annual total number of cases
No Change in the distribution of *V. vulnificus*	**Baseline**	**2007 – 2018**	10.8	59.3	19.0	59
	SSP126	**2041-2060**	10.8	73.3	32.9	101
		2081-2100	10.8	83.3	43.6	138
	SSP370	**2041-2060**	10.8	59.3	31.7	80
		2081-2100	10.8	50.0	41.7	81

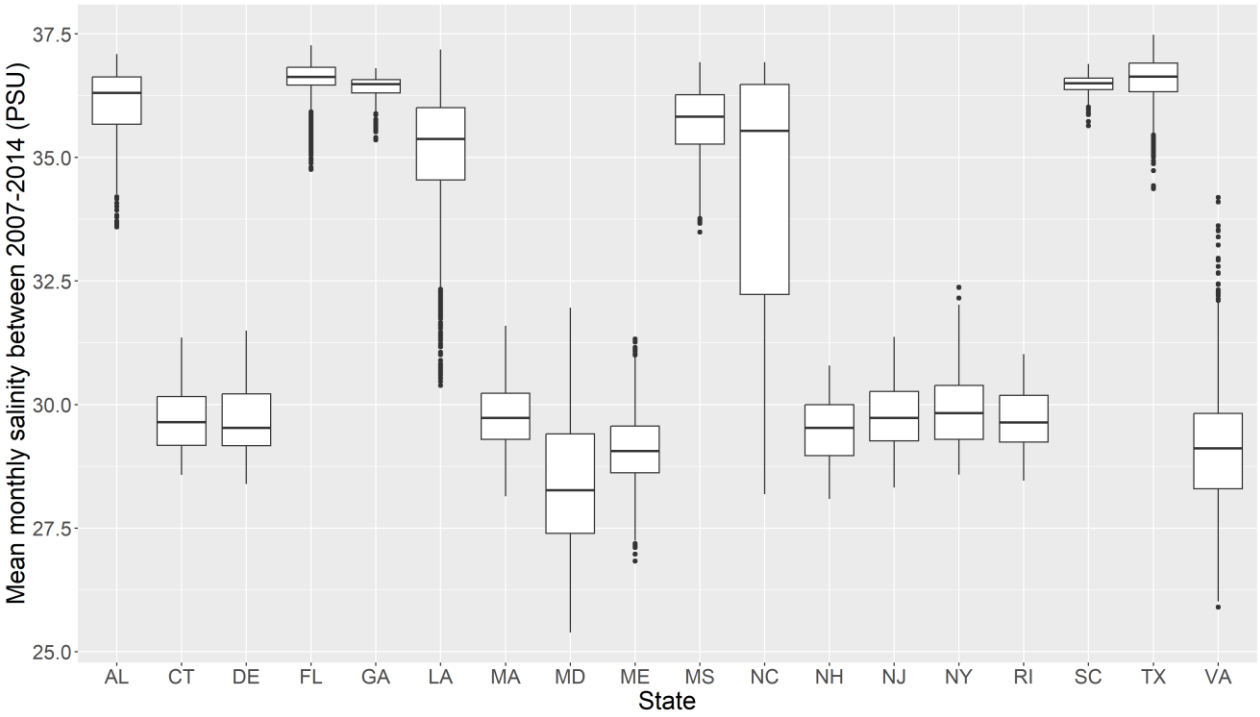

Figure S1 Boxplot of mean monthly salinity concentration (PSU) for every 25 km x 25 km coastal grid cell in the study area 2007-2014 subdivided by state.

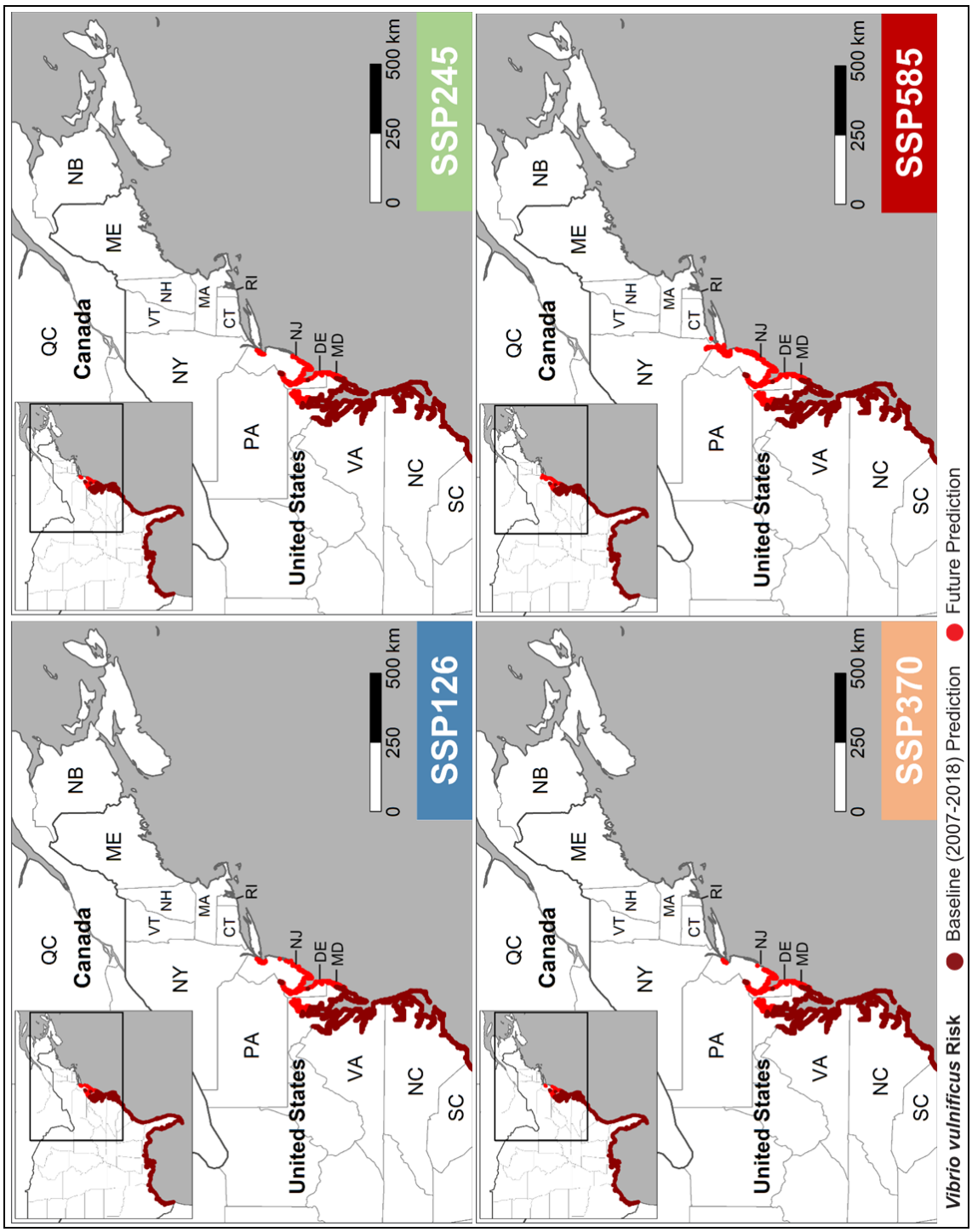

Figure S2 Tmean model prediction of *V. vulnificus* human wound infection risk averaged across seven CMIP6 global climate models between 2021 – 2040 under CMIP6 Shared Socioeconomic Pathway (SSPs) SSP126, SSP245, SSP370 and SSP585.

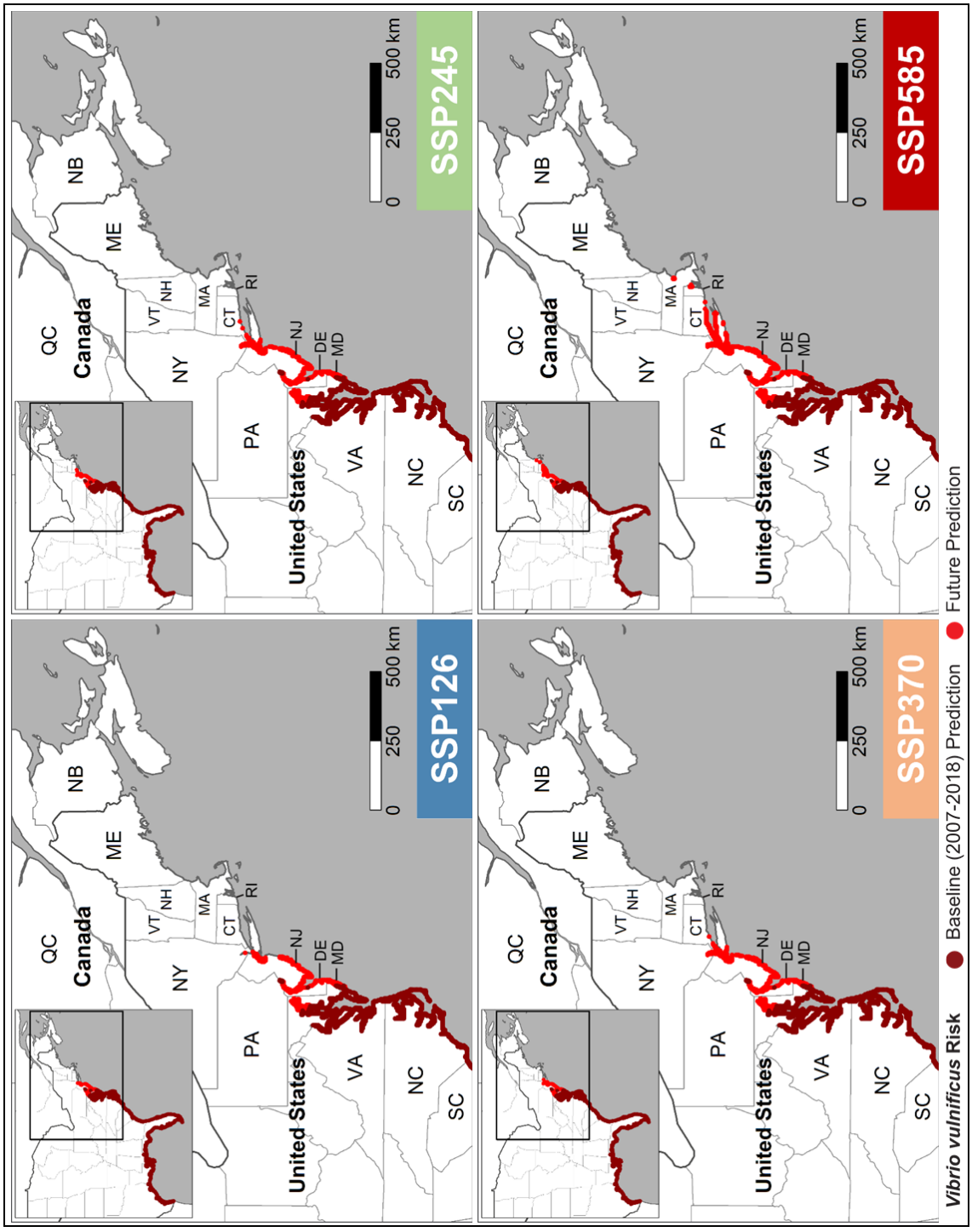

Figure S3 As Figure S2 but for 2041 – 2060.

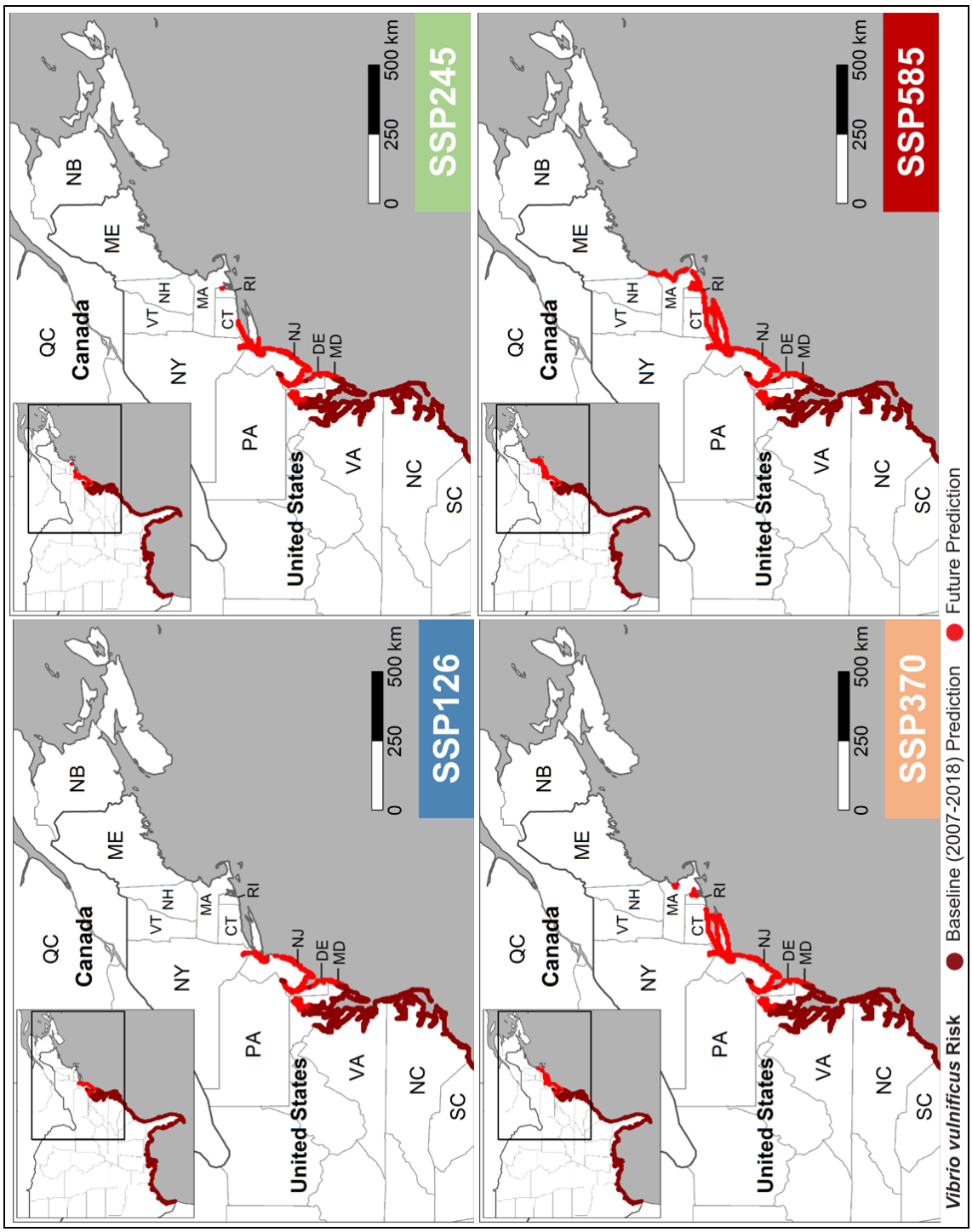

Figure S4 As Figure S2 but for 2061 – 2080.

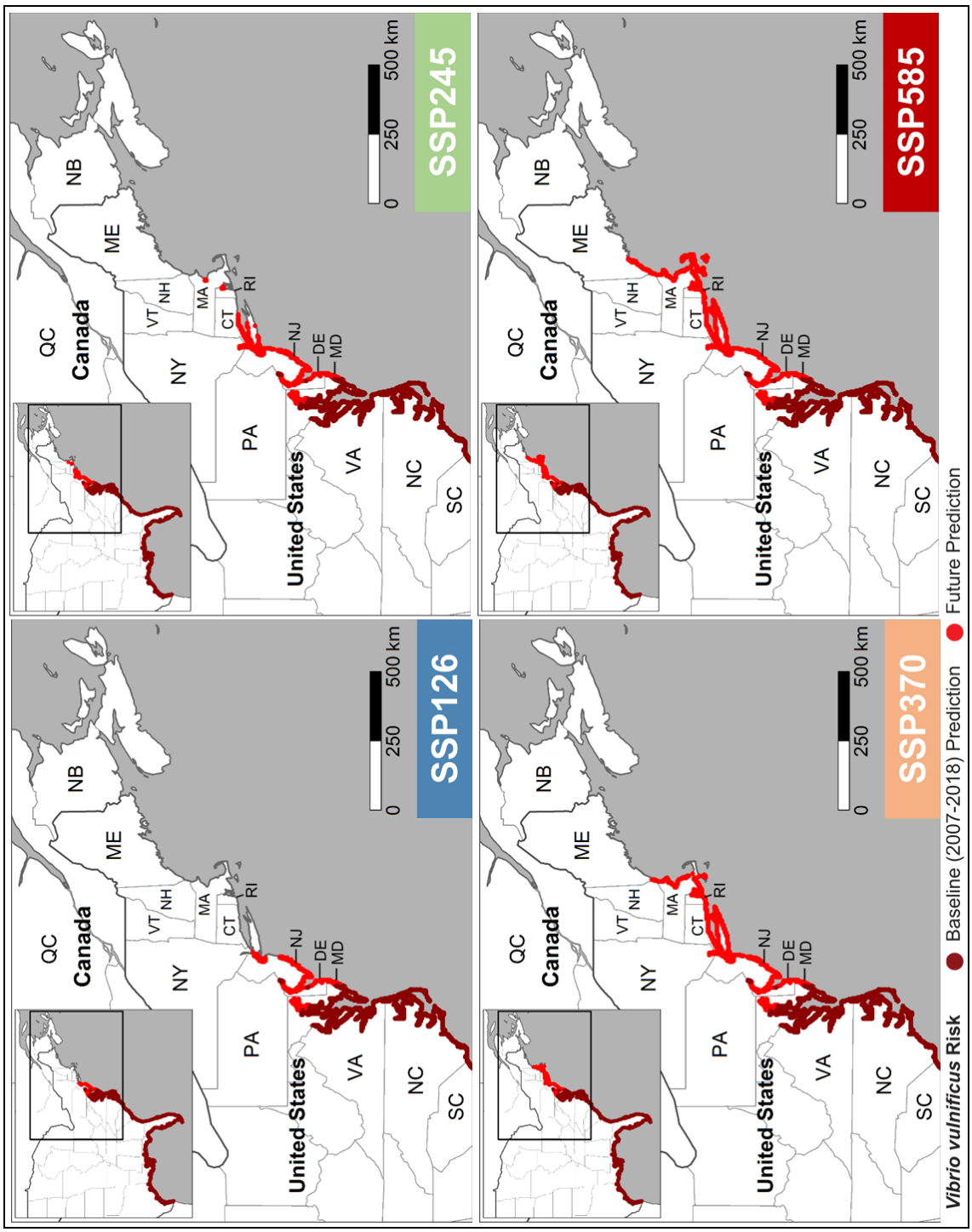

Figure S5 As Figure S2 but for 2081 – 2100.

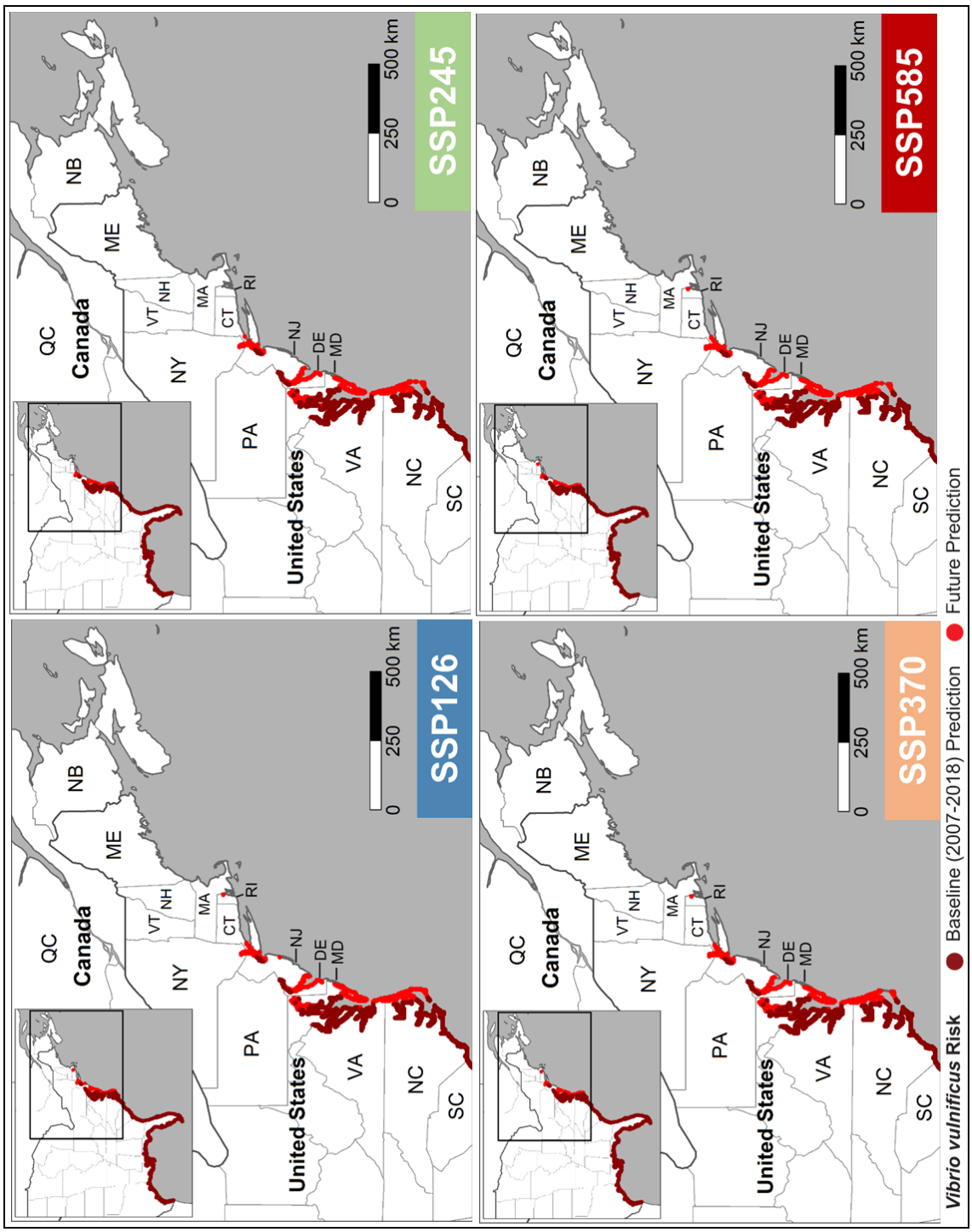

Figure S6 Tmax model prediction of *V. vulnificus* human wound infection risk averaged across seven CMIP6 global climate models between 2021 – 2040 under CMIP6 Shared Socioeconomic Pathway (SSPs) SSP126, SSP245, SSP370 and SSP585.

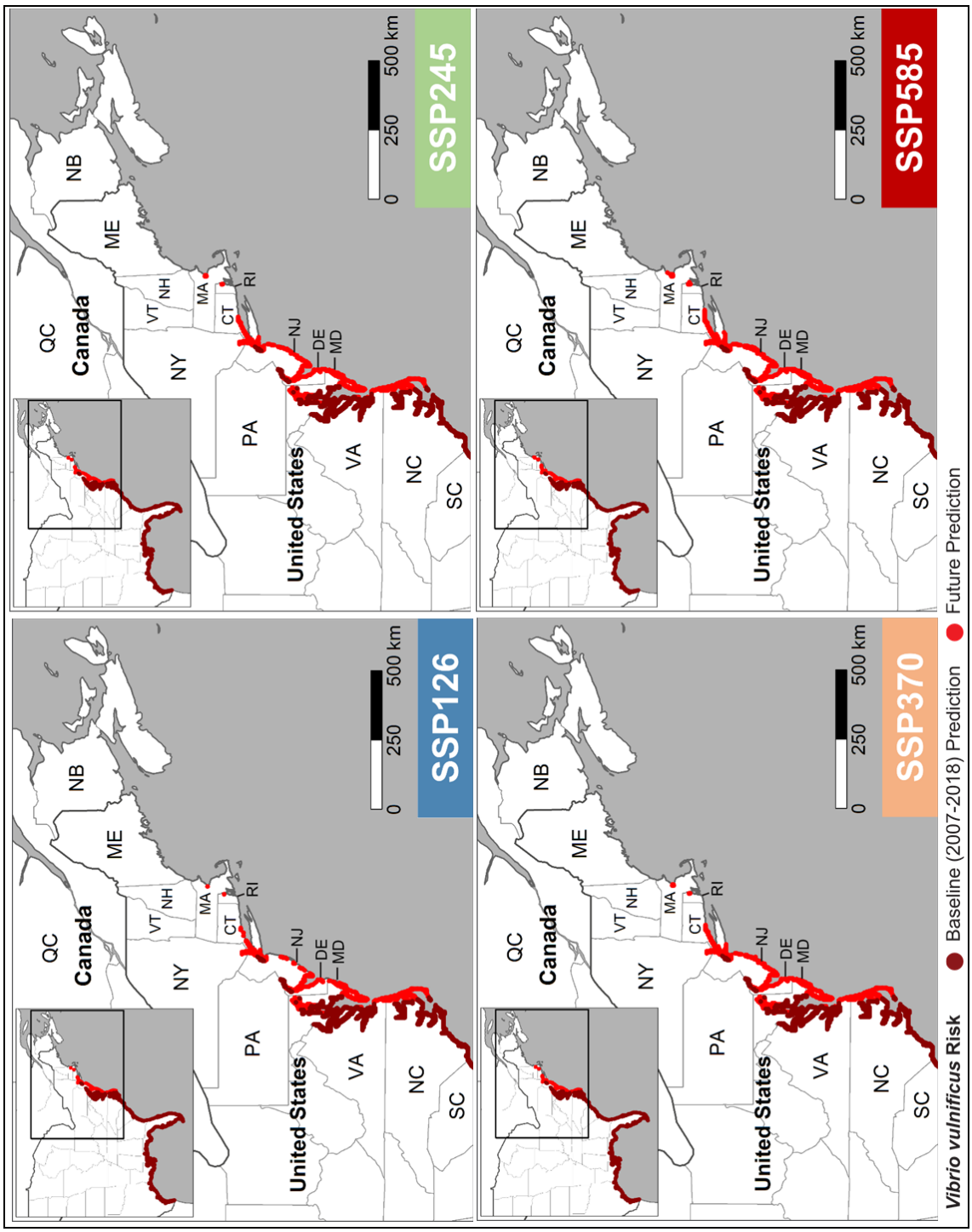

Figure S7 As Figure S6 but for 2041 – 2060.

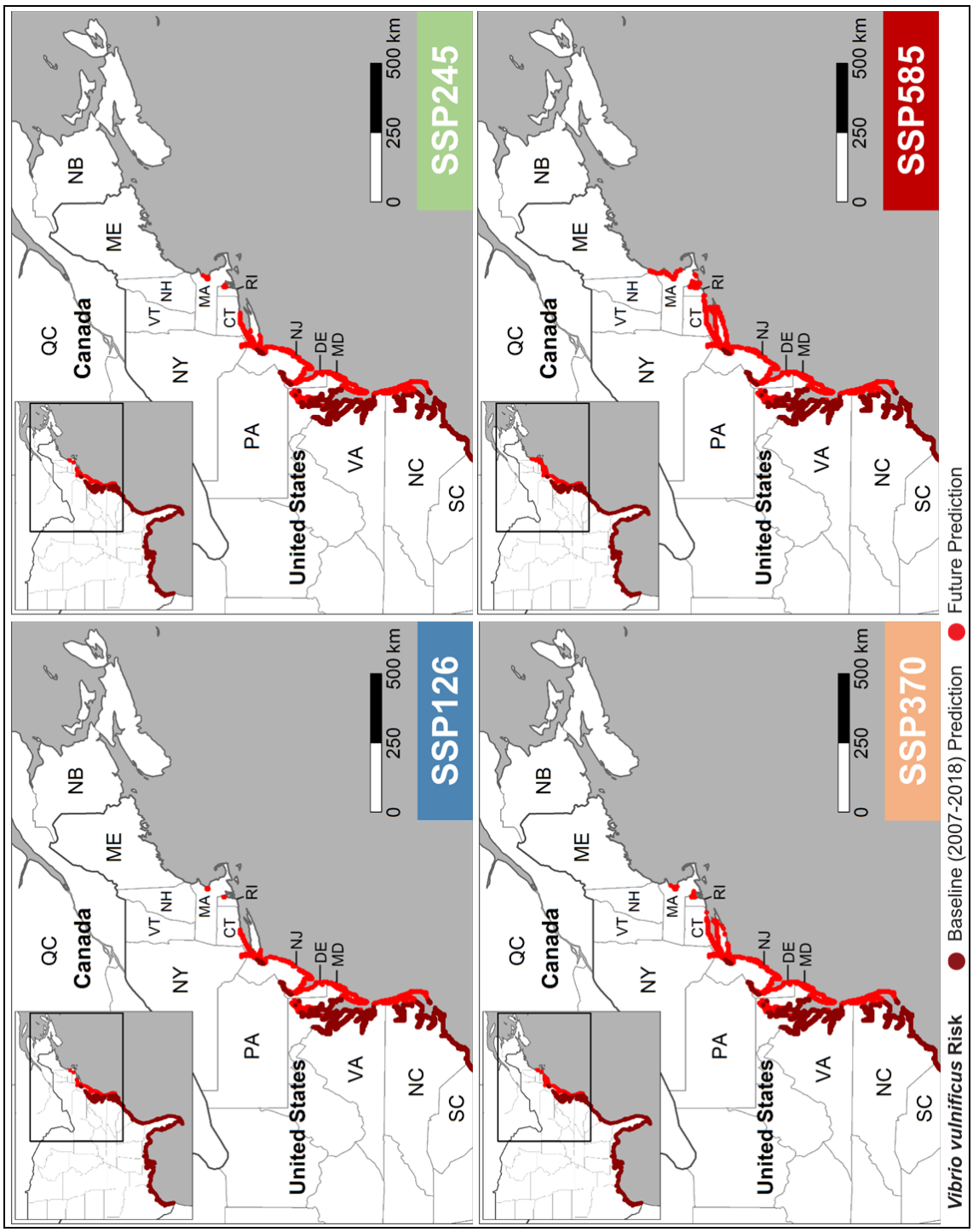

Figure S8 As Figure S6 but for 2061 – 2080.

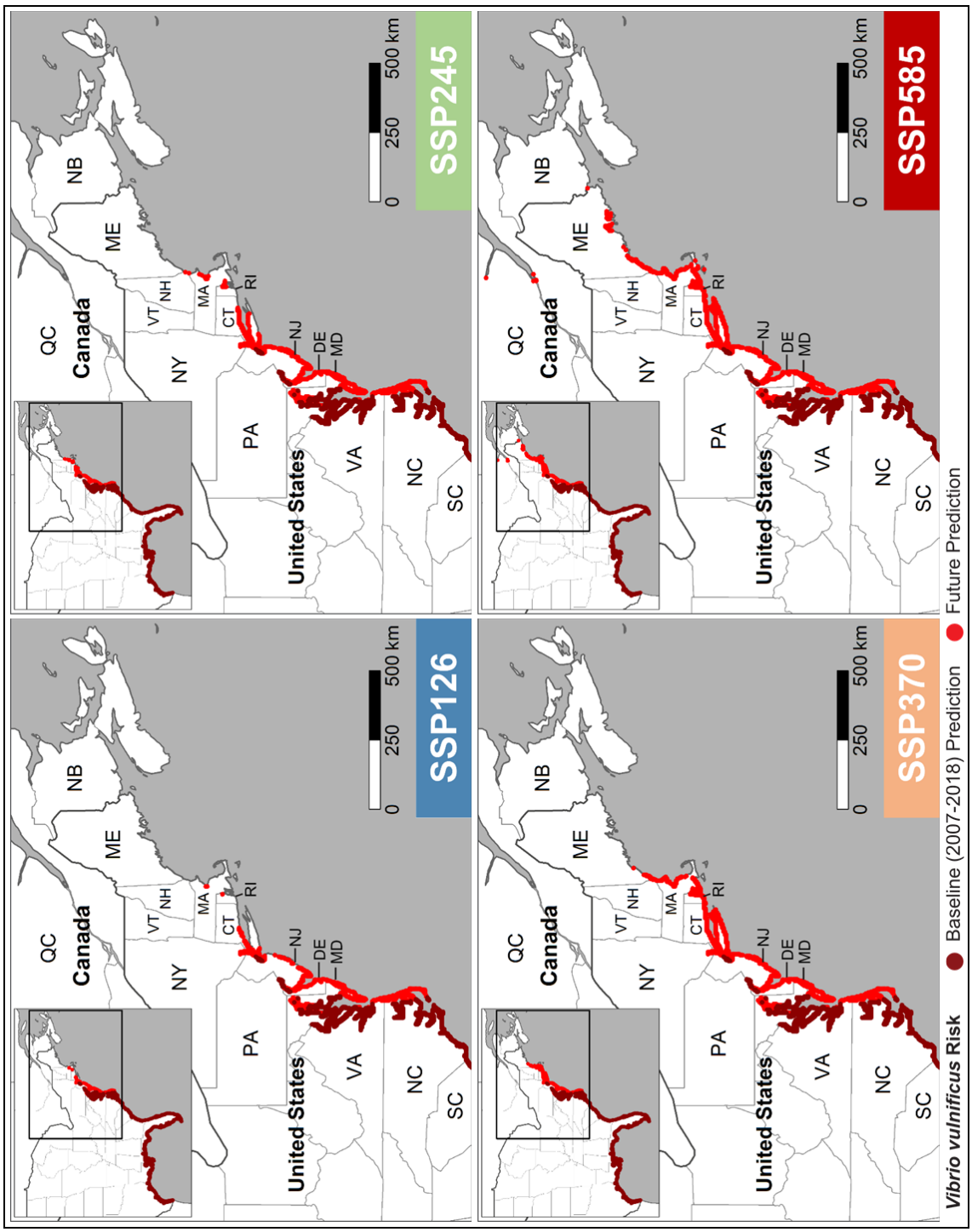

Figure S9 As Figure S6 but for 2081 – 2100.

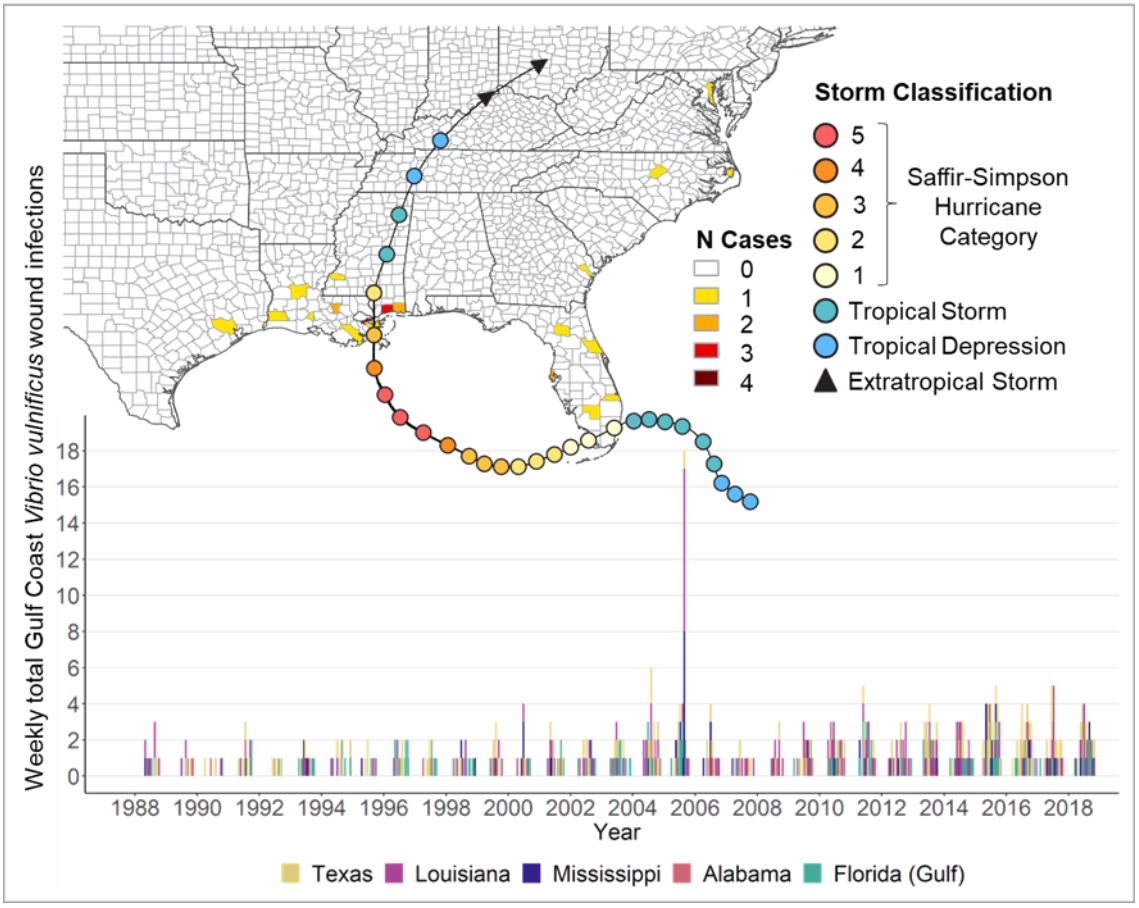

Figure S10 Top: Storm track of Hurricane Katrina, August 2005, with county-level reports of *V. vulnificus* wound infections for 2005 following Hurricane Katrina (23/08/2005 onwards). Bottom: Total weekly *V. vulnificus* wound infection case numbers for Gulf Coast States (stacked). Only infections reported within 200 km of the coast are included.

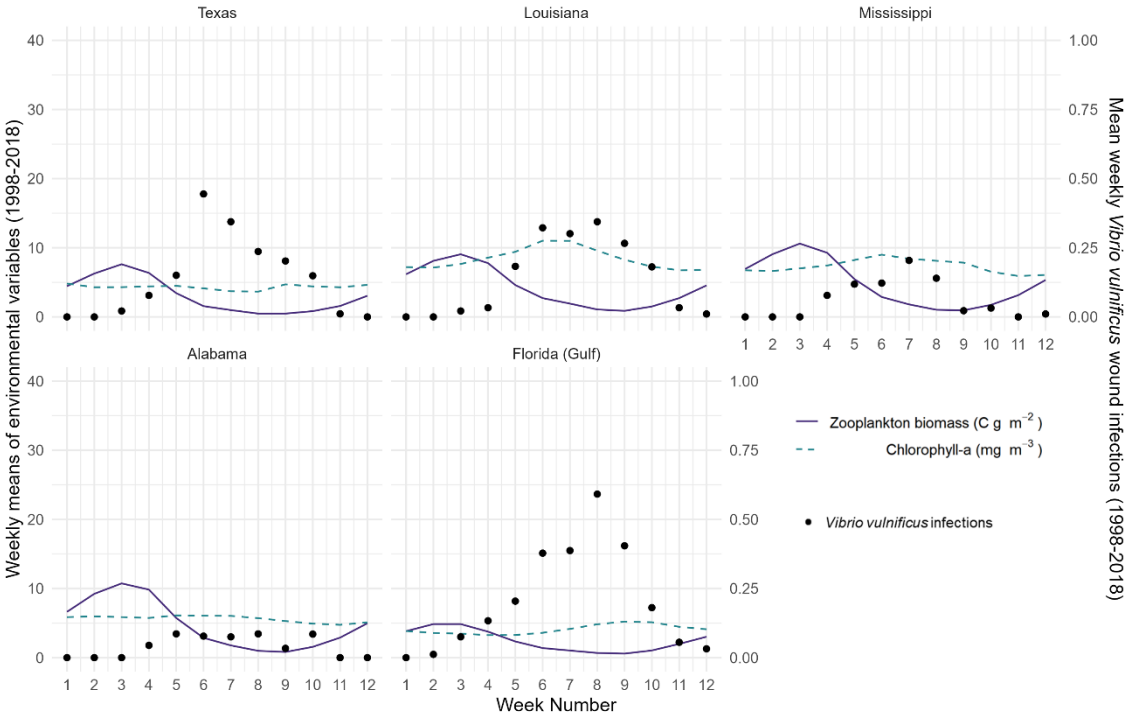

Figure S11 Monthly chlorophyll-a and zooplankton biomass with number of *V. vulnificus* wound infections for US Gulf Coast states averaged over 1993-2018 time-period. Environmental means are weighted by population count within 200 km of the coast.

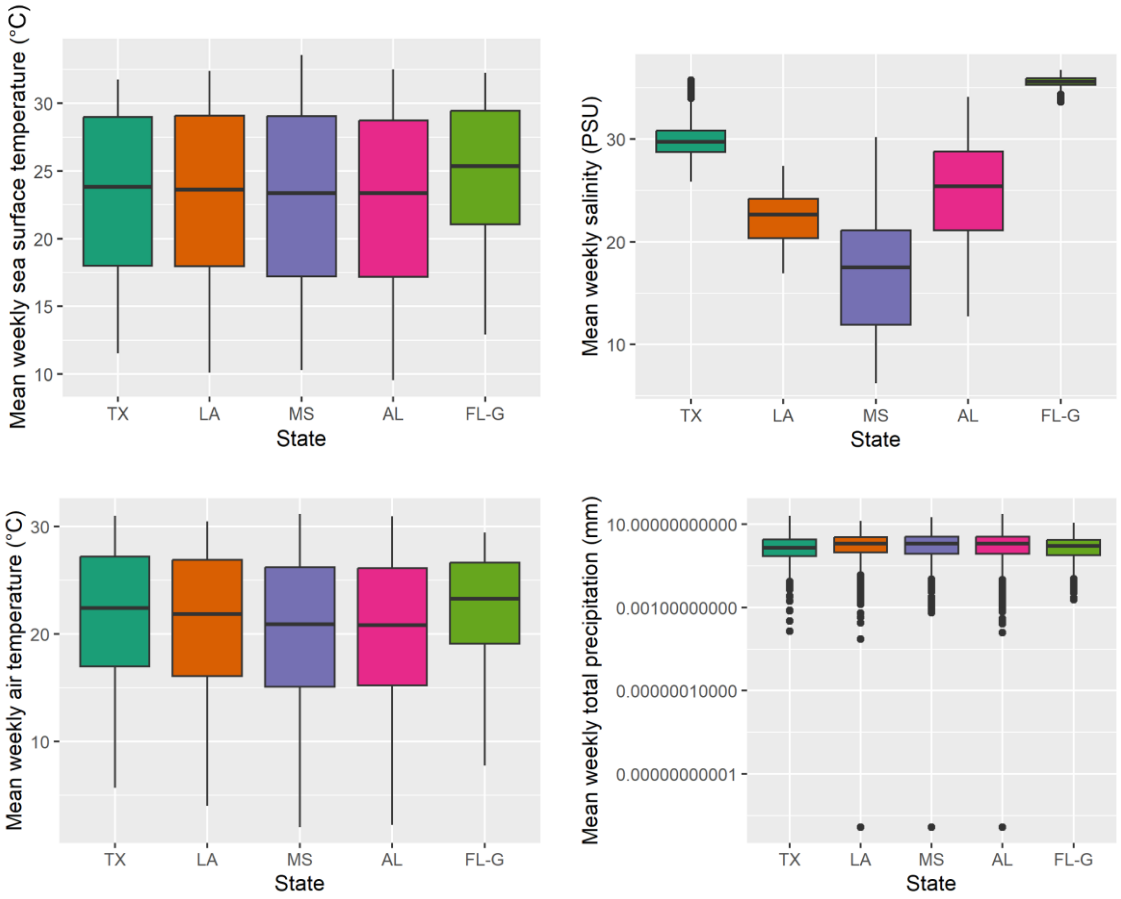

Figure S12 Distribution of mean weekly coastal conditions weighted by population density of US Gulf Coast states between 1993-2018.

Table S5 Initial model sets predicting incidence of *V. vulnificus* infection in a given week based on highest Akaike weight (w_i). Results shown for a sea surface temperature (sst) model set and air temperature (temp) model set, which each contain 63 possible combinations of environmental variables. Model sets include a 'null' model (intercept and random effect of US state only) and 'baseline' model which contains variables present in all environmental models. K indicates the number of parameters in each model. Model results were generated for and averaged over 100 random subsets of the dataset: AIC corrected for large K relative to sample size (AIC_c), difference in AIC_c from the best model (Δ_i), area under the ROC curve (AUC) and Akaike weight (w_i).

Rank (n = 65)	Model[a, b]	K	Mean (n = 100)			
			AIC_c	Δ_i	AUC	w_i
Sea surface temperature set						
1	sst weekmean	18	765.696	1.153	0.818	0.053
2	sst weekmax	18	766.054	1.511	0.818	0.051
3	sst weekmean + totprec weekmean	19	766.436	1.893	0.818	0.037
4	sst weekmin	18	766.666	2.124	0.818	0.036
5	sst weekmax + totprec weekmean	19	766.679	2.136	0.818	0.036
6	sst weekmean + totprec weekmax	19	766.654	2.111	0.818	0.033
7	sst weekmax + totprec weekmax	19	766.888	2.345	0.818	0.032
8	sst weekmean + totprec weekmin	19	767.014	2.471	0.817	0.028
9	sst weekmax + totprec weekmin	19	767.379	2.836	0.817	0.027
10	sst weekmin + totprec weekmean	19	767.451	2.908	0.818	0.027
11	sal weekmin + sst weekmean	19	767.124	2.581	0.816	0.026
12	sal weekmin + sst weekmax	19	767.478	2.935	0.816	0.026

[a]All environmental models and the baseline model contain a random effect for US state, 3rd order polynomial terms of year, dummy month variables and binary term for whether it is a public holiday (state or federal) or not. [b]Predictor labels: weekmin = weekly minimum, weekmean = weekly mean, weekmax = weekly maximum, sst = sea surface temperature (°C), temp = air temperature (°C), sal = salinity (PSU), totprec = total precipitation (mm).

Table S5 continued…

Rank (n = 65)	Model[a, b]	K	Mean (n = 100)			
			AIC_c	Δ_i	AUC	w_i
13	sal weekmax + sst weekmean	19	767.133	2.590	0.817	0.026
14	sal weekmax + sst weekmax	19	767.452	2.909	0.817	0.025
15	sal weekmean + sst weekmean	19	767.169	2.626	0.817	0.025
16	sal weekmean + sst weekmax	19	767.508	2.965	0.817	0.025
17	sst weekmin + totprec weekmax	19	767.680	3.137	0.818	0.023
18	sst weekmin + totprec weekmin	19	767.974	3.432	0.817	0.021
19	sal weekmax + sst weekmean + totprec weekmean	20	767.866	3.323	0.817	0.018
20	sal weekmax + sst weekmin	19	768.118	3.575	0.817	0.018
21	sal weekmin + sst weekmin	19	768.116	3.573	0.816	0.018
22	sal weekmax + sst weekmax + totprec weekmean	20	768.065	3.523	0.817	0.018
23	sal weekmin + sst weekmean + totprec weekmean	20	767.887	3.344	0.817	0.017
24	sal weekmean + sst weekmin	19	768.154	3.611	0.817	0.017
25	sal weekmean + sst weekmean + totprec weekmean	20	767.911	3.368	0.817	0.017
26	sal weekmin + sst weekmax + totprec weekmean	20	768.121	3.578	0.816	0.017
27	sal weekmean + sst weekmax + totprec weekmean	20	768.129	3.586	0.817	0.017
28	sal weekmax + sst weekmean + totprec weekmax	20	768.099	3.556	0.817	0.016
29	sal weekmin + sst weekmean + totprec weekmax	20	768.102	3.560	0.816	0.016
30	sal weekmin + sst weekmax + totprec weekmax	20	768.329	3.786	0.816	0.015
31	sal weekmax + sst weekmax + totprec weekmax	20	768.294	3.751	0.817	0.015

[a]All environmental models and the baseline model contain a random effect for US state, 3rd order polynomial terms of year, dummy month variables and binary term for whether it is a public holiday (state or federal) or not. [b]Predictor labels: weekmin = weekly minimum, weekmean = weekly mean, weekmax = weekly maximum, sst = sea surface temperature (°C), temp = air temperature (°C), sal = salinity (PSU), totprec = total precipitation (mm).

Table S5 continued…

Rank (n = 65)	Model[a, b]	Mean (n = 100)				
		K	AIC_c	Δ_i	AUC	w_i
32	sal weekmean + sst weekmean + totprec weekmax	20	768.135	3.593	0.817	0.015
33	sal weekmean + sst weekmax + totprec weekmax	20	768.347	3.804	0.817	0.015
34	sal weekmin + sst weekmean + totprec weekmin	20	768.452	3.909	0.815	0.014
35	sal weekmin + sst weekmax + totprec weekmin	20	768.813	4.270	0.815	0.013
36	sal weekmax + sst weekmax + totprec weekmin	20	768.778	4.235	0.816	0.013
37	sal weekmax + sst weekmean + totprec weekmin	20	768.454	3.911	0.816	0.013
38	sal weekmax + sst weekmin + totprec weekmean	20	768.895	4.352	0.817	0.013
39	sal weekmean + sst weekmean + totprec weekmin	20	768.494	3.952	0.816	0.013
40	sal weekmean + sst weekmax + totprec weekmin	20	768.840	4.297	0.816	0.013
41	sal weekmin + sst weekmin + totprec weekmean	20	768.919	4.376	0.817	0.012
42	sal weekmean + sst weekmin + totprec weekmean	20	768.938	4.395	0.817	0.012
43	sal weekmax + sst weekmin + totprec weekmax	20	769.139	4.597	0.817	0.011
44	sal weekmin + sst weekmin + totprec weekmax	20	769.147	4.604	0.816	0.011
45	sal weekmean + sst weekmin + totprec weekmax	20	769.175	4.632	0.817	0.011
46	sal weekmin + sst weekmin + totprec weekmin	20	769.433	4.890	0.815	0.010
47	sal weekmax + sst weekmin + totprec weekmin	20	769.429	4.886	0.816	0.010
48	sal weekmean + sst weekmin + totprec weekmin	20	769.469	4.927	0.816	0.010
49	baseline model	17	778.148	13.606	0.816	0.002
50	totprec weekmean	18	778.204	13.661	0.817	0.001

[a]All environmental models and the baseline model contain a random effect for US state, 3rd order polynomial terms of year, dummy month variables and binary term for whether it is a public holiday (state or federal) or not. [b]Predictor labels: weekmin = weekly minimum, weekmean = weekly mean, weekmax = weekly maximum, sst = sea surface temperature (°C), temp = air temperature (°C), sal = salinity (PSU), totprec = total precipitation (mm).

Table S5 continued…

Rank (n = 65)	Model[a, b]	K	Mean (n = 100) AIC$_c$	Δ_i	AUC	w_i
51	sal weekmax	18	778.815	14.273	0.817	0.001
52	totprec weekmax	18	778.400	13.858	0.817	0.001
53	sal weekmean	18	779.103	14.560	0.817	0.001
54	sal weekmax + totprec weekmean	19	778.823	14.280	0.817	0.001
55	sal weekmin	18	779.406	14.864	0.816	0.001
56	sal weekmax + totprec weekmax	19	779.094	14.551	0.817	0.001
57	totprec weekmin	18	779.487	14.945	0.815	0.001
58	sal weekmean + totprec weekmean	19	779.094	14.552	0.817	0.001
59	sal weekmean + totprec weekmax	19	779.349	14.806	0.817	0.001
60	sal weekmin + totprec weekmean	19	779.392	14.849	0.817	0.001
61	sal weekmin + totprec weekmax	19	779.628	15.085	0.817	0.001
62	sal weekmax + totprec weekmin	19	780.151	15.609	0.816	0.001
63	sal weekmean + totprec weekmin	19	780.446	15.903	0.816	0.001
64	sal weekmin + totprec weekmin	19	780.755	16.212	0.815	0.000
65	null model	2	988.338	223.795	0.646	0.000
Air temperature set						
1	temp_weekmean	18	765.875	1.099	0.817	0.074
2	temp_weekmin	18	766.275	1.500	0.818	0.065
3	temp_weekmean + totprec_weekmin	19	767.066	2.290	0.816	0.043

[a]All environmental models and the baseline model contain a random effect for US state, 3rd order polynomial terms of year, dummy month variables and binary term for whether it is a public holiday (state or federal) or not. [b]Predictor labels: weekmin = weekly minimum, weekmean = weekly mean, weekmax = weekly maximum, sst = sea surface temperature (°C), temp = air temperature (°C), sal = salinity (PSU), totprec = total precipitation (mm).

Table S5 continued…

Rank (n = 65)	Model[a, b]	Mean (n = 100)				
		K	AIC_c	Δ_i	AUC	w_i
4	temp_weekmean + totprec_weekmax	19	767.100	2.324	0.817	0.040
5	sal_weekmax + temp_weekmean	19	767.147	2.371	0.817	0.039
6	temp_weekmean + totprec_weekmean	19	767.118	2.342	0.817	0.039
7	temp_weekmin + totprec_weekmin	19	767.561	2.786	0.817	0.037
8	sal_weekmin + temp_weekmean	19	767.294	2.519	0.816	0.037
9	sal_weekmean + temp_weekmean	19	767.265	2.490	0.816	0.037
10	temp_weekmin + totprec_weekmean	19	767.556	2.781	0.818	0.036
11	temp_weekmin + totprec_weekmax	19	767.563	2.787	0.818	0.035
12	sal_weekmax + temp_weekmin	19	767.564	2.789	0.818	0.034
13	sal_weekmean + temp_weekmin	19	767.678	2.902	0.818	0.031
14	sal_weekmin + temp_weekmin	19	767.718	2.942	0.817	0.030
15	sal_weekmin + temp_weekmean + totprec_weekmin	20	768.498	3.723	0.815	0.022
16	sal_weekmax + temp_weekmean + totprec_weekmin	20	768.380	3.605	0.816	0.022
17	sal_weekmean + temp_weekmean + totprec_weekmin	20	768.488	3.713	0.815	0.021
18	sal_weekmax + temp_weekmean + totprec_weekmax	20	768.385	3.609	0.817	0.021
19	sal_weekmax + temp_weekmean + totprec_weekmean	20	768.381	3.605	0.817	0.021
20	sal_weekmin + temp_weekmean + totprec_weekmax	20	768.521	3.745	0.816	0.020
21	sal_weekmean + temp_weekmean + totprec_weekmax	20	768.494	3.718	0.816	0.020
22	sal_weekmax + temp_weekmin + totprec_weekmin	20	768.882	4.106	0.817	0.019

[a]All environmental models and the baseline model contain a random effect for US state, 3rd order polynomial terms of year, dummy month variables and binary term for whether it is a public holiday (state or federal) or not. [b]Predictor labels: weekmin = weekly minimum, weekmean = weekly mean, weekmax = weekly maximum, sst = sea surface temperature (°C), temp = air temperature (°C), sal = salinity (PSU), totprec = total precipitation (mm).

Table S5 continued…

Rank (n = 65)	Model[a, b]	K	Mean (n = 100) AIC$_c$	Δ_i	AUC	w_i
23	sal_weekmin + temp_weekmean + totprec_weekmean	20	768.537	3.762	0.816	0.019
24	sal_weekmean + temp_weekmean + totprec_weekmean	20	768.502	3.726	0.816	0.019
25	sal_weekmax + temp_weekmin + totprec_weekmean	20	768.841	4.066	0.818	0.019
26	sal_weekmax + temp_weekmin + totprec_weekmax	20	768.868	4.092	0.818	0.018
27	sal_weekmean + temp_weekmin + totprec_weekmin	20	768.993	4.217	0.817	0.018
28	sal_weekmin + temp_weekmin + totprec_weekmin	20	769.020	4.244	0.816	0.017
29	sal_weekmean + temp_weekmin + totprec_weekmean	20	768.957	4.181	0.817	0.017
30	sal_weekmin + temp_weekmin + totprec_weekmean	20	769.001	4.225	0.817	0.016
31	sal_weekmean + temp_weekmin + totprec_weekmax	20	768.974	4.198	0.817	0.016
32	sal_weekmin + temp_weekmin + totprec_weekmax	20	769.009	4.234	0.817	0.016
33	temp_weekmax	18	771.492	6.716	0.816	0.009
34	temp_weekmax + totprec_weekmax	19	772.361	7.586	0.816	0.006
35	temp_weekmax + totprec_weekmin	19	772.648	7.873	0.815	0.006
36	sal_weekmax + temp_weekmax	19	772.539	7.763	0.816	0.005
37	temp_weekmax + totprec_weekmean	19	772.385	7.610	0.816	0.005
38	sal_weekmean + temp_weekmax	19	772.738	7.963	0.816	0.005
39	sal_weekmin + temp_weekmax	19	772.889	8.114	0.815	0.005
40	sal_weekmax + temp_weekmax + totprec_weekmean	20	773.412	8.636	0.816	0.003
41	sal_weekmax + temp_weekmax + totprec_weekmax	20	773.433	8.658	0.816	0.003

[a]All environmental models and the baseline model contain a random effect for US state, 3rd order polynomial terms of year, dummy month variables and binary term for whether it is a public holiday (state or federal) or not. [b]Predictor labels: weekmin = weekly minimum, weekmean = weekly mean, weekmax = weekly maximum, sst = sea surface temperature (°C), temp = air temperature (°C), sal = salinity (PSU), totprec = total precipitation (mm).

Table S5 continued…

Rank (n = 65)	Model[a, b]	Mean (n = 100)				
		K	AIC_c	Δ_i	AUC	w_i
42	sal_weekmax + temp_weekmax + totprec_weekmin	20	773.759	8.984	0.815	0.003
43	sal_weekmean + temp_weekmax + totprec_weekmean	20	773.609	8.833	0.816	0.003
44	sal_weekmean + temp_weekmax + totprec_weekmax	20	773.616	8.840	0.816	0.003
45	sal_weekmean + temp_weekmax + totprec_weekmin	20	773.947	9.171	0.815	0.003
46	sal_weekmin + temp_weekmax + totprec_weekmax	20	773.757	8.981	0.815	0.003
47	sal_weekmin + temp_weekmax + totprec_weekmean	20	773.765	8.989	0.815	0.003
48	sal_weekmin + temp_weekmax + totprec_weekmin	20	774.077	9.301	0.814	0.003
49	baseline model	17	778.148	13.373	0.816	0.002
50	sal_weekmax	18	778.815	14.040	0.817	0.001
51	totprec_weekmax	18	778.400	13.625	0.817	0.001
52	totprec_weekmean	18	778.204	13.428	0.817	0.001
53	sal_weekmean	18	779.103	14.328	0.817	0.001
54	sal_weekmax + totprec_weekmean	19	778.823	14.047	0.817	0.001
55	sal_weekmax + totprec_weekmax	19	779.094	14.318	0.817	0.001
56	sal_weekmin	18	779.406	14.631	0.816	0.001
57	totprec_weekmin	18	779.487	14.712	0.815	0.001
58	sal_weekmean + totprec_weekmean	19	779.094	14.319	0.817	0.001
59	sal_weekmean + totprec_weekmax	19	779.349	14.573	0.817	0.001
60	sal_weekmin + totprec_weekmean	19	779.392	14.616	0.817	0.001

[a]All environmental models and the baseline model contain a random effect for US state, 3rd order polynomial terms of year, dummy month variables and binary term for whether it is a public holiday (state or federal) or not. [b]Predictor labels: weekmin = weekly minimum, weekmean = weekly mean, weekmax = weekly maximum, sst = sea surface temperature (°C), temp = air temperature (°C), sal = salinity (PSU), totprec = total precipitation (mm).

Table S5 continued…

Rank (n = 65)	Model[a, b]	Mean (n = 100)				
		K	AIC_c	Δ_i	AUC	w_i
61	sal_weekmin + totprec_weekmax	19	779.628	14.853	0.817	0.001
62	sal_weekmax + totprec_weekmin	19	780.151	15.376	0.816	0.001
63	sal_weekmean + totprec_weekmin	19	780.446	15.670	0.816	0.001
64	sal_weekmin + totprec_weekmin	19	780.755	15.980	0.815	0.000
65	null model	2	988.338	223.562	0.646	0.000

[a]All environmental models and the baseline model contain a random effect for US state, 3rd order polynomial terms of year, dummy month variables and binary term for whether it is a public holiday (state or federal) or not. [b]Predictor labels: weekmin = weekly minimum, weekmean = weekly mean, weekmax = weekly maximum, sst = sea surface temperature (°C), temp = air temperature (°C), sal = salinity (PSU), totprec = total precipitation (mm).

Table S6 Standardised coefficient estimates (β), standard errors, relative predictor importance (Σw_i) and 95% confidence intervals of coefficients shown. Each value is averaged over all models in each model set (n = 65) and 100 random subsets of the dataset. Confidence intervals that do not overlap 0 are highlighted in bold.

Rank	Predictor[a]	β	SE	Σw_i	95% CIs	
					Lower	Upper
Sea surface temperature set						
1	sst weekmean	1.371	0.381	0.367	**0.624**	**2.117**
2	sst weekmax	1.346	0.379	0.359	**0.602**	**2.089**
3	sst weekmin	1.301	0.374	0.260	**0.567**	**2.035**
4	totprec weekmean	-0.091	0.096	0.245	-0.278	0.097
5	totprec weekmax	-0.079	0.098	0.217	-0.271	0.112
6	sal weekmax	-0.113	0.249	0.200	-0.601	0.375
7	sal weekmin	-0.010	0.254	0.198	-0.508	0.488
8	sal weekmean	-0.073	0.254	0.193	-0.571	0.425
9	totprec weekmin	-0.010	0.096	0.188	-0.199	0.179
Air temperature set						
1	temp weekmean	1.137	0.322	0.494	**0.505**	**1.769**
2	temp weekmin	1.025	0.296	0.423	**0.446**	**1.605**
3	totprec weekmin	0.021	0.097	0.216	-0.170	0.212
4	sal weekmax	-0.176	0.252	0.211	-0.669	0.318
5	totprec weekmean	-0.067	0.096	0.205	-0.255	0.122
6	totprec weekmax	-0.064	0.098	0.204	-0.255	0.128
7	sal weekmean	-0.132	0.256	0.195	-0.634	0.369
8	sal weekmin	-0.067	0.259	0.194	-0.574	0.439
9	temp weekmax	0.838	0.308	0.068	**0.235**	**1.441**

[a]Predictor labels: weekmin = weekly minimum, weekmean = weekly mean, weekmax = weekly maximum, sst = sea surface temperature (°C), temp = air temperature (°C), sal = salinity (PSU), totprec = total precipitation (mm).

Table S7 Change in model AIC corrected for large number of parameters relative to sample size (ΔAIC_c) and area under the ROC curve (Δ AUC) with addition of La Niña, El Niño and hurricane predictors. All values have been averaged across 100 subsets of the dataset.

	Rank	Model[a, b]	+ La Niña		+ El Niño		+ hurricanes		+ La Niña + hurricanes		+ El Niño + hurricanes	
			ΔAIC_c	Δ AUC	ΔAIC_c	Δ AUC	ΔAIC_c	Δ AUC	ΔAIC_c	Δ AUC	ΔAIC_c	Δ AUC
Sea surface temperature set	1	sst weekmean	-1.248	0.001	-0.018	0.001	-0.490	0.000	-0.823	0.001	-0.812	0.001
	2	sst weekmean + totprec weekmean	-1.630	0.001	-0.067	0.001	-0.875	0.000	-1.543	0.001	-1.298	0.001
	3	sal weekmax + sst weekmean	-1.367	0.001	-0.029	0.001	-0.588	0.000	-0.930	0.001	-0.923	0.001
	4	sal weekmax + sst weekmean + totprec weekmean	-1.758	0.001	-0.080	0.001	-0.971	0.000	-1.650	0.001	-1.410	0.001
	5	totprec weekmean	-0.565	0.000	0.320	0.000	-0.892	0.000	-0.577	0.000	-0.924	0.001
	6	sal weekmax	-0.339	0.000	0.340	0.000	-0.414	0.000	0.176	-0.001	-0.357	0.000
	7	sal weekmax + totprec weekmean	-0.744	0.001	0.260	0.001	-0.861	0.000	-0.612	0.001	-0.945	0.001
Air temperature set	1	temp weekmean	-1.434	0.001	0.093	0.001	-0.436	0.000	-0.948	0.001	-0.634	0.001
	2	temp weekmean + totprec weekmin	-1.507	0.001	0.070	0.001	-0.517	0.000	-0.997	0.001	-0.745	0.001
	3	sal weekmax + temp weekmean	-1.567	0.001	0.068	0.001	-0.502	0.000	-1.035	0.000	-0.722	0.001
	4	sal weekmax + temp weekmean + totprec weekmin	-1.646	0.001	0.051	0.001	-0.598	-0.001	-1.099	0.000	-0.842	0.001
	5	sal weekmax	-0.339	0.000	0.340	0.000	-0.414	0.000	0.176	-0.001	-0.357	0.000
	6	totprec weekmin	-0.288	0.000	0.401	0.001	-0.511	0.000	0.125	0.000	-0.405	0.001
	7	sal weekmax + totprec weekmin	-0.454	0.000	0.343	0.000	-0.510	0.000	0.071	0.000	-0.456	0.000

[a]All environmental models and the baseline model contain a random effect for US state, 3rd order polynomial terms of year, dummy month variables and binary term for whether it is a public holiday (state or federal) or not. [b]Predictor labels: weekmin = weekly minimum, weekmean = weekly mean, weekmax = weekly maximum, sst = sea surface temperature (°C), temp = air temperature (°C), sal = salinity (PSU), totprec = total precipitation (mm).

Table S8 Change in model AIC corrected for large number of parameters relative to sample size (ΔAIC_c) and area under the ROC curve (Δ AUC) with addition of chlorophyll-a (mg m^{-3}) and zooplankton biomass (C g m^{-2}) predictors. All values have been averaged across model results generated from 100 subsets of the dataset. Model sets were rerun on 1998-2018 data to match the availability of plankton data.

	Rank	Model[a, b]	+ chlorophyll a		+ zooplankton		+ chlorophyll a + zooplankton	
			ΔAIC_c	Δ AUC	ΔAIC_c	Δ AUC	ΔAIC_c	Δ AUC
Sea surface temperature set	1	sst weekmean	1.435	-0.001	0.298	-0.001	1.634	-0.001
	2	sst weekmean + totprec weekmean	1.467	-0.001	0.330	0.000	1.713	-0.001
	3	sal weekmax + sst weekmean	1.261	-0.002	0.149	-0.001	1.419	-0.002
	4	sal weekmax + sst weekmean + totprec weekmean	1.291	-0.001	0.188	-0.001	1.492	-0.002
	5	totprec weekmean	1.512	-0.001	1.430	-0.001	2.950	-0.002
	6	sal weekmax	1.359	-0.001	1.394	0.000	2.754	-0.001
	7	sal weekmax + totprec weekmean	1.379	-0.001	1.392	-0.001	2.771	-0.002
Air temperature set	1	temp weekmean	1.513	-0.001	1.158	-0.001	2.666	-0.001
	2	temp weekmean + totprec weekmin	1.524	-0.001	1.172	0.000	2.688	-0.001
	3	sal weekmax + temp weekmean	1.290	-0.001	1.173	-0.001	2.479	-0.002
	4	sal weekmax + temp weekmean + totprec weekmin	1.299	-0.001	1.186	-0.001	2.498	-0.002
	5	sal weekmax	1.359	-0.001	1.394	0.000	2.754	-0.001
	6	totprec weekmin	1.530	-0.001	1.442	-0.001	2.982	-0.002
	7	sal weekmax + totprec weekmin	1.376	0.000	1.398	0.000	2.775	-0.001

[a]All environmental models and the baseline model contain a random effect for US state, 3rd order polynomial terms of year, dummy month variables and binary term for whether it is a public holiday (state or federal) or not. [b]Predictor labels: weekmin = weekly minimum, weekmean = weekly mean, weekmax = weekly maximum, sst = sea surface temperature (°C), temp = air temperature (°C), sal = salinity (PSU), totprec = total precipitation (mm).

Table S9 Linear regression results air temperature ~ month (Gulf Coast).

Variable	Estimate	Standard Error	t-value	p-value
(Intercept)	20.72	0.10	199.60	<0.0001
Aug	7.16	0.15	49.19	<0.0001
Dec	-6.19	0.15	-42.44	<0.0001
Feb	-5.99	0.15	-40.21	<0.0001
Jan	-7.53	0.15	-51.86	<0.0001
Jul	7.09	0.15	48.73	<0.0001
Jun	6.30	0.15	42.91	<0.0001
Mar	-3.46	0.15	-23.78	<0.0001
May	3.69	0.15	25.39	<0.0001
Nov	-2.81	0.15	-19.12	<0.0001
Oct	1.81	0.15	12.48	<0.0001
Sep	5.50	0.15	37.45	<0.0001

R^2: 0.825

Table S10 Linear regression results air temperature ~ month (Atlantic Coast).

Variable	Estimate	Standard Error	t-value	p-value
(Intercept)	12.82	0.13	95.41	<0.0001
Aug	11.31	0.19	60.03	<0.0001
Dec	-6.44	0.19	-34.09	<0.0001
Feb	-8.25	0.19	-42.82	<0.0001
Jan	-9.03	0.19	-48.05	<0.0001
Jul	11.81	0.19	62.67	<0.0001
Jun	9.19	0.19	48.38	<0.0001
Mar	-5.08	0.19	-26.97	<0.0001
May	4.71	0.19	25.05	<0.0001
Nov	-1.97	0.19	-10.36	<0.0001
Oct	3.28	0.19	17.46	<0.0001
Sep	8.50	0.19	44.73	<0.0001

R^2: 0.675

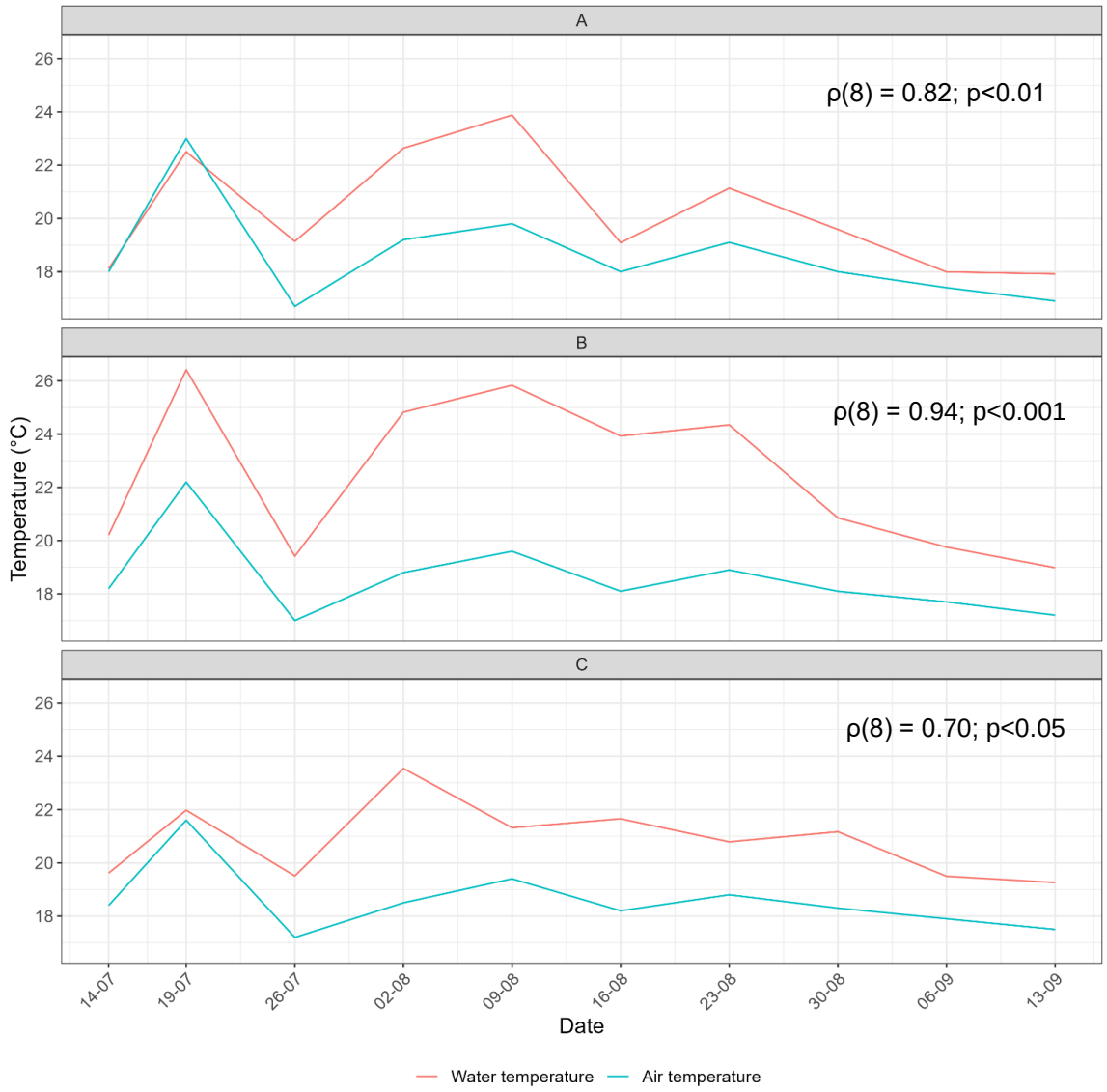

Figure S13 In situ water temperature and local air temperature from Visual Crossing on sampling dates. Result of Spearman's rank correlations between the two forms of temperature shown for each site.

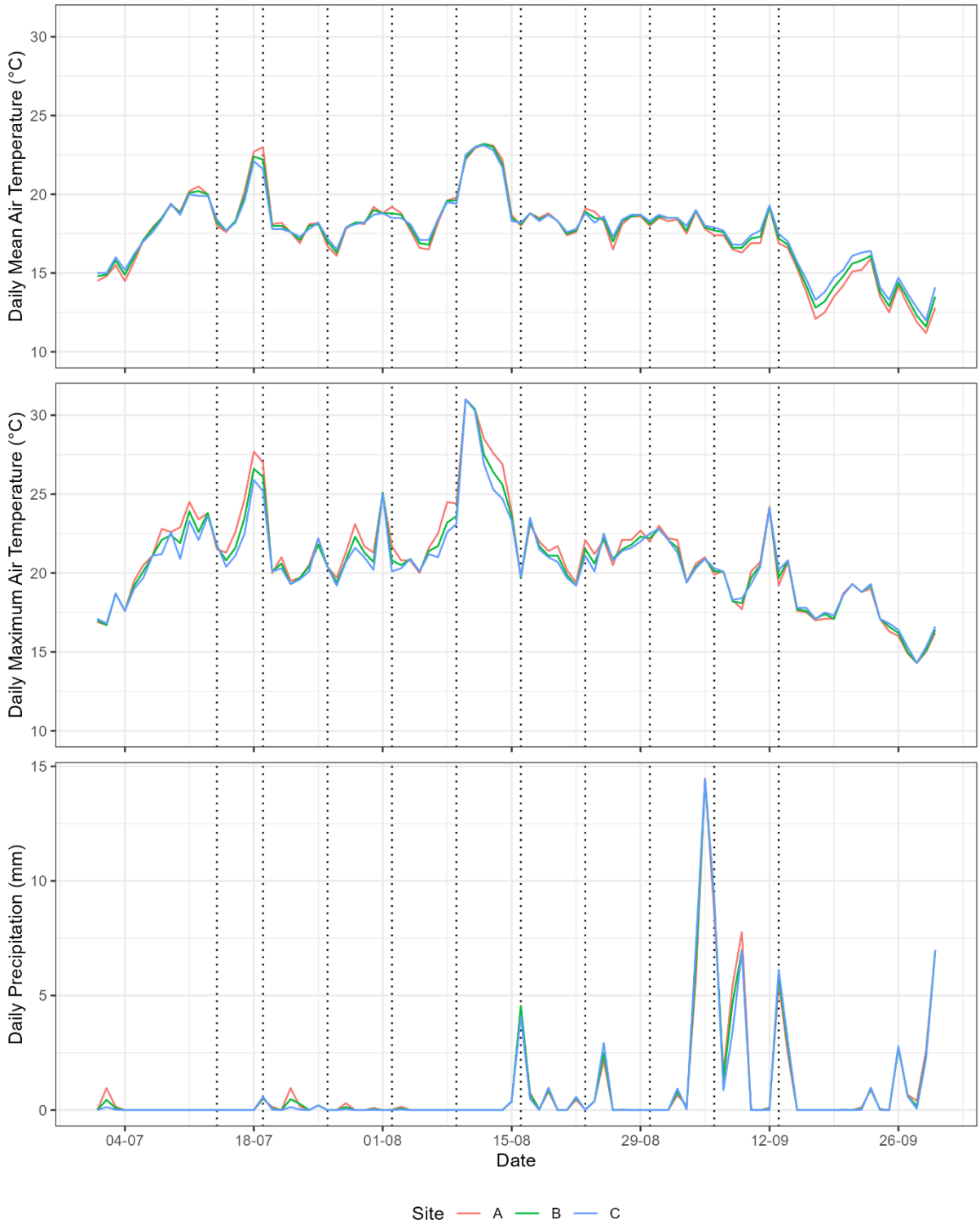

Figure S14 Daily weather conditions near sites A-C including mean air temperature, maximum air temperature and precipitation between 01/07/2022 to 30/09/2022 from Visual Crossing. Dotted lines indicate the dates samples taken.

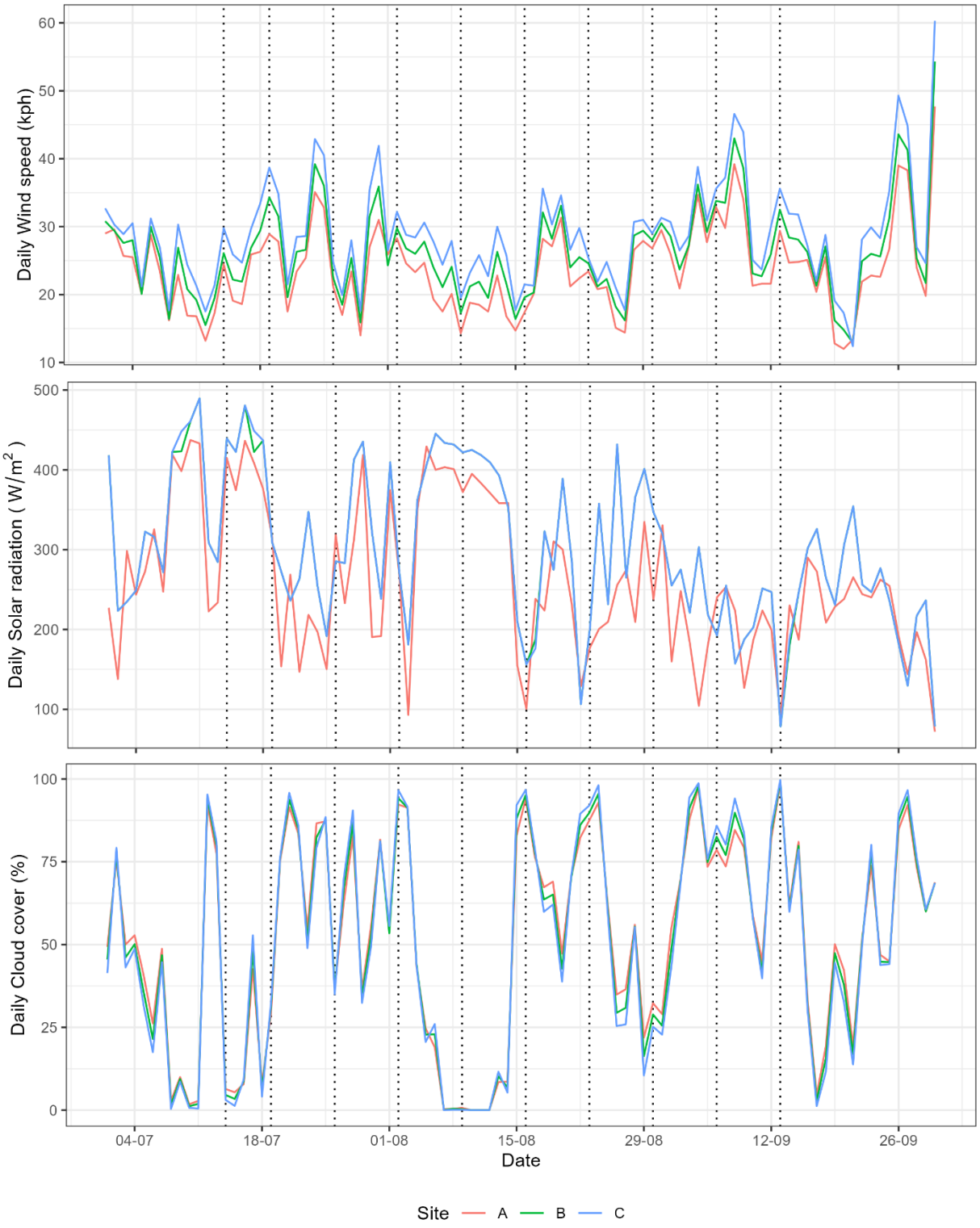

Figure S15 Daily weather conditions near sites A-C including wind speed, solar radiation, and cloud cover between 01/07/2022 to 30/09/2022 from Visual Crossing. Dotted lines indicate the dates samples taken.

Table S11 Example morphologies of *Vibrio* species on VID and TCBS media isolated from coastal lagoon water during the study.

Vibrio alginolyticus on VID: “creamy”		
A	Creamy pink; mucoid; ~3-5 mm	22/072L
	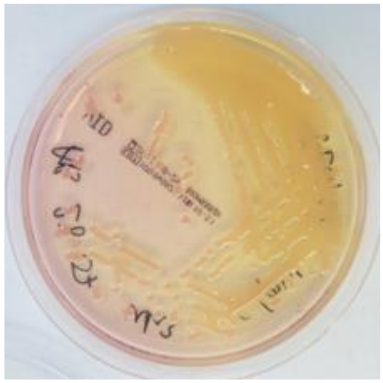	
B	Purple; mucoid; ~3 mm	22/029L
	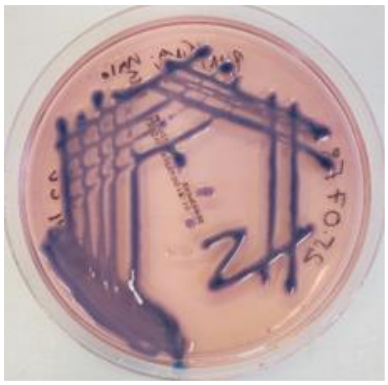	
C	Pink; ~2-3 mm	22/255L
		

Table S11 continued…

Vibrio alginolyticus on VID: “creamy”		
D	Dark blue; ~1-3 mm	22/045L
	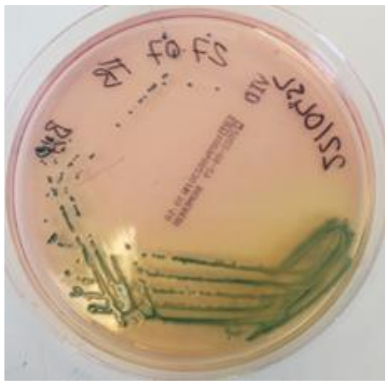	
E	Purple; ~2 mm	22/088L (Va PCR positive, 16S: *Gromontia hollisae*)
		
Vibrio alginolyticus on TCBS: “yellow”		
F	Yellow	22/073L
		

Table S11 continued…

Vibrio alginolyticus on TCBS: “yellow”		
G	Creamy; translucent centre; filamentous margin	22/154L
	 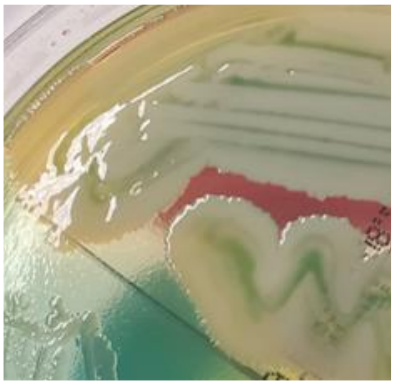	
H	Yellow turning green	22/081L
	 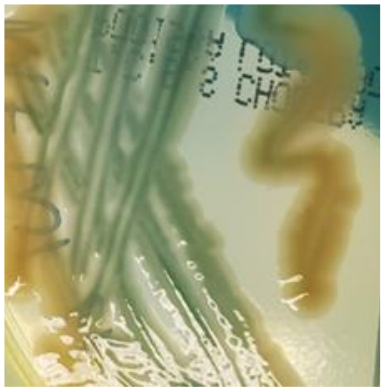	
Vibrio parahaemolyticus on VID: “pink”		
I	Dark pink; mucoid; ~1-2 mm	22/258L
	 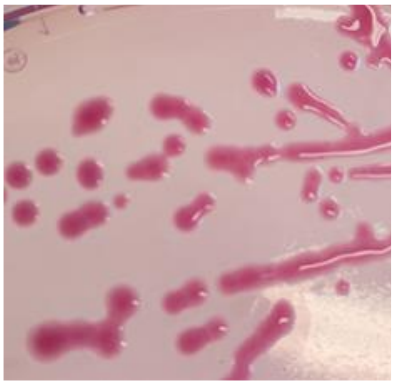	

Table S11 continued…

Vibrio parahaemolyticus on VID: “pink”		
G	Pink; <1 mm	22/141L
	 	
H	Purple; <1 mm	22/233L
	 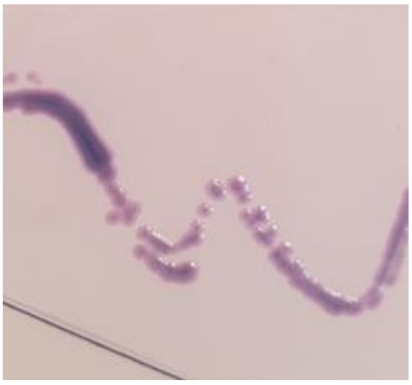	
Vibrio parahaemolyticus on TCBS: “green”		
I	Green; ~2-4 mm	22/094L
	 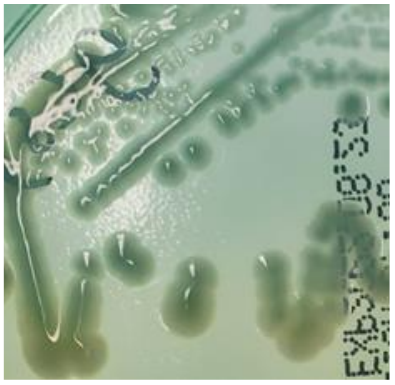	

Table S11 continued…

Vibrio cholerae on VID: “bluish-green to green”		
J	Blue; <1 mm	22/071L
	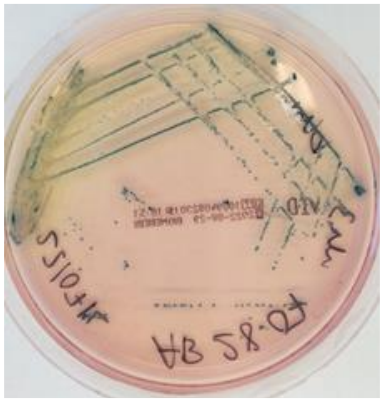 	
K	Pink; ~1 mm	22/157L
	 	
Vibrio cholerae on TCBS: “yellow”		
L	Yellow; ~1 mm	22/219L
	 	

Glossary

Bacteraemia[1]	Presence of live bacteria in the bloodstream, a form of sepsis.
(Liver) cirrhosis[1]	Irreversible scarring of the liver commonly caused by alcohol consumption and viral hepatitis.
Endotoxic (septic) shock, septicaemia, systemic Infection[2]	A life-threatening condition where the overreaction of the immune system to infection causes damage to the body's own tissues and organs.
Gastroenteritis[2]	Inflammation of the stomach and bowel, caused by infection.
Hemochromatosis[1]	An inherited disorder characterized by abnormally high absorption of iron by the intestinal tract, resulting in excessive storage of iron, particularly in the liver, skin, pancreas, heart, joints, and testes.
Necrotising fasciitis[2]	Serious bacterial infection of subdermal tissue and surrounding muscles and organs.
Surgical debridement[3]	A procedure to remove all infected and dead tissue from a skin wound.

[1]MedicineNet)

[2]NHS (www.nhs.uk)

[3]UCSF Department of Surgery (https://surgery.ucsf.edu)

References

Abd, H., Weintraub, A., Sandström, G., 2005. Intracellular survival and replication of Vibrio cholerae O139 in aquatic free-living amoebae. Environmental Microbiology 7, 1003–1008. https://doi.org/10.1111/j.1462-2920.2005.00771.x

Aiyar, S.E., Gaal, T., Gourse, R.L., 2002. rRNA Promoter Activity in the Fast-Growing Bacterium Vibrio natriegens. Journal of Bacteriology 184, 1349 LP – 1358. https://doi.org/10.1128/JB.184.5.1349-1358.2002

Alam, M.J., Tomochika, K.I., Miyoshi, S.I., Shinoda, S., 2002. Environmental investigation of potentially pathogenic Vibrio parahaemolyticus in the Seto-Inland Sea, Japan. FEMS Microbiol Lett 208, 83–87. https://doi.org/10.1111/j.1574-6968.2002.tb11064.x

Albertini, M.C., Accorsi, A., Teodori, L., Pierfelici, L., Uguccioni, F., Rocchi, M.B.L., Burattini, S., Citterio, B., 2006. Use of multiparameter analysis for Vibrio alginolyticus viable but nonculturable state determination. Cytometry Part A 69A, 260–265. https://doi.org/10.1002/cyto.a.20263

Allen, H.K., Donato, J., Wang, H.H., Cloud-Hansen, K.A., Davies, J., Handelsman, J., 2010. Call of the wild: Antibiotic resistance genes in natural environments. Nature Reviews Microbiology 8, 251–259. https://doi.org/10.1038/nrmicro2312

Almagro-Moreno, S., Martinez-Urtaza, J., Pukatzki, S., 2023. Vibrio Infections and the Twenty-First Century, in: Almagro-Moreno, S., Pukatzki, S. (Eds.), Vibrio Spp. Infections, Advances in Experimental Medicine and Biology. Springer International Publishing, Cham, pp. 1–16. https://doi.org/10.1007/978-3-031-22997-8_1

Altekruse, S.F., Bishop, R.D., Baldy, L.M., Thompson, S.G., Wilson, S.A., Ray, B.J., Griffin, P.M., 2000. Vibrio gastroenteritis in the US Gulf of Mexico region: The role of raw oysters. Epidemiology and Infection 124, 489–495. https://doi.org/10.1017/S0950268899003714

Amaral-Zettler, L.A., Zettler, E.R., Mincer, T.J., 2020. Ecology of the plastisphere. Nat Rev Microbiol 18, 139–151. https://doi.org/10.1038/s41579-019-0308-0

Amaro, C., Carmona-Salido, H., 2023. Vibrio vulnificus, an Underestimated Zoonotic Pathogen, in: Advances in Experimental Medicine and Biology. pp. 175–194.

Amato, E., Riess, M., Thomas-Lopez, D., Linkevicius, M., Pitkänen, T., Wołkowicz, T., Rjabinina, J., Jernberg, C., Hjertqvist, M., MacDonald, E., Antony-Samy, J.K., Bjerre, K.D., Salmenlinna, S., Fuursted, K., Hansen, A., Naseer, U., 2022. Epidemiological and microbiological investigation of a large increase in vibriosis, northern Europe, 2018. Eurosurveillance 27, 2101088. https://doi.org/10.2807/1560-7917.ES.2022.27.28.2101088

Anderson, A.M.L., Varkey, J.B., Petti, C.A., Liddle, R.A., Frothingham, R., Woods, C.W., 2004. Non-o1 Vibrio cholerae septicemia: Case report, discussion of literature, and relevance to bioterrorism. Diagnostic Microbiology and Infectious Disease 49, 295–297. https://doi.org/10.1016/j.diagmicrobio.2004.04.016

Anderson, L.E., Plummer, M.L., 2017. Recreational Demand for Shellfish Harvesting Under Environmental Closures. Marine Resource Economics 32, 43–57. https://doi.org/10.1086/688975

Andersson, A., Meier, H.E.M., Ripszam, M., Rowe, O., Wikner, J., Haglund, P., Eilola, K., Legrand, C., Figueroa, D., Paczkowska, J., Lindehoff, E., Tysklind, M., Elmgren, R., 2015. Projected future climate change and Baltic Sea ecosystem management. Ambio 44, 345–356. https://doi.org/10.1007/s13280-015-0654-8

Andrews, L., Jahncke, M., Mallikarjunan, K., 2003. Low Dose Gamma Irradiation to Reduce Pathogenic Vibrios in Live Oysters (Crassostrea virginica). Journal of Aquatic Food Product Technology 12, 71–82. https://doi.org/10.1300/J030v12n03_07

Andrews, L.S., Park, D.L., Chen, Y.P., 2000. Low temperature pasteurization to reduce the risk of vibrio infections from raw shell-stock oysters. Food Additives and Contaminants 17, 787–791. https://doi.org/10.1080/026520300415336

Archer, E.J., Baker-Austin, C., Osborn, T.J., Jones, N.R., Martínez-Urtaza, J., Trinanes, J., Oliver, J.D., González, F.J.C., Lake, I.R., 2023. Climate warming and increasing Vibrio vulnificus infections in North America. Sci Rep 13, 3893. https://doi.org/10.1038/s41598-023-28247-2

Asplund, M.E., Rehnstam-Holm, A.S., Atnur, V., Raghunath, P., Saravanan, V., Härnström, K., Collin, B., Karunasagar, I., Godhe, A., 2011. Water column dynamics of Vibrio in relation to phytoplankton community composition and environmental conditions in a tropical coastal area. Environmental Microbiology 13, 2738–2751. https://doi.org/10.1111/j.1462-2920.2011.02545.x

Aunkham, A., Zahn, M., Kesireddy, A., Pothula, K.R., Schulte, A., Baslé, A., Kleinekathöfer, U., Suginta, W., Van Den Berg, B., 2018. Structural basis for chitin acquisition by marine Vibrio species. Nature Communications 9, 1–14. https://doi.org/10.1038/s41467-017-02523-y

Ayala, A.J., Kabengele, K., Almagro-Moreno, S., Ogbunugafor, C.B., 2023. Meteorological associations of Vibrio vulnificus clinical infections in tropical settings: Correlations with air pressure, wind speed, and temperature. PLOS Neglected Tropical Diseases 17, e0011461. https://doi.org/10.1371/journal.pntd.0011461

Ayala, A.J., Ogbunugafor, C.B., 2023. When Vibrios Take Flight: A Meta-Analysis of Pathogenic Vibrio Species in Wild and Domestic Birds. Adv Exp Med Biol 1404, 295–336. https://doi.org/10.1007/978-3-031-22997-8_15

Badley, A., Phillips, B., Haldane, D.J.M., Dalton, M.T., 1990. Pathogenic marine vibrio species in selected Nova Scotian recreational coastal waters. Canadian Journal of Public Health 81, 263–267.

Badr, H.S., Zaitchik, B.F., Kerr, G.H., Nguyen, N.-L.H., Chen, Y.-T., Hinson, P., Colston, J.M., Kosek, M.N., Dong, E., Du, H., Marshall, M., Nixon, K., Mohegh, A., Goldberg, D.L., Anenberg, S.C., Gardner, L.M., 2023. Unified real-time environmental-epidemiological data for multiscale modeling of the COVID-19 pandemic. Sci Data 10, 367. https://doi.org/10.1038/s41597-023-02276-y

Baker-Austin, C., Jenkins, C., Dadzie, J., Mestanza, O., Delgado, E., Powell, A., Bean, T., Martinez-Urtaza, J., 2020. Genomic epidemiology of domestic and travel-associated Vibrio parahaemolyticus infections in the UK, 2008–2018. Food Control 115, 107244. https://doi.org/10.1016/j.foodcont.2020.107244

Baker-Austin, C., McArthur, J.V., Lindell, A.H., Wright, M.S., Tuckfield, R.C., Gooch, J., Warner, L., Oliver, J., Stepanauskas, R., 2009. Multi-site analysis reveals

widespread antibiotic resistance in the marine pathogen Vibrio vulnificus. Microbial Ecology 57, 151–159. https://doi.org/10.1007/s00248-008-9413-8

Baker-Austin, C., McArthur, J.V., Tuckfield, R.C., Najarro, M., Lindell, A.H., Gooch, J., Stepanauskas, R., 2008. Antibiotic resistance in the shellfish pathogen Vibrio parahaemolyticus isolated from the coastal water and sediment of Georgia and South Carolina, {USA}. Journal of Food Protection 71, 2552–2558. https://doi.org/10.4315/0362-028x-71.12.2552

Baker-Austin, C., Oliver, J.D., 2018. Vibrio vulnificus: new insights into a deadly opportunistic pathogen. Environmental Microbiology 20, 423–430. https://doi.org/10.1111/1462-2920.13955

Baker-Austin, C., Oliver, J.D., 2016. Rapidly developing and fatal Vibrio vulnificus wound infection. IDCases 6, 13. https://doi.org/10.1016/j.idcr.2016.07.014

Baker-Austin, C., Oliver, J.D., Alam, M., Ali, A., Waldor, M.K., Qadri, F., Martinez-Urtaza, J., 2018. Vibrio spp. infections. Nature Reviews Disease Primers 4, 1–19. https://doi.org/10.1038/s41572-018-0005-8

Baker-Austin, C., Stockley, L., Rangdale, R., Martinez-Urtaza, J., 2010. Environmental occurrence and clinical impact of Vibrio vulnificus and Vibrio parahaemolyticus: a European perspective. Environmental Microbiology Reports 2, 7–18. https://doi.org/10.1111/j.1758-2229.2009.00096.x

Baker-Austin, C., Trinanes, J., Gonzalez-Escalona, N., Martinez-Urtaza, J., 2017. Non-Cholera Vibrios: The Microbial Barometer of Climate Change. Trends in Microbiology 25, 76–84. https://doi.org/10.1016/j.tim.2016.09.008

Baker-Austin, C., Trinanes, J., Martinez-Urtaza, J., 2020. The new tools revolutionizing *Vibrio* science. Environmental Microbiology 22, 4096–4100. https://doi.org/10.1111/1462-2920.15083

Baker-Austin, C., Trinanes, J.A., Salmenlinna, S., Löfdahl, M., Siitonen, A., Taylor, N.G.H., Martinez-Urtaza, J., 2016. Heat Wave-Associated Vibriosis, Sweden and Finland, 2014. Emerg Infect Dis 22, 1216–1220. https://doi.org/10.3201/eid2207.151996

Baker-Austin, C., Trinanes, J.A., Taylor, N.G.H., Hartnell, R., Siitonen, A., Martinez-Urtaza, J., 2013. Emerging Vibrio risk at high latitudes in response to ocean warming. Nature Climate Change 3, 73–77. https://doi.org/10.1038/nclimate1628

Barberi, O.N., Byron, C.J., Burkholder, K.M., St. Gelais, A.T., Williams, A.K., 2020. Assessment of bacterial pathogens on edible macroalgae in coastal waters. J Appl Phycol 32, 683–696. https://doi.org/10.1007/s10811-019-01993-5

Bartoń, K., 2023. MuMIn: Multi-Model Inference.

Basher, Z., Bowden, D.A., Costello, M.J., 2014. Diversity and Distribution of Deep-Sea Shrimps in the Ross Sea Region of Antarctica. PLOS ONE 9, e103195. https://doi.org/10.1371/journal.pone.0103195

Bates, D., Maechler, M., Bolker, B., Walker, S., 2015. Fitting Linear Mixed-Effects Models Using lme4. Journal of Statistical Software 67, 1–48. https://doi.org/10.18637/jss.v067.i01

Becker, E.A., Forney, K.A., Fiedler, P.C., Barlow, J., Chivers, S.J., Edwards, C.A., Moore, A.M., Redfern, J.V., 2016. Moving Towards Dynamic Ocean Management: How Well Do Modeled Ocean Products Predict Species Distributions? Remote Sensing 8, 149. https://doi.org/10.3390/rs8020149

Bej, A.K., Patterson, D.P., Brasher, C.W., Vickery, M.C.L., Jones, D.D., Kaysner, C.A., 1999. Detection of total and hemolysin-producing Vibrio parahaemolyticus in shellfish using multiplex PCR amplification of tl, tdh and trh. Journal of Microbiological Methods 36, 215–225. https://doi.org/10.1016/S0167-7012(99)00037-8

Belkin, I.M., 2009. Rapid warming of Large Marine Ecosystems. Progress in Oceanography 81, 207–213. https://doi.org/10.1016/j.pocean.2009.04.011

Bell, G.D., Chelliah, M., 2006. Leading Tropical Modes Associated with Interannual and Multidecadal Fluctuations in North Atlantic Hurricane Activity. Journal of Climate 19, 590–612. https://doi.org/10.1175/JCLI3659.1

Bellomo, K., Angeloni, M., Corti, S., von Hardenberg, J., 2021. Future climate change shaped by inter-model differences in Atlantic meridional overturning circulation response. Nat Commun 12, 3659. https://doi.org/10.1038/s41467-021-24015-w

Berdalet, E., Fleming, L.E., Gowen, R., Davidson, K., Hess, P., Backer, L.C., Moore, S.K., Hoagland, P., Enevoldsen, H., 2015. Marine harmful algal blooms, human health and wellbeing: challenges and opportunities in the 21st century. Journal of the Marine Biological Association of the United Kingdom. Marine Biological Association of the United Kingdom 2015, 10.1017/S0025315415001733. https://doi.org/10.1017/S0025315415001733

Bindoff, N.L., Cheung, W.W.L., Kairo, J.G., Arístegui, J., Guinder, V.A., Hallberg, R., Hilmi, N., Jiao, N., Karim, M.S., Levin, L., O'Donoghue, S., Purca Cuicapusa, S.R., Rinkevich, B., Suga, T., Tagliabue, A., Williamson, P., 2019. Changing Ocean, Marine Ecosystems, and Dependent Communities, in: Pörtner, H.O., Roberts, D.C., Masson-Delmotte, V., Zhai, P., Tignor, M., Poloczanska, E., Mintenbeck, K., Alegría, A., Nicolai, M., Okem, A., Petzold, J., Rama, B., Weyer, N.M. (Eds.), IPCC Special Report on the Ocean and Cryosphere in a Changing Climate. pp. 447–588. https://www.ipcc.ch/report/srocc/

Blackwell, K.D., Oliver, J.D., 2008. The ecology of Vibrio vulnificus, Vibrio cholerae, and Vibrio parahaemolyticus in North Carolina Estuaries. Journal of Microbiology 46, 146–153. https://doi.org/10.1007/s12275-007-0216-2

Blokesch, M., 2014. The Lifestyle of Vibrio cholerae Fosters Gene Transfers: Growing on chitinous surfaces helps these bacteria to initiate horizontal gene transfer and, perhaps, to swap pathogenic traits. Microbe Magazine 9, 64–70. https://doi.org/10.1128/microbe.9.64.1

Böer, S.I., Heinemeyer, E.A., Luden, K., Erler, R., Gerdts, G., Janssen, F., Brennholt, N., 2013. Temporal and Spatial Distribution Patterns of Potentially Pathogenic Vibrio spp. at Recreational Beaches of the German North Sea. Microbial Ecology 65, 1052–1067. https://doi.org/10.1007/s00248-013-0221-4

Boucher, O., Servonnat, J., Albright, A.L., Aumont, O., Balkanski, Y., Bastrikov, V., Bekki, S., Bonnet, R., Bony, S., Bopp, L., Braconnot, P., Brockmann, P., Cadule, P., Caubel, A., Cheruy, F., Codron, F., Cozic, A., Cugnet, D., D'Andrea, F., Davini, P., de Lavergne, C., Denvil, S., Deshayes, J., Devilliers, M., Ducharne, A., Dufresne, J.-L., Dupont, E., Éthé, C., Fairhead, L., Falletti, L., Flavoni, S., Foujols, M.-A., Gardoll, S., Gastineau, G., Ghattas, J., Grandpeix, J.-Y., Guenet, B., Guez, L., E., Guilyardi, E., Guimberteau, M., Hauglustaine, D., Hourdin, F., Idelkadi, A., Joussaume, S., Kageyama, M., Khodri, M., Krinner, G., Lebas, N., Levavasseur,

G., Lévy, C., Li, L., Lott, F., Lurton, T., Luyssaert, S., Madec, G., Madeleine, J.-B., Maignan, F., Marchand, M., Marti, O., Mellul, L., Meurdesoif, Y., Mignot, J., Musat, I., Ottlé, C., Peylin, P., Planton, Y., Polcher, J., Rio, C., Rochetin, N., Rousset, C., Sepulchre, P., Sima, A., Swingedouw, D., Thiéblemont, R., Traore, A.K., Vancoppenolle, M., Vial, J., Vialard, J., Viovy, N., Vuichard, N., 2020. Presentation and Evaluation of the IPSL-CM6A-LR Climate Model. Journal of Advances in Modeling Earth Systems 12, e2019MS002010. https://doi.org/10.1029/2019MS002010

Boughey, K.L., Lake, I.R., Haysom, K.A., Dolman, P.M., 2011. Improving the biodiversity benefits of hedgerows: How physical characteristics and the proximity of foraging habitat affect the use of linear features by bats. Biological Conservation 144, 1790–1798. https://doi.org/10.1016/j.biocon.2011.02.017

Boutayeb, A., Boutayeb, S., 2005. The burden of non communicable diseases in developing countries. International Journal for Equity in Health 4, 2. https://doi.org/10.1186/1475-9276-4-2

Bowers, D.G., Brett, H.L., 2008. The relationship between CDOM and salinity in estuaries: An analytical and graphical solution. Journal of Marine Systems 73, 1–7. https://doi.org/10.1016/j.jmarsys.2007.07.001

Bowley, J., Baker-Austin, C., Michell, S., Lewis, C., 2022. Pathogens transported by plastic debris: does this vector pose a risk to aquatic organisms? Emerging Topics in Life Sciences ETLS20220022. https://doi.org/10.1042/ETLS20220022

Bowley, J., Baker-Austin, C., Porter, A., Hartnell, R., Lewis, C., 2021. Oceanic Hitchhikers – Assessing Pathogen Risks from Marine Microplastic. Trends in Microbiology 29, 107–116. https://doi.org/10.1016/j.tim.2020.06.011

Brehm, T.T., Berneking, L., Rohde, H., Chistner, M., Schlickewei, C., Sena Martins, M., Schmiedel, S., 2020. Wound infection with Vibrio harveyi following a traumatic leg amputation after a motorboat propeller injury in Mallorca, Spain: a case report and review of literature. BMC Infectious Diseases 20, 104. https://doi.org/10.1186/s12879-020-4789-2

Brehm, T.T., Berneking, L., Sena Martins, M., Dupke, S., Jacob, D., Drechsel, O., Bohnert, J., Becker, K., Kramer, A., Christner, M., Aepfelbacher, M., Schmiedel, S., Rohde, H., 2021a. Heatwave-associated Vibrio infections in Germany, 2018

and 2019. Eurosurveillance 26. https://doi.org/10.2807/1560-7917.ES.2021.26.41.2002041

Brehm, T.T., Dupke, S., Hauk, G., Fickenscher, H., Rohde, H., Berneking, L., 2021b. [Non-cholera Vibrio species - currently still rare but growing danger of infection in the North Sea and the Baltic Sea]. Internist (Berl) 62, 876–886. https://doi.org/10.1007/s00108-021-01086-x

Brooke, J.S., 2012. Stenotrophomonas maltophilia: an Emerging Global Opportunistic Pathogen. Clin Microbiol Rev 25, 2–41. https://doi.org/10.1128/CMR.00019-11

Brumfield, K.D., Chen, A.J., Gangwar, M., Usmani, M., Hasan, N.A., Jutla, A.S., Huq, A., Colwell, R.R., 2023a. Environmental Factors Influencing Occurrence of Vibrio parahaemolyticus and Vibrio vulnificus. Appl Environ Microbiol e0030723. https://doi.org/10.1128/aem.00307-23

Brumfield, K.D., Moiz, U., Sanneri, S., Komalpreet, S., Mayank, G., Hasan Nur A., Netherland Michael, Deliz Katherine, Angelini Christine, Beatty Norman L., Huq Anwar, Jutla Antarpreet S., Colwell Rita R., 2023b. Genomic diversity of Vibrio spp. and metagenomic analysis of pathogens in Florida Gulf coastal waters following Hurricane Ian. mBio 0, e01476-23. https://doi.org/10.1128/mbio.01476-23

Brumfield, K.D., Usmani, M., Chen, K.M., Gangwar, M., Jutla, A.S., Huq, A., Colwell, R.R., 2021. Environmental parameters associated with incidence and transmission of pathogenic Vibrio spp. Environmental Microbiology. https://doi.org/10.1111/1462-2920.15716

Bullington, J.A., Golder, A.R., Steward, G.F., McManus, M.A., Neuheimer, A.B., Glazer, B.T., Nigro, O.D., Nelson, C.E., 2022. Refining real-time predictions of Vibrio vulnificus concentrations in a tropical urban estuary by incorporating dissolved organic matter dynamics. Science of The Total Environment 829, 154075. https://doi.org/10.1016/j.scitotenv.2022.154075

Burnham, K.P., Anderson, D.R., 2004. Multimodel Inference: Understanding AIC and BIC in Model Selection. Sociological Methods & Research 33, 261–304. https://doi.org/10.1177/0049124104268644

Burnham, K.P., Anderson, D.R., 2002. Model Selection and Multi-Model Inference : A Practical Information-Theoretic Approach. Springer, Secaucus, UNITED STATES.

Cai, J., Han, H., Song, Z., Li, C., Zhou, J., 2006. Isolation and characterization of pathogenic Vibrio alginolyticus from diseased postlarval abalone, Haliotis diversicolor supertexta (Lischke). Aquaculture Research 37, 1222–1226. https://doi.org/10.1111/j.1365-2109.2006.01552.x

Cavicchioli, R., Ripple, W.J., Timmis, K.N., Azam, F., Bakken, L.R., Baylis, M., Behrenfeld, M.J., Boetius, A., Boyd, P.W., Classen, A.T., Crowther, T.W., Danovaro, R., Foreman, C.M., Huisman, J., Hutchins, D.A., Jansson, J.K., Karl, D.M., Koskella, B., Welch, D.B.M., Martiny, J.B.H., Moran, M.A., Orphan, V.J., Reay, D.S., Remais, J.V., Rich, V.I., Singh, B.K., Stein, L.Y., Stewart, F.J., Sullivan, M.B., Oppen, M.J.H. van, Weaver, S.C., Webb, E.A., Webster, N.S., 2019. Scientists' warning to humanity: microorganisms and climate change. Nature Reviews Microbiology 1. https://doi.org/10.1038/s41579-019-0222-5

Ceccarelli, D., Hasan, N.A., Huq, A., Colwell, R.R., 2013. Distribution and dynamics of epidemic and pandemic Vibrio parahaemolyticus virulence factors. Frontiers in Cellular and Infection Microbiology 3, 1–9. https://doi.org/10.3389/fcimb.2013.00097

Center for International Earth Science Information Network - CIESIN - Columbia University, 2018a. Gridded Population of the World, Version 4 (GPWv4): Basic Demographic Characteristics, Revision 11.

Center for International Earth Science Information Network - CIESIN - Columbia University, 2018b. Gridded Population of the World, Version 4 (GPWv4): Population Count Adjusted to Match 2015 Revision of UN WPP Country Totals, Revision 11.

Center for International Earth Science Information Network - CIESIN - Columbia University, 2018c. Gridded Population of the World, Version 4 (GPWv4): Population Count, Revision 11.

Center for International Earth Science Information Network - CIESIN - Columbia University, United Nations Food and Agriculture Programme - FAO, Centro

Internacional de Agricultura Tropical - CIAT, 2005. Gridded Population of the World, Version 3 (GPWv3): Population Count Grid.

Centers for Disease Control and Prevention, 2023. Health Alert Network (HAN) - 00497 | Severe Vibrio vulnificus Infections in the United States Associated with Warming Coastal Waters [WWW Document]. URL https://emergency.cdc.gov/han/2023/han00497.asp (accessed 9.24.23).

Centers for Disease Control and Prevention, 2022. Cholera and Other Vibrio Illness Surveillance (COVIS) | Vibrio Illness (Vibriosis) | CDC [WWW Document]. URL https://www.cdc.gov/vibrio/surveillance.html (accessed 7.28.23).

Centers for Disease Control and Prevention, 2019. Vibrio Species Causing Vibriosis: Questions and Answers [WWW Document]. URL https://www.cdc.gov/vibrio/faq.html (accessed 12.4.19).

Centers for Disease Control and Prevention, 2015. FoodNet Surveillence [WWW Document]. URL https://www.cdc.gov/foodnet/surveillance.html (accessed 12.5.19).

Centers for Disease Control and Prevention, 1999. Outbreak of Vibrio parahaemolyticus Infection Associated with Eating Raw Oysters and Clams Harvested from Long Island Sound — Connecticut, New Jersey, and New York, 1998. Morbidity and Mortality Weekly Report 48, 48–51. https://doi.org/10.1001/jama.281.8.696

Centers for Disease Control and Prevention, 1998. Parahaemolyticus Outbreak 1997 Pacific Northwest. Morbidity and Mortality Weekly Report 47, 457–462. https://doi.org/10.1001/jama.280.6.504

Centers for Disease Control and Prevention (CDC), 2005. Vibrio illnesses after hurricane katrina - Multiple States, August-September 2005. Morbidity and Mortality Weekly Report 54, 928–931.

Cervino, J.M., Thompson, F.L., Gomez-Gil, B., Lorence, E.A., Goreau, T.J., Hayes, R.L., Winiarski-Cervino, K.B., Smith, G.W., Hughen, K., Bartels, E., 2008. The Vibrio core group induces yellow band disease in Caribbean and Indo-Pacific reef-building corals. Journal of Applied Microbiology 105, 1658–1671. https://doi.org/10.1111/j.1365-2672.2008.03871.x

Chang, W., Cheng, J., Allaire, J., Sievert, C., Schloerke, B., Xie, Y., Allen, J., McPherson, J., Dipert, A., Borges, B., 2022. shiny: Web Application Framework for R.

Chao, W.N., Tsai, C.F., Chang, H.R., Chan, K.S., Su, C.H., Lee, Y.T., Ueng, K.C., Chen, C.C., Chen, S.C., Lee, M.C., 2013. Impact of timing of surgery on outcome of Vibrio vulnificus-related necrotizing fasciitis. American Journal of Surgery 206, 32–39. https://doi.org/10.1016/j.amjsurg.2012.08.008

Chase, E., Young, S., Harwood, V.J., 2015. Sediment and vegetation as reservoirs of Vibrio vulnificus in the Tampa Bay Estuary and Gulf of Mexico. Applied and Environmental Microbiology 81, 2489–2494. https://doi.org/10.1128/{AEM}.03243-14

Chen, F.-R., Liu, P.-C., Lee, K.-K., 2000. Lethal Attribute of Serine Protease Secreted by Vibrio alginolyticus Strains in Kuruma Prawn Penaeus japonicus. Zeitschrift für Naturforschung C 55, 94–99. https://doi.org/10.1515/znc-2000-1-218

Chen, Y., Ai, X., Yang, Y., 2022. Vibrio cholerae: a pathogen shared by human and aquatic animals. The Lancet Microbe 3, e402. https://doi.org/10.1016/S2666-5247(22)00125-2

Chen, Y.-T., Tang, H.-J., Chao, C.-M., Lai, C.-C., 2015. Clinical Manifestations of Non-O1 Vibrio cholerae Infections. PLOS ONE 10, e0116904. https://doi.org/10.1371/journal.pone.0116904

Cherrie, M.P.C., Nichols, G., Iacono, G.L., Sarran, C., Hajat, S., Fleming, L.E., 2018. Pathogen seasonality and links with weather in England and Wales: a big data time series analysis. BMC Public Health 18, 1067. https://doi.org/10.1186/s12889-018-5931-6

Chicco, D., 2017. Ten quick tips for machine learning in computational biology. BioData Mining 10, 1–17. https://doi.org/10.1186/s13040-017-0155-3

Chin, T.M., Vazquez-Cuervo, J., Armstrong, E.M., 2017. A multi-scale high-resolution analysis of global sea surface temperature. Remote Sensing of Environment 200, 154–169. https://doi.org/10.1016/j.rse.2017.07.029

Christidis, N., McCarthy, M., Stott, P.A., 2020. The increasing likelihood of temperatures above 30 to 40 °C in the United Kingdom. Nature Communications 11, 3093. https://doi.org/10.1038/s41467-020-16834-0

Climate Reanalyzer, Climate Change Institute, University of Maine, 2023. Daily Sea Surface Temperature [WWW Document]. URL https://climatereanalyzer.org/clim/sst_daily/ (accessed 8.20.23).

Coerdt, K.M., Khachemoune, A., 2021. Vibrio vulnificus: Review of Mild to Life-threatening Skin Infections. Cutis 107. https://doi.org/10.12788/cutis.0183

Cohen, Darryl.T., 2018. Coastline County Population Continues to Grow: 60 Million Live in the Path of Hurricanes [WWW Document]. URL https://www.census.gov/library/stories/2018/08/coastal-county-population-rises.html (accessed 5.29.20).

Collins, M., Sutherland, M., Bouwer, L., Cheong, S.M., Frölicher, T., Jacot Des Combes, H., Koll Roxy, M., Losada, I., McInnes, K., Ratter, B., Rivera-Arriaga, E., Susanto, R.D., Swingedouw, D., Tibig, L., 2019. Extremes, Abrupt Changes and Managing Risks, in: Pörtner, H.-O., Roberts, D.C., Masson-Delmotte, V., Zhai, P., Tignor, M., Poloczanska, E., Mintenbeck, K., Alegría, A., Nicolai, M., Okem, A., Petzold, J., Rama, B., Weyer, N.M. (Eds.), {IPCC} Special Report on the Ocean and Cryosphere in a Changing Climate. pp. 3–63.

Colón-González, F.J., Harris, I., Osborn, T.J., Bernardo, C.S.S., Peres, C.A., Hunter, P.R., Warren, R., Vuurene, D. van, Lake, I.R., 2018. Limiting global-mean temperature increase to 1.5–2 °C could reduce the incidence and spatial spread of dengue fever in Latin America. PNAS 115, 6243–6248. https://doi.org/10.1073/pnas.1718945115

Colwell, R.R., 2000. Viable but nonculturable bacteria: A survival strategy. Journal of Infection and Chemotherapy 6, 121–125. https://doi.org/10.1007/PL00012151

Colwell, R.R., 1996. Global climate and infectious disease: The cholera paradigm. Science 274, 2025–2031. https://doi.org/10.1126/science.274.5295.2025

Conchon, A., 2016. Modélisation du zooplancton et du micronecton marins (phdthesis). Université de La Rochelle.

Connecticut State Department of Public Health, 2023. Vibrio [WWW Document]. CT.gov - Connecticut's Official State Website. URL https://portal.ct.gov/DPH/Press-Room/Press-Releases---2023/Vibrio (accessed 9.3.23).

Constantin de Magny, G., Hasan, N.A., Roche, B., 2014. How community ecology can improve our understanding of cholera dynamics. Front Microbiol 5, 137. https://doi.org/10.3389/fmicb.2014.00137

Cook, D.W., Bowers, J.C., DePaola, A., 2002. Density of total and pathogenic (tdh+) Vibrio parahaemolyticus in Atlantic and Gulf Coast molluscan shellfish at harvest. Journal of Food Protection 65, 1873–1880. https://doi.org/10.4315/0362-028X-65.12.1873

Coombes, E.G., Jones, A.P., Sutherland, W.J., 2008. The biodiversity implications of changes in coastal tourism due to climate change. Environmental Conservation 35, 319–330. https://doi.org/10.1017/S0376892908005134

Copernicus Climate Data Store, 2019. Ocean colour daily data from 1997 to present derived from satellite observations. https://doi.org/10.24381/cds.f85b319d

Copernicus Marine Service, 2023a. Atlantic - European North West Shelf - Ocean Physics Analysis and Forecast. https://doi.org/10.48670/moi-00054

Copernicus Marine Service, 2023b. North West Shelf Region, Bio-Geo-Chemical, L4, monthly means and interpolated daily observation. https://doi.org/10.48670/moi-00119

Copernicus Marine Service, 2022a. Global Ocean Physics Reanalysis. https://doi.org/10.48670/moi-00021

Copernicus Marine Service, 2022b. Global ocean low and mid trophic levels biomass content hindcast. https://doi.org/10.48670/moi-00020

Cornes, R.C., Tinker, J., Hermanson, L., Oltmanns, M., Hunter, W.R., Lloyd-Hartley, H., Kent, E.C., Rabe, B., Renshaw, R., 2023. The impacts of climate change on sea temperature around the UK and Ireland. MCCIP Science Review 2023. https://doi.org/10.14465/2022.reu08.tem

Coutard, F., Crassous, P., Droguet, M., Gobin, E., Colwell, R.R., Pommepuy, M., Hervio-Heath, D., 2007. Recovery in culture of viable but nonculturable Vibrio parahaemolyticus: Regrowth or resuscitation? ISME Journal 1, 111–120. https://doi.org/10.1038/ismej.2007.1

Czajkowski, M., Ahtiainen, H., Artell, J., Budziński, W., Hasler, B., Hasselström, L., Meyerhoff, J., Nõmmann, T., Semeniene, D., Söderqvist, T., Tuhkanen, H., Lankia, T., Vanags, A., Zandersen, M., Zylicz, T., Hanley, N., 2015. Valuing the commons: An international study on the recreational benefits of the Baltic Sea. Journal of Environmental Management 156, 209–217. https://doi.org/10.1016/j.jenvman.2015.03.038

Daniels, N.A., 2011. Vibrio vulnificus oysters: Pearls and perils. Clinical Infectious Diseases 52, 788–792. https://doi.org/10.1093/cid/ciq251

Dechet, A.M., Yu, P.A., Koram, N., Painter, J., 2008. Nonfoodborne Vibrio Infections: An Important Cause of Morbidity and Mortality in the United States, 1997–2006. Clinical Infectious Diseases 46, 970–976. https://doi.org/10.1086/529148

Deeb, R., Tufford, D., Scott, G.I., Moore, J.G., Dow, K., 2018. Impact of Climate Change on Vibrio vulnificus Abundance and Exposure Risk. Estuaries and Coasts 41, 2289–2303. https://doi.org/10.1007/s12237-018-0424-5

DePaola, A., Nordstrom, J.L., Bowers, J.C., Wells, J.G., Cook, D.W., 2003. Seasonal abundance of total and pathogenic Vibrio parahaemolyticus in Alabama oysters. Applied and Environmental Microbiology 69, 1521–1526. https://doi.org/10.1128/AEM.69.3.1521-1526.2003

Deshayes, S., Daurel, C., Cattoir, V., Parienti, J.J., Quilici, M.L., de La Blanchardière, A., 2015. Non-O1, non-O139 Vibrio cholerae bacteraemia: case report and literature review. SpringerPlus 4, 1–9. https://doi.org/10.1186/s40064-015-1346-3

Dieckmann, R., Strauch, E., Alter, T., 2010. Rapid identification and characterization of Vibrio species using whole-cell MALDI-TOF mass spectrometry. J Appl Microbiol 109, 199–211. https://doi.org/10.1111/j.1365-2672.2009.04647.x

Diner, R.E., Kaul, D., Rabines, A., Zheng, H., Steele, J.A., Griffith, J.F., Allen, A.E., 2021. Pathogenic Vibrio Species Are Associated with Distinct Environmental Niches and Planktonic Taxa in Southern California ({USA}) Aquatic Microbiomes. mSystems e0057121. https://doi.org/10.1128/{mSystems}.00571-21

Ditlevsen, P., Ditlevsen, S., 2023. Warning of a forthcoming collapse of the Atlantic meridional overturning circulation. Nat Commun 14, 4254. https://doi.org/10.1038/s41467-023-39810-w

Dormann, C.F., Calabrese, J.M., Guillera-Arroita, G., Matechou, E., Bahn, V., Bartoń, K., Beale, C.M., Ciuti, S., Elith, J., Gerstner, K., Guelat, J., Keil, P., Lahoz-Monfort, J.J., Pollock, L.J., Reineking, B., Roberts, D.R., Schröder, B., Thuiller, W., Warton, D.I., Wintle, B.A., Wood, S.N., Wüest, R.O., Hartig, F., 2018. Model averaging in ecology: a review of Bayesian, information-theoretic, and tactical approaches for predictive inference. Ecological Monographs 88, 485–504. https://doi.org/10.1002/ecm.1309

Dubert, J., Romalde, J.L., Spinard, E.J., Nelson, D.R., Gomez-Chiarri, M., Barja, J.L., 2016. Reclassification of the larval pathogen for marine bivalves Vibrio tubiashii subsp. europaeus as Vibrio europaeus sp. nov. International Journal of Systematic and Evolutionary Microbiology 66, 4791–4796. https://doi.org/10.1099/ijsem.0.001431

E. U. Directive, 2006. 7/EC of the European Parliament and of the Council of 15 February 2006 concerning the management of bathing water quality and repealing Directive 76/160/EEC. Official Journal of the European Union 2013, L64.

Eagon, R.G., 1962. Pseudomonas natriegens, a marine bacterium with a generation time of less than 10 minutes. J Bacteriol 83, 736–737. https://doi.org/10.1128/jb.83.4.736-737.1962

Ebi, K.L., Åström, C., Boyer, C.J., Harrington, L.J., Hess, J.J., Honda, Y., Kazura, E., Stuart-Smith, R.F., Otto, F.E.L., 2020. Using Detection And Attribution To Quantify How Climate Change Is Affecting Health. Health Affairs 39, 2168–2174. https://doi.org/10.1377/hlthaff.2020.01004

Ebi, K.L., Ogden, N.H., Semenza, J.C., Woodward, A., 2017. Detecting and Attributing Health Burdens to Climate Change. Environ Health Perspect 125, 085004. https://doi.org/10.1289/EHP1509

Edouard, S., Daumas, A., Branger, S., Durand, J.-M., Raoult, D., Fournier, P.-E., 2009. Grimontia hollisae, a potential agent of gastroenteritis and bacteraemia in the Mediterranean area. Eur J Clin Microbiol Infect Dis 28, 705–707. https://doi.org/10.1007/s10096-008-0678-0

Eiler, A., Gonzalez-Rey, C., Allen, S., Bertilsson, S., 2007. Growth response of Vibrio cholerae and other Vibrio spp. to cyanobacterial dissolved organic matter and

temperature in brackish water. FEMS Microbiology Ecology 60, 411–418. https://doi.org/10.1111/j.1574-6941.2007.00303.x

Eiler, A., Johansson, M., Bertilsson, S., 2006. Environmental influences on Vibrio populations in northern temperate and boreal coastal waters (Baltic and Skagerrak Seas). Applied and Environmental Microbiology 72, 6004–6011. https://doi.org/10.1128/AEM.00917-06

Elliott, L.R., White, M.P., Sarran, C., Grellier, J., Garrett, J.K., Scoccimarro, E., Smalley, A.J., Fleming, L.E., 2019. The effects of meteorological conditions and daylight on nature-based recreational physical activity in England. Urban Forestry and Urban Greening 42, 39–50. https://doi.org/10.1016/j.ufug.2019.05.005

Engdaw, M.M., Steiner, A.K., Hegerl, G.C., Ballinger, A.P., 2023. Attribution of observed changes in extreme temperatures to anthropogenic forcing using CMIP6 models. Weather and Climate Extremes 39, 100548. https://doi.org/10.1016/j.wace.2023.100548

Engel, M.F., Muijsken, M.A., Mooi-Kokenberg, E., Kuijper, E.J., van Westerloo, D.J., 2016. Vibrio cholerae non-O1 bacteraemia: description of three cases in the Netherlands and a literature review. Euro Surveillance 21. https://doi.org/10.2807/1560-7917.ES.2016.21.15.30197

Epstein, P.R., 2001. Climate change and emerging infectious diseases. Microbes and Infection 3, 747–754. https://doi.org/10.1016/s1286-4579(01)01429-0

Erler, R., Wichels, A., Heinemeyer, E.-A., Hauk, G., Hippelein, M., Reyes, N.T., Gerdts, G., 2015. VibrioBase: A MALDI-TOF MS database for fast identification of Vibrio spp. that are potentially pathogenic in humans. Systematic and Applied Microbiology 38, 16–25. https://doi.org/10.1016/j.syapm.2014.10.009

Esteves, K., Hervio-Heath, D., Mosser, T., Rodier, C., Tournoud, M., Jumas-Bilak, E., Colwell, R.R., Monfort, P., 2015. Rapid Proliferation of Vibrio parahaemolyticus, Vibrio vulnificus, and Vibrio cholerae during Freshwater Flash Floods in French Mediterranean Coastal Lagoons. Frontiers in Microbiology 81, 7600–7609. https://doi.org/10.1128/AEM.01848-15.Editor

European Centre for Disease Prevention and Control, 2016. Vibrio Map Viewer [WWW Document]. URL https://e3geoportal.ecdc.europa.eu/SitePages/Vibrio Map Viewer.aspx (accessed 5.27.20).

Eyring, V., Bony, S., Meehl, G.A., Senior, C.A., Stevens, B., Stouffer, R.J., Taylor, K.E., 2016. Overview of the Coupled Model Intercomparison Project Phase 6 (CMIP6) experimental design and organization. Geoscientific Model Development 9, 1937–1958. https://doi.org/10.5194/gmd-9-1937-2016

Farrell, M.L., Joyce, A., Duane, S., Fitzhenry, K., Hooban, B., Burke, L.P., Morris, D., 2021. Evaluating the potential for exposure to organisms of public health concern in naturally occurring bathing waters in Europe: A scoping review. Water Res 206, 117711. https://doi.org/10.1016/j.watres.2021.117711

Faruque, S.M., Mekalanos, J.J., 2012. Phage-bacterial interactions in the evolution of toxigenic Vibrio cholerae. Virulence 3, 556–565. https://doi.org/10.4161/viru.22351

Feng, X., Haines, K., de Boisséson, E., 2018. Coupling of surface air and sea surface temperatures in the CERA-20C reanalysis. Quarterly Journal of the Royal Meteorological Society 144, 195–207. https://doi.org/10.1002/qj.3194

Fernández-Rendón, C.L., Barrera-Escorcia, G., Wong-Chang, I., Vázquez Botello, A., Gómez-Gil, B., Lizárraga-Partida, M.L., 2019. Toxigenic V. cholerae, V. parahaemolyticus, and V. vulnificus in oysters from the Gulf of Mexico and sold in Mexico City. International Journal of Environmental Health Research 29, 430–440. https://doi.org/10.1080/09603123.2018.1548696

Fick, S.E., Hijmans, R.J., 2017. WorldClim 2: new 1-km spatial resolution climate surfaces for global land areas. International Journal of Climatology 37, 4302–4315. https://doi.org/10.1002/joc.5086

Filazzola, A., Xie, G., Barrett, K., Dunn, A., Johnson, M.T.J., MacIvor, J.S., 2022. Using smartphone-GPS data to quantify human activity in green spaces. PLOS Computational Biology 18, e1010725. https://doi.org/10.1371/journal.pcbi.1010725

Fleischmann, S., Herrig, I., Wesp, J., Stiedl, J., Reifferscheid, G., Strauch, E., Alter, T., Brennholt, N., 2022. Prevalence and Distribution of Potentially Human

Pathogenic Vibrio spp. on German North and Baltic Sea Coasts. Front Cell Infect Microbiol 12, 846819. https://doi.org/10.3389/fcimb.2022.846819

Fong, C.R., Gaynus, C.J., Carpenter, R.C., 2020. Extreme rainfall events pulse substantial nutrients and sediments from terrestrial to nearshore coastal communities: a case study from French Polynesia. Sci Rep 10, 2955. https://doi.org/10.1038/s41598-020-59807-5

Ford, C.L., Powell, A., Lau, D.Y.L., Turner, A.D., Dhanji-Rapkova, M., Martinez-Urtaza, J., Baker-Austin, C., 2020. Isolation and characterization of potentially pathogenic *Vibrio* species in a temperate, higher latitude hotspot. Environmental Microbiology Reports 12, 424–434. https://doi.org/10.1111/1758-2229.12858

Frankignoulle, M., Distèche, A., 1984. CO2 chemistry in the water column above a posidonia seagrass bed and related air-sea exchanges. Oceanologica Acta 7.

Freeman, E.A., Moisen, G.G., 2008. A comparison of the performance of threshold criteria for binary classification in terms of predicted prevalence and kappa. Ecological Modelling 217, 48–58. https://doi.org/10.1016/j.ecolmodel.2008.05.015

Frischkorn, K.R., Stojanovski, A., Paranjpye, R., 2013. Vibrio parahaemolyticus type IV pili mediate interactions with diatom-derived chitin and point to an unexplored mechanism of environmental persistence. Environmental Microbiology 15, 1416–1427. https://doi.org/10.1111/1462-2920.12093

Froelich, B., Bowen, J., Gonzalez, R., Snedeker, A., Noble, R., 2013. Mechanistic and statistical models of total vibrio abundance in the neuse river estuary. Water Research 47, 5783–5793. https://doi.org/10.1016/j.watres.2013.06.050

Froelich, B.A., Ayrapetyan, M., Fowler, P., Oliver, J.D., Noble, R.T., 2015. Development of a matrix tool for the prediction of Vibrio species in oysters harvested from North Carolina. Applied and Environmental Microbiology 81, 1111–1119. https://doi.org/10.1128/AEM.03206-14

Froelich, B.A., Noble, R.T., 2016. Vibrio bacteria in raw oysters: Managing risks to human health. Philosophical Transactions of the Royal Society B: Biological Sciences. https://doi.org/10.1098/rstb.2015.0209

Frölicher, T.L., Laufkötter, C., 2018. Emerging risks from marine heat waves. Nat Commun 9, 650. https://doi.org/10.1038/s41467-018-03163-6

Galbraith, P.S., Larouche, P., Chassé, J., Petrie, B., 2012. Sea-surface temperature in relation to air temperature in the Gulf of St. Lawrence: Interdecadal variability and long term trends. Deep Sea Research Part {II}: Topical Studies in Oceanography 77–80, 10–20. https://doi.org/10.1016/j.dsr2.2012.04.001

Galvis, F., Ageitos, L., Martínez-Matamoros, D., Barja, J.L., Rodríguez, J., Lemos, M.L., Jiménez, C., Balado, M., 2020. The marine bivalve molluscs pathogen Vibrio neptunius produces the siderophore amphibactin which is widespread in molluscs microbiota. Environmental Microbiology n/a, 5467–5482. https://doi.org/10.1111/1462-2920.15312

Garnier, M., Labreuche, Y., Garcia, C., Robert, M., Nicolas, J.L., 2007. Evidence for the involvement of pathogenic bacteria in summer mortalities of the Pacific oyster Crassostrea gigas. Microb Ecol 53, 187–196. https://doi.org/10.1007/s00248-006-9061-9

Ghosh, T., 2012. Sustainable Coastal Tourism: Problems and Management Options. Journal of Geography and Geology 4, 163–169. https://doi.org/10.5539/jgg.v4n1p163

Gildas Hounmanou, Y.M., Engberg, J., Bjerre, K.D., Holt, H.M., Olesen, B., Voldstedlund, M., Dalsgaard, A., Ethelberg, S., 2023. Correlation of High Seawater Temperature with Vibrio and Shewanella Infections, Denmark, 2010-2018. Emerg Infect Dis 29, 605–608. https://doi.org/10.3201/eid2903.221568

Gonzalez, D.J., Gonzalez, R.A., Froelich, B.A., Oliver, J.D., Noble, R.T., McGlathery, K.J., 2014. Non-native macroalga may increase concentrations of Vibrio bacteria on intertidal mudflats. Marine Ecology Progress Series 505, 29–36. https://doi.org/10.3354/meps10771

González-Escalona, N., Cachicas, V., Acevedo, C., Rioseco, M.L., Vergara, J.A., Cabello, F., Romero, J., Espejo, R.T., 2005. Vibrio parahaemolyticus diarrhea, Chile, 1998 and 2004. Emerging infectious diseases 11, 129–131. https://doi.org/10.3201/eid1101.040762

González-Escalona, N., Gavilan, R.G., Brown, E.W., Martinez-Urtaza, J., 2015. Transoceanic spreading of pathogenic strains of Vibrio parahaemolyticus with distinctive genetic signatures in the {recA} gene. Plos One 10, e0117485. https://doi.org/10.1371/journal.pone.0117485

Governor Kathy Hochul, 2023. Following Death in Suffolk County Tied to Rare Vibrio Vulnificus Bacteria, Governor Hochul Updates New Yorkers on Public Health Precautions and Ongoing Preparedness Efforts | Governor Kathy Hochul [WWW Document]. URL https://www.governor.ny.gov/news/following-death-suffolk-county-tied-rare-vibrio-vulnificus-bacteria-governor-hochul-updates (accessed 9.3.23).

Grantz, K.H., Meredith, H.R., Cummings, D.A.T., Metcalf, C.J.E., Grenfell, B.T., Giles, J.R., Mehta, S., Solomon, S., Labrique, A., Kishore, N., Buckee, C.O., Wesolowski, A., 2020. The use of mobile phone data to inform analysis of COVID-19 pandemic epidemiology. Nat Commun 11, 4961. https://doi.org/10.1038/s41467-020-18190-5

Greenfield, D.I., Gooch Moore, J., Stewart, J.R., Hilborn, E.D., George, B.J., Li, Q., Dickerson, J., Keppler, C.K., Sandifer, P.A., 2017. Temporal and Environmental Factors Driving Vibrio Vulnificus and V. Parahaemolyticus Populations and Their Associations With Harmful Algal Blooms in South Carolina Detention Ponds and Receiving Tidal Creeks. GeoHealth 1, 306–317. https://doi.org/10.1002/2017GH000094

Gudmundsson, E., Asche, F., Nielsen, M., 2006. Revenue Distribution Through The Seafood Value Chain. FAO Fisheries Circular 1019, 42.

Gugliandolo, C., Irrera, G.P., Lentini, V., Maugeri, T.L., 2008. Pathogenic Vibrio, Aeromonas and Arcobacter spp. associated with copepods in the Straits of Messina (Italy). Mar Pollut Bull 56, 600–606. https://doi.org/10.1016/j.marpolbul.2007.12.001

Guillod, C., Ghitti, F., Mainetti, C., 2019. Vibrio parahaemolyticus Induced Cellulitis and Septic Shock after a Sea Beach Holiday in a Patient with Leg Ulcers. Case Reports in Dermatology 11, 94–100. https://doi.org/10.1159/000499478

Gurevitz, J.M., Ceballos, L.A., Gaspe, M.S., Alvarado-Otegui, J.A., Enríquez, G.F., Kitron, U., Gürtler, R.E., 2011. Factors Affecting Infestation by Triatoma infestans

in a Rural Area of the Humid Chaco in Argentina: A Multi-Model Inference Approach. PLoS Negl Trop Dis 5, e1349. https://doi.org/10.1371/journal.pntd.0001349

Gyraite, G., Kataržytė, M., Overlingė, D., Vaičiūtė, D., Jonikaitė, E., Schernewski, G., 2020. Skip the Dip—Avoid the Risk? Integrated Microbiological Water Quality Assessment in the South-Eastern Baltic Sea Coastal Waters. Water 12, 3146. https://doi.org/10.3390/w12113146

Hajima, T., Watanabe, M., Yamamoto, A., Tatebe, H., Noguchi, M.A., Abe, M., Ohgaito, R., Ito, Akinori, Yamazaki, D., Okajima, H., Ito, Akihiko, Takata, K., Ogochi, K., Watanabe, S., Kawamiya, M., 2020. Development of the MIROC-ES2L Earth system model and the evaluation of biogeochemical processes and feedbacks. Geoscientific Model Development 13, 2197–2244. https://doi.org/10.5194/gmd-13-2197-2020

Hajima, T., Watanabe, M., Yamamoto, A., Tatebe, H., Noguchi, M.A., Abe, M., Ohgaito, R., Ito, Akinori, Yamazaki, D., Okajima, H., Ito, Akihiko, Takata, K., Ogochi, K., Watanabe, S., Kawamiya, M., 2019. Description of the MIROC-ES2L Earth system model andevaluation of its climate–biogeochemical processes and feedbacks (preprint). Climate and Earth System Modeling. https://doi.org/10.5194/gmd-2019-275

Hall-Stoodley, L., Costerton, J.W., Stoodley, P., 2004. Bacterial biofilms: From the natural environment to infectious diseases. Nature Reviews Microbiology 2, 95–108. https://doi.org/10.1038/nrmicro821

Halpern, M., Izhaki, I., 2017. Fish as hosts of Vibrio cholerae. Frontiers in Microbiology 8, 1–7. https://doi.org/10.3389/fmicb.2017.00282

Harlock, M., Quinn, S., Turnbull, A.R., 2022. Emergence of non-choleragenic Vibrio infections in Australia. Commun Dis Intell (2018) 46. https://doi.org/10.33321/cdi.2022.46.8

Harris, I., Jones, P.D., Osborn, T.J., Lister, D.H., 2014. Updated high-resolution grids of monthly climatic observations - the CRU TS3.10 Dataset. International Journal of Climatology 34, 623–642. https://doi.org/10.1002/joc.3711

Harrison, J., Nelson, K., Morcrette, H., Morcrette, C., Preston, J., Helmer, L., Titball, R.W., Butler, C.S., Wagley, S., 2022. The increased prevalence of Vibrio species and the first reporting of Vibrio jasicida and Vibrio rotiferianus at UK shellfish sites. Water Research 211, 117942. https://doi.org/10.1016/j.watres.2021.117942

Hartley, J.W., West, E., Gothard, W.P., Hanan, H.W.I., 1991. Vibrio alginolyticus in the U.K. Journal of Infection 23, 223. https://doi.org/10.1016/0163-4453(91)92596-W

Hassan, C., 2022. Dangerous flesh-eating bacterial infections increased in Florida after Hurricane Ian [WWW Document]. CNN. URL https://www.cnn.com/2022/10/18/health/rare-bacteria-hurricane-ian-floodwaters/index.html (accessed 8.20.23).

Hauer, M., Center for International Earth Science Information Network - CIESIN - Columbia University, 2021. Georeferenced U.S. County-Level Population Projections, Total and by Sex, Race and Age, Based on the SSPs, 2020-2100.

Hausfather, Z., Peters, G., P., 2020. Emissions – the 'business as usual' story is misleading. Nature 577, 618–620. https://doi.org/10.1038/d41586-020-00177-3

Hays, G.C., Richardson, A.J., Robinson, C., 2005. Climate change and marine plankton. Trends in Ecology and Evolution 20, 337–344. https://doi.org/10.1016/j.tree.2005.03.004

Heisler, J., Glibert, P.M., Burkholder, J.M., Anderson, D.M., Cochlan, W., Dennison, W.C., Dortch, Q., Gobler, C.J., Heil, C.A., Humphries, E., Lewitus, A., Magnien, R., Marshall, H.G., Sellner, K., Stockwell, D.A., Stoecker, D.K., Suddleson, M., 2008. Eutrophication and harmful algal blooms: A scientific consensus. Harmful Algae 8, 3–13. https://doi.org/10.1016/j.hal.2008.08.006

Heng, S.P., Letchumanan, V., Deng, C.Y., Ab Mutalib, N.S., Khan, T.M., Chuah, L.H., Chan, K.G., Goh, B.H., Pusparajah, P., Lee, L.H., 2017. Vibrio vulnificus: An environmental and clinical burden. Frontiers in Microbiology 8. https://doi.org/10.3389/fmicb.2017.00997

Henson, S.A., Cael, B.B., Allen, S.R., Dutkiewicz, S., 2021. Future phytoplankton diversity in a changing climate. Nat Commun 12, 5372. https://doi.org/10.1038/s41467-021-25699-w

Hernández-Cabanyero, C., Sanjuán, E., Fouz, B., Pajuelo, D., Vallejos-Vidal, E., Reyes-López, F.E., Amaro, C., 2020. The Effect of the Environmental Temperature on the Adaptation to Host in the Zoonotic Pathogen Vibrio vulnificus. Frontiers in Microbiology 11, 1–17. https://doi.org/10.3389/fmicb.2020.00489

Herring, S.C., Christidis, N., Hoell, A., Hoerling, M.P., Stott, P.A., 2020. Explaining Extreme Events of 2018 from a Climate Perspective. Bulletin of the American Meteorological Society 101, S1–S128. https://doi.org/10.1175/bams-explainingextremeevents2016.1

Hinder, S.L., Hays, G.C., Edwards, M., Roberts, E.C., Walne, A.W., Gravenor, M.B., 2012. Changes in marine dinoflagellate and diatom abundance under climate change. Nature Climate Change 2, 271–275. https://doi.org/10.1038/nclimate1388

Hinestrosa, F., Madeira, R.G., Bourbeau, P.P., 2007. Severe Gastroenteritis and Hypovolemic Shock Caused by *Grimontia* (*Vibrio*) *hollisae* Infection. J Clin Microbiol 45, 3462–3463. https://doi.org/10.1128/JCM.01205-07

Hlady, W.G., Klontz, K.C., 1996. The epidemiology of Vibrio infections in Florida, 1981-1993. Journal of Infectious Diseases 173, 1176–1183. https://doi.org/10.1093/infdis/173.5.1176

Hoegh-Guldberg, Jacob, O.D., Taylor, M., Bindi, M., Brown, S., Camilloni, I., Diedhiou, A., Djalante, R., Ebi, K.L., Engelbrecht, F., J.Guiot, Hijioka, Y., Mehrotra, S., Payne, A., Seneviratne, S.I., Thomas, A., Warren, R., Zhou, G., 2018. Impacts of 1.5°C of Global Warming on Natural and Human Systems. Global Warming of 1.5 ^{o}C. An IPCC Special Report on the impacts of global warming of 1.5°C above pre-industrial levels and related global greenhouse gas emission pathways, in the context of strengthening the global response to the threat of climate change 175–311.

Hollis, D.G., Weaver, R.E., Baker, C.N., Thornsberry, C., 1976. Halophilic Vibrio species isolated from blood cultures. J Clin Microbiol 3, 425–431.

Honda, T., Abad-Lapuebla, M.A., Ni, Y., Yamamoto, K., Miwatani, T., 1991. Characterization of a new thermostable direct haemolysin produced by a Kanagawa-phenomenon-negative clinical isolate of Vibrio parahaemolyticus. Microbiology 137, 253–259. https://doi.org/10.1099/00221287-137-2-253

Hong, J., Steen, C., Wong, E., Keong, B., 2020. *Shewanella*: an important, emerging and lethal pathogen in a patient with recurrent presentations of cholangitis. BMJ Case Rep 13, e237655. https://doi.org/10.1136/bcr-2020-237655

Hooper, W.L., Barrow, G.I., Mcnab, D.J.N., 1974. VIBRIO PARAHÆMOLYTICUS FOOD-POISONING IN BRITAIN. The Lancet 303, 1100–1102. https://doi.org/10.1016/S0140-6736(74)90570-4

Hosmer, D.W., Jr., Lemeshow, S., Sturdivant, R.X., 2013. Applied Logistic Regression. John Wiley & Sons, Incorporated, Newark, UNITED STATES.

Hsieh, J.L., Fries, J.S., Noble, R.T., 2008. Dynamics and predictive modelling of Vibrio spp. in the Neuse River Estuary, North Carolina, USA. Environmental Microbiology 10, 57–64. https://doi.org/10.1111/j.1462-2920.2007.01429.x

Hsieh, J.L., Fries, J.S., Noble, R.T., 2007. Vibrio and phytoplankton dynamics during the summer of 2004 in a eutrophying estuary. Ecological Applications 17, 102–109. https://doi.org/10.1890/05-1274.1

Huang, B., Liu, C., Banzon, V., Freeman, E., Graham, G., Hankins, B., Smith, T., Zhang, H.-M., 2021. Improvements of the Daily Optimum Interpolation Sea Surface Temperature (DOISST) Version 2.1. Journal of Climate 34, 2923–2939. https://doi.org/10.1175/JCLI-D-20-0166.1

Huang, K.C., Weng, H.H., Yang, T.Y., Chang, T.S., Huang, T.W., Lee, M.S., 2016. Distribution of fatal vibrio vulnificus necrotizing skin and soft-tissue infections a systematic review and meta-analysis. Medicine (United States) 95, 1–8. https://doi.org/10.1097/MD.0000000000002627

Huehn, S., Eichhorn, C., Urmersbach, S., Breidenbach, J., Bechlars, S., Bier, N., Alter, T., Bartelt, E., Frank, C., Oberheitmann, B., Gunzer, F., Brennholt, N., Boeer, S., Appel, B., Dieckmann, R., Strauch, E., 2014. Pathogenic vibrios in environmental, seafood and clinical sources in Germany. Int. J. Med. Microbiol. 304, 843–850. https://doi.org/10.1016/j.ijmm.2014.07.010

Hugo, G., 2011. Future demographic change and its interactions with migration and climate change. Global Environmental Change 21, S21–S33. https://doi.org/10.1016/j.gloenvcha.2011.09.008

Hunt, D.E., Gevers, D., Vahora, N.M., Polz, M.F., 2008. Conservation of the chitin utilization pathway in the Vibrionaceae. Applied and Environmental Microbiology 74, 44–51. https://doi.org/10.1128/AEM.01412-07

Huq, A., Small, E.B., West, P.A., Huq, M.I., Rahman, R., Colwell, R.R., 1983. Ecological relationships between Vibrio cholerae and planktonic crustacean copepods. Applied and Environmental Microbiology 45, 275–283. https://doi.org/10.1128/aem.45.1.275-283.1983

Intergovernmental Panel on Climate Change (IPCC) (Ed.), 2022. Annex I: Glossary, in: Global Warming of 1.5°C: IPCC Special Report on Impacts of Global Warming of 1.5°C above Pre-Industrial Levels in Context of Strengthening Response to Climate Change, Sustainable Development, and Efforts to Eradicate Poverty. Cambridge University Press, Cambridge, pp. 541–562. https://doi.org/10.1017/9781009157940.008

IPCC, 2022. Climate Change 2022: Impacts, Adaptation and Vulnerability. Contribution of Working Group II to the Sixth Asessment Report of the Intergovernmental Panel on Climate Change. Cambridge University Press.

IPCC, 2021. Climate Change 2021: The Physical Science Basis. Contribution of Working Group I to the Sixth Assessment Report of the Intergovernmental Panel on Climate Change. https://doi.org/10.1017/9781009157896

IPCC, 2014. Climate Change 2014: Synthesis Report. Contribution of Working Groups I, II and III to the Fifth Assessment Report of the Intergovernmental Panel on Climate Change. IPCC, Geneva, Switzerland. https://doi.org/10.1016/S0022-0248(00)00575-3

Islam, M.S., Drasar, B.S., Sack, R.B., 1994. The Aquatic Flora and Fauna as Reservoirs of Vibrio cholerae: A Review. Journal of Diarrhoeal Diseases Research 12, 87–96.

Islam, M.S., Rahim, Z., Alam, M.J., Begum, S., Moniruzzaman, S.M., Umeda, A., Amako, K., Albert, M.J., Sack, R.B., Huq, A., Colwell, R.R., 1999. Association of Vibrio cholerae O1 with the cyanobacterium, Anabaena sp., elucidated by polymerase chain reaction and transmission electron microscopy. Transactions of the Royal Society of Tropical Medicine and Hygiene 93, 36–40. https://doi.org/10.1016/S0035-9203(99)90171-2

Jacobs, J.M., Rhodes, M., Brown, C.W., Hood, R.R., Leight, A., Long, W., Wood, R., 2014. Modeling and forecasting the distribution of Vibrio vulnificus in Chesapeake Bay. Journal of Applied Microbiology 117, 1312–1327. https://doi.org/10.1111/jam.12624

Jacobs, J.M., Rhodes, M., Brown, C.W., Hood, R.R., Leight, A., Long, W., Wood, R., 2010. Predicting the Distribution of Vibrio vulnificus in Chesapeake Bay. {NOAA} Technical Memorandum {NOS} {NCCOS} 112 24.

Jacobs Slifka, K.M., Newton, A.E., Mahon, B.E., 2017. Vibrio alginolyticus infections in the USA, 1988-2012. Epidemiology and Infection 145, 1491–1499. https://doi.org/10.1017/S0950268817000140

Janecko, N., Bloomfield, S.J., Palau, R., Mather, A.E., 2021. Whole genome sequencing reveals great diversity of Vibrio spp in prawns at retail. Microb Genom 7, 000647. https://doi.org/10.1099/mgen.0.000647

Jiang, L., O'Neill, B.C., Zoraghein, H., Dahlke, S., 2020. Population scenarios for U.S. states consistent with shared socioeconomic pathways. Environmental Research Letters 15. https://doi.org/10.1088/1748-9326/aba5b1

Johnson, E.E., Escobar, L.E., Zambrana-Torrelio, C., 2019. An Ecological Framework for Modeling the Geography of Disease Transmission. Trends in Ecology and Evolution 34, 655–668. https://doi.org/10.1016/j.tree.2019.03.004

Jones, B., O'Neill, B.C., 2016. Spatially explicit global population scenarios consistent with the Shared Socioeconomic Pathways. Environmental Research Letters 11, 084003. https://doi.org/10.1088/1748-9326/11/8/084003

Jones, M.K., Oliver, J.D., 2009. Vibrio vulnificus: Disease and pathogenesis. Infection and Immunity 77, 1723–1733. https://doi.org/10.1128/IAI.01046-08

Julie, D., Solen, L., Antoine, V., Jaufrey, C., Annick, D., Dominique, H.-H., Deter, J., Lozach, S., Véron, A., Chollet, J., Derrien, A., Hervio-Heath, D., 2010. Ecology of pathogenic and non-pathogenic Vibrio parahaemolyticus on the French Atlantic coast. Effects of temperature, salinity, turbidity and chlorophyll a. Environmental Microbiology 12, 929–937. https://doi.org/10.1111/j.1462-2920.2009.02136.x

Julien, J., Ayer, T., Bethea, E.D., Tapper, E.B., Chhatwal, J., 2020. Projected prevalence and mortality associated with alcohol-related liver disease in the USA, 2019-40: a modelling study. Lancet Public Health 5, e316–e323. https://doi.org/10.1016/S2468-2667(20)30062-1

Kalvaitienė, G., Vaičiūtė, D., Bučas, M., Gyraitė, G., Kataržytė, M., 2023. Macrophytes and their wrack as a habitat for faecal indicator bacteria and Vibrio in coastal marine environments. Marine Pollution Bulletin 194, 115325. https://doi.org/10.1016/j.marpolbul.2023.115325

Kaneko, T., Colwell, R.R., 1975. Adsorption of Vibrio parahaemolyticus onto Chitin and Copepods. Applied Microbiology 29, 269–274. https://doi.org/10.1128/aem.29.2.269-274.1975

Kaneko, T., Colwell, R.R., 1973. Ecology of Vibrio parahaemolyticus in Chesapeake Bay. Journal of Bacteriology 113, 24–32. https://doi.org/10.1128/jb.113.1.24-32.1973

Kang, N.-Y., Elsner, J.B., 2015. Trade-off between intensity and frequency of global tropical cyclones. Nature Clim Change 5, 661–664. https://doi.org/10.1038/nclimate2646

Kang, S.-J., Jung, S.-I., Peck, K.R., 2020. Historical and Clinical Perspective of Vibrio vulnificus Infections in Korea. Infect Chemother 52, 245–251. https://doi.org/10.3947/ic.2020.52.2.245

Kelly, M.T., 1982. Effect of temperature and salinity on Vibrio (Beneckea) vulnificus occurrence in a gulf coast environment. Applied and Environmental Microbiology 44, 820–824. https://doi.org/10.1128/aem.44.4.820-824.1982

Kendon, M., 2022. Unprecedented extreme heatwave, July 2022. Met Office.

Kendon, M., McCarthy, M., Jevrejeva, S., Matthews, A., Williams, J., Sparks, T., West, F., 2023. State of the UK Climate 2022. International Journal of Climatology 43, 1–83. https://doi.org/10.1002/joc.8167

Khan, F.A., Fisher, M.A., Khakoo, R.A., 2007. Association of hemochromatosis with infectious diseases: expanding spectrum. International Journal of Infectious Diseases 11, 482–487. https://doi.org/10.1016/j.ijid.2007.04.007

Kim, I.-G., Lee, M.-H., Jung, S.-Y., Song, J.J., Oh, T.-K., Yoon, J.-H., 2005. Exiguobacterium aestuarii sp. nov. and Exiguobacterium marinum sp. nov., isolated from a tidal flat of the Yellow Sea in Korea. International Journal of Systematic and Evolutionary Microbiology 55, 885–889. https://doi.org/10.1099/ijs.0.63308-0

Kim, Y.B., Okuda, J., Matsumoto, C., Takahashi, N., Hashimoto, S., Nishibuchi, M., 1999. Identification of Vibrio parahaemolyticus strains at the species level by PCR targeted to the toxR gene. J Clin Microbiol 37, 1173–1177. https://doi.org/10.1128/JCM.37.4.1173-1177.1999

Kim, Y.-H., Min, S.-K., Zhang, X., Sillmann, J., Sandstad, M., 2020. Evaluation of the CMIP6 multi-model ensemble for climate extreme indices. Weather and Climate Extremes 29, 100269. https://doi.org/10.1016/j.wace.2020.100269

King, M., Rose, L., Fraimow, H., Nagori, M., Danish, M., Doktor, K., 2019. Vibrio vulnificus infections from a previously nonendemic area. Annals of Internal Medicine 171, 520–521. https://doi.org/10.7326/L19-0133

Klontz, K.C., 1988. Syndromes of Vibrio vulnificus Infections. Annals of Internal Medicine 109, 318. https://doi.org/10.7326/0003-4819-109-4-318

Knabb, R.D., Rhome, J.R., Brown, D.P., 2023. Tropical Cyclone Report Hurricane Katrina 23-30 August 2005. National Hurricane Center.

Kuhn, M., 2021. caret: Classification and Regression Training.

Kuo, Y.L., Shieh, S.J., Chiu, H.Y., Lee, J.W., 2007. Necrotizing fasciitis caused by Vibrio vulnificus: Epidemiology, clinical findings, treatment and prevention. European Journal of Clinical Microbiology and Infectious Diseases 26, 785–792. https://doi.org/10.1007/s10096-007-0358-5

Kural, A.G., Chen, H., 2008. Conditions for a 5-log reduction of Vibrio vulnificus in oysters through high hydrostatic pressure treatment. International Journal of Food Microbiology 122, 180–187. https://doi.org/10.1016/j.ijfoodmicro.2007.11.074

Labreuche, Y., Lambert, C., Soudant, P., Boulo, V., Huvet, A., Nicolas, J.-L., 2006. Cellular and molecular hemocyte responses of the Pacific oyster, Crassostrea gigas, following bacterial infection with Vibrio aestuarianus strain 01/32. Microbes and Infection 8, 2715–2724. https://doi.org/10.1016/j.micinf.2006.07.020

Lake, I.R., Colón-González, F.J., Takkinen, J., Rossi, M., Sudre, B., Dias, J.G., Tavoschi, L., Joshi, A., Semenza, J.C., Nichols, G., Gomes Dias, J., Tavoschi, L., Joshi, A., Semenza, J.C., Nichols, G., 2019. Exploring Campylobacter seasonality across Europe using The European Surveillance System (TESSy), 2008 to 2016. Euro Surveillance 24. https://doi.org/10.2807/1560-7917.{ES}.2019.24.13.180028

Lamb, J.B., van de Water, J.A.J.M., Bourne, D.G., Altier, C., Hein, M.Y., Fiorenza, E.A., Abu, N., Jompa, J., Harvell, C.D., 2017. Seagrass ecosystems reduce exposure to bacterial pathogens of humans, fishes, and invertebrates. Science 355, 731–733. https://doi.org/10.1126/science.aal1956

Laskowski-Arce, M.A., Orth, K., 2008. Acanthamoeba castellanii promotes the survival of Vibrio parahaemolyticus. Applied and Environmental Microbiology 74, 7183–7188. https://doi.org/10.1128/AEM.01332-08

Le Roux, F., Wegner, K.M., Baker-Austin, C., Vezzulli, L., Osorio, C.R., Amaro, C., Ritchie, J.M., Defoirdt, T., Destoumieux-Garzón, D., Blokesch, M., Mazel, D., Jacq, A., Cava, F., Gram, L., Wendling, C.C., Strauch, E., Kirschner, A., Huehn, S., 2015. The emergence of Vibrio pathogens in Europe: Ecology, evolution and pathogenesis (Paris, 11-12 March 2015). Frontiers in Microbiology 6, 1–8. https://doi.org/10.3389/fmicb.2015.00830

Lehmann, A., Myrberg, K., Post, P., Chubarenko, I., Dailidiene, I., Hinrichsen, H.-H., Hüssy, K., Liblik, T., Meier, H.E.M., Lips, U., Bukanova, T., 2022. Salinity dynamics of the Baltic Sea. Earth System Dynamics 13, 373–392. https://doi.org/10.5194/esd-13-373-2022

Lehodey, P., Conchon, A., Senina, I., Domokos, R., Calmettes, B., Jouanno, J., Hernandez, O., Kloser, R., 2015. Optimization of a micronekton model with acoustic data. ICES Journal of Marine Science 72, 1399–1412. https://doi.org/10.1093/icesjms/fsu233

Lehodey, P., Murtugudde, R., Senina, I., 2010. Bridging the gap from ocean models to population dynamics of large marine predators: A model of mid-trophic functional groups. Progress in Oceanography 84, 69–84. https://doi.org/10.1016/j.pocean.2009.09.008

Leng, F., Lin, S., Wu, W., Zhang, J., Song, J., Zhong, M., 2019. Epidemiology, pathogenetic mechanism, clinical characteristics, and treatment of Vibrio

vulnificus infection: a case report and literature review. European Journal of Clinical Microbiology and Infectious Diseases 38, 1999–2004. https://doi.org/10.1007/s10096-019-03629-5

Leonelli, S., Tempini, N., 2021. Where health and environment meet: the use of invariant parameters in big data analysis. Synthese 198, 2485–2504. https://doi.org/10.1007/s11229-018-1844-2

Letchumanan, V., Yin, W.F., Lee, L.H., Chan, K.G., 2015. Prevalence and antimicrobial susceptibility of Vibrio parahaemolyticus isolated from retail shrimps in Malaysia. Frontiers in Microbiology 6, 1–11. https://doi.org/10.3389/fmicb.2015.00033

Levin, S.A., 1992. The Problem of Pattern and Scale in Ecology: The Robert H. MacArthur Award Lecture. Ecology 73, 1943–1967. https://doi.org/10.2307/1941447

Levine, W.C., Griffin, P.M., 1993. Vibrio infections on the Gulf Coast: results of first year of regional surveillance. Gulf Coast Vibrio Working Group. J Infect Dis 167, 479–483. https://doi.org/10.1093/infdis/167.2.479

Li, H., Qiao, G., Li, Q., Zhou, W., Won, K.M., Xu, D.-H., Park, S.-I., 2010. Biological characteristics and pathogenicity of a highly pathogenic Shewanella marisflavi infecting sea cucumber, Apostichopus japonicus. Journal of Fish Diseases 33, 865–877. https://doi.org/10.1111/j.1365-2761.2010.01189.x

Li, Xinyao, Wu, Y., Sun, X., Ma, J., Li, Xiaofeng, Liu, C., Xie, H., 2020. Non-O1/non-O139 Vibrio cholerae bacteraemia in mainland China from 2005 to 2019: clinical, epidemiological and genetic characteristics. Epidemiology and Infection 148, e186. https://doi.org/10.1017/S0950268820001545

Lin, B., Wang, Z., Malanoski, A.P., O'Grady, E.A., Wimpee, C.F., Vuddhakul, V., Alves Jr, N., Thompson, F.L., Gomez-Gil, B., Vora, G.J., 2010. Comparative genomic analyses identify the Vibrio harveyi genome sequenced strains BAA-1116 and HY01 as Vibrio campbellii. Environmental Microbiology Reports 2, 81–89. https://doi.org/10.1111/j.1758-2229.2009.00100.x

Lindsey, R., 2017. How El Niño and La Niña affect the winter jet stream and U.S. climate [WWW Document]. URL http://www.climate.gov/news-features/featured-

images/how-el-ni%C3%B1o-and-la-ni%C3%B1a-affect-winter-jet-stream-and-us-climate (accessed 6.8.23).

Lipp, E.K., Rodriguez-Palacios, C., Rose, J.B., 2001. Occurrence and distribution of the human pathogen Vibrio vulnificus in a subtropical Gulf of Mexico estuary. Hydrobiologia 460, 165–173. https://doi.org/10.1023/A:1013127517860

Liu, C., Lu, J., Su, Y.C., 2009. Effects of flash freezing, followed by frozen storage, on reducing Vibrio parahaemolyticus in pacific raw oysters (Crassostrea gigas). Journal of Food Protection 72, 174–177. https://doi.org/10.4315/0362-028X-72.1.174

Liu, W., Xie, S.-P., Liu, Z., Zhu, J., 2017. Overlooked possibility of a collapsed Atlantic Meridional Overturning Circulation in warming climate. Science Advances 3, e1601666. https://doi.org/10.1126/sciadv.1601666

Logar-Henderson, C., Ling, R., Tuite, A.R., Fisman, D.N., 2019. Effects of large-scale oceanic phenomena on non-cholera vibriosis incidence in the United States: implications for climate change. Epidemiol. Infect. 147, e243. https://doi.org/10.1017/S0950268819001316

López-Cortés, A., Schumann, P., Pukall, R., Stackebrandt, E., 2006. Exiguobacterium mexicanum sp. nov. and Exiguobacterium artemiae sp. nov., isolated from the brine shrimp Artemia franciscana. Syst Appl Microbiol 29, 183–190. https://doi.org/10.1016/j.syapm.2005.09.007

Luk, S.Y., Hoagland, P., Rheuban, J.E., Costa, J.E., Doney, S.C., 2019. Modeling the effect of water quality on the recreational shellfishing cultural ecosystem service of Buzzards Bay, Massachusetts. Marine Pollution Bulletin 140, 364–373. https://doi.org/10.1016/j.marpolbul.2018.12.047

Luo, P., Hu, C., 2008. Vibrio alginolyticus gyrB sequence analysis and gyrB-targeted PCR identification in environmental isolates. Dis Aquat Organ 82, 209–216. https://doi.org/10.3354/dao01984

Mahmud, Z.H., Neogi, S.B., Kassu, A., Wada, T., Islam, M.S., Nair, G.B., Ota, F., 2007. Seaweeds as a reservoir for diverse Vibrio parahaemolyticus populations in Japan. International Journal of Food Microbiology 118, 92–96. https://doi.org/10.1016/j.ijfoodmicro.2007.05.009

Main, C.R., Salvitti, L.R., Whereat, E.B., Coyne, K.J., 2015. Community-Level and species-specific associations between phytoplankton and particle-associated Vibrio species in delaware's inland bays. Applied and Environmental Microbiology 81, 5703–5713. https://doi.org/10.1128/AEM.00580-15

Mälzer, H.-J., aus der Beek, T., Müller, S., Gebhardt, J., 2016. Comparison of different model approaches for a hygiene early warning system at the lower Ruhr River, Germany. International Journal of Hygiene and Environmental Health, Safe Ruhr 219, 671–680. https://doi.org/10.1016/j.ijheh.2015.06.005

Marion, G.M., Millero, F.J., Camões, M.F., Spitzer, P., Feistel, R., Chen, C.-T.A., 2011. pH of seawater. Marine Chemistry 126, 89–96. https://doi.org/10.1016/j.marchem.2011.04.002

Marti, E., Variatza, E., Balcazar, J.L., 2014. The role of aquatic ecosystems as reservoirs of antibiotic resistance. Trends Microbiol 22, 36–41. https://doi.org/10.1016/j.tim.2013.11.001

Martinez-Urtaza, J., Huapaya, B., Gavilan, R.G., Blanco-Abad, V., Ansede-Bermejo, J., Cadarso-Suarez, C., Figueiras, A., Trinanes, J., 2008. Emergence of asiatic vibrio diseases in south america in phase with El Niño. Epidemiology 19, 829–837. https://doi.org/10.1097/EDE.0b013e3181883d43

Martinez-Urtaza, J., Trinanes, J., Gonzalez-Escalona, N., Baker-Austin, C., 2016. Is El Niño a long-distance corridor for waterborne disease? Nature Microbiology 1, 1–3. https://doi.org/10.1038/nmicrobiol.2016.18

Matz, C., McDougald, D., Moreno, A.M., Yung, P.Y., Yildiz, F.H., Kjelleberg, S., 2005. Biofilm formation and phenotypic variation enhance predation-driven persistence of Vibrio cholerae. Proceedings of the National Academy of Sciences of the United States of America 102, 16819–16824. https://doi.org/10.1073/pnas.0505350102

Mayry, J., Mac, R., Huynh, M., Mitra, S., 2022. Development of a Low-Cost Lateral Flow Assay for Rapid Detection of Vibrio Cholerae. Meet. Abstr. MA2022-01, 2190. https://doi.org/10.1149/MA2022-01532190mtgabs

McDougald, D., Rice, S.A., Weichart, D., Kjelleberg, S., 1998. Nonculturability: Adaptation or debilitation? FEMS Microbiology Ecology 25, 1–9. https://doi.org/10.1016/S0168-6496(97)00063-9

McLaughlin, J.B., DePaola, M.P.H., Bopp, C.A., Martinek, K.A., Napolilli, N.P., Allison, C.G., Murray, S.L., Thompson, E.C., Bird, M.M., Middaugh, J.P., 2005. Outbreak of Vibrio parahaemolyticus Gastroenteritis Associated with Alaskan Oysters. The New England Journal of Medicine 353, 1463–1470. https://doi.org/10.1056/NEJMoa051594

Merkel, S.M., Alexander, S., Zufall, E., Oliver, J.D., Huet-hudson, Y.M., 2001. Essential Role for Estrogen in Protection against. Society 69, 6119–6122. https://doi.org/10.1128/IAI.69.10.6119

Miles, D.W., Ross, T., Olley, J., McMeekin, T.A., 1997. Development and evaluation of a predictive model for the effect of temperature and water activity on the growth rate of Vibrio parahaemolyticus. International Journal of Food Microbiology 38, 133–142. https://doi.org/10.1016/S0168-1605(97)00100-1

Miles, M.V.P., Alexander, K.M., Wright, K.C., Miller, R.P., Lindsey, L.J., Burkett, J.L., Kahn, S.A., 2023. Vibrio vulnificus Soft Tissue Infections in the Southern Gulf Coast Region. Am Surg 89, 147–149. https://doi.org/10.1177/0003134820951500

Moisen, G., Freeman, E., 2008. PresenceAbsence: An R Package for Presence Absence Analysis. Journal of Statistical Software 23.

Mora, C., McKenzie, T., Gaw, I.M., Dean, J.M., von Hammerstein, H., Knudson, T.A., Setter, R.O., Smith, C.Z., Webster, K.M., Patz, J.A., Franklin, E.C., 2022. Over half of known human pathogenic diseases can be aggravated by climate change. Nat. Clim. Chang. 12, 869–875. https://doi.org/10.1038/s41558-022-01426-1

Morgan, D., Ozanne-Smith, J., 2013. Identification of observed factors that predict bather water-immersions at beaches. Ocean & Coastal Management 84, 180–183. https://doi.org/10.1016/j.ocecoaman.2013.08.006

Motes, M.L., DePaola, A., Cook, D.W., Veazey, J.E., Hunsucker, J.C., Garthright, W.E., Blodgett, R.J., Chirtel, S.J., 1998. Influence of water temperature and salinity on Vibrio vulnificus in Northern Gulf and Atlantic Coast oysters (Crassostrea

virginica). Applied and Environmental Microbiology 64, 1459–1465. https://doi.org/10.1128/{AEM}.64.4.1459-1465.1998

Mougin, J., Flahaut, C., Roquigny, R., Bonnin-Jusserand, M., Grard, T., Le Bris, C., 2020. Rapid Identification of Vibrio Species of the Harveyi Clade Using MALDI-TOF MS Profiling With Main Spectral Profile Database Implemented With an In-House Database: Luvibase. Frontiers in Microbiology 11.

Moussa, M., Cauvin, E., Le Piouffle, A., Lucas, O., Bidault, A., Paillard, C., Benoit, F., Thuillier, B., Treilles, M., Travers, M.A., Garcia, C., 2021. A MALDI-TOF MS database for fast identification of Vibrio spp. potentially pathogenic to marine mollusks. Appl Microbiol Biotechnol 105, 2527–2539. https://doi.org/10.1007/s00253-021-11141-0

Muñoz Sabater, J., 2019. ERA5-Land hourly data from 1950 to present. https://doi.org/10.24381/cds.e2161bac

Murage, P., Hajat, S., Kovats, R.S., 2017. Effect of night-time temperatures on cause and age-specific mortality in London. Environ Epidemiol 1, e005. https://doi.org/10.1097/EE9.0000000000000005

Nalin, D.R., Daya, V., Reid, A., Levine, M.M., Cisneros, L., 1979. Adsorption and growth of Vibrio cholerae on chitin. Infection and Immunity 25, 768–770. https://doi.org/10.1128/iai.25.2.768-770.1979

National Centers for Coastal Ocean Science (NCCOS), 2021. Phytoplankton Monitoring Network: 20 Years of Citizen Science and Still Growing (Video) [WWW Document]. NCCOS Coastal Science Website. URL https://coastalscience.noaa.gov/news/phytoplankton-monitoring-network-20-years-of-citizen-science-and-still-growing/ (accessed 8.30.23).

NCDHHS, 2023. NCDHHS Urges Caution After Three Deaths Due to Vibrio this Summer | NCDHHS [WWW Document]. URL https://www.ncdhhs.gov/news/press-releases/2023/07/28/ncdhhs-urges-caution-after-three-deaths-due-vibrio-summer (accessed 9.3.23).

Neogi, S.B., Koch, B.P., Schmitt-Kopplin, P., Pohl, C., Kattner, G., Yamasaki, S., Lara, R.J., 2011. Biogeochemical controls on the bacterial populations in the eastern Atlantic Ocean. Biogeosciences 8, 3747–3759. https://doi.org/b

Neumann, B., Vafeidis, A.T., Zimmermann, J., Nicholls, R.J., 2015. Future coastal population growth and exposure to sea-level rise and coastal flooding--a global assessment. Plos One 10, e0118571. https://doi.org/10.1371/journal.pone.0118571

Newton, A., Kendall, M., Vugia, D.J., Henao, O.L., Mahon, B.E., 2012. Increasing rates of vibriosis in the United States, 1996-2010: Review of surveillance data from 2 systems. Clinical Infectious Diseases 54, 391–395. https://doi.org/10.1093/cid/cis243

Nigro, O.D., Hou, A., Vithanage, G., Fujioka, R.S., Steward, G.F., 2011. Temporal and spatial variability in culturable pathogenic Vibrio spp. in Lake Pontchartrain, Louisiana, following hurricanes Katrina and Rita. Applied and Environmental Microbiology 77, 5384–5393. https://doi.org/10.1128/{AEM}.02509-10

Nigro, O.D., Steward, G.F., 2015. Differential specificity of selective culture media for enumeration of pathogenic vibrios: Advantages and limitations of multi-plating methods. Journal of Microbiological Methods 111, 24–30. https://doi.org/10.1016/j.mimet.2015.01.014

Nijdam, D., Rood, T., Westhoek, H., 2012. The price of protein: Review of land use and carbon footprints from life cycle assessments of animal food products and their substitutes. Food Policy 37, 760–770. https://doi.org/10.1016/j.foodpol.2012.08.002

Nishibuchi M, Kaper J B, 1985. Nucleotide sequence of the thermostable direct hemolysin gene of Vibrio parahaemolyticus. Journal of Bacteriology 162, 558–564. https://doi.org/10.1128/jb.162.2.558-564.1985

NOAA, 2023a. NOAA predicts a near-normal 2023 Atlantic hurricane season [WWW Document]. URL https://www.noaa.gov/news-release/2023-atlantic-hurricane-season-outlook (accessed 5.8.23).

NOAA, 2023b. Assessing the Global Climate in July 2023 [WWW Document]. National Centers for Environmental Information (NCEI). URL https://www.ncei.noaa.gov/news/global-climate-202307 (accessed 9.3.23).

NOAA, 2022. Commercial Shellfish Aquaculture on the West Coast | NOAA Fisheries [WWW Document]. URL https://www.fisheries.noaa.gov/west-

coast/aquaculture/commercial-shellfish-aquaculture-west-coast (accessed 8.17.23).

Noorian, P., Hoque, M.M., Espinoza-Vergara, G., McDougald, D., 2023. Environmental Reservoirs of Pathogenic Vibrio spp. and Their Role in Disease: The List Keeps Expanding, in: Almagro-Moreno, S., Pukatzki, S. (Eds.), Vibrio Spp. Infections, Advances in Experimental Medicine and Biology. Springer International Publishing, Cham, pp. 99–126. https://doi.org/10.1007/978-3-031-22997-8_6

Norel, M., Kałczyński, M., Pińskwar, I., Krawiec, K., Kundzewicz, Z.W., 2021. Climate Variability Indices—A Guided Tour. Geosciences 11, 128. https://doi.org/10.3390/geosciences11030128

Nowakowska, J., Oliver, J.D., 2013. Resistance to environmental stresses by Vibrio vulnificus in the viable but nonculturable state. FEMS Microbiology Ecology 84, 213–222. https://doi.org/10.1111/1574-6941.12052

Oberbeckmann, S., Fuchs, B.M., Meiners, M., Wichels, A., Wiltshire, K.H., Gerdts, G., 2012. Seasonal Dynamics and Modeling of a Vibrio Community in Coastal Waters of the North Sea. Microbial Ecology 63, 543–551. https://doi.org/10.1007/s00248-011-9990-9

Oberbeckmann, S., Wichels, A., Wiltshire, K.H., Gerdts, G., 2011. Occurrence of Vibrio parahaemolyticus and Vibrio alginolyticus in the German Bight over a seasonal cycle. Antonie van Leeuwenhoek, International Journal of General and Molecular Microbiology 100, 291–307. https://doi.org/10.1007/s10482-011-9586-x

Okada, K., Iida, T., Kita-Tsukamoto, K., Honda, T., 2005. Vibrios commonly possess two chromosomes. Journal of Bacteriology 187, 752–757. https://doi.org/10.1128/JB.187.2.752-757.2005

Oliver, J.D., 2015. The Biology of Vibrio vulnificus. Microbiology Spectrum 3, 1–10. https://doi.org/10.1128/microbiolspec.ve-0001-2014

Oliver, J.D., 2013. Vibrio vulnificus: Death on the Half Shell. A Personal Journey with the Pathogen and its Ecology. Microbial Ecology 65, 793–799. https://doi.org/10.1007/s00248-012-0140-9

Oliver, J.D., 2005a. The viable but nonculturable state in bacteria. Journal of Microbiology 43 Spec No, 93–100.

Oliver, J.D., 2005b. The viable but non-culturable state in the human pathogen Vibrio vulnificus. Journal of Microbiology 43, 93–100.

Oliver, J.D., 2005c. Wound infections caused by Vibrio vulnificus and other marine bacteria. Epidemiology and Infection 133, 383–391. https://doi.org/10.1017/S0950268805003894

Oliver, J.D., Nilsson, L., Kjelleberg, S., 1991. Formation of nonculturable Vibrio vulnificus cells and its relationship to the starvation state. Applied and Environmental Microbiology 57, 2640–2644. https://doi.org/10.1128/aem.57.9.2640-2644.1991

O'Neill, B.C., Kriegler, E., Riahi, K., Ebi, K.L., Hallegatte, S., Carter, T.R., Mathur, R., van Vuuren, D.P., 2014. A new scenario framework for climate change research: The concept of shared socioeconomic pathways. Climatic Change 122, 387–400. https://doi.org/10.1007/s10584-013-0905-2

Orihuela-Pinto, B., England, M.H., Taschetto, A.S., 2022. Interbasin and interhemispheric impacts of a collapsed Atlantic Overturning Circulation. Nat. Clim. Chang. 12, 558–565. https://doi.org/10.1038/s41558-022-01380-y

Osorio, C.R., Vences, A., Matanza, X.M., Terceti, M.S., 2018. Photobacterium damselae subsp. damselae, a generalist pathogen with unique virulence factors and high genetic diversity. J Bacteriol 200, e00002-00018. https://doi.org/10.1128/JB.00002-18

Ou, T.Y., Liu, J.W., Leu, H.S., 2003. Independent prognostic factors for fatality in patients with invasive Vibrio cholerae non-O1 infections. Journal of Microbiology, Immunology and Infection 36, 117–122.

Park, S., Kim, I.K., Kim, W., Yoon, J.-H., 2020. Shewanella insulae sp. nov., isolated from a tidal flat. Int J Syst Evol Microbiol 70, 3872–3877. https://doi.org/10.1099/ijsem.0.004252

Parveen, S., Hettiarachchi, K.A., Bowers, J.C., Jones, J.L., Tamplin, M.L., McKay, R., Beatty, W., Brohawn, K., Dasilva, L.V., DePaola, A., 2008. Seasonal distribution of total and pathogenic Vibrio parahaemolyticus in Chesapeake Bay oysters and waters. International Journal of Food Microbiology 128, 354–361. https://doi.org/10.1016/j.ijfoodmicro.2008.09.019

Parveen, S., Jacobs, J., Ozbay, G., Chintapenta, L.K., Almuhaideb, E., Meredith, J., Ossai, S., Abbott, A., Grant, A., Brohawn, K., Chigbu, P., Richards, G.P., 2020. Seasonal and Geographical Differences in Total and Pathogenic Vibrio parahaemolyticus and Vibrio vulnificus Levels in Seawater and Oysters from the Delaware and Chesapeake Bays Determined Using Several Methods. Appl Environ Microbiol 86, e01581-20. https://doi.org/10.1128/AEM.01581-20

Payne, S.M., Mey, A.R., Wyckoff, E.E., 2016. Vibrio Iron Transport: Evolutionary Adaptation to Life in Multiple Environments. Microbiology and Molecular Biology Reviews 80, 69–90. https://doi.org/10.1128/mmbr.00046-15

Paz, S., Bisharat, N., Paz, E., Kidar, O., Cohen, D., 2007. Climate change and the emergence of Vibrio vulnificus disease in Israel. Environmental Research 103, 390–396. https://doi.org/10.1016/j.envres.2006.07.002

Pezzlo, M., Valter, P.J., Burns, M.J., 1979. Wound infection associated with Vibrio alginolyticus. American Journal of Clinical Pathology 71, 476–478. https://doi.org/10.1093/ajcp/71.4.476

Pfeffer, C.S., Hite, F.M., Oliver, J.D., 2003. Ecology of Vibrio vulnificus in estuarine waters of eastern North Carolina. Applied and Environmental Microbiology 69, 3526–3531. https://doi.org/10.1128/AEM.69.6.3526-3531.2003

Phuvasate, S., Chen, M.H., Su, Y.C., 2012. Reductions of Vibrio parahaemolyticus in Pacific oysters (Crassostrea gigas) by depuration at various temperatures. Food Microbiology 31, 51–56. https://doi.org/10.1016/j.fm.2012.02.004

Powell, A., Baker-Austin, C., Wagley, S., Bayley, A., Hartnell, R., 2013. Isolation of Pandemic Vibrio parahaemolyticus from UK Water and Shellfish Produce. Microbial Ecology 65, 924–927. https://doi.org/10.1007/s00248-013-0201-8

Prado, S., Dubert, J., da Costa, F., Martínez-Patiño, D., Barja, J.L., 2014. Vibrios in hatchery cultures of the razor clam, Solen marginatus (Pulteney). Journal of Fish Diseases 37, 209–217. https://doi.org/10.1111/jfd.12098

Pruzzo, C., Gallo, G., Canesi, L., 2005. Persistence of vibrios in marine bivalves: The role of interactions with haemolymph components. Environmental Microbiology 7, 761–772. https://doi.org/10.1111/j.1462-2920.2005.00792.x

Pruzzo, C., Vezzulli, L., Colwell, R.R., 2008. Global impact of Vibrio cholerae interactions with chitin. Environmental Microbiology 10, 1400–1410. https://doi.org/10.1111/j.1462-2920.2007.01559.x

Public Health Agency of Sweden, 2023. Vibrioinfektioner – sjukdomsstatistik [WWW Document]. URL https://www.folkhalsomyndigheten.se/folkhalsorapportering-statistik/statistik-a-o/sjukdomsstatistik/vibrioinfektioner/ (accessed 9.23.23).

Public Health Agency of Sweden, 2019. Vibrioinfektioner – sjukdomsstatistik [WWW Document]. URL https://www.folkhalsomyndigheten.se/folkhalsorapportering-statistik/statistik-a-o/sjukdomsstatistik/vibrioinfektioner/?t=county&base=domestic (accessed 11.25.19).

Pujalte, M.-J., Ortigosa, M., Urdaci, M.-C., Garay, E., Grimont, P.A.D., 1993. Vibrio mytili sp. nov., from Mussels. International Journal of Systematic and Evolutionary Microbiology 43, 358–362. https://doi.org/10.1099/00207713-43-2-358

Quinn, T.P., Le, V., Cardilini, A.P.A., 2021. Test set verification is an essential step in model building. Methods in Ecology and Evolution 12, 127–129. https://doi.org/10.1111/2041-210X.13495

R Core Team, 2022. R: A Language and Environment for Statistical Computing.

R Core Team, 2021. R: A Language and Environment for Statistical Computing.

Ralston, E.P., Kite-Powell, H., Beet, A., 2011. An estimate of the cost of acute health effects from food- and water-borne marine pathogens and toxins in the USA. Journal of Water and Health 9, 680–694. https://doi.org/10.2166/wh.2011.157

Ramirez, M., Domínguez-Borbor, C., Salazar, L., Debut, A., Vizuete, K., Sonnenholzner, S., Alexis, F., Rodríguez, J., 2022. The probiotics Vibrio diabolicus (Ili), Vibrio hepatarius (P62), and Bacillus cereus sensu stricto (P64) colonize internal and external surfaces of Penaeus vannamei shrimp larvae and protect it against Vibrio parahaemolyticus. Aquaculture 549, 737826. https://doi.org/10.1016/j.aquaculture.2021.737826

Ramírez Villegas, J., Jarvis, A., 2010. Downscaling Global Circulation Model Outputs: The Delta Method Decision and Policy Analysis Working Paper No. 1 (Working Paper). International Center for Tropical Agriculture.

Randa, M.A., Polz, M.F., Lim, E., 2004. Effects of Temperature and Salinity on Vibrio vulnificus Population Dynamics as Assessed by Quantitative PCR. Applied and Environmental Microbiology 70, 5469 LP – 5476. https://doi.org/10.1128/AEM.70.9.5469-5476.2004

Raszl, S.M., Froelich, B.A., Vieira, C.R.W.W., Blackwood, A.D., Noble, R.T., 2016. Vibrio parahaemolyticus and Vibrio vulnificus in South America: water, seafood and human infections. Journal of Applied Microbiology 121, 1201–1222. https://doi.org/10.1111/jam.13246

Reilly, G.D., Reilly, C.A., Smith, E.G., Baker-Austin, C., 2011. Vibrio alginolyticus-associated wound infection acquired in British waters, Guernsey, July 2011. Eurosurveillance 16, 3. https://doi.org/10.2807/ese.16.42.19994-en

Reusch, T.B.H., Schubert, P.R., Marten, S.-M., Gill, D., Karez, R., Busch, K., Hentschel, U., 2021. Lower Vibrio spp. abundances in Zostera marina leaf canopies suggest a novel ecosystem function for temperate seagrass beds. Mar Biol 168, 149. https://doi.org/10.1007/s00227-021-03963-3

Reverter, M., Sarter, S., Caruso, D., Avarre, J.-C., Combe, M., Pepey, E., Pouyaud, L., Vega-Heredía, S., de Verdal, H., Gozlan, R.E., 2020. Aquaculture at the crossroads of global warming and antimicrobial resistance. Nat Commun 11, 1870. https://doi.org/10.1038/s41467-020-15735-6

Rhoads, J., 2006. Post-Hurricane Katrina challenge: Vibrio vulnificus. Journal of the American Academy of Nurse Practitioners 18, 318–324. https://doi.org/10.1111/j.1745-7599.2006.00139.x

Riahi, K., van Vuuren, D.P., Kriegler, E., Edmonds, J., O'Neill, B.C., Fujimori, S., Bauer, N., Calvin, K., Dellink, R., Fricko, O., Lutz, W., Popp, A., Cuaresma, J.C., KC, S., Leimbach, M., Jiang, L., Kram, T., Rao, S., Emmerling, J., Ebi, K., Hasegawa, T., Havlik, P., Humpenöder, F., Da Silva, L.A., Smith, S., Stehfest, E., Bosetti, V., Eom, J., Gernaat, D., Masui, T., Rogelj, J., Strefler, J., Drouet, L., Krey, V., Luderer, G., Harmsen, M., Takahashi, K., Baumstark, L., Doelman, J.C., Kainuma, M., Klimont, Z., Marangoni, G., Lotze-Campen, H., Obersteiner, M., Tabeau, A., Tavoni, M., 2017. The Shared Socioeconomic Pathways and their energy, land use, and greenhouse gas emissions implications: An overview.

Global Environmental Change 42, 153–168. https://doi.org/10.1016/j.gloenvcha.2016.05.009

Rippey, S.R., 1994. Infectious diseases associated with molluscan shellfish consumption. Clinical Microbiology Reviews 7, 419–425. https://doi.org/10.1128/CMR.7.4.419

Rivas, A., Lemos, M., Osorio, C., 2013. Photobacterium damselae subsp. damselae, a bacterium pathogenic for marine animals and humans. Frontiers in Microbiology 4.

Robin, X., Turck, N., Hainard, A., Tiberti, N., Lisacek, F., Sanchez, J.-C., Müller, M., 2011. pROC: an open-source package for R and S+ to analyze and compare ROC curves. BMC Bioinformatics 12, 77. https://doi.org/10.1186/1471-2105-12-77

Robinson, L.M., Elith, J., Hobday, A.J., Pearson, R.G., Kendall, B.E., Possingham, H.P., Richardson, A.J., 2011. Pushing the limits in marine species distribution modelling: lessons from the land present challenges and opportunities. Global Ecology and Biogeography 20, 789–802. https://doi.org/10.1111/j.1466-8238.2010.00636.x

Rojas, R., Blanco-Hortas, A., Kehlet-Delgado, H., Lema, A., Miranda, C.D., Romero, J., Martínez, P., Barja, J.L., Dubert, J., 2021. First description outside Europe of the emergent pathogen Vibrio europaeus in shellfish aquaculture. Journal of Invertebrate Pathology 180, 107542. https://doi.org/10.1016/j.jip.2021.107542

Rong, R., Lin, H., Wang, J., Khan, M.N., Li, M., 2014. Reductions of Vibrio parahaemolyticus in oysters after bacteriophage application during depuration. Aquaculture 418–419, 171–176. https://doi.org/10.1016/j.aquaculture.2013.09.028

Roszak, D.B., Colwell, R.R., 1987. Survival strategies of bacteria in the natural environment. Microbiological reviews 51, 365–379.

Ruppert, J., Panzig, B., Guertler, L., Hinz, P., Schwesinger, G., Felix, S.B., Friesecke, S., 2004. Two cases of severe sepsis due to Vibrio vulnificus wound infection acquired in the Baltic Sea. European Journal of Clinical Microbiology and Infectious Diseases 23, 912–915. https://doi.org/10.1007/s10096-004-1241-2

Sajja, K.C., Mohan, D.P., Rockey, D.C., 2014. Age and ethnicity in cirrhosis. Journal of investigative medicine : the official publication of the American Federation for Clinical Research 62, 920–926. https://doi.org/10.1097/JIM.0000000000000106

Sakihara, E., Noge, I., Suzuyama, H., Takeoka, H., Nabeshima, S., 2023. Vibrio vulnificus sepsis after shrimp shelling in a patient with preexisting primary biliary cholangitis: a case report. J Med Case Rep 17, 27. https://doi.org/10.1186/s13256-023-03767-7

Scaglione, S., Kliethermes, S., Cao, G., Shoham, D., Durazo, R., Luke, A., Volk, M.L., 2015. The epidemiology of cirrhosis in the United States a population-based study. Journal of Clinical Gastroenterology 49, 690–696. https://doi.org/10.1097/MCG.0000000000000208

Schets, F.M., Berg, H.H.J.L. van den, Demeulmeester, A.A., Dijk, E. van, Rutjes, S.A., Hooijdonk, H.J.P. van, Husman, A.M. de R., 2006. Vibrio alginolyticus infections in the Netherlands after swimming in the North Sea. Weekly releases (1997–2007) 11, 3077. https://doi.org/10.2807/esw.11.45.03077-en

Schets, F.M., van den Berg, H.H.J.L.J.L., Marchese, A., Garbom, S., de Roda Husman, A.M., 2011. Potentially human pathogenic vibrios in marine and fresh bathing waters related to environmental conditions and disease outcome. International Journal of Hygiene and Environmental Health 214, 399–406. https://doi.org/10.1016/j.ijheh.2011.05.003

Schulzweida, U., 2019. CDO User Guide (1.9.8). https://doi.org/10.5281/zenodo.7112925

Schütt, E.M., Hundsdörfer, M.A.J., von Hoyningen-Huene, A.J.E., Lange, X., Koschmider, A., Oppelt, N., 2023. First Steps towards a near Real-Time Modelling System of Vibrio vulnificus in the Baltic Sea. International Journal of Environmental Research and Public Health 20, 5543. https://doi.org/10.3390/ijerph20085543

Séférian, R., Nabat, P., Michou, M., Saint-Martin, D., Voldoire, A., Colin, J., Decharme, B., Delire, C., Berthet, S., Chevallier, M., Sénési, S., Franchisteguy, L., Vial, J., Mallet, M., Joetzjer, E., Geoffroy, O., Guérémy, J.-F., Moine, M.-P., Msadek, R., Ribes, A., Rocher, M., Roehrig, R., Salas-y-Mélia, D., Sanchez, E., Terray, L., Valcke, S., Waldman, R., Aumont, O., Bopp, L., Deshayes, J., Éthé, C., Madec,

G., 2019. Evaluation of CNRM Earth System Model, CNRM-ESM2-1: Role of Earth System Processes in Present-Day and Future Climate. Journal of Advances in Modeling Earth Systems 11, 4182–4227. https://doi.org/10.1029/2019MS001791

Seidel, J., Whiting, P.C., Edbrooke, D.L., 2006. The costs of intensive care. Continuing Education in Anaesthesia, Critical Care and Pain 6, 160–163. https://doi.org/10.1093/bjaceaccp/mkl030

Semenza, J.C., Trinanes, J., Lohr, W., Sudre, B., Löfdahl, M., Martinez-Urtaza, J., Nichols, G.L., Rocklöv, J., 2017. Environmental Suitability of Vibrio Infections in a Warming Climate: An Early Warning System. Environmental Health Perspectives 125, 107004. https://doi.org/10.1289/EHP2198

Semmler, T., Danilov, S., Gierz, P., Goessling, H.F., Hegewald, J., Hinrichs, C., Koldunov, N., Khosravi, N., Mu, L., Rackow, T., Sein, D.V., Sidorenko, D., Wang, Q., Jung, T., 2020. Simulations for CMIP6 With the AWI Climate Model AWI-CM-1-1. Journal of Advances in Modeling Earth Systems 12, e2019MS002009. https://doi.org/10.1029/2019MS002009

Semmler, T., Danilov, S., Rackow, T., Sidorenko, D., Barbi, D., Hegewald, J., Sein, D., Wang, Q., Jung, T., 2018. AWI AWI-CM1.1MR model output prepared for CMIP6 CMIP historical. Version 20201215. https://doi.org/10.22033/ESGF/CMIP6.2686

Shaw, K.S., Rosenberg Goldstein, R.E., He, X., Jacobs, J.M., Crump, B.C., Sapkota, A.R., 2014. Antimicrobial susceptibility of Vibrio vulnificus and Vibrio parahaemolyticus recovered from recreational and commercial areas of Chesapeake Bay and Maryland Coastal Bays. PLoS ONE 9, e89616. https://doi.org/10.1371/journal.pone.0089616

Sheahan, M., Gould, C.A., Neumann, J.E., Kinney, P.L., Hoffmann, S., Fant, C., Wang, X., Kolian, M., 2022. Examining the Relationship between Climate Change and Vibriosis in the United States: Projected Health and Economic Impacts for the 21st Century. Environ Health Perspect 130, 087007. https://doi.org/10.1289/EHP9999a

Sheikh, H.I., John, A., Musa, N., abdulrazzak, L.A., Alfatama, M., Fadhlina, A., 2022a. Vibrio spp. and Their Vibriocin as a Vibriosis Control Measure in Aquaculture.

Appl Biochem Biotechnol 194, 4477–4491. https://doi.org/10.1007/s12010-022-03919-3

Sheikh, H.I., Najiah, M., Fadhlina, A., Laith, A.A., Nor, M.M., Jalal, K.C.A., Kasan, N.A., 2022b. Temperature Upshift Mostly but not Always Enhances the Growth of Vibrio Species: A Systematic Review. Frontiers in Marine Science 9. https://doi.org/10.3389/fmars.2022.959830

Shikuma, N.J., Hadfield, M.G., 2010. Marine biofilms on submerged surfaces are a reservoir for Escherichia coli and Vibrio cholerae. Biofouling 26, 39–46. https://doi.org/10.1080/08927010903282814

Shinoda, S., 2011. Sixty years from the discovery of Vibrio parahaemolyticus and some recollections. Biocontrol Science. https://doi.org/10.4265/bio.16.129

Sodders, N., Stockdale, K., Baker, K., Ghanem, A., Vieth, B., Harder, T., 2023. Notes from the Field: Vibriosis Cases Associated with Flood Waters During and After Hurricane Ian — Florida, September–October 2022. MMWR Morb Mortal Wkly Rep 72, 497–498. https://doi.org/10.15585/mmwr.mm7218a5

Sohrabi, H., Majidi, M.R., Khaki, P., Jahanban-Esfahlan, A., de la Guardia, M., Mokhtarzadeh, A., 2022. State of the art: Lateral flow assays toward the point-of-care foodborne pathogenic bacteria detection in food samples. Compr Rev Food Sci Food Saf 21, 1868–1912. https://doi.org/10.1111/1541-4337.12913

Srinivas, J., Pillai, M., Vinod, V., Dinesh, R.K., 2015. Skin and Soft Tissue Infections due to Shewanella algae – An Emerging Pathogen. J Clin Diagn Res 9, DC16–DC20. https://doi.org/10.7860/JCDR/2015/12152.5585

Sterk, A., Schets, F.M., Husman, A.M. de R., de Nijs, T., Schijven, J.F., 2015. Effect of Climate Change on the Concentration and Associated Risks of Vibrio Spp. in Dutch Recreational Waters. Risk Anal. 35, 1717–1729. https://doi.org/10.1111/risa.12365

Strom, M.S., Paranjpye, R.N., 2000. Epidemiology and pathogenesis of Vibrio vulnificus. Microbes and Infection 2, 177–188. https://doi.org/10.1016/S1286-4579(00)00270-7

Su, Y.C., Liu, C., 2007. Vibrio parahaemolyticus: A concern of seafood safety. Food Microbiology 24, 549–558. https://doi.org/10.1016/j.fm.2007.01.005

Svitil, A.L., Chadhain, S., Moore, J.A., Kirchman, D.L., Ní Chadhain, S.M., Moore, J.A., Kirchman, D.L., 1997. Chitin Degradation Proteins Produced by the Marine Bacterium Vibrio harveyi Growing on Different Forms of Chitin. Applied and Environmental Microbiology 63, 408–413. https://doi.org/10.1128/aem.63.2.408-413.1997

Swart, N.C., Cole, J.N.S., Kharin, V.V., Lazare, M., Scinocca, J.F., Gillett, N.P., Anstey, J., Arora, V., Christian, J.R., Hanna, S., Jiao, Y., Lee, W.G., Majaess, F., Saenko, O.A., Seiler, C., Seinen, C., Shao, A., Sigmond, M., Solheim, L., von Salzen, K., Yang, D., Winter, B., 2019. The Canadian Earth System Model version 5 (CanESM5.0.3). Geoscientific Model Development 12, 4823–4873. https://doi.org/10.5194/gmd-12-4823-2019

Symonds, M.R.E., Moussalli, A., 2011. A brief guide to model selection, multimodel inference and model averaging in behavioural ecology using Akaike's information criterion. Behavioral Ecology and Sociobiology 65, 13–21.

Tack, D.M., Ray, L., Griffin, P.M., Cieslak, P.R., Dunn, J., Rissman, T., Jervis, R., Lathrop, S., Muse, A., Duwell, M., Smith, K., Tobin-D'Angelo, M., Vugia, D.J., Zablotsky Kufel, J., Wolpert, B.J., Tauxe, R., Payne, D.C., 2020. Preliminary Incidence and Trends of Infections with Pathogens Transmitted Commonly Through Food - Foodborne Diseases Active Surveillance Network, 10 U.S. Sites, 2016-2019. MMWR. Morbidity and mortality weekly report 69, 509–514. https://doi.org/10.15585/mmwr.mm6917a1

Takemura, A.F., Chien, D.M., Polz, M.F., 2014. Associations and dynamics of vibrionaceae in the environment, from the genus to the population level. Frontiers in Microbiology 5, 1–26. https://doi.org/10.3389/fmicb.2014.00038

Tantillo, G.M., Fontanarosa, M., Di Pinto, A., Musti, M., 2004. Updated perspectives on emerging vibrios associated with human infections. Letters in Applied Microbiology 39, 117–126. https://doi.org/10.1111/j.1472-765X.2004.01568.x

Tatebe, H., Ogura, T., Nitta, T., Komuro, Y., Ogochi, K., Takemura, T., Sudo, K., Sekiguchi, M., Abe, M., Saito, F., Chikira, M., Watanabe, S., Mori, M., Hirota, N., Kawatani, Y., Mochizuki, T., Yoshimura, K., Takata, K., O'ishi, R., Yamazaki, D., Suzuki, T., Kurogi, M., Kataoka, T., Watanabe, M., Kimoto, M., 2019. Description and basic evaluation of simulated mean state, internal variability, and climate

sensitivity in MIROC6. Geoscientific Model Development 12, 2727–2765. https://doi.org/10.5194/gmd-12-2727-2019

The CMIP6 landscape, 2019. . Nature Climate Change 9, 727. https://doi.org/10.1038/s41558-019-0599-1

Thickman, J.D., Gobler, C.J., 2017. The ability of algal organic matter and surface runoff to promote the abundance of pathogenic and non-pathogenic strains of Vibrio parahaemolyticus in Long Island Sound, USA. PLoS ONE 12, 1–17. https://doi.org/10.1371/journal.pone.0185994

Thompson, F.L., Iida, T., Swings, J., 2004. Biodiversity of vibrios. Microbiol Mol Biol Rev 68, 403–431, table of contents. https://doi.org/10.1128/MMBR.68.3.403-431.2004

Thompson, F.L., Thompson, C.C., Hoste, B., Vandemeulebroecke, K., Gullian, M., Swings, J., 2003. Vibrio fortis sp. nov. and Vibrio hepatarius sp. nov., isolated from aquatic animals and the marine environment. Int J Syst Evol Microbiol 53, 1495–1501. https://doi.org/10.1099/ijs.0.02658-0

Thompson, J.R., Randa, M.A., Marcelino, L.A., Tomita-Mitchell, A., Lim, E., Polz, M.F., 2004. Diversity and dynamics of a North Atlantic coastal Vibrio community. Applied and Environmental Microbiology 70, 4103–4110. https://doi.org/10.1128/AEM.70.7.4103-4110.2004

Tiwari, A., Oliver, D.M., Bivins, A., Sherchan, S.P., Pitkänen, T., 2021. Bathing Water Quality Monitoring Practices in Europe and the United States. Int J Environ Res Public Health 18, 5513. https://doi.org/10.3390/ijerph18115513

Toubiana, M., Fernandez, D., Filho, J.-E.M., Garnier, J., Castro, R.R. de, Bonnet, M.-P., Colwell, R.R., Monfort, P., 2019. Occurence of Vibrio parahaemolyticus, Vibrio vulnificus and Vibrio cholerae in the urbanized Guaraja bay, Amazonia, Brasil. Presented at the Vibrio 2019. The 8th biennial International Conference on the Biology of Vibrios.

Trinanes, J., Martinez-Urtaza, J., 2021. Future scenarios of risk of Vibrio infections in a warming planet: a global mapping study. The Lancet Planetary Health 5, e426–e435. https://doi.org/10.1016/S2542-5196(21)00169-8

Tseng, S.-Y., Liu, P.-Y., Lee, Y.-H., Wu, Z.-Y., Huang, C.-C., Cheng, C.-C., Tung, K.-C., 2018. The Pathogenicity of Shewanella algae and Ability to Tolerate a Wide Range of Temperatures and Salinities. Can J Infect Dis Med Microbiol 2018, 6976897. https://doi.org/10.1155/2018/6976897

Turner, J.W., Good, B., Cole, D., Lipp, E.K., 2009. Plankton composition and environmental factors contribute to Vibrio seasonality. ISME Journal 3, 1082–1092. https://doi.org/10.1038/ismej.2009.50

Turner, J.W., Malayil, L., Guadagnoli, D., Cole, D., Lipp, E.K., 2014. Detection of Vibrio parahaemolyticus, Vibrio vulnificus and Vibrio cholerae with respect to seasonal fluctuations in temperature and plankton abundance. Environmental Microbiology 16, 1019–1028. https://doi.org/10.1111/1462-2920.12246

Twedt, R.M., Spaulding, P.L., Hall, H.E., 1969. Morphological, cultural, biochemical, and serological comparison of Japanese strains of Vibrio parahemolyticus with related cultures isolated in the United States. J Bacteriol 98, 511–518. https://doi.org/10.1128/jb.98.2.511-518.1969

Uh, Y., Park, J.-S.S., Hwang, G.-Y.Y., Jang, I.-H.H., Yoon, K.-J.J., Park, H.-C.C., Hwang, S.-O.O., 2001. Vibrio alginolyticus acute gastroenteritis: report of two cases. Clinical Microbiology and Infection 7, 104–106. https://doi.org/10.1046/j.1469-0691.2001.00207.x

UK Health Security Agency, 2018. What is Whole Genome Sequencing? - UK Health Security Agency [WWW Document]. URL https://ukhsa.blog.gov.uk/2018/05/01/what-is-whole-genome-sequencing/ (accessed 11.20.23).

Ulitzur, S., 1974. Vibrio parahaemolyticus andVibrio alginolyticus: Short generation-time marine bacteria. Microb Ecol 1, 127–135. https://doi.org/10.1007/BF02512384

UN DESA, 2019. World population prospects 2019, United Nations. Department of Economic and Social Affairs. World Population Prospects 2019.

United Nations, 2016. Report of the Conference of the Parties on its twenty-first session, held in Paris from 30 November to 13 December 2015.

United Nations Department of Economic and Social Affairs, 2023. World Social Report 2023: Leaving No One Behind in an Ageing World, World Social Report. United Nations. https://doi.org/10.18356/9789210019682

United Nations, Department of Economic and Social Affairs, P.D., 2015. World Population Ageing 2015, World Population Ageing 2015 Report. United Nations, New York. https://doi.org/10.21615/cesp.12.1.3

United States Environmental Protection Agency, 2013. Impacts of Climate Change on the Occurrence of Harmful Algal Blooms.

Urbanczyk, Y., Ogura, Y., Hayashi, T., Urbanczyk, H., 2015. Description of a novel marine bacterium, Vibrio hyugaensis sp. nov., based on genomic and phenotypic characterization. Systematic and Applied Microbiology 38, 300–304. https://doi.org/10.1016/j.syapm.2015.04.001

Urkawa, H., Rivera, I.N.G., 2006. The Biology of Vibrios, in: Thompson, F.L., Austin, B., Swings, J.G. (Eds.), The Biology of Vibrios, Monograph, ASM Press. ASM Press, Washington, D.C.

U.S. Department of Agriculture (USDA), 2020. Economic Research Service (ERS). Cost Estimates of Foodborne Illnesses.

US Environmental Protection Agency, 2001. Protocol for Developing Pathogen TMDLs. EPA, U.S. Environmental Protection Agency, Office of Water (4503F). Washington, DC.

van Zyl, G.U., 2022. , in: Rezaei, N. (Ed.), Encyclopedia of Infection and Immunity. Elsevier, pp. 463–479.

Vasey, J., Jones, D., Deng, C.H., Hedderley, D., Martinez-Urtaza, J., Powell, A., Wang, J., Wright, J., Merien, A.-M.P., Fletcher, G.C., Vidovic, S., 2023. Comparative genomics uncovered differences between clinical and environmental populations of Vibrio parahaemolyticus in New Zealand. Microbial Genomics 9, 001037. https://doi.org/10.1099/mgen.0.001037

Velazquez-Roman, J., León-Sicairos, N., Hernandez-Diaz, L., Canizalez-Roman, A., 2014. Pandemic Vibrio parahaemolyticus O3:K6 on the American continent. Frontiers in Cellular and Infection Microbiology 3.

Velez, K.E.C., Leighton, R.E., Decho, A.W., Pinckney, J.L., Norman, R.S., 2023. Modeling pH and Temperature Effects as Climatic Hazards in Vibrio Vulnificus and Vibrio Parahaemolyticus Planktonic Growth and Biofilm Formation. GeoHealth 7, e2022GH000769. https://doi.org/10.1029/2022GH000769

Vellinga, M., Wood, R.A., 2002. Global Climatic Impacts of a Collapse of the Atlantic Thermohaline Circulation. Climatic Change 54, 251–267. https://doi.org/10.1023/A:1016168827653

Verschuere, L., Heang, H., Criel, G., Sorgeloos, P., Verstraete, W., 2000. Selected Bacterial Strains Protect Artemia spp. from the Pathogenic Effects of Vibrio proteolyticus CW8T2. Appl Environ Microbiol 66, 1139–1146.

Vezzulli, L., Baker-Austin, C., Kirschner, A., Pruzzo, C., Martinez-Urtaza, J., 2020. Global emergence of environmental non-O1/O139 Vibrio cholerae infections linked with climate change: a neglected research field? Environmental Microbiology 22, 4342–4355. https://doi.org/10.1111/1462-2920.15040

Vezzulli, L., Colwell, R.R., Pruzzo, C., 2013. Ocean Warming and Spread of Pathogenic Vibrios in the Aquatic Environment. Microbial Ecology 65, 817–825. https://doi.org/10.1007/s00248-012-0163-2

Vezzulli, L., Grande, C., Reid, P.C., Hélaouët, P., Edwards, M., Höfle, M.G., Brettar, I., Colwell, R.R., Pruzzo, C., 2016. Climate influence on Vibrio and associated human diseases during the past half-century in the coastal North Atlantic. Proceedings of the National Academy of Sciences of the United States of America 113, E5062–E5071. https://doi.org/10.1073/pnas.1609157113

Vezzulli, L., Pezzati, E., Brettar, I., Höfle, M., Pruzzo, C., 2015. Effects of Global Warming on Vibrio Ecology. https://doi.org/10.1128/microbiolspec.VE-0004-2014

Vezzulli, L., Pezzati, E., Moreno, M., Fabiano, M., Pane, L., Pruzzo, C., The VibrioSea Consortium, 2009. Benthic ecology of Vibrio spp. and pathogenic Vibrio species in a coastal Mediterranean environment (La Spezia Gulf, Italy). Microb Ecol 58, 808–818. https://doi.org/10.1007/s00248-009-9542-8

Vezzulli, L., Pruzzo, C., Huq, A., Colwell, R.R., 2010. Environmental reservoirs of Vibrio cholerae and their role in cholera. Environmental Microbiology Reports 2, 27–33. https://doi.org/10.1111/j.1758-2229.2009.00128.x

Voldoire, A., 2018. CNRM-CERFACS CNRM-CM6-1 model output prepared for CMIP6 CMIP. https://doi.org/10.22033/ESGF/CMIP6.1375

Voldoire, A., Saint-Martin, D., Sénési, S., Decharme, B., Alias, A., Chevallier, M., Colin, J., Guérémy, J.-F., Michou, M., Moine, M.-P., Nabat, P., Roehrig, R., Salas y Mélia, D., Séférian, R., Valcke, S., Beau, I., Belamari, S., Berthet, S., Cassou, C., Cattiaux, J., Deshayes, J., Douville, H., Ethé, C., Franchistéguy, L., Geoffroy, O., Lévy, C., Madec, G., Meurdesoif, Y., Msadek, R., Ribes, A., Sanchez-Gomez, E., Terray, L., Waldman, R., 2019. Evaluation of CMIP6 DECK Experiments With CNRM-CM6-1. Journal of Advances in Modeling Earth Systems 11, 2177–2213. https://doi.org/10.1029/2019MS001683

von Hammerstein, H., Setter, R.O., van Aswegen, M., Currie, J.J., Stack, S.H., 2022. High-Resolution Projections of Global Sea Surface Temperatures Reveal Critical Warming in Humpback Whale Breeding Grounds. Frontiers in Marine Science 9.

Wagley, S., Borne, R., Harrison, J., Baker-Austin, C., Ottaviani, D., Leoni, F., Vuddhakul, V., Titball, R.W., 2018. Galleria mellonella as an infection model to investigate virulence of Vibrio parahaemolyticus. Virulence 9, 197–207. https://doi.org/10.1080/21505594.2017.1384895

Wagley, S., Morcrette, H., Kovacs-Simon, A., Yang, Z.R., Power, A., Tennant, R.K., Love, J., Murray, N., Titball, R.W., Butler, C.S., 2021. Bacterial dormancy: A subpopulation of viable but non-culturable cells demonstrates better fitness for revival. {PLoS} Pathogens 17, e1009194. https://doi.org/10.1371/journal.ppat.1009194

Wang, B., Luo, X., Yang, Y.-M., Sun, W., Cane, M.A., Cai, W., Yeh, S.-W., Liu, J., 2019. Historical change of El Niño properties sheds light on future changes of extreme El Niño. Proceedings of the National Academy of Sciences 116, 22512–22517. https://doi.org/10.1073/pnas.1911130116

Wang, D., Zhang, D., Chen, W., Yu, S., Shi, X., 2010. Retention of Vibrio parahaemolyticus in oyster tissues after chlorine dioxide treatment. International Journal of Food Microbiology 137, 76–80. https://doi.org/10.1016/j.ijfoodmicro.2009.10.022

Wang, X., Zhang, H., Bertone, E., Stewart, R.A., Hughes, S.P., 2021. Coupled data-driven and process-based model for fluorescent dissolved organic matter

prediction in a shallow subtropical reservoir. Environmental Modelling & Software 141, 105053. https://doi.org/10.1016/j.envsoft.2021.105053

Warnock, E.W., MacMath, T.L., 1993. Primary vibrio vulnificus septicemia. Journal of Emergency Medicine 11, 153–156. https://doi.org/10.1016/0736-4679(93)90510-E

Warszawski, L., Frieler, K., Huber, V., Piontek, F., Serdeczny, O., Schewe, J., 2014. The Inter-Sectoral Impact Model Intercomparison Project (ISI–MIP): Project framework. Proc Natl Acad Sci USA 111, 3228. https://doi.org/10.1073/pnas.1312330110

Washington State Department of Health, 2021. High heat, low tide likely triggering spike in shellfish-linked infections [WWW Document]. Washington State Department of Health. URL https://doh.wa.gov/newsroom/high-heat-low-tide-likely-triggering-spike-shellfish-linked-infections (accessed 8.17.23).

Weis, K.E., Hammond, R.M., Hutchinson, R., Blackmore, C.G.M., 2011. Vibrio illness in Florida, 1998-2007. Epidemiology and Infection 139, 591–598. https://doi.org/10.1017/S0950268810001354

Weisburg, W.G., Barns, S.M., Pelletier, D.A., Lane, D.J., 1991. 16S ribosomal DNA amplification for phylogenetic study. Journal of Bacteriology 173, 697–703. https://doi.org/10.1128/jb.173.2.697-703.1991

Westrich, J.R., Ebling, A.M., Landing, W.M., Joyner, J.L., Kemp, K.M., Griffin, D.W., Lipp, E.K., 2016. Saharan dust nutrients promote Vibrio bloom formation in marine surface waters. Proceedings of the National Academy of Sciences of the United States of America 113, 5964–5969. https://doi.org/10.1073/pnas.1518080113

Wetz, J., Blackwood, A., Fries, J., Williams, Z., Noble, R., 2008. Trends in total Vibrio spp. and Vibrio vulnificus concentrations in the eutrophic Neuse River Estuary, North Carolina, during storm events. Aquat. Microb. Ecol. 53, 141–149. https://doi.org/10.3354/ame01223

Wetz, J.J., Blackwood, A.D., Fries, J.S., Williams, Z.F., Noble, R.T., 2014. Quantification of Vibrio vulnificus in an Estuarine Environment: a Multi-Year Analysis Using QPCR. Estuaries and Coasts 37, 421–435. https://doi.org/10.1007/s12237-013-9682-4

Whittingham, M.J., Stephens, P.A., Bradbury, R.B., Freckleton, R.P., 2006. Why do we still use stepwise modelling in ecology and behaviour? Journal of Animal Ecology 75, 1182–1189. https://doi.org/10.1111/j.1365-2656.2006.01141.x

Winder, M., Sommer, U., 2012. Phytoplankton response to a changing climate. Hydrobiologia 698, 5–16. https://doi.org/10.1007/s10750-012-1149-2

Wong, H.C., Wang, P., 2004. Induction of viable but nonculturable state in Vibrio parahaemolyticus and its susceptibility to environmental stresses. Journal of Applied Microbiology 96, 359–366. https://doi.org/10.1046/j.1365-2672.2004.02166.x

World Health Organisation, 2023. Disease Outbreak News; Cholera – Global situation [WWW Document]. URL https://www.who.int/emergencies/disease-outbreak-news/item/2023-DON437 (accessed 9.24.23).

World Meteorological Organisation, 2021. State of the Global Climate 2020 (No. WMO-No. 1264).

Wright, A.C., Hill, R.T., Johnson, J.A., Roghman, M.C., Colwell, R.R., Morris, J.G., 1996. Distribution of Vibrio vulnificus in the Chesapeake Bay. Applied and Environmental Microbiology 62, 717–724. https://doi.org/10.1128/aem.62.2.717-724.1996

Wright, A.C., Simpson, L.M., Oliver, J.D., 1981. Role of iron in the pathogenesis of Vibrio vulnificus infections. Infection and Immunity 34, 503–507. https://doi.org/10.1128/iai.34.2.503-507.1981

Wu, B., Liang, W., Kan, B., 2016. Growth phase, oxygen, temperature, and starvation affect the development of viable but non-culturable state of Vibrio cholerae. Frontiers in Microbiology 7, 1–9. https://doi.org/10.3389/fmicb.2016.00404

Wu, Y., Miao, C., Sun, Y., AghaKouchak, A., Shen, C., Fan, X., 2021. Global Observations and CMIP6 Simulations of Compound Extremes of Monthly Temperature and Precipitation. GeoHealth 5, e2021GH000390. https://doi.org/10.1029/2021GH000390

Xin, X., Zhang, J., Zhang, F., Wu, T., Shi, X., Li, J., Chu, M., Liu, Q., Yan, J., Ma, Q., Wei, M., 2018. BCC BCC-CSM2MR model output prepared for CMIP6 CMIP. https://doi.org/10.22033/ESGF/CMIP6.1725

Yamaguchi, R., Rodgers, K.B., Timmermann, A., Stein, K., Schlunegger, S., Bianchi, D., Dunne, J.P., Slater, R.D., 2022. Trophic level decoupling drives future changes in phytoplankton bloom phenology. Nat. Clim. Chang. 12, 469–476. https://doi.org/10.1038/s41558-022-01353-1

Yang, F., Xu, L., Huang, W., Li, F., 2022. Highly lethal Vibrio parahaemolyticus strains cause acute mortality in Penaeus vannamei post-larvae. Aquaculture 548, 737605. https://doi.org/10.1016/j.aquaculture.2021.737605

Yang, X., Zhao, P., Dong, Y., Chen, S., Shen, H., Jiang, G., Zhu, H., Dong, J., Gao, S., 2021. An isothermal recombinase polymerase amplification and lateral flow strip combined method for rapid on-site detection of Vibrio vulnificus in raw seafood. Food Microbiology 98, 103664. https://doi.org/10.1016/j.fm.2020.103664

Ying, N., Wang, Y., Song, X., Yang, L., Qin, B., Wu, Y., Fang, W., 2021. Lateral flow colorimetric biosensor for detection of Vibrio parahaemolyticus based on hybridization chain reaction and aptamer. Mikrochim Acta 188, 381. https://doi.org/10.1007/s00604-021-05031-5

Zanna, L., Khatiwala, S., Gregory, J.M., Ison, J., Heimbach, P., 2019. Global reconstruction of historical ocean heat storage and transport. Proc. Natl. Acad. Sci. U.S.A. 116, 1126–1131. https://doi.org/10.1073/pnas.1808838115

Zettler, E.R., Mincer, T.J., Amaral-Zettler, L.A., 2013. Life in the “plastisphere”: Microbial communities on plastic marine debris. Environmental Science and Technology 47, 7137–7146. https://doi.org/10.1021/es401288x

Zhang, H., Yang, Z., Zhou, Y., Bao, H., Wang, R., Li, T., Pang, M., Sun, L., Zhou, X., 2018. Application of a phage in decontaminating Vibrio parahaemolyticus in oysters. International Journal of Food Microbiology 275, 24–31. https://doi.org/10.1016/j.ijfoodmicro.2018.03.027

Zhang, L., Orth, K., 2013. Virulence determinants for Vibrio parahaemolyticus infection. Current Opinion in Microbiology, Host–microbe interactions: bacteria 16, 70–77. https://doi.org/10.1016/j.mib.2013.02.002

Zhang, X., Huang, B.-W., Zheng, Y.-D., Xin, L.-S., Chen, W.-B., Yu, T., Li, C., Wang, C.-M., Bai, C.-M., 2023. Identification and Characterization of Infectious Pathogens

Associated with Mass Mortalities of Pacific Oyster (Crassostrea gigas) Cultured in Northern China. Biology 12, 759. https://doi.org/10.3390/biology12060759

Zhang, X.-H., He, X., Austin, B., 2020. Vibrio harveyi: a serious pathogen of fish and invertebrates in mariculture. Mar Life Sci Technol 2, 231–245. https://doi.org/10.1007/s42995-020-00037-z

Zhang, X.-J., Qin, G.-M., Bing, X.-W., Yan, B.-L., Liang, L.-G., 2011. Molecular and phenotypic characterization of Vibrio aestuarianus, a pathogen of the cultured tongue sole, Cynoglossus semilaevis Günther. Journal of Fish Diseases 34, 57–64. https://doi.org/10.1111/j.1365-2761.2010.01212.x